

UC Riverside

UC Riverside Electronic Theses and Dissertations

Title

Conservation Genetic Assessment of the Island Night Lizard, *Xantusia riversiana*, Under Contemporary and Future Environmental Conditions

Permalink

<https://escholarship.org/uc/item/9qj134ng>

Author

Rice, Stephen Edward

Publication Date

2017

Copyright Information

This work is made available under the terms of a Creative Commons Attribution License, available at <https://creativecommons.org/licenses/by/4.0/>

Peer reviewed|Thesis/dissertation

UNIVERSITY OF CALIFORNIA
RIVERSIDE

AND

SAN DIEGO STATE UNIVERSITY

Conservation Genetic Assessment of the Island Night Lizard, *Xantusia riversiana*, Under
Contemporary and Future Environmental Conditions.

A Dissertation submitted in partial satisfaction
of the requirements for the degree of

Doctor of Philosophy

in

Evolutionary Biology

by

Stephen Edward Rice

September 2017

Dissertation Committee:

Dr. Rulon Clark, Co-Chairperson
Dr. Kurt Anderson, Co-Chairperson
Dr. Andrew Bohonak
Dr. Helen Regan
Dr. John Gatesy

The Dissertation of Stephen Edward Rice is approved:

Committee Co-Chairperson

Committee Co-Chairperson

University of California, Riverside
San Diego State University

ACKNOWLEDGEMENTS

This research presented in this dissertation would not be possible without the assistance of numerous field assistants, colleagues, the logistical support of San Clemente Island Naval Base and Channel Islands National Park Service, and the support of the San Diego Chapter of the ARCS Foundation as well as my friends and family.

Support for this research came from United States Department of Defense (Award Number W9126G-12-2-0060) and the Southern California Research and Learning Center (Award Number S18309). I would like to thank the National Park Service and San Clemente Island Naval Base for access to their respective islands and providing landscape-level GIS layers. I also thank Dr. Alan Flint (USGS) for providing the downscaled climate data for Chapter 3, and the staff at the Savannah River Ecology Research Laboratory for development of the 23 microsatellite loci used in this dissertation. In addition I would like to thank Drs. R. Clark (SDSU), A. Bohonak (SDSU), H. Regan (UCR), K. Anderson (UCR), and J. Gatesy (UCR) for serving on the dissertation committee and providing feedback on the chapters.

DEDICATION

I dedicate this dissertation to my mother, Darlene Rice, for her tireless efforts in providing encouragement throughout my research and dissertation and for instilling in me a shared work ethic and value of education. I could not have done this without her. I also dedicate this dissertation to my father and step-mother Paul and Janice Norton in addition to the rest of my family. This work is especially dedicated to my niece Jayna and cousins Rilee, Mateo, Taya, and Angelita whose excitement, enthusiasm, and interest have offered both refreshment and encouragement throughout my research career. Finally, I dedicate this dissertation to the memory of my grandparents, Nell and EJ Rice, and great-grandmother, Edna Wiseman, who passed long before I started this journey but whose influences set me on the path.

ABSTRACT OF THE DISSERTATION

Conservation Genetic Assessment of the Island Night Lizard, *Xantusia riversiana*, Under Contemporary and Future Environmental Conditions.

by

Stephen Edward Rice

Doctor of Philosophy, Graduate Program in Evolutionary Biology
University of California, Riverside and San Diego State University, September 2017
Dr. Rulon Clark and Dr. Kurt Anderson, Co-Chairpersons

The island night lizard, *Xantusia riversiana*, is a reptile endemic to three California Channel Islands that was recently delisted from the Endangered Species Act. Several long-term ecological studies have characterized the species throughout its range, yet aspects of the species ecology remain unresolved including sensitivity to climatic change. I collected 917 lizards from the full range of the subspecies *X. r. reticulata* on Santa Barbara Island and San Clemente Island and genotyped all individuals at 23 microsatellite loci. I used these genetic data to determine contemporary patterns in genetic structure and landscape-level correlates with genetic divergence on each island. I found significant population structure on each island and effects of fragmentation from crystalline ice plant, coastal cholla cactus, secondary roadways, and canyons. I used genetic and capture data to identify average parent-offspring differences of 14 m on Santa Barbara Island and 41 m on San Clemente Island. I found that related individuals >0.8 years old were more likely to be captured together on both islands, suggesting the presence of cryptic sociality. Spatial autocorrelation analyses of inter-individual genetic distances revealed different scales of spatial independence on each island (102 - 169 m on

SBI and 955 - 1,424 m on SCI). These results suggest scale-dependent effects of each island below which individuals are more genetically related than expected by chance and may indicate a patch size for familial territory or ranges. I leveraged capture data and historical climate data to construct species distribution models (SDMs) focused on Santa Barbara and San Clemente Islands and projected to the year 2100 under climate change. These models predicted >93% loss in suitable habitat by 2038. I used the SDM for Santa Barbara Island and the results of genetic and spatial analyses to parameterize stochastic demogenetic simulations to determine the sensitivity of island night lizards to climate change using a coupled niche population model framework. These simulations demonstrate *X. riversiana* is highly vulnerable to climate change with expected minimum abundances of 0% - 1% of contemporary population size. Conservation implications and management suggestions are discussed throughout each chapter.

Table of Contents

Introduction.....	1
Chapter 1: Factors affecting intra-island genetic connectivity and diversity of an abundant and widespread island endemic, the San Clemente Island night lizard.	6
Abstract	6
Introduction	7
Materials and Methods	10
Results	18
Discussion	24
Literature Cited	32
Figures	40
Tables	45
Chapter 2: Elucidating dispersal ecology of reclusive species through genetic analyses of parentage and relatedness: the island night lizard (<i>Xantusia riversiana</i>) as a case study. 47	47
Abstract	47
Introduction	48
Methods	51
Results	56
Discussion	57
Literature Cited	64
Figures	68
Tables	72
Chapter 3: Demogenetic simulations reveal fragmenting effects of climate change on insular lizard populations.....	75
Abstract	75
Introduction	76
Methods	79
Results	85
Discussion	86
Literature Cited	95
Figures	98
Tables	103
Conclusions.....	105
Appendix A: Microsatellite loci primers and replication files.....	111
Appendix B: Individual capture data and genotypes	131
Appendix C: Chapter 1 supplementary material.....	238
Appendix D: Chapter 2 supplementary material	263
Appendix E: Chapter 3 supplementary material.....	267

List of Figures

Chapter 1

Figure 1.1. Location of Channel Islands inhabited by the island night lizard.....	40
Figure 1.2. San Clemente Island collection sites with coancestry proportions.....	41
Figure 1.3. Santa Barbara Island collection sites with coancestry proportions.....	42
Figure 1.4 San Clemente Island landscape effects	43
Figure 1.5 Santa Barbara Island landscape effects.....	44

Chapter 2

Figure 2.1. Correlogram of Moran's I on Santa Barbara Island	68
Figure 2.2. Correlogram of Moran's I on San Clemente Island.....	69
Figure 2.3. Variogram analyses for Santa Barbara Island.....	70
Figure 2.4. Variogram analyses for San Clemente Island	71

Chapter 3

Figure 3.1. Percentage of contemporary suitable habitat patches remaining on both Santa Barbara Island and San Clemente Island	98
Figure 3.2. Mean global F_{st} with standard deviations	99
Figure 3.3. Quasi-extinction for distance and connectivity models 2007-2038.....	100
Figure 3.4. Quasi-extinction for connectivity models 2007-2069	101
Figure 3.5. Quasi-extinction for connectivity models 2007-2100	102

Appendix C

Figure C.8. Collection sites on San Clemente Island and associated habitat	249
Figure C.9. Collection sites on Santa Barbara Island and associated habitat	250
Figure C.10. San Clemente Island barplot for the Structure 2-cluster solution.....	251
Figure C.11. San Clemente Island DAPC density plot for sequential k-means 2-cluster solution and associated BIC plot.....	252
Figure C.12. Santa Barbara Island barplot for the Structure 4-cluster solution.....	253
Figure C.13. Santa Barbara Island DAPC density plot for sequential k-means 2-cluster solution and associated BIC plot.....	254
Figure C.14. San Clemente Island IBD, IBR, IBB null models	255
Figure C.15. Santa Barbara Island IBD and IBR null model plots.....	256
Figure C.16. San Clemente Island IBR conductance analysis.....	257
Figure C.17. San Clemente Island IBR resistance analysis	258
Figure C.18. San Clemente Island IBR plots.....	259
Figure C.19. Santa Barbara Island IBR conductance analysis.....	260
Figure C.20. Santa Barbara Island IBR resistance analysis.....	261
Figure C.21. Santa Barbara Island IBR plots.....	262

Appendix D

Figure D.1. Graph of raw data contributing to Santa Barbara Island DyadML analyses	263
Figure D.2. Graph of raw data contributing to Santa Barbara Island DPS analyses	264

Figure D.3. Graph of raw data contributing to San Clemente Island DyadML analyses	265
Figure D.4. Graph of raw data contributing to San Clemente Island DPS analyses	266

Appendix E

Figure E.2. Contemporary (2007) habitat suitability	268
Figure E.3. 2038 CanESM 4.5 habitat suitability	269
Figure E.4. 2038 CanESM 8.5 habitat suitability	270
Figure E.5. 2038 Miroc 4.5 habitat suitability	271
Figure E.6. 2038 Miroc 8.5 habitat suitability	272
Figure E.7. 2069 CanESM 4.5 habitat suitability	273
Figure E.8. 2069 CanESM 8.5 habitat suitability	274
Figure E.9. 2069 Miroc 4.5 habitat suitability	275
Figure E.10. 2069 Miroc 8.5 habitat suitability	276
Figure E.11. 2100 CanESM 4.5 habitat suitability	277
Figure E.12. 2100 CanESM 8.5 habitat suitability	278
Figure E.13. 2100 Miroc 4.5 habitat suitability	279
Figure E.14. 2100 Miroc 8.5 habitat suitability	280

List of Tables

Chapter 1	
Table 1.1. San Clemente Island competing conductance and resistance models.....	45
Table 1.2. Santa Barbara Island competing conductance and resistance models.....	46
Chapter 2	
Table 2.1. Isolation by distance model results	72
Table 2.2. Pairwise distances among relatives	73
Table 2.3. Logistic regression on distance matrices results	74
Chapter 3	
Table 3.1. Environmental and topographic predictors	103
Table 3.2. Proportional EMA by year, climate change scenario, and model	104
Appendix A	
Table A.2. Microsatellite primers and genotyping notes	112
Appendix B	
Table B.1. Individual capture data from San Clemente Island	131
Table B.2. Individual capture data from Santa Barbara Island	147
Table B.3. Individual genetic data from San Clemente Island.....	155
Table B.4. Individual genetic data from Santa Barbara Island	210
Appendix C	
Table C.3. Summary statistics for each island and collection site	243
Table C.4. San Clemente Island collection site pairwise Fsts with 95% confidence intervals	245
Table C.5. Santa Barbara Island collection site pairwise Fsts with 95% confidence intervals	246
Table C.6. San Clemente Island single-variable multiple regression on distance matrices results	247
Table C.7. Santa Barbara Island single-variable multiple regression on distance matrices results	248
Appendix E	
Table E.1. Life history parameters for <i>Xantusia riversiana</i> simulations.....	267

INTRODUCTION

In order to mitigate the consequences of anthropogenic environmental change, a thorough understanding of the patterns and processes leading to diversification and extinction is needed (Kinnison et al. 2007). The largest anthropogenic effect, global climate change, is expected to most strongly affect species with restricted geographic ranges, specialized niches, limited dispersal capacity, and small effective population sizes (reviewed in Oliver and Morecroft 2014). Insular species may be especially vulnerable to ecological disturbances, including habitat modifications due to climate change or invasions by non-native species (e.g. Gillespie et al. 2008).

Among vertebrate taxa, reptiles are considered indicator species of climate change due to their sensitivity to environmental conditions. Projections indicate 11-49% of endemic reptiles will face extinction in the coming decades (Thomas et al. 2004; Urban et al. 2014). Sinervo et al. (2010) concluded that 58% of the fence lizard species studied would be extinct by 2080 and further estimated a global loss of 30% of all lizard species by 2080. These estimates were based on climatic correlations of temperature with thermoregulation and the downstream effects on growth, maintenance, and reproduction. Sinervo et al. (2010) identified two key life history traits correlated with increased extinction risk due to increased temperature: 1) viviparity, presumably due to compromised embryonic development, and 2) thermoconformation (non-basking lizards) due to the lower average body temperatures and critical thermal maxima. A more complete understanding of the effects of climate change on viviparous thermoconforming

lizards is needed to identify strategies which may mitigate losses due to global climate change.

Conservation assessments of the sensitivity of species to climate change have generally focused on population viability analyses (PVA). PVAs are commonly used to evaluate the effects habitat changes on species distribution and extinction risks but rarely incorporate genetic data (Fordham et al. 2014; Frankham et al. 2014). However, a component of some PVAs, species distribution models (SDM), have been used to explain observed genetic patterns (e.g. Knowles et al. 2007). Research methods which integrate these approaches to identify past, present, and future distributions by incorporating genetic and genomic data have been proposed (McCallum et al. 2013; Velo-Anton et al. 2013; Fordham et al. 2014). Recent advances in these efforts include individual-based simulations which can couple species niche, population demography, and genetics to perform PVAs designed to model demographic and genetic changes through time. These modeling methods are known as demogenetic simulations (Landguth et al. 2017) and represent a methodological advancement which can yield insight into the demographic and genetic effects of climate change.

I used an insular lizard endemic to the California Channel Islands, *Xantusia riversiana reticulata*, as the focal system to integrate genetic and demographic research designed to understand the sensitivity of this species to habitat modifications, identify key life history parameters, and model the effects of climate change. The island night lizard is an ideal candidate to integrate genetic and demographic approaches as key components of its life history suggest a high threat from environmental change:

viviparity, biennial reproduction, long lifespan, thermoconformation, restricted range, and limited dispersal ability (Fellers and Drost 1991; Mautz et al. 1992; Mautz 1993; Fellers et al. 1998). Yet, due to the abundance of lizards and generalist habitat requirements, climate change is not anticipated to impact this species beyond indirect effects (United States Fish and Wildlife Service 2014).

The research undertaken for this dissertation is divided into 3 chapters each designed to inform conservation and management of this species while providing data necessary for demogenetic model construction. Chapter 1 used microsatellite data with capture locations to assess landscape-level factors correlated with genetic connectivity of *X. riversiana* on San Clemente and Santa Barbara Islands and characterized the contemporary population structure and genetic patterns on each island. Chapter 2 used genetic and capture data from Chapter 1 to characterize dispersal on each island and identified the relevant spatial scales for modeling individual-based patterns. Chapter 3 used genetic structure from Chapter 1 and dispersal parameters from Chapter 2 to inform demogenetic simulations which were used to evaluate the effects of climate change on demographic and genetic patterns to the year 2100 on Santa Barbara Island.

Literature Cited

- Fellers GM, Drost CA (1991) Ecology of the island night lizard, *Xantusia riversiana*, on Santa Barbara Island, California. *Herpetological Monographs*, 5, 28-78.
- Fellers GM, Drost CA, Mautz WJ, Murphey T (1998) Ecology of the island night lizard, *Xantusia riversiana*, on San Nicolas Island, California. Prepared for the US Navy by the USGS, Western Ecological Research Center, Pt. Reyes Field Station, Pt. Reyes National Seashore, CA.
- Fordham DA, Brook BW, Moritz C, Nogues-Bravo D (2014) Better forecasts of range dynamics using genetic data. *Trends in Ecology and Evolution*, 29, 436-443.
- Frankham R, Bradshaw CJA, Brook BW (2014) Genetics in conservation management: Revised recommendations for the 50/500 rules, Red List criteria and population viability analyses. *Biological Conservation*, 170, 56-63.
- Gillespie RG, Claridge EM, Roderick GE (2008) Biodiversity dynamics in isolated island communities: interaction between natural and human-mediated processes. *Molecular Ecology*, 17, 45-57.
- Kinnison MT, Hendry AP, Stockwell CA (2007) Contemporary evolution meets conservation biology II: impediments to integration and application. *Ecological Resources*, 22, 947-954.
- Knowles LL, Carstens BC, Keat ML (2007) Coupling genetic and ecological-niche models to examine how past population distributions contribute to divergence. *Current Biology*, 17, 940-946.
- Landguth EL, Bearlin A, Day CC, Dunham J (2017) CDMetaPOP: an individual-based, eco-evolutionary model for spatially explicit simulation of landscape demogenetics. *Methods in Ecology and Evolution*, 8(1), 4–11.
<https://doi.org/10.1111/2041-210X.12608>
- Mautz WJ (1993). Ecology and energetics of the island night lizard, *Xantusia riversiana*, on San Clemente Island, California. Pp. 417-428, In: F. G. Hochberg (ed.), *Third California Islands symposium: Recent advances in research on the California Islands*. Santa Barbara Museum of Natural History, Santa Barbara, CA. 661 pp.
- Mautz WJ, Daniels CB, Bennett AF (1992) Thermal dependence of locomotion and aggression in a Xantusiid lizard. *Herpetologica*, 48, 271-279.

- McCallum KP, Guerin GR, Breed MF, Lowe AJ (2013) Combining population genetics, species distribution modeling and field assessments to understand a species vulnerability to climate change. *Austral Ecology*, 39, 17-28.
- Oliver TH, Morecroft MD (2014) Interactions between climate change and land use change on biodiversity: attribution, problems, risks, and opportunities. *WIREs Climate Change*, 5, 317-335.
- Sinervo B, Mendez-de-la-Cruz F, Miles DB, Heulin B, Bastiaans E, Villagran -Santa Cruz M, Lara-Resendiz R, Martinez-Mendez R, Calderon-Espinosa ML, Meza-Lazaro RN, Gadsden H, Avila, M Morando, IJ De la Riva, PV Sepulveda, CFD Rocha, N Ibarguengoytia, CA Puntriano LJ, Massot M, Lepetz V, Oksanen TA, Chapple DG, Bauer AM, Branch WR, Clobert J, Sites Jr JW (2010) Erosion of lizard diversity by climate change and altered thermal niches. *Science*, 328, 894-899.
- Thomas CD, Cameron A, Green RE, Bakkenes M, Beaumont LJ, Collingham YC, Erasmus BFN, de Siqueira MF, Grainger A, Hannah L, Hughes L, Huntley B, van Jaarsveld, GF Midgley, L Miles, MA Ortega-Huerta, A T Peterson, OL Phillips AS, Williams SE (2004) Extinction risk from climate change. *Nature*, 427, 145-148.
- United States Fish and Wildlife Service (2014) Island night lizard (*Xantusia riversiana*) final Post-Delisting Monitoring Plan. U.S. Fish and Wildlife Service, Carlsbad Fish and Wildlife Office, Carlsbad, California.
- Urban MC, Richardson JL, Freidenfelds NA (2014) Plasticity and genetic adaptation mediate amphibian and reptile responses to climate change. *Evolutionary Applications*, 7, 88-103.
- Velo-Anton G, Parra JL, Parra-Olea G, Zamudio KR (2013) Tracking climate change in a dispersal-limited species: reduced spatial and genetic connectivity in a montane salamander. *Molecular Ecology*, 22, 3261-3278.

Chapter 1: Factors affecting intra-island genetic connectivity and diversity of an abundant and widespread island endemic, the San Clemente Island night lizard.

Stephen E. Rice¹ and Rulon W. Clark¹

1. San Diego State University, Dept of Biology, 5500 Campanile Drive, San Diego, California, 92182

Abstract

Habitat fragmentation and loss are fundamental conservation concerns. Because protected areas are often “habitat islands” isolated by human development, studies of physical islands which document genetic patterns associated with natural and artificial fragmentation may provide insight into the management of anthropogenic habitat islands. The San Clemente Island night lizard, *Xantusia riversiana reticulata*, is a regionally abundant endemic to two California Channel Islands, each with a history of anthropogenic disturbance. We genotyped 917 individuals at 23 microsatellite loci to quantify population structure and identify natural and anthropogenic landscape features correlated with genetic divergence between collection sites. Each well-sampled collection site was a distinct genepool, pairwise F_{st} values were small but significant, and STRUCTURE detected 2 populations on San Clemente Island and 4 populations on Santa Barbara Island. Active sand dunes on San Clemente Island were a barrier whereas cholla phase maritime desert scrub, secondary roadways, and canyons were resistant surfaces. Resistant surfaces on Santa Barbara Island were woolly seablite, crystalline iceplant, and barren ground. Conductive habitat included California boxthorn and prickly pear cactus on both islands with additional minor features unique to each island. These results can

inform management plans on each island by identifying habitat targets for mitigation and restoration efforts to improve connectivity. Our results highlight the need for considering fine-scale features correlated with contemporary and historical patterns of fragmentation, especially in small and isolated habitats.

Introduction

Habitat fragmentation by anthropogenic modifications, such as changes in land use and habitat availability, can decrease metapopulation connectivity, increase genetic divergence, and increase extinction risks (e.g. Frankham 2005; Sumner 2005; Vandergast et al. 2016). A common conservation paradigm presents fragmented and isolated habitat patches as hospitable islands surrounded by an inhospitable matrix, similar to oceanic islands, although species' responses to the matrix can vary even among closely related syntopic species (e.g. Hokit et al. 1999; Ricketts 2001; Prugh et al. 2008). An extension of this island metaphor includes the subdivision of habitat fragments into management areas, which may be managed by independent agencies without the ability to modify or improve the intervening habitat matrix. Studies which provide a generalizable approach to identify both common and site-specific strategies may prove invaluable in the management of fragmented and isolated habitat patches.

Oceanic islands are often considered natural laboratories in which evolutionary processes can be studied in closed systems, under more well-defined spatial and temporal scales. Due to their limited sizes and isolated nature, island ecosystems may be highly susceptible to ecological disturbances (e.g. Biber 2002; Gillespie et al. 2008; Harradine et al. 2015). Research on these islands can inform conservation and management science by

providing comparisons with fragmented mainland ecosystems, which often operate as “habitat islands” due to changes in community composition, connectivity, and decreased population sizes (e.g. Hokit et al. 1999; Driscoll 2004; Wang et al. 2009). Additionally, studies on islands with a history of anthropogenic disturbance may identify vital resources for protection and allow for the investigation of broader questions regarding species persistence, interdependent relationships among native species, and ecosystem “economics” (e.g. Leigh et al. 2009).

The California Channel Islands are small oceanic islands off of the coast of Southern California which may yield insight into the effects of habitat fragmentation and alteration due to their long-term natural fragmentation and recent anthropogenic modifications. Each island is characterized by a Mediterranean climate with differences in island size, total precipitation, and average temperatures. Each island has a history of habitat degradation and disturbance from anthropogenic activities, including the introduction of grazing animals, non-native vegetation, and various levels of human habitation. By quantifying the contemporary genetic patterns of island endemics, researchers can provide a baseline for monitoring efforts (*sensu* Schwartz et al. 2007; reviewed in Stetz et al. 2011), a framework for investigating the potential effects of management actions or habitat modifications, and the tools to infer potential effects of environmental change in the near-future (e.g. Row et al. 2014).

Reptiles are an excellent group for studies of fragmentation due to their intermediate dispersal distances, relatively high population densities, plasticity of responses, thermal physiology, and potential vulnerability to habitat modifications (e.g.

Hokit et al. 1999; Jordan and Snell 2008; Wang et al. 2009; Tseng et al. 2015). Projections indicate 11-49% of endemic reptiles will face extinction in the coming decades (Thomas et al. 2004; Urban et al. 2014) and a study by Sinervo et al. (2010) estimated a global loss of 30% of all lizard species by 2080 due to thermal physiology alone. Even for highly abundant species within a confined area, dispersal limitations paired with habitat sensitivity could lead to a range of evolutionary responses between extinction and fine-scale speciation (e.g. Gillespie et al. 2008; Tseng et al. 2015).

The island night lizard, *Xantusia riversiana* (Cope 1883), is an endemic to 3 California Channel Islands: Santa Barbara Island, San Clemente Island, and San Nicolas Island (Figure 1.1). Island night lizards are habitat generalists, but display preferences towards prime habitat on each island (Fellers and Drost 1991; Mautz 1993; Fellers et al. 1998). Prime habitat on San Clemente and Santa Barbara Islands consists of California boxthorn (*Lycium californicum*), prickly pear cactus (*Opuntia littoralis*), and rocky areas which may support abundances in excess of 3,200 individual/ha (Fellers and Drost 1991; Mautz 1993). Ecological research on San Clemente Island has identified island night lizard utilization of all habitats except for deep canyons, sand dunes, and canyon woodland (Mautz 1993). On Santa Barbara Island, lizards are found primarily in prime habitat to the exclusion of grasslands (Fellers and Drost 1991). Island night lizards on San Nicolas Island are considered a distinct subspecies, *X. r. riversiana* (Smith 1946), from the San Clemente Island night lizard (*X. r. riversiana*) and display different habitat utilization and overall life history patterns (Fellers et al. 1998).

Even though the island night lizard is locally abundant, several life history traits make this long-lived species potentially vulnerable to habitat change and fragmentation: slow growth, late maturity, viviparity, and very low dispersal distances (Fellers and Drost 1991; Mautz 1993). We examined population structure and contemporary landscape correlates of genetic differentiation of *X. r. riversiana* throughout its range. We hypothesized that collection sites within islands would display only minor patterns of genetic differentiation due to large population sizes and near-continuous distribution patterns. We also hypothesized that any detected genetic differentiation would be described as correlations of genetic distance with geographic distance and landscape resistance due to limited movement distances and habitat utilizations (Fellers and Drost 1991; Mautz 1993). We analyzed population genetic structure using genepool delimitation, F-statistics, and Bayesian approaches. We examined the correlation of genetic distance between collections sites with geographic distance and resistance due to landscape factors using multiple regression on distance matrices. To support monitoring efforts, we estimated population genetic parameters for each collection site to serve as reference values for any future comparisons.

Materials and Methods

Field Sites and Sample Collection

We collected samples on San Clemente Island from February through November of 2013 and Santa Barbara Island from May through September 2015. Collection sites were selected based on distance from other collection sites and habitat features to support field collections. San Clemente Island collection sites (Figure 1.2 and Appendix C.8)

were selected to provide systematic coverage of the island as well as contrasts at different scales near features of interest: roadways, sand dunes, and areas of habitat transition.

Collection sites on Santa Barbara Island (Figure 1.3 and Appendix C.9) were chosen to provide systematic sampling across the maximum distance of the island; samples were also collected from encountered individuals opportunistically.

Island night lizards were captured by turning cover items and setting live traps in prime habitat along well-worn trails. When multiple lizards were encountered, we made attempts to capture and sample all lizards. Target sample size for each collection site was a minimum of 30 individuals (Hale et al. 2012). Captured lizards were processed following the United States Geological Survey herpetofaunal monitoring protocols (Fisher et al. 2008), sex was determined by probing lizards ≥ 60 mm snout-vent length (Fellers and Drost 1991) and GPS coordinates were recorded with hand-held units with an estimated accuracy of 5 m. Tissue samples consisted of toes that were clipped at the distal knuckle, which also served as a unique 4-digit identification, and a 10 mm segment from the tail tip. Tissues were preserved in 95% ethanol and stored at -20°C .

Sampling and Genotyping

We collected tissue samples from 605 island night lizards at 18 collection sites on San Clemente Island and 312 island night lizards from 7 collection sites and 3 smaller opportunistic areas on Santa Barbara Island (Appendix B). We extracted DNA with a standard salt digestion (Appendix A.1) and genotyped individuals at 23 polymorphic microsatellite loci arranged into 8 reactions (Rice et al. 2016, Appendix A.2). We scored alleles twice with GENEMAPPER vers 4.0 (Applied Biosystems) for consistency; loci

missing data or with inconsistent allele calls were reamplified and rescored to generate a consensus genotype. We assessed error rates associated with allele calls (Pompanon et al. 2005) by extracting and genotyping 35 individuals on San Clemente Island and 16 individuals on Santa Barbara Island a second time.

Quality Control

We removed individuals from analyses if amplification was successful at fewer than 16 loci. We removed first-order relatives (full-sibling, parent-offspring) from data sets for each island through a consensus approach. Pairwise relationships were inferred for samples within each collection site and were considered first-order relatives when at least 2 of 3 methods inferred the relationship. The methods we chose for inference were COLONY (Jones and Wang 2010), CERVUS (Kalinowski et al. 2007), and the DyadML estimator as calculated in COANCESTRY (Wang 2011). Individuals were removed from each data set to retain the largest sample size. Final data sets with relatives removed were used in all further analyses.

We evaluated the quality of each locus for each island at the level of collection sites following Selkoe and Toonen (2006). We examined loci for linkage disequilibrium (LD) and conformance to Hardy-Weinberg and random mating proportions (HWE) in GENEPOP vers 4.5 (Rousset 2008) with p-values corrected for multiple comparisons through sequential Bonferroni testing (Holm 1979). We assessed the presence of null alleles with MICROCHECKER vers 2.2.3 (Van Oosterhout et al. 2004). We examined the putative neutrality of loci with the program LOSITAN (Beaumont and Nichols 1996; Antao et al. 2008) under the infinite alleles model and neutral F_{st} estimation. Loci were

removed from data sets if LOSITAN detected selection, null alleles occurred in a majority of sampled sites, when in LD with another locus, or amplification occurred in less than 75% of individuals. We used the package DIVERSITY (Keenan et al. 2013) in the R statistical environment (R Core Team 2016) and GENEPOP to generate summary statistics for each collection site and each island (Appendix C.3).

Population Structure

We delineated genepools on each island following Waples and Gaggiotti (2006). We conducted an exact test for genetic differentiation for all pairs of collection sites in GENEPOP. We combined probabilities with Fisher's method (Fisher 1932) using 0.0001 as the lower bound for individual test probabilities; combined probabilities were corrected using sequential Bonferroni testing. Collection sites were aggregated if no significant difference was found and the procedure was repeated until all pairwise comparisons were significant.

We estimated the degree and significance of genetic differentiation between collection sites with ≥ 20 individuals with Weir and Cockerham's (1984) estimate of F_{st} with 95% bias corrected confidence intervals generated by 1,000 bootstraps over individuals in DIVERSITY. We defined differentiation as significant when the confidence interval did not overlap 0.

We used the program STRUCTURE (Pritchard et al. 2000; Falush et al. 2003) to estimate the number of populations on each island (K) using data from all collection sites. We used values of K from 1 to 18 for San Clemente Island and 1 to 10 for Santa Barbara Island. Analyses for both island consisted of 20 runs with a 500,000 burn-in period and

1,000,000 MCMC iterations under the admixture model with uncorrelated and correlated allele frequency models (Pritchard et al. 2010). We used the Evanno et al. (2005) method as implemented in STRUCTURE HARVESTER (Earl and vonHoldt 2012) to estimate the number of populations. We generated ancestry matrices with the greedy algorithm in the program CLUMPP (Jakobsson and Rosenberg 2007) to produce barplots with the program DISTRUCT (Rosenberg 2004) for the best supported value of K for each island.

Additionally, we utilized the multivariate technique Discriminant Analysis of Principal Components (DAPC, Jombart et al. 2010) as implemented in the R package ADEGENET (Jombart 2008) to assess the number of genetic clusters useful for statistical classification of the data. We used sequential k-means clustering as implemented with the *find.clusters* function and retained all principal components. The number of clusters chosen for each island corresponded to the lowest value(s) for the Bayesian Information Criteria. The results of k-means clustering were used as group assignments for DAPC analyses, in which we retained 150 principal components for analyses and all eigenvalues.

Isolation by Distance and Isolation by Resistance Analyses

We used the isolation by resistance (IBR, McRae 2006) framework to model conductance and resistance of landscape features on each island. The IBR framework used circuit theory to model pairwise connectivity between collection sites as electrical current iterated across all possible paths for each raster map. The value of raster cells within maps were used to assign the relative cost of movement across a raster cell. Greater values in resistance models increased effective distances between collection sites

whereas greater values in conductance models reduced the effective distance between collection sites. Raster cells assigned a value of 1 approximate log-transformed geographic distance (Lee-Yaw et al. 2009) and are used as the reference value within models. IBR models were compared to the null model of isolation by distance (IBD, Wright 1943). IBD is the observation of spatial autocorrelation within the genetic data (reviewed in Meirmans 2012).

To assess the degree and significance of IBD on each island we employed non-parametric rank-based multiple regression on distance matrices (MRDM, Lichstein 2007) using the function *MRM* in the R package *ECODIST* (Goslee and Urban 2007) with 10,000 permutations, pairwise F_{st} as the response variable, and pairwise Euclidean distance as the predictor. As an extension of the Mantel test framework, results of MRDM are comparable to Mantel results with a single predictor matrix. We used *CIRCUITSCAPE* (McRae and Beier 2007) for IBR analyses in which we modeled conductance and resistance of landscape elements separately on each island. Resistance and conductance were modeled separately to clearly delineate landscape features with positive and negative correlations with pairwise genetic distances. Only those collection sites with at least 20 individuals were included in IBD and IBR analyses.

The methods used to construct raster maps and evaluate model fit were consistent between islands; however, the resolution of the data and the thematic content of GIS layers differed due to coarseness of GIS data. Input rasters were made with *QGIS* (*QGIS* Development Team, 2016). Raster cell values for each feature ranged from 2 (low), 50 (moderate), and 100 (high) (Appendix C.6 and C.7). These values were not chosen to

identify or represent the true values of landscape features. Resistance values were chosen to identify candidate landscape features and attribute a coarse value to each for modelling purposes only, as the relative difference between features is important in model construction and selection. Collection sites were represented as focal regions composed of the minimum-spanning convex hulls generated from capture coordinates.

We used non-parametric MRDM with 10,000 permutations to assess the categorical features for each island. Models ranged from single features to full models of all statistically supported features. Single features entered the model-building framework (Appendix C.1) if their inclusion was significant and the coefficient of determination (R^2) was greater than the null model. The null model consisted of all features with a resistance value of 1. Resistance-distance matrices for single features were used to estimate the regression effect of higher-order models with MRDM (Appendix C.2). We constructed the top 10% of estimated models for each GIS layer and additive models across GIS layers for each island. In additive models, raster cells had either a cumulative value based on the presence of all features in the cell, values for each distinct feature class, or 1 when no focal feature was present.

We used a consensus approach for model selection which considered the ranked-order of best models across MRDM, corrected Akaike information criterion (AICc), and marginal R^2_{β} (Edwards et al. 2008). We used the *lmer* function in the R package LME4 (Bates et al. 2015) to construct maximum-likelihood population effects (MLPE) models (Clarke et al. 2002) fit with residual maximum likelihood (REML) estimation with collection site as a random factor. We used the *KRmodcomp* function in the R package

PBKRTEST (Halekoh and Højsgaard 2014) to calculate the marginal R_p^2 from the MLPE models (Appendix S3). We calculated AICc with the R package MUMIN (Bartoń 2016) for MLPE models fit without REML estimation, as variables which contributed the fixed effects differed between models (reviewed in Van Strien et al. 2012).

San Clemente Island

Resistance-based analyses of San Clemente Island focused on three categorical GIS layers: vegetation type (RECON, Inc 2012), roadways type (Naval Facilities and Engineering Command South West (NAVFACSW), date unknown), and canyon length (NAVFACSW, date unknown). We estimated the coarseness of resolution of the GIS data to be 1 ha, therefore all raster maps were produced with 100 m cell size.

Vegetation was parsed into 11 classes based on least-cost transect analysis groupings (Appendix C.8). Due to a strong signal of genetic differentiation, we investigated different null models for IBR analyses (see results). The null model best supported by MRDM analyses modeled active sand dunes as an absolute barrier, which was then coded as no data in all maps. Roadways were divided into two classifications: paved roads, which served as primary traffic conduits along the spine of the island and within more populated areas, and secondary roads, which were generally unpaved access roads (Appendix C.8). We applied a 5 m buffer to all road types to eliminate breaks in the linear features when rasterized. Canyons were divided into three length classes of small (0-499 ft), medium (500-999 ft), and large ($\geq 1,000$ ft).

Santa Barbara Island

Resistance-based analyses of Santa Barbara Island focused on three layers: vegetation type (National Park Service (NPS), 2010) (Appendix C.9), western seagull (*Larus occidentalis*) nesting sites, and home ranges of a small population of potential predators, barn owls (*Tyto alba*). There are no roads on Santa Barbara Island. Vegetation was classified into 14 groups based on dominant vegetation alliances; due to observations of woolly seablite (*Suaeda taxifolia*) provisional shrubland alliance transitioning seasonally into crystalline iceplant (*Mesembryanthemum crystallinum*) dominated habitat (pers. comm., Rodriguez 2016) we grouped these alliances into a single class. The presence of western seagull nesting colonies was included in resistance analyses by digitizing seabird nesting locations from 2015 (NPS 2015) and assigned the full range of resistance values (data not shown). Barn owl home ranges were digitized from Figure 1 of Thomsen et al. (2014) and classified as with the western gull resistance analysis (data not shown). Resolution on vegetation data was listed as 1 ft (NPS 2010); however raster maps were generated with a cell size of 5 m for all layers due to the uncertainty in GPS coordinates.

Results

Quality Control

No loci were discarded due to LD or non-robust amplification. Three different loci on each island differed significantly from HWE; however, these loci were not removed on this finding alone. A single locus (Xari22) was removed due to null alleles in 12 of 18 collection sites on San Clemente Island; no loci were removed from the Santa

Barbara Island data set due to null alleles. The program LOSITAN identified 2 loci (Xari33, Xari44) as under selection for San Clemente Island and 2 loci (Xari18, Xari30) as under selection for Santa Barbara Island. These loci were removed from further analyses within each respective data set. Final data sets consisted of 20 loci for San Clemente Island and 21 loci for Santa Barbara Island (Appendix A.2).

The per-allele error rates associated with genotyping were 0.062% for San Clemente Island and 0.272% for Santa Barbara Island. Rates of non-robust amplification were 7.14% for San Clemente Island and 3.80% for Santa Barbara Island. We removed 18 individuals from the San Clemente Island data set due to missing data; no individuals were removed from the Santa Barbara Island data set for this reason. The consensus approach revealed 75 first-order relationships among 114 individuals on San Clemente Island and 65 first-order relationships among 97 individuals on Santa Barbara Island. We removed 53 individuals from the San Clemente Island data set and 41 individuals from the Santa Barbara Island data set due to these relationships. These removals resulted in sample sizes of 534 individuals from San Clemente Island and 271 from Santa Barbara Island.

Summary Statistics

Sample sizes for San Clemente Island collection sites ranged from 12-70 individuals. Rarefied allelic richness ranged from 5.46 to 9.31; excluding the only collection site with fewer than 20 individuals allelic richness ranged from 6.28 to 11.0. Observed heterozygosity ranged from 0.62 to 0.88 whereas expected heterozygosity ranged from 0.69 to 0.87. Only collection site 8 had significant departure from HWE

after applying sequential Bonferroni corrections. Collection site 8, which is a coastal site bordered by ocean and active sand dunes on all but one side, also had the lowest allelic richness, observed heterozygosity, and expected heterozygosity.

Sample sizes for Santa Barbara Island collection sites ranged from 21-60 individuals and 8-12 individuals for three opportunistic collection areas. Rarified allelic richness based on all collection sites ranged from 5.62 to 6.65. Removal of the three opportunistic sites resulted in allelic richness ranging from 7.17 to 8.65. Observed heterozygosity ranged from 0.76 to 0.85 for focal sites and up to 0.89 for opportunistic areas. Expected heterozygosity ranged similarly from 0.78 to 0.83. No significant departures from HWE were detected.

Population Structure

All collection sites on San Clemente Island were identified as distinct genepools through contingency table analysis of allele frequencies; combined p-values ranged from functionally 0 to 1.02×10^{-5} . Two collection sites on Santa Barbara Island were aggregated (LC and GC) whereas all other sites were distinct genepools with p-values ranging from functionally 0 to 1.71×10^{-7} . Aggregated summary statistics for LC and GC are presented in Appendix C.3; however, due to the limited sample size of LC, LC and GC were not aggregated for further analyses.

Pairwise F_{st} values between collection sites revealed subtle but significant structure on San Clemente Island (Appendix C.4) with values ranging from 0.0022 to 0.1278. The largest values for F_{st} involved collection site 8. The best supported clustering solution found by STRUCTURE for San Clemente Island was $K=2$ (Figure 1.2

and Appendix C.10). Sequential k-means clustering supported values of K ranging from 2 to 4 (Appendix C.11).

On Santa Barbara Island pairwise F_{st} also showed subtle but significant structure (Appendix C.5) with values ranging from 0.0199 to 0.0590. STRUCTURE analyses with correlated and uncorrelated allele frequencies converged on solutions of K=4 and K=7; both models were detected using the Evanno et al. (2005) method but the magnitude of peaks differed between allele frequency model. We chose the solution of K=4 (Figure 1.3 and Appendix C.12) as the K=7 solution displayed clusters with minimal contributions. Sequential k-means clustering supported K=2 (Appendix C.13).

Isolation by Distance

We detected significant IBD on both San Clemente Island and Santa Barbara Island. On San Clemente Island, initial analyses of the 17 collection sites resulted in no detection of IBD ($p=0.145$, $R^2=0.0249$; Appendix C.14); we attribute this to the non-linear and non-monotonic relationship between F_{st} and Euclidean distance which resulted from the strong signal of genetic differentiation between collection site 8 and all other sites. Removal of this site as an outlier resulted in a significant finding of IBD among the remaining 16 collection sites ($p=0.001$, $R^2=0.2060$). Santa Barbara Island also displayed significant patterns of IBD when evaluated with the 7 primary collection sites ($p=0.0174$, $R^2=0.4258$, Appendix C.15).

Isolation by Resistance Models

San Clemente Island

As with IBD analyses, IBR analyses were sensitive to the inclusion of collection site 8. We evaluated 4 models to determine if the observed patterns could be attributed to either collection site 8 or active sand dunes acting as a barrier. The best supported model placed active sand dunes as a complete barrier ($p=0.0005$, $R^2=0.2602$, Appendix C.14), followed by a distance-only model with collection site 8 removed ($p=0.0020$, $R^2=0.1121$), collection site 8 removed and active sand dunes as a complete barrier ($p=0.0096$, $R^2=0.0848$), and the distance-only model with all collection sites ($p=0.0149$, $R^2=0.0681$). We chose to model active sand dunes as a complete barrier in all further models.

Models of conductance (Table 1.1, Figure 1.4) that included California boxthorn (boxthorn) and prickly pear cactus (prickly pear) had the strongest support across methods. Four models were equivalent in significance ($p=0.0001$, R^2 range: 0.6433-0.6602). Ranking these models by AICc led to equivalence between two models that differed only by the inclusion of grasslands as low conductance; the model with the lowest AICc (-957.56) and highest R^2_{β} value (0.7257) contained both grasslands and small canyons as low conductance (Appendix C.16).

Models of resistance (Table 1.1, Figure 1.4) with cholla phase maritime desert scrub (cholla), canyons, and secondary roads were best supported across methods. Corrected AIC could not differentiate between the best models as all contained the same features (AICc: -972.94 to -974.47). In the top performing models cholla, medium-sized

canyons, and secondary roadways were moderate resistance whereas large canyons were moderate to high resistance (Appendix C.17). The model best supported by MRDM ($p=0.0001$, $R^2=0.5125$) and R^2_{β} (0.8606) was a model with cholla, medium-sized canyons, and secondary roads with moderate resistance and large canyons with high resistance.

Santa Barbara Island

The distance-only null model on Santa Barbara Island was significant ($p=0.0214$, $R^2=0.4804$; Appendix C.15). Models of conductance (Table 1.2, Figure 1.5) which included boxthorn and prickly pear had the best support across methods. The R^2 for conductance models ranged from 0.8596 to 0.8877. The model with the greatest R^2 had both boxthorn and prickly pear with high conductance and giant coreopsis (*Leptosyne gigantean*) habitat as low conductance ($p=0.0008$, Figure 1.5 and Appendix C.19). Eight models had AICc values within 2 units of the top model (AICc range -151.976 to -153.318). The model best supported within this subset by R^2_{β} (0.8718) was congruent with the MRDM results. Statistical methods did not show congruence among model rankings after the best supported model.

Models of resistance which included woolly seablite (seablite) and crystalline iceplant (iceplant) as moderately resistant were the best supported models (Table 1.2, Figure 1.5). Seven models had equivalent R^2 (0.8582) and highly significant p-values ($p=0.0003$ to 0.0007). These models were parsed into two groups by AICc; the best supported group had AICc values of -149.043 to -150.066 and differed only in the resistance value assigned to barren ground and inclusion of needle goldfields (*Lasthenia*

gracilis). The models with the greatest R^2_{β} contained seablite and iceplant as low resistance with barren ground as moderate ($R^2_{\beta}=0.8867$) and high resistance ($R^2_{\beta}=0.8853$); these models fell within the range of the AICc subset but had much lower R^2 values (0.6919 and 0.6879 respectively). We chose the model in which combined seablite and iceplant with barren ground and common fiddleneck with moderate resistance (Figure 1.5 and Appendix C.20) as increased resistance and habitat types failed to greatly improve the model (Table 1.2).

Discussion

We conducted a detailed genetic assessment of *X. riversiana* on San Clemente Island and Santa Barbara Island to inform conservation and management approaches. We utilized island-wide sampling with 23 microsatellite loci to estimate baseline parameters for each collection site, quantify population structure, and identify landscape factors correlated with genetic divergence on each island. We found island night lizards were admixed on each island with shallow, but significant, population structure. Each island displayed patterns of IBD with conductance through California boxthorn and prickly pear cactus. Active sand dunes were identified as a barrier to gene flow on San Clemente Island but absent on Santa Barbara Island. Habitat resistance patterns were unique to each island and included both natural and anthropogenic features.

Population Structure

STRUCTURE characterized San Clemente Island as 2 genetic clusters associated with the northern and southern ends with strong admixture across the island. This pattern could result from the clustered sampling of a ubiquitously distributed organism

characterized by neighbor-mating or limited dispersal (Schwartz and McKelvey 2009). However, the congruence between genepool delineation, multivariate approaches, and pairwise F_{st} corroborate the inferences made by STRUCTURE.

Surprisingly, Santa Barbara Island displayed a greater degree of population structure than San Clemente Island, despite its much smaller size. The STRUCTURE results sorted the island samples into a western population on Webster Point, a northern population along Cliff Canyon, a multi-site mid-island cluster, and a south-eastern cluster. The western and northern clusters displayed relatively little admixture whereas the other clusters were more strongly admixed. Sequential k-means clustering supported a similar pattern with the western and northern collection sites clustering separately from all others. Similarly, genepool delineation and pairwise F_{st} corroborated the STRUCTURE findings, revealing significant differentiation even for those sites <400 m apart.

It is notable that the global F_{st} estimates for San Clemente Island and Santa Barbara Island were remarkably similar (0.0341 and 0.0346 respectively) despite large differences in island size and sampling scale. Thus, genetic structure on each island may be, in part, explained by IBD due to limited dispersal distances. While dispersal estimates are absent from the literature, displacement distances on San Clement Island averaged 3 m (Mautz 1993) with a maximum observation of 29 m (Mautz et al. 1992).

Isolation by Resistance: Conductance Models

California boxthorn and prickly pear cactus support the greatest abundances of island night lizards and are prime habitat types indicated for continued monitoring under the United States Fish and Wildlife Service post-delisting plan (USFWS 2014). Our

analyses identified these habitats as highly conductive, thus corroborating the ecological data (Fellers and Drost 1991; Mautz 1993). Surprisingly, grasslands were also identified as conductive on San Clemente Island even though ecological data suggested grasslands are poor habitat (Fellers and Drost 1991). This may be attributable to the presence of cover items, such as rocks, within the San Clemente Island grasslands. As thermoconformers (Regal 1968; Fellers and Drost 1991) cover items are important landscape features for thermal regulation and any habitat with suitable cover may be conductive. For example, island night lizards on San Nicolas Island can be found in beach habitat with little vegetation, so long as cover rocks are present (Fellers et al. 1998). The best supported conductance model for Santa Barbara Island contained only one additional habitat type, giant coreopsis, as weakly conductive. The distribution of this habitat type on Santa Barbara Island is such that it is generally contiguous with prime habitat so it is difficult to analyze the importance of this habitat type on its own.

Isolation by Sand Dunes

Active sand dunes along the north coast of San Clemente Island were the only habitat we identified as a barrier. This habitat was best modeled as an absolute barrier to dispersal, which is supported by Mautz (1993). It is likely that this finding could hold true on San Nicolas Island as well; however the effect of sand dunes on this island has yet to be assessed. There are no sand dunes present on Santa Barbara Island.

Isolation by Resistance Models

San Clemente Island

Models of habitat resistance were not congruent between the two islands, with no features identified as resistant on both islands. This finding probably reflects differences in topography, the extent of certain vegetation types, and anthropogenic development. On San Clemente Island we identified cholla, secondary roadways, and medium and large canyons as resistant features. The association of canyons with increased genetic differentiation between collection sites is supported by ecological research, and may be due to both difficulty in crossing and lack of resources (Mautz 1993).

The establishment of the Naval base in the early 19th century and subsequent infrastructure and training activities also appear to have an effect, as secondary roadways impede connectivity. It is of note that the primary roadway was not identified as a resistant surface, even though it is paved and has more traffic. However, this primary road is one relatively short road running down the middle of the island, whereas the network of secondary roads is extensive and bisects multiple collection sites within prime habitat, thereby increasing its detectable effect.

The habitat type most strongly associated with genetic differentiation was cholla, a vegetation community that is distributed extensively on San Clemente Island but not on Santa Barbara Island. Coastal cholla may act as a resistant surface as the spines readily pierce flesh and could injure or debilitate fleeing or dispersing individuals (personal obs.). The large cholla patch separating the collection sites at the southern end of San Clemente Island is of particular interest as it could easily limit the dispersal of individuals

across the landscape. The increased disturbance to the southern portion of the island through active bombardment may further propagate cholla, thus increasing its density and distribution within the bombardment areas.

Santa Barbara Island

While resistance model selection was not congruent for Santa Barbara Island, two habitat types were consistently included: seablite grouped with iceplant and barren ground. Due to the spatial and temporal transitions between seablite and iceplant habitat types (pers. comm., Rodriguez 2016), we could not determine the independent contributions of these habitat types to genetic differentiation. Iceplant can modify soil composition through the deposition of retained salt deposits, rendering areas unsuitable for other vegetation (Vivrette and Muller 1977). This may limit the cover for foraging, thermoregulation, or dispersal due to barren areas which result from plant death (Fellers and Drost 1991). The identification of barren ground on Santa Barbara Island as resistant is unsurprising and attributable to the lack of cover and soil fissures used by island night lizards.

The absence of grassland habitats from the final resistance models is notable. Fellers and Drost (1991) found that lizards were largely absent from grasslands with capture effort equivalent to that of seablite and iceplant dominated habitat. The identification of common fiddleneck and needle goldfields within similarly supported resistance models are not congruent with the dietary analyses nor ecological study of Fellers and Drost (1991). These habitat types were identified through statistical optimization and could represent biases in this process. However, these habitats represent

herbaceous cover types which offer little shelter or resources to island night lizards and are adjacent to other resistant features. The NP collection site occurred primarily within a habitat dominated by needle goldfields; however a large number of rocks were present, thus supplementing the available cover. It is likely that when herbaceous cover is dense enough to cause refugial fissures in the soil (Fellers and Drost 1991) or supplemented by cover items within the habitat, resistance may be minimized.

Management Implications

The island night lizard is an abundant island endemic with a restricted range which was delisted from the Endangered Species Act in 2014 contingent on monitoring over a 10-year period (USFWS 2014). While active management is no longer required, actions should be identified to better support the monitoring framework. Our genetic analyses indicate that management actions common to both islands should focus on protecting and restoring prime habitat to improve connectivity and localized abundances.

Management action focused on mitigating the impact of resistant surfaces on island night lizard populations would be unique not only to each island, but also to differing sections of San Clemente Island. On San Clemente Island, natural population fragmentation results from canyons and active sand dunes. We recommend that mitigation efforts be applied to secondary roadways by limiting the fragmentation of prime habitat and adding cover items or corridors to provide a more permeable surface. Within the bombardment area, the propagation of cholla should be minimized through more targeted training activities to avoid spreading propagules. On Santa Barbara Island,

we recommend removing crystalline iceplant and restoring native vegetation to improve the quality of the habitat matrix and supporting connectivity between collection sites.

Our study methodology can be generalized to the inference of connectivity patterns within Southern California where native habitat is fragmented by anthropogenic modifications, infrastructure, and invasive species. For example, the California Floristic Province is under increasing synergistic threats from climate change, urbanization, and altered fire regimes (e.g. Syphard et al. 2007; Regan et al. 2012). Management strategies to maintain population persistence for many species will likely need to incorporate information on conductance and resistance for habitat patches that increasingly act in isolation. As many management actions are spatially explicit, it is increasingly important to characterize genetic patterns using spatially explicit methods (Schaffer et al. 2015).

An exemplar region which could benefit from such an approach is the peninsular region of Southern California, Point Loma. This region is predicted to experience increased extinction risks of plant and animal species (e.g. Lawson 2011) and genetic studies of lizards (Luckau 2015) and small mammals (Lion 2016) reveal consistent patterns of significant genetic differentiation and decreased genetic diversity. These increased extinction risks are further complicated by multiple managing agencies and land use practices throughout the relatively small peninsula. The modeling frameworks we present can be applied to Point Loma to support management efforts of each species by identifying resistant features for mitigation efforts within each fine-scale management area while simultaneously identifying key landscape features within and between management areas which support connectivity. We encourage the comparison of fine-

scale patterns within and between regional management units to identify common mitigation strategies within and between protected areas. Resistance-based analyses may identify unique features acting at relatively fine scales that could be actively managed to better sustain local demes or populations by increasing the prime habitat area and improve the matrix quality (e.g. Fahrig 2001).

Literature Cited

- Antao T, Lopes A, Lopes RJ, Beja-Pereira A, Luikart G (2008) Lositan: A workbench to detect molecular adaptation based on a Fst-outlier method. *BMC Bioinformatics*, 9, 323.
- Bartoń K (2016) MuMIn: multi-model inference. R package, version 1.15.6. Available online: <http://r-forge.r-project.org/projects/mumin/>
- Bates D, Maechler M, Bolker B, Walker S (2015) Fitting Linear Mixed-Effects Models Using lme4. *Journal of Statistical Software*, 67:1-48.
- Beaumont MA, Nichols RA (1996) Evaluating loci for use in the genetic analysis of population structure. *Proceedings of the Royal Society of London. Series B: Biological Sciences*, 263, 1619-1626.
- Biber E (2002) Patterns of endemic extinctions among island bird species. *Ecography*, 25, 661-676.
- Brownstein MJ, Carpten JD, Smith JR (1996) Modulation of non-templated nucleotide addition by Taq DNA polymerase: primer modifications that facilitate genotyping. *BioTechniques*, 20, 1004-1010.
- Clarke RT, Rothery P, Raybould AF (2002) Confidence limits for regression relationships between distance matrices: estimating gene flow with distance. *Journal of Agricultural Biological and Environmental Statistics*, 7, 361–372.
- Cope ED (1883) Note on a species of Xantusia. In: *Proceedings of the Academy of Natural Sciences of Philadelphia 1884* (ed Nolan EJ), pp. 29-32. Academy of Natural Sciences of Philadelphia, PA.
- Driscoll D (2004) Extinction and outbreaks accompany fragmentation of a reptile community. *Ecological Applications*, 14, 220-240.
- Earl DA, vonHoldt BM (2012) Structure Harvester: a website and program for visualizing structure output and implementing the Evanno method. *Conservation Genetics Resources*, 4, 359-361.
- Edwards LJ, Muller KE, Wolfinger RD, Qaqish BF, Schabenberger O (2008) An R^2 statistic for fixed effects in the linear mixed model. *Statistics in Medicine*, 27, 6137-6157.

- Evanno G, Regnaut S, Goudet J (2005) Detecting the number of clusters of individuals using the software structure: a simulation study. *Molecular Ecology*, 14, 2611-2620.
- Fahrig L (2001) How much habitat is enough? *Biological Conservation*, 100, 65-74.
- Falush D, Stephens M, Pritchard JK (2003) Inference of population structure using multilocus genotype data: linked loci and correlated allele frequencies. *Genetics*, 164, 1567-1587.
- Fellers GM, Drost CA (1991) Ecology of the island night lizard, *Xantusia riversiana*, on Santa Barbara Island, California. *Herpetological Monographs*, 5, 28-78.
- Fellers GM, Drost CA, Mautz WJ, Murphey T (1998) Ecology of the island night lizard, *Xantusia riversiana*, on San Nicolas Island, California. Prepared for the US Navy by the USGS, Western Ecological Research Center, Pt. Reyes Field Station, Pt. Reyes National Seashore, CA.
- Fisher RA (1932) *Statistical Methods for Research Workers*. Oliver and Boyd, Edinburgh.
- Fisher R, Stokes D, Rochester C, Brehme C, Hathaway S, Case T (2008) *Herpetological monitoring using a pitfall trapping design in southern California*. U. S. Geological Survey Techniques and Methods 2-A5.
- Frankham R (2005) Genetics and extinction. *Biological Conservation* 126:131-140.
- Gillespie RG, Claridge EM, Roderick GE (2008) Biodiversity dynamics in isolated island communities: interaction between natural and human-mediated processes. *Molecular Ecology*, 17, 45-57.
- Goslee SC, Urban DL (2007) The ecodist package for dissimilarity-based analysis of ecological data. *Journal Statistical Software*, 22, 1-19.
- Hale ML, Burg TM, Steeves TE (2012) Sampling for microsatellite-based population genetic studies: 25 to 30 individuals per population is enough to accurately estimate allele frequencies. *PLoS One*, 7, e45170.
- Halekoh U, Højsgaard S (2014) A Kenward-Roger Approximation and Parametric Bootstrap Methods for Tests in Linear Mixed Models - The R Package pbkrtest. *Journal Statistical Software*, 59, 1-30.

- Harradine E, How RA, Schmitt LH, Spencer PBS (2015) Island size and remoteness have major conservation significance for how spatial diversity is partitioned in skinks. *Biodiversity and Conservation*, 24, 2011-2029.
- Hokit GD, Stith BM, Branch LC (1999) Effects of landscape structure in Florida scrub: a population perspective. *Ecological Applications*, 9, 124-134.
- Holm S (1979) A simple sequentially rejective multiple test procedure. *Scandinavian Journal of Statistics*, 6, 65-70.
- Jakobsson M, Rosenberg NA (2007) Clump: a cluster matching and permutation program for dealing with label switching and multimodality in analysis of population structure. *Bioinformatics*, 23, 1801-1806.
- Jombart T (2008) Adegnet: a R package for the multivariate analysis of genetic markers. *Bioinformatics*, 24, 1403-1405.
- Jombart T, Devillard S, Balloux F (2010) Discriminant analysis of principal components: a new method for the analysis of genetically structured populations. *BMC Genetics*, 11, 94. doi:10.1186/1471-2156-11-94.
- Jones OR, Wang J (2010) Colony: a program for parentage and sibship inference from multilocus genotype data. *Molecular Ecology Resources*, 10, 551-555.
- Jordan MA, Snell HL (2008) Historical fragmentation of islands and genetic drift in populations of Galapagos lava lizards (*Microlophus albemarlensis* complex). *Molecular Ecology*, 17, 1224-1237.
- Kalinowski ST, Taper ML, Marshall TC (2007) Revising how the computer program CERVUS accommodates genotyping error increases success in paternity assignment. *Molecular Ecology*, 16, 1099-1106.
- Keenan K, McGinnity P, Cross TF, Crozier WW, Prodohl PA (2013) Diversity: an R package for the estimation and exploration of population genetics parameters and their associated errors. *Methods in Ecology and Evolution*, 4, 782-788.
- Lawson DM (2011) Multi-species conservation in the context of global change. Ph.D. Dissertation, University of California, Davis.
- Lee-Yaw JA, Davidson A, McRae BH, Green DM (2009) Do landscape processes predict phylogeographic patterns in the wood frog? *Molecular Ecology*, 18, 1863-1874.
- Leigh EG Jr, Vermeij GJ, Wikelski M (2009) What do human economies, large islands and forest fragments reveal about the factors limiting ecosystem evolution?

Journal of Evolutionary Biology, 22, 1-12, doi: 10.1111/j.1420-9101.2008.01624.x

- Lichstein JW (2007) Multiple regression on distance matrices: a multivariate spatial analysis tool. *Plant Ecology*, 188, 117-131.
- Luckau TK (2015) Comparative conservation genetics of two sympatric lizard species across multiple landscapes in San Diego Country. MSc Thesis, San Diego State University.
- Lion K (2016) A comparative study of genetic patterns in two closely related and sympatric *Peromyscus* species. MSc Thesis, San Diego State University.
- Mautz WJ (1993) Ecology and energetics of the island night lizard, *Xantusia riversiana*, on San Clemente Island, California. In: Third California Islands symposium: Recent advances in research on the California Islands (ed Hochberg FG), pp. 417-428. Santa Barbara Museum of Natural History, Santa Barbara, CA.
- Mautz WJ, Daniels CB, Bennett AF (1992) Thermal dependence of locomotion and aggression in a Xantusiid lizard. *Herpetologica*, 48, 271-279.
- McRae, BH (2006) Isolation by resistance. *Evolution*, 60, 1551-1561.
- McRae BH, Beier P (2007) Circuit theory predicts gene flow in plant and animal populations. *Proceedings of the National Academy of Sciences USA*, 104, 19885-19890.
- Meirmans PG (2012) The trouble with isolation by distance. *Molecular Ecology*, 21, 2839-2846.
- Naval Facilities and Engineering Command South West (NAVFACSW)(Date Unknown) Spatial data developed by NAVFACSW.
- National Institute of Standards and Technology (NIST) (2005) Primer Tools. Available online: <http://yellow.nist.gov:8444/dnaAnalysis/primerToolsPage.do>.
- National Park Service (2010) Channel Islands National Park, Santa Barbara Island vegetation map final draft.
- National Park Service (2015) Channel Islands National Park, Santa Barbara Island seabird nesting locations.
- Pompanon F, Bonin A, Bellemain E, Taberlet P (2005) Genotyping errors: causes, consequences and solutions. *Nature Reviews Genetics*, 6, 847-859.

- Pritchard JK, Stephens M, Donnelly P (2000) Inference of population structure using multilocus genotype data. *Genetics*, 155, 945-959.
- Pritchard JK, Wen X, Falush D (2010) Documentation for structure software: version 2.3.
- Prugh LR, Hodges KE, Sinclair ARE, Brashares JS (2008) Effect of habitat area and isolation on fragmented animal populations. *Proceedings of the National Academy of Sciences USA*, 105, 20770-20775.
- QGIS Development Team (2016) QGIS Geographic Information System. Open Source Geospatial Foundation Project. Available online: <<http://qgis.osgeo.org>>.
- R Core Team (2016) R: A language and environment for statistical computing. R Foundation for Statistical Computing, Vienna, Austria. Available online: <https://www.R-project.org/>.
- RECON Environmental, Inc (2012) San Clemente Island vegetation mapping: How GIS helped two botanists map 36,000 acres in five field days. Poster accessible online: http://www.recon-us.com/services/biological-res/san_clemente_island/san_clemente_poster.pdf.
- Regal PJ (1968) An analysis of heat seeking in a lizard. Ph.D. Dissertation, University of California, Los Angeles.
- Regan HM, Syphard AD, Franklin J, Swab RM, Markovchick L, Flint AL, Flint, LE, Zedler PH (2012) Evaluation of assisted colonization strategies under global change for a rare, fire-dependent plant. *Global Change Biology*, 18, 936-947.
- Rice SE, Beasley RR, Lance SL, Jones KL, Clark RW (2016) Development of 24 polymorphic microsatellite markers for the Island Night Lizard (*Xantusia riversiana*) in Microsatellite records for volume 8, issue 2. *Conservation Genetics Resources*, 8, 169-196 doi: 10.1007/s12686-016-0549-4
- Ricketts TH (2001) The matrix matters: effective isolation in fragmented landscapes. *American Naturalist*, 158, 87-99.
- Rosenberg NA (2004) Distruct: a program for the graphical display of population structure. *Molecular Ecology Notes*, 4, 137-138.
- Rousset F (2008) Genepop'007: a complete re-implementation of the genepop software for Windows and Linux. *Molecular Ecology Resources*, 8, 103-106.

- Row JR, Wilson PJ, Gomez C, Koen EL, Bowman J, Thorton D, Murray D (2014) The subtle role of climate change on population genetic structure in Canada lynx. *Global Change Biology*, 20, 2076-2086.
- Shaffer HB, Gidiş M, McCartney-Melstad E, Neal KM, Oyamaguchi HM, Tellez M, Toffelmier EM (2015) Conservation genetics and genomics of amphibians and reptiles. *Annual Review of Animal Biosciences*, 3, 113-138.
- Schwartz MK, McKelvey KS (2009) Why sampling scheme matters: the effect of sampling scheme on landscape genetic results. *Conservation Genetics*, 10, 441-452.
- Schwartz MK, Luikart G, Waples R (2007) Genetic monitoring as a promising tool for conservation and management. *Trends in Ecology and Evolution*, 22, 25-33.
- Selkoe KA, Toonen RJ (2006) Microsatellites for ecologists: a practical guide to using and evaluating microsatellite markers. *Ecology Letters*, 9, 615-629.
- Sinervo B, Mendez-de-la-Cruz F, Miles DB, Heulin B, Bastiaans E, Villagran -Santa Cruz M, Lara-Resendiz R, Martinez-Mendez R, Calderon-Espinosa ML, Meza-Lazaro RN, Gadsden H, Avila, M Morando, IJ De la Riva, PV Sepulveda, CFD Rocha, N Iburguengoytia, CA Puntriano LJ, Massot M, Lepetz V, Oksanen TA, Chapple DG, Bauer AM, Branch WR, Clobert J, Sites Jr JW (2010) Erosion of lizard diversity by climate change and altered thermal niches. *Science*, 328, 894-899.
- Smith HM (1946) A subspecies of the lizard *Xantusia riversiana*. *Journal of the Washington Academy of Sciences*, 36, 392-393.
- Stetz, JB, Kendall KC, Vojta CD, GeM Working Group (2011) Genetic monitoring for managers: a new online resource. *Journal of Fish and Wildlife Management*, 2, 216-219.
- Sumner J (2005) Decreased relatedness between male prickly forest skinks (*Gnypetoscincus queenslandiae*) in habitat fragments. *Conservation Genetics*, 6, 333-340.
- Sunnucks P (2011) Towards modelling persistence in woodland birds: the role of genetics. *Emu*, 111, 19-39.
- Syphard AD, Clarke KC, Franklin J (2007). Simulating fire frequency and urban growth in southern California coastal shrublands, USA. *Landscape Ecology*, 22, 431-445.

- Thomas CD, Cameron A, Green RE, Bakkenes M, Beaumont LJ, Collingham YC, Erasmus BFN, de Siqueira MF, Grainger A, Hannah L, Hughes L, Huntley B, van Jaarsveld AS, Midgley GF, Miles L, Ortega-Huerta MA, Peterson AT, Phillips OL, Williams SE (2004) Extinction risk from climate change. *Nature*, 427, 145-148.
- Thomsen, SK, Kroeger CE, Bloom PH, Harvey AL (2014) Space use and home-range size of barn owls on Santa Barbara Island. *Monographs of the Western North American Naturalist*, 7, 339-347.
- Tseng S-P, Wang C-J, Li S-H, L S-M (2015) Within-island speciation with an exceptional case of distinct separation between two sibling lizard species divided by a narrow stream. *Molecular Phylogenetics and Evolution*, 90, 164-175.
- United States Fish and Wildlife Service (USFWS) (2014) Island night lizard (*Xantusia riversiana*) final Post-Delisting Monitoring Plan. U.S. Fish and Wildlife Service, Carlsbad Fish and Wildlife Office, Carlsbad, California.
- Urban MC, Richardson JL, Freidenfelds NA (2014) Plasticity and genetic adaptation mediate amphibian and reptile responses to climate change. *Evolutionary Applications*, 7, 88-103.
- Van Oosterhout C, Hutchinson WF, Wills DP, Shipley P (2004) Micro-checker: software for identifying and correcting genotyping errors in microsatellite data. *Molecular Ecology Notes*, 4, 535-538.
- Van Strien MJ, Keller D, Holderegger R (2012) A new analytical approach to landscape genetic modelling: least-cost transect analysis and linear mixed models. *Molecular Ecology*, 21,4010-4023.
- Vandergast AG, Wood DA, Thompson AR, Fisher M, Barrows CW, Grant TJ (2016) Drifting to oblivion? Rapid genetic differentiation in an endangered lizard following habitat fragmentation and drought. *Diversity and Distributions*, 22, 344-357.
- Vivrette NJ, Muller CH (1977) Mechanism of invasion and dominance of coastal grassland by *Mesembryanthemum crystallinum*. *Ecological Monographs*, 47, 301-318.
- Wang J (2011) Coancestry: a program for simulating, estimating and analyzing relatedness and inbreeding coefficients. *Molecular Ecology Resources*, 11, 141-145.

Wang Y, Zhang J, Feeley KJ, Jiang P, Ding P (2009) Life-history traits associated with fragmentation vulnerability of lizards in the Thousand Island Lake, China. *Animal Conservation*, 12, 329-337.

Waples RS, Gaggiotti O (2006) What is a population? An empirical evaluation of some genetic methods for identifying the number of gene pools and their degree of connectivity. *Molecular Ecology*, 15, 1419-1439.

Weir BS, Cockerham CC (1984) Estimating F-statistics for the analysis of population structure. *Evolution*, 38, 1358-1370.

Wright S (1943) Isolation by distance. *Genetics*, 28, 114-138.

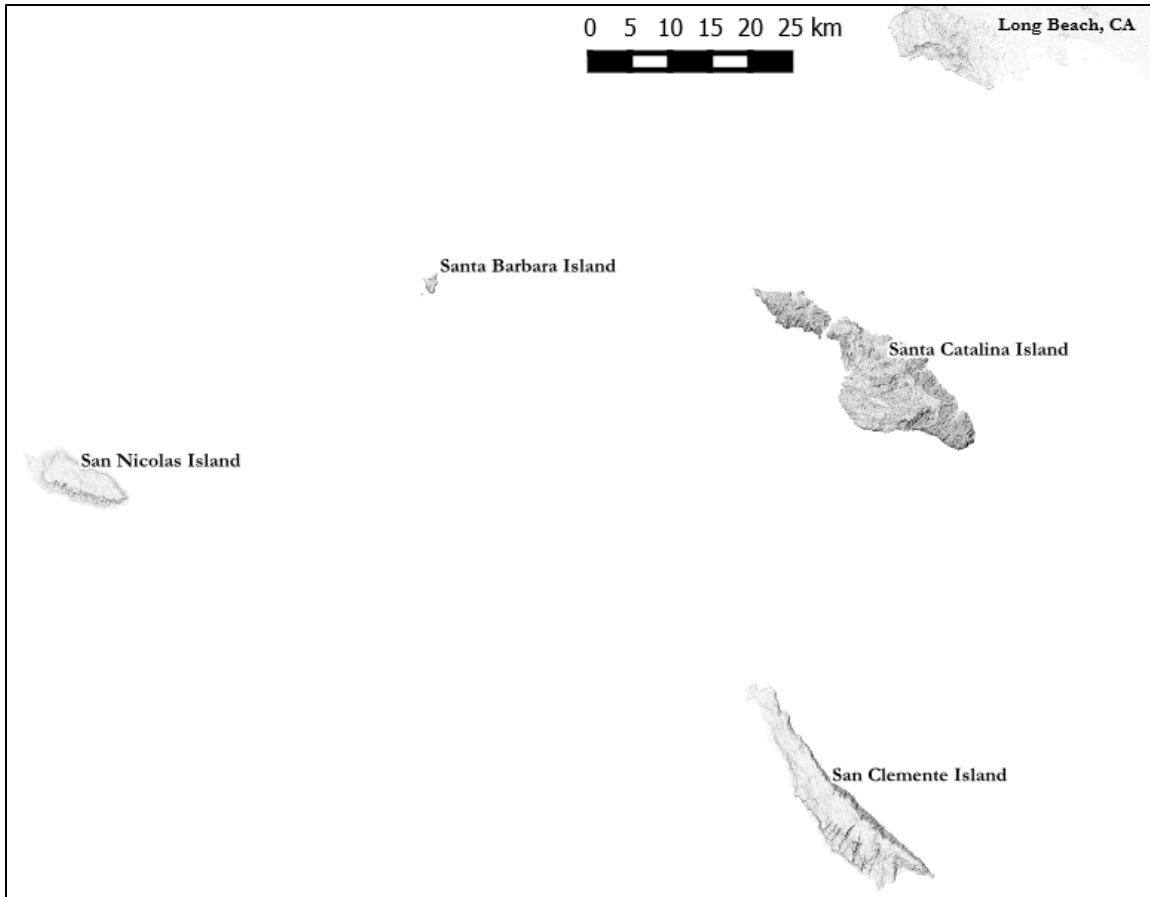


Figure 1.1. Location of Channel Islands inhabited by the island night lizard. The island night lizard is endemic to 3 Channel Island: San Clemente Island, Santa Barbara Island, and San Nicolas Island.

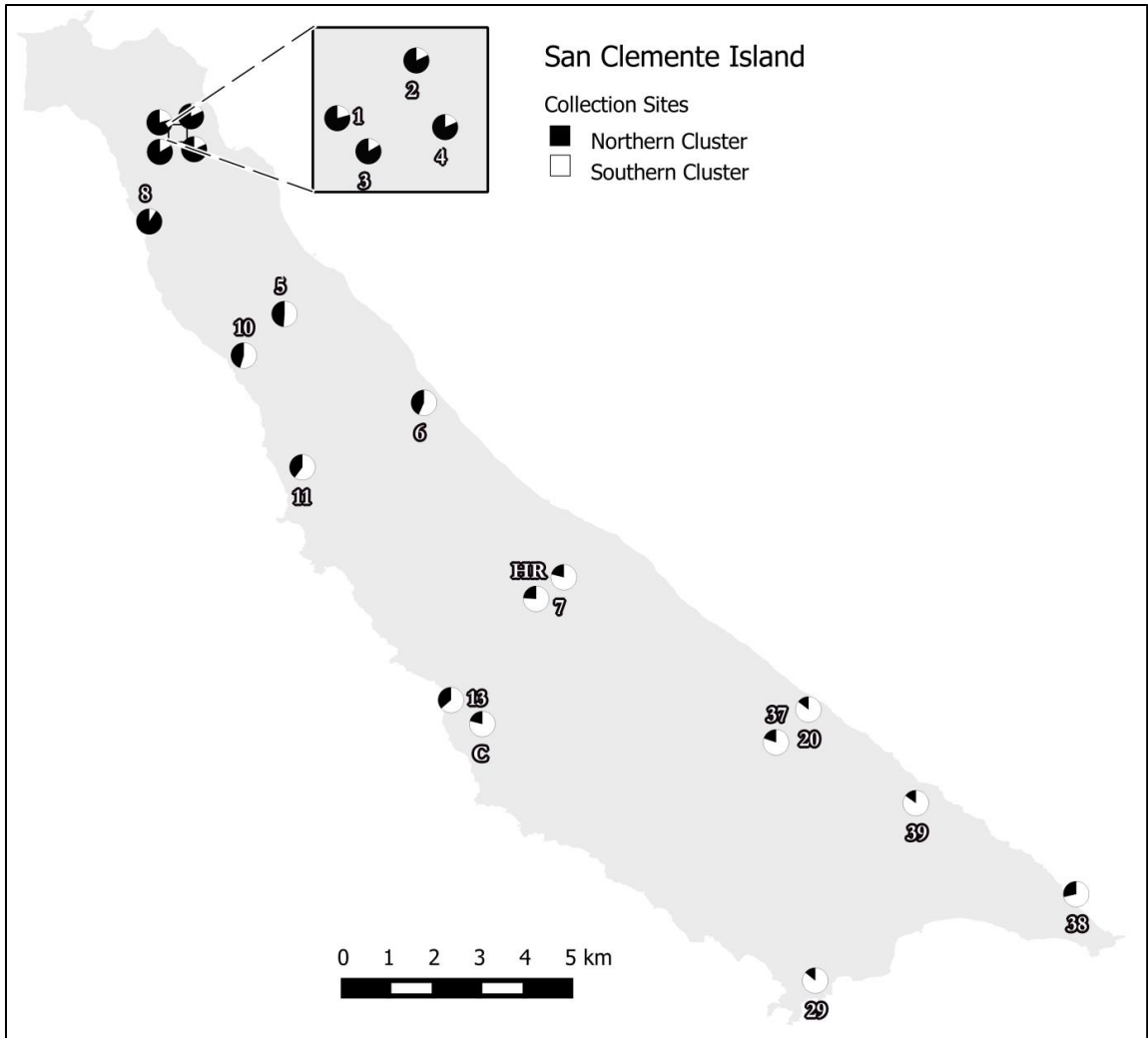


Figure 1.2. San Clemente Island collection sites with coancestry proportions. All collection sites on San Clemente Island are shown. Pie charts represent the site-level coancestry proportions for the STRUCTURE solution $K=2$ as calculated from the CLUMPP outputs. STRUCTURE barplot is shown in Appendix C.10.

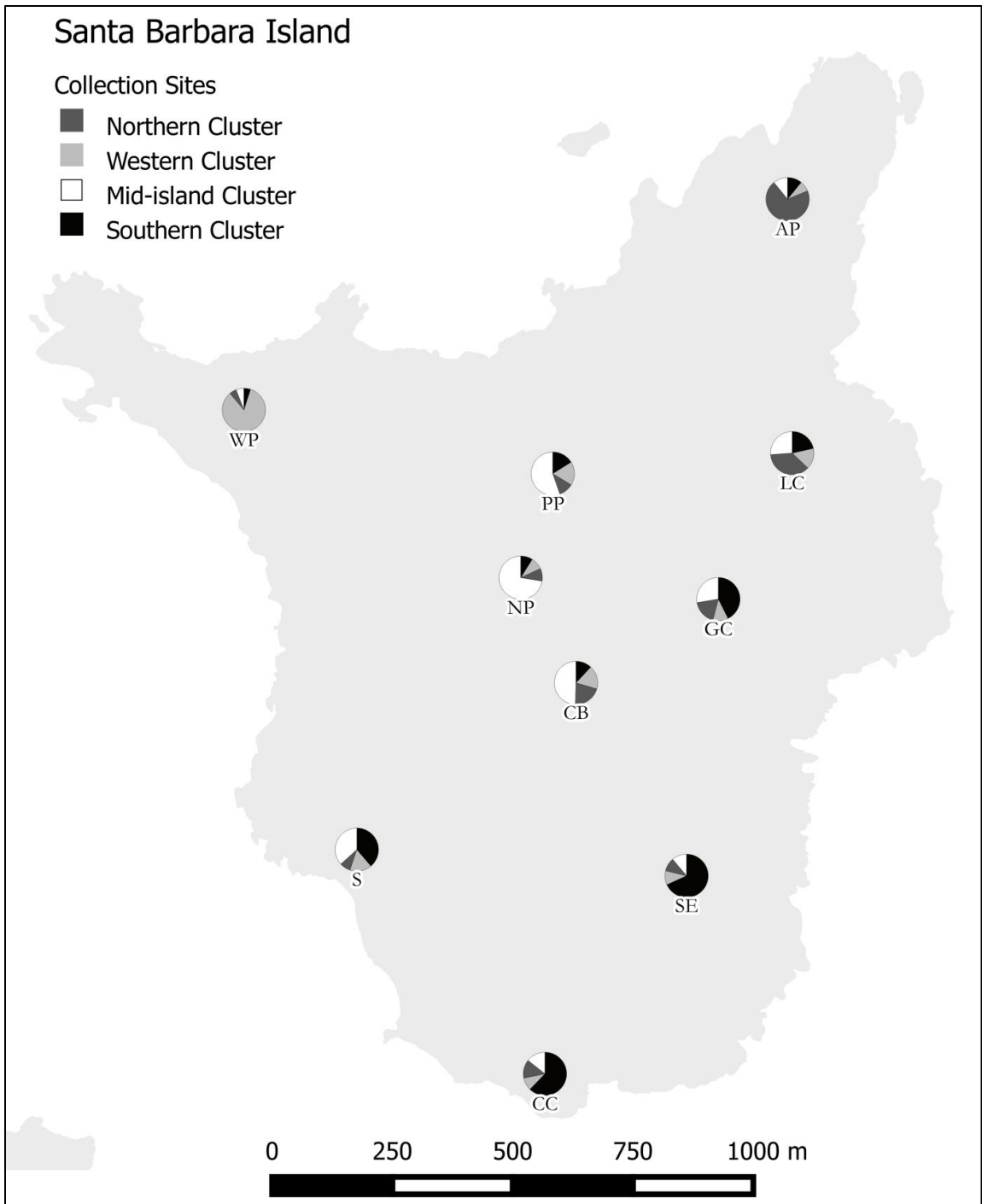


Figure 1.3. Santa Barbara Island collection sites with coancestry proportions. All collection sites on San Clemente Island are shown. Pie charts represent the site-level coancestry proportions for the STRUCTURE solution $K=4$ as calculated from the CLUMPP outputs. STRUCTURE barplot is shown in Appendix C.12.

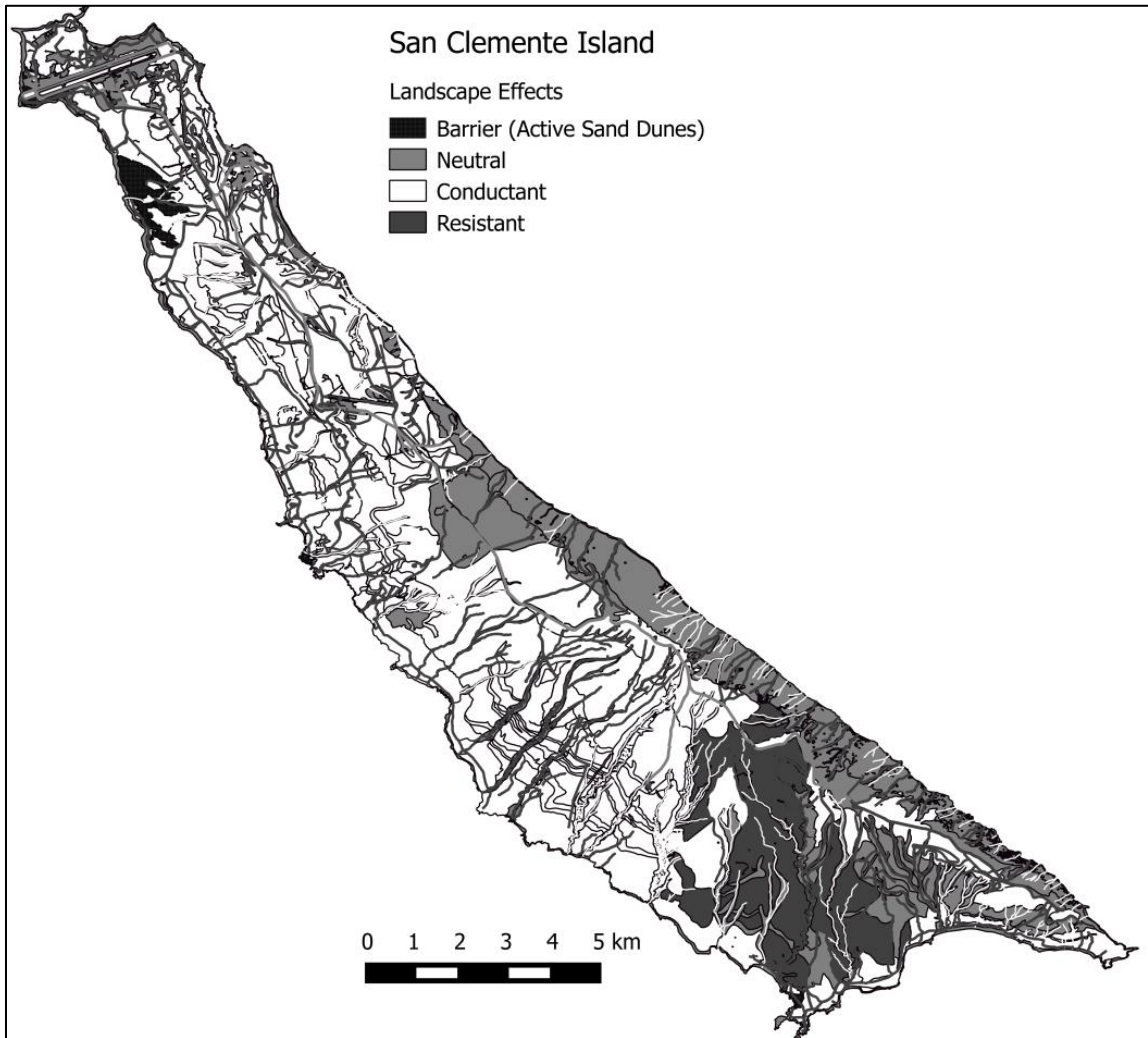


Figure 1.4. San Clemente Island landscape effects. The landscape-level features identified by analyses (see results) incorporated as a composite image. See Figure 1. 2 for location of collection sites. Active sand dunes were identified as a barrier (black). Landscape features which were neither conductant nor resistant were given values of 1 and considered neutral (gray). Conductant features (California boxthorn, prickly pear cactus, grasslands, and canyons < 500ft in length) are shown in white. Resistant habitat (cholla phase maritime desert scrub secondary roadways, canyons > 500ft in length) are shown in dark gray. See Appendix C for specific landscape features and models.

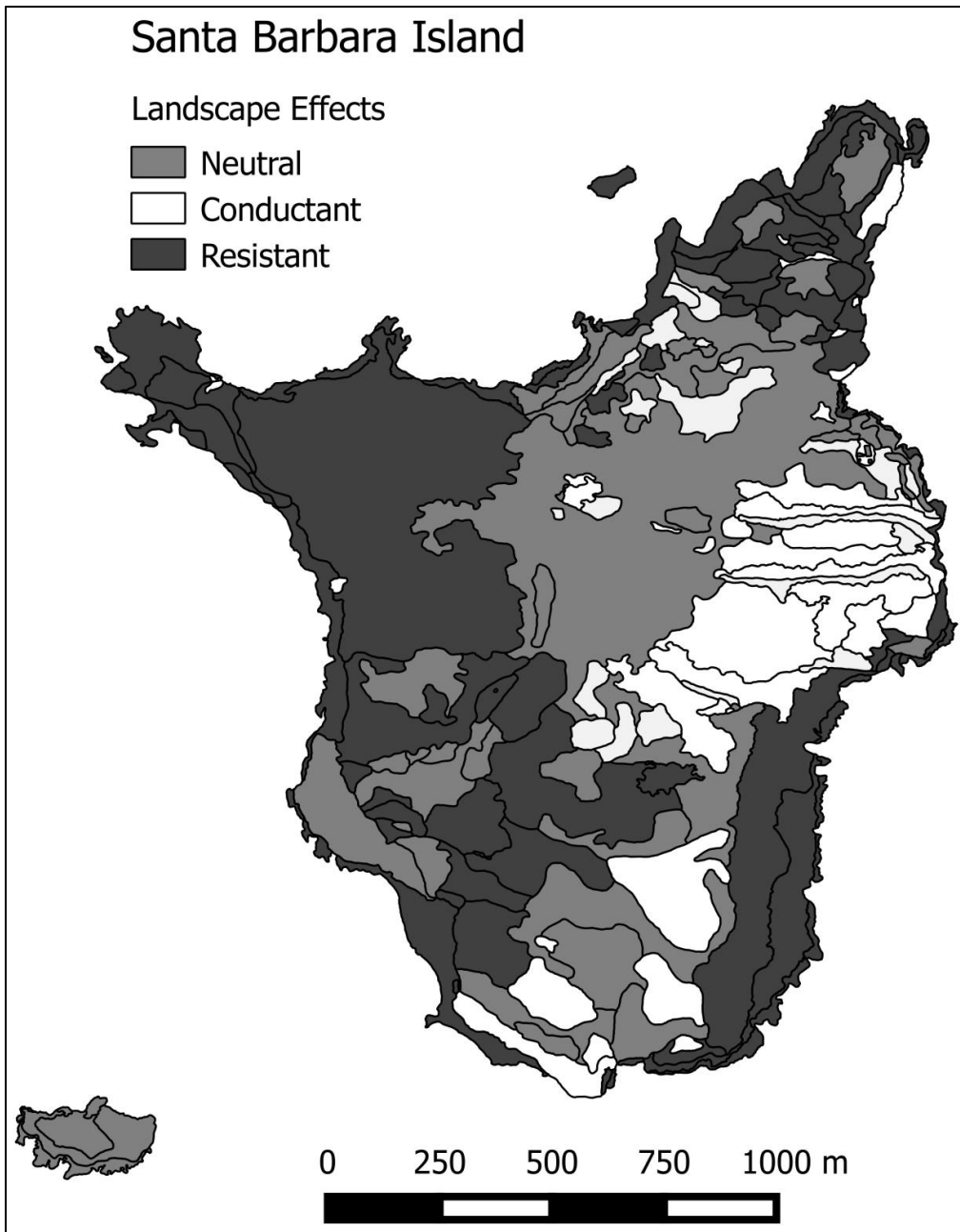


Figure 1.5. Santa Barbara Island landscape effects. The landscape-level features identified by analyses (see results) incorporated as a composite image. See Figure 1. 3 for location of collection sites. Landscape features which were neither conductant nor resistant were given values of 1 and considered neutral (gray). Conductant features (California boxthorn, prickly pear cactus, and giant coreopsis) are shown in white. Resistant habitat (woolly seablite with crystalline iceplant, barren ground, and common fiddleneck) are shown in dark gray. See Appendix C for specific landscape features and models.

Table 1.1. San Clemente Island competing conductance and resistance models. The best-supported conductance and resistance models for each layer are shown with the associated p-value (p) and coefficient of determination from non-parametric rank-based regressions (R^2) from the resulting MRDM analysis. The corrected AIC value (AICc) and R^2_{β} value are also presented (see text for methods).

	p	R^2	AICc	R^2_{β}
Null	0.0005	0.2602	-912.35	0.2825
Conductance Models				
Null + California boxthorn (100c) + Prickly pear cactus (100c)	0.0001	0.6554	-951.04	0.5630
Null + California boxthorn (100c) + Prickly pear cactus (100c) + Grassland (2c)	0.0001	0.6433	-952.10	0.6769
Null + California boxthorn (100c) + Prickly pear cactus (100c) + Canyons < 500 ft (2c)	0.0001	0.6602	-955.75	0.6116
Null + California boxthorn (100c) + Prickly pear cactus (100c) + Grassland (2c) + Canyons < 500 ft (2c)	0.0001	0.6461	-957.56	0.7257
Resistance Models				
Null + Cholla (50r) + Secondary Roads (50r) + Canyons 500-1000 ft (50r) + Canyons > 1000 ft (50r)	0.0002	0.5039	-974.47	0.8607
Null + Cholla (50r) + Secondary Roads (50r) + Canyons 500-1000 ft (50r) + Canyons > 1000 ft (100r)	0.0001	0.5125	-974.39	0.8606
Null + Cholla (50r) + Secondary Roads (50r) + Canyons 500-1000 ft (50r) + Canyons > 1000 ft (50r) + Canyons < 500 ft (2r)	0.0002	0.5137	-973.19	0.8445
Null + Cholla (50r) + Secondary Roads (50r) + Canyons 500-1000 ft (50r) + Canyons > 1000 ft (100r) + Canyons < 500 ft (2r)	0.0004	0.5175	-972.94	0.8427

Table 1.2. Santa Barbara Island competing conductance and resistance models. The best-supported conductance and resistance models for each layer are shown with the associated p-value (p) and coefficient of determination for non-parametric rank-based regressions (R^2) from the resulting MRDM analysis. The corrected AIC value (AICc) and R^2_{β} value are also presented (see text for methods).

	p	R^2	AICc	R^2_{β}
Null	0.0212	0.4804	-140.12	0.6911
Conductance Models				
Null + California Boxthorn(100c)+ Prickly pear cactus (50c) + Common fiddleneck (2c)	0.0013	0.8611	-151.98	0.8614
Null + California Boxthorn(100c)+ Prickly pear cactus (50c) + Needle goldfields (2c)	0.0003	0.8801	-151.98	0.8624
Null + California Boxthorn(100c)+ Prickly pear cactus (2c)	0.0002	0.8653	-152.12	0.8667
Null + California Boxthorn(50c)+ Prickly pear cactus (2c)	0.0012	0.8617	-152.36	0.8683
Null + California Boxthorn(100c)+ Prickly pear cactus (50c) + Giant Coreopsis (2c)	0.0005	0.8677	-153.13	0.8716
Null + California Boxthorn(100c)+ Prickly pear cactus (100c)+ Giant Coreopsis (2c)	0.0008	0.8877	-153.19	0.8718
Null + California Boxthorn(100c)+ Prickly pear cactus (50c) + Oatgrass (2c)	0.0006	0.8693	-153.23	0.8709
Null + California Boxthorn(100c)+ Prickly pear cactus (100c) + Oatgrass (2c)	0.0010	0.8693	-153.32	0.8713
Resistance Models				
Null + Seablite with iceplant (50r) + Barren ground (100r) + Common fiddleneck (50r)	0.0003	0.8582	-149.69	0.8076
Null + Seablite with iceplant (50r) + Barren ground (50r) + Common fiddleneck (50r)	0.0005	0.8582	-149.39	0.7490
Null + Seablite with iceplant (50r) + Barren ground (100r) + Common fiddleneck (50r) + Needle goldfields (100r)	0.0004	0.8582	-149.04	0.8371
Null + Seablite with iceplant (50r) + Barren ground (50r) + Common fiddleneck (50r) + Needle goldfields (100r)	0.0005	0.8582	-150.07	0.8704
Null + Seablite with iceplant (2r) + Barren ground (50r)	0.0027	0.6919	-150.22	0.8867

Chapter 2: Elucidating dispersal ecology of reclusive species through genetic analyses of parentage and relatedness: the island night lizard (*Xantusia riversiana*) as a case study.

Stephen E. Rice¹ and Rulon W. Clark¹

1. San Diego State University, Dept of Biology, 5500 Campanile Drive, San Diego, California, 92182

Abstract

Characterizing dispersal and movement patterns are vital to understanding the evolutionary ecology of species. For many reclusive species, such as reptiles, the observation of direct dispersal may be difficult or intractable. However, indirect genetic methods may be used to characterize dispersal distances and patterns. We used genetic and capture data from the island night lizard (*Xantusia riversiana*) to estimate natal dispersal distances through indirect genetic methods, characterize movement and space use patterns, and compare these distances to previous estimates made from more traditional ecological approaches. We found no evidence of sex-biased dispersal. Indirect estimates of natal dispersal were greater than the previous field-based estimates with average distances of 14 m on Santa Barbara Island (SBI) and 41 m on San Clemente Island (SCI). Wright's σ was estimated at 16 m on SBI and 19 m on SCI. Correlograms of Moran's I revealed large differences in the scale of spatial autocorrelation between islands (SBI=375 m, SCI=1,813 m) which was corroborated by variograms of inter-individual genetic difference (102 - 169 m on SBI and 955 - 1,424 m on SCI) . A permutation logistic regression revealed that related individuals >0.8 years old were more

likely to be captured together on both islands. Overall, our findings suggest that field-based estimates of individual displacement within this species may underestimate genetic dispersal. Furthermore, characterization of capture patterns and relatedness revealed kin-affiliative behavior in *X. riversiana*, which may be indicative of delayed dispersal and cryptic sociality. We suggest indirect inferences of natal dispersal should focus on parentage analyses and Wright's σ for parameter estimation of individual movement, whereas the ranges identified by spatial autocorrelation and variograms are likely to be relevant at the larger patch scales. These results highlight the power of relatedness-based analyses for characterizing aspects of the movement ecology of reclusive species that may be difficult to observe directly.

Introduction

The dispersal and movement of organisms is a fundamental process in population biology, yet may be difficult to characterize even in abundant species. Dispersal studies provide insight into the evolutionary ecology of focal species and inform conservation planning and management (e.g. Bowler and Benton 2005; Hawkes 2009; Dussex et al. 2016). Dispersal, defined here as the movement of individuals away from their natal sites, may be quantified directly through long-term capture-mark-recapture (CMR) studies and spatial monitoring or indirectly through genetic inference methods.

Both direct and indirect approaches to characterizing dispersal have limitations. Direct observations of dispersal are labor intensive and time consuming, resulting in reduced sample sizes that may underestimate typical dispersal rates and distances (e.g. Dussex et al. 2016) whereas genetic inference may be complicated through modeling

assumptions and challenges in study design and sample collection (Broquet and Petit 2009). While few studies use both direct and indirect inference methods, the proliferation of genetic methods has led to a variety of analytical approaches to detect dispersed individuals (Manel et al. 2005), categorize age and sex biases in dispersal patterns, and characterize dispersal distances (Goudet et al. 2002; Broquet and Petit 2009). The processes and potential confounds of these methods are important to understand, as incorporating unrealistic assumptions or parameters within spatial models of dispersal may yield inaccurate results and directly impact the efficacy of management actions (Bowler and Benton 2005; Hawkes 2009). However, for reclusive species the characterization of dispersal from field data may be especially problematic due to low probabilities of recapture (e.g. Pimm et al. 2015); thus indirect methods are a compelling tool for characterizing dispersal patterns and distances.

Genetic methods are an increasingly common tool for elucidating species dispersal ecology. Recently, Moore et al (2014) used parentage analyses with pairwise distances between dyad members to characterize condition-dependent dispersal patterns in American black bears. Dussex et al (2016) found that assignment methods were generally inconsistent with CMR and parentage analyses inferences. Furthermore, they found that parentage analyses were the most powerful approach at fine scales for elucidating dispersal ecology of the greater white-toothed shrew. In addition to understanding dispersal, managers often need to determine the spatial extent over which landscape influences a focal species (Jackson and Fahrig 2014). Jackson and Fahrig (2014) found that the scale at which landscape structure affects species varies with the

population outcome measured. The simulation study conducted by Jackson and Fahrig (2014) suggested that the landscape scale for population persistence should be a lower bound for conservation as the scale needed to support genetic diversity was much larger. Taken together, statistical methods that help characterize the dispersal of species and the scale at which landscape affects genetic structure can provide vital information in the context of conservation.

The island night lizard (*Xantusia riversiana*) was recently delisted from the Endangered Species Act and provides a unique opportunity to evaluate the utility of indirect methods to elucidate dispersal ecology. This species is well studied with few documented predators and exists in discrete insular populations with regional abundances of 3,200 individuals/ha in prime habitat (Fellers and Drost 1991). Even with long-term study, direct observations of individual movement suggest very small individual displacement distances of 3 to 6 m (Fellers and Drost 1991; Mautz 1993). The dearth of information on island night lizard dispersal ecology is a direct obstacle to modelling metapopulation dynamics and extinction risk due to climatic change.

We applied genetic inference methods to characterize dispersal ecology and infer natal dispersal distances in *X. riversiana* on two of the three California Channel Islands this species is known to occupy. We used genetic and capture data from our landscape genetics analysis (Chapter 1) to characterize dispersal ecology and space use. The goal of this study was to leverage existing data to assess different techniques for estimating dispersal from genetic data and compare these patterns to values derived from ecological studies.

Methods

Study System and Data

Island night lizards are endemic to three California Channel Islands, two of which were evaluated in Chapter 1: Santa Barbara Island (SBI) and San Clemente Island (SCI). In brief, we captured 917 island night lizards across both islands utilizing a clustered sampling approach. Individuals were genotyped at 23 microsatellite loci (Rice et al. 2016; Appendices A, B) and first-order relatives, defined as parent-offspring and full siblings, were identified using a consensus approach between three methods: COLONY (Jones and Wang 2010), CERVUS (Kalinowski et al 2007), and the DyadML estimator (Milligan 2003) as calculated in COANCESTRY (Wang 2011). The current study draws on the capture data, individual genetic profiles, relatedness, and relationship analyses from Chapter 1.

Statistical Approaches

We used 4 approaches to quantify dispersal distances in the island night lizard: pairwise distances between relationships, estimation of Wright's gene-dispersal distance (Wright 1946), correlograms of Moran's I (reviewed in Hardy and Vekemans 1999), and range estimates from variograms (reviewed in Wagner et al. 2005). We characterized sex-biases in dispersal using the approach of Goudet et al. (2002). We evaluated predictors of co-capture among individuals with a permutation based logistic regression on distance matrices (LRDM, Prunier et al. 2015). Statistical analyses were carried out in R (R Core Team 2016) using the packages ADEGENET (Jombart 2008), HIERFSTAT (Goudet and Jombart 2015), COIN (Hothorn et al. 2006), PHYLIN (Tarroso et al. 2015), and FMSB

(Nakazawa 2015). We estimated Wright's gene dispersal distance, σ , and Moran's I using the program SPAGEDI (Hardy and Vekemans 2002).

Indirect Estimate of Natal Dispersal: Distances Between First-Order Relatives

The pairwise distances between parents and offspring have been demonstrated to be a powerful tool in the characterization of dispersal ecology (e.g. Moore et al. 2014; Dussex et al. 2016). We utilized the data from Chapter 1 (Appendix B) to characterize distances between inferred relationship classes. First-order relatives consisted of individuals identified through the consensus method used in Chapter 1 wherein dyads were considered first-order relatives when the inferred relationship was parent-offspring, full sibling, or the relatedness coefficient, DyadML, was greater than 0.35. Relationship classes of parent-offspring, full sibling, and half sibling were inferred by COLONY. Unrelated samples were all relationships not detected by COLONY.

We used an approximate general independent test of distances between ordered relationship groups in the package COIN to test whether pairwise geographic distances differed between relationship groups within and between islands. To correct for the presence of neonates captured in close proximity to adults, we present analyses based on the full data sets and data sets consisting only of individuals greater than 40 mm snout-to-vent length (SVL) which equates to approximately 0.8 years old (Fellers and Drost 1991).

Indirect Estimate of Natal Dispersal: Gene Dispersal Distance, Wright's σ

Wright (1946) described an isolation by distance model in which the genetic neighborhood is a 2-dimensional area in which most mating events occur. This model can be used to estimate σ from a regression of the inter-individual genetic distance, Rousset's

a (Rousset 2000), on the logarithm of the inter-individual geographic distance (Rousset 2000; Hardy et al. 2006). We assumed drift-migration equilibrium and estimated σ , interpreted as mean natal dispersal distance, for each island across 3 distance classes and 5 density estimates (Table 2.1). Density estimates were based on the average effective population size per sample site as estimated by the linkage-disequilibrium method (Hill 1981) and confidence intervals from the program NEESTIMATOR (Do et al. 2014). Additional estimates of density were derived from the census population size over the entire area of each island and the prime-habitat area listed in the United States Fish and Wildlife Service post-delisting monitoring plan (USFWS 2014).

Scales of Spatial Genetic Autocorrelation: Individual Allele Frequencies

Moran's I is a common measure of spatial autocorrelation of individual allele frequencies (Hardy and Vekemans 1999). Moran's I was calculated for each pairwise distance bin, set at increments of 150 m for SBI and 500 m for SCI, and significance was tested with 1,000 permutations. The increments for distance bins were assigned based on the smallest distance at which all bins had observations. For each island, we produced a correlogram of Moran's I at each distance class. The distance at which the value of Moran's I became ≤ 0 was interpreted as the point at which individual allele frequencies were no longer spatially autocorrelated. We interpreted this point as the average maximum dispersal distance of island night lizards (e.g. Yaegashi et al. 2014).

Scales of Spatial Genetic Autocorrelation: Inter-individual Genetic Distances

Variograms assess the spatial autocorrelation of a variable by depicting the semivariance (defined as half the variance of all pairwise differences) against distance,

and may identify the spatial scale of dispersal processes (Le Corre et al 1998; Dutech et al. 2008). The empirical data was used to generate a variogram which was then fit with a theoretical variogram with parameters for nugget (semivariance associated with non-spatial effects), sill (the value at which semivariance stabilizes), and range (the scale of effect or threshold of spatial independence) (Wagner et al. 2005). There are few guidelines for determining the increment or maximum distances considered in empirical variograms; therefore, we followed the conventions of using the minimum lag distances which produced a minimum of 30 observations per bin and limited variograms to one-half the maximum pairwise distance compared (Rossi et al. 1992). Lag distances differed between Moran's I and variogram analyses, due to variogram constraint to a smaller maximum distance.

We used the package PHYLIN to produce empirical and theoretical variograms. For theoretical variograms, exponential models were fit to all data sets with the nugget set to the semivariance of the first distance bin and the remaining parameters estimated within the package. The variogram approach implemented in PHYLIN requires pairwise distance variables; therefore we evaluated DPS, an inter-individual genetic distance calculated as $1 - \text{proportion of shared alleles in ADEGENET}$, and a measure of (un)relatedness by subtracting DyadML values from 1, the theoretical maximum probability under identity by descent (Milligan 2003).

Characterizing Sex-Biased Dispersal

The methods of Goudet et al (2002) identify a permutation t-test approach to test for sex-biases in dispersal based on four metrics derived from genetic data for individuals

of each sex: mean and variance of the corrected assignment index (mAIC and vAIC, respectively), Fst, and Fis. However, these methods have been reported to perform well only in the presence of strong sex-biased dispersal (Goudet et al. 2002). Statistical tests to detect sex bias were conducted in the package HIERFSTAT with the metrics mAIC, vAIC, Fst, and Fis (Goudet et al. 2002). Significance for comparisons based on mAIC and vAIC were ran with 10,000 permutations whereas tests based on Fst and Fis were based on 1,000 permutations due to computational constraints.

Predictors of Co-capture

We used an extension of permutation based LRDM (Prunier et al. 2015) to assess whether the probability of capturing individuals together could be attributed to the predictors of pairwise sex, sexual maturity, relatedness, or relationship. We used a binary response variable with success defined as being captured together. Predictors were pairwise distance matrices with sex and sexual maturity coded as categorical comparisons.

Models were constructed from single variable up to full models; due to the highly collinear nature of DyadML and COLONY-inferred relationships (data not shown) these predictors were not included in the same models. Logistic regression models were constructed with the *glm* function and a binomial ‘logit’ link. Nagelkerke’s R^2 (Smith and McKenna 2013; Prunier et al. 2015) was calculated for each model using the *NagelkerkeR2* function in the package FMSB and served as the reference distribution statistic for determining significance by permuting the binary response matrix 10,000 times and recalculating Nagelkerke’s R^2 for each permutation. Semi-standardized beta

weights for the full models were calculated as in Prunier et al. (2015) with the odd's ratios calculated as the exponentiated semi-standardized beta weights following King (2007).

Results

Mean pairwise distances (Table 2.2) between all relationship groups were significantly different within both islands ($p < 2.2 \times 10^{-16}$). Post-hoc comparison of mean pairwise distances between relationship groups revealed that full sibling dyad and parent-offspring dyad distances were not significantly different for either island (SBI $p=0.1017$, SCI $p=0.7566$); all other comparisons were significant at the $p<0.005$ level. After controlling for young of year (SVL < 40 mm) mean pairwise distances were significantly different between islands for first-order relationship ($p=0.0062$) and parent-offspring dyads ($p=0.0228$). When controlling for young of year, mean parent-offspring distance for SBI was 14 m and 41 m on SCI.

The gene dispersal estimate, σ , ranged between 7 m and 31 m for SBI and 7 m to 23 m for SCI. Estimates of σ were robust to the inclusion of young of year and consistent across different distance classes when density was constant; however, estimates were sensitive to density estimates (Table 2.1). Constraining density estimates to average effective density (N_e/km^2) across sample locations resulted in estimates of 16 m for SBI and 19 m for SCI for full data sets and 16 m for SBI and 18 m for SCI when young of year were removed.

Moran's I revealed that spatial autocorrelation on SBI was significantly positive ($p\leq 0.005$) at distances less than 375 m, after which Moran's I became negative (Figure

2.1). On SCI, spatial autocorrelation was significantly positive ($p \leq 0.001$) up to distances of 1,395 m and had standard errors overlapping 0 at a distance of 1,813 m (Figure 2.2). Variograms based on relatedness had higher support, as indicated by R^2 , than those based on DPS for both islands (Figures 2.3, 2.4). On SBI, the range for the 1-DyadML variogram was 102 m whereas SCI had a range estimate of 955 m. The genetic distance measure, DPS, resulted in greater range estimates on both islands (SBI=169 m, SCI =1,424 m).

Our characterization of dispersal ecology revealed no statistical support for sex-biased dispersal on either island. Exploratory LRDM analyses revealed that relatedness and relationship were the only significant predictors of co-capture when controlling for young of year on each island (Table 2.3). Pairs of individuals were 1.066 times more likely to be captured at the same point with a one standard deviation change in DyadML relatedness on SBI and 1.031 times more likely on SCI. To examine the predictive ability of these patterns we utilized a traditional logistic regression with SBI as the training data set and SCI as the test data set. Both DyadML relatedness values and COLONY-inferred relationships had high accuracy (0.9996) and low misclassification (0.0004) rates when predicting capture success.

Discussion

We found inferred parent-offspring distances were between 2 and 13 times greater than the individual displacement distances from long-term CMR studies (Fellers and Drost 1991; Mautz 1993). We provided the first quantitative estimates of dispersal distances in the species (14 m on SBI and 41 m on SCI) and found spatial autocorrelation

of allele frequencies, genetic distance, and relatedness at previously unrecorded scales. The LRDM approach of Prunier et al. (2015) resulted in relatedness and relationships being the strongest predictors of island night lizard co-captures, suggesting a cryptic social structure with kin-affiliative behavior.

Indirect Estimates of Natal Dispersal: Distances Between First-Order Relatives

Fellers and Drost (1991) found 12 juveniles on SBI 30 m to 40 m from prime habitat over a 6 year study and surmised these represented juvenile dispersal events, whereas individual recapture data suggested average displacements of 5.6 m. While there is no value for juvenile dispersal distances on SCI, Mautz (1993) found that individuals relocated only an average of 3 m from previous capture sites. Our findings provide the first quantitative estimates of juvenile dispersal distances. Although the distance between parent-offspring pairs is approximately 3 times shorter than the estimates of Fellers and Drost (1991), our estimates are approximately 2.5 times greater than the observed movement distances on SBI and 13 times greater than those on SCI.

Moore et al. (2014) and Dussex et al. (2016) both found parentage analyses more accurate in describing dispersal ecology than alternate genetic methods. Our results support the utility of parentage and kinship analyses in characterizing natal movement, especially when focused on parent-offspring pairs. Estimation of first-order relationships as described in Chapter 1 and their pairwise differences may be informative in the characterization of dispersal when few parent-offspring comparisons are available. The mean distances inferred for first-order relationships differed between islands, potentially due to differences in island scale and population densities. It is notable that the maximum

distance between first-order relatives is very close (SBI=158.63 m, SCI=156.75 m) between both islands, although these maximums belong to different relationship groups (full sibling and parent-offspring respectively) for each island.

Indirect Estimates of Natal Dispersal: Gene Dispersal Distance, Wright's σ

Estimates of gene dispersal were remarkably close between each island and were within 2 m of parent-offspring distances for the full data sets on each island. The discrepancy between parent-offspring distance and σ for SCI upon removal of neonates may be attributable to changes in sample size and analytical method. Future research should consider simulation-based approaches to evaluate the accuracy of these metrics compared to the known simulation parameters. However, when estimating parameters for natural populations characterized by an isolation by distance pattern, parentage analyses and σ appear to yield consistent results.

Scales of Spatial Genetic Autocorrelation: Individual Allele Frequencies

Correlograms of Moran's I have been used to understand the scale of autocorrelation within allele frequencies and interpreted to provide an estimate of dispersal distance (e.g. Epperson and Li 1997; Yaegashi et al. 2014). The interpretation of the correlogram's x-intercept as average maximum dispersal distance is uncommon in the literature. This method returned notable differences between islands as Moran's I crossed the x-axis at 375 m for SBI and 1,813 m for SCI. These scales are much larger than the displacement estimates from long-term field studies and our dispersal estimates from parentage analyses and σ . Thus, we recommend that studies focused on estimating

dispersal distances should favor parentage analyses or gene dispersal distances over spatial autocorrelation analyses.

Scales of Spatial Genetic Autocorrelation: Inter-individual Genetic Distances

Dispersal distances estimated from variogram ranges were also incongruent with parentage analyses but provided smaller estimates of the scale of spatial autocorrelation than Moran's I. The use of variograms to estimate dispersal has not been formally studied and has been only suggested in the literature (Dutech et al. 2008). The range estimates could denote the scale of spatial genetic structure (Wagner et al. 2005), connectivity among localized groups (Le Corre et al. 1998), or the "patch size" of the process evaluated (Legendre and Fortin 1989). Because we generated distance measures from the proportion of shared alleles and relatedness our estimates may denote the "patch size" of relatedness, or may indicate familial territories. More meaningful biological interpretation of these results will require long-term telemetry paired with parentage analyses to provide data on individual movement and more thorough interpretation of spatial genetic patterns. However, simulation-based approaches may offer a more tractable solution to determine whether range estimates produced from spatial autocorrelation and variogram analyses are congruent with known or simulated dispersal patterns.

Predictors of Co-capture

Pairwise relatedness and relationships were the best predictors of capturing individuals together on both islands. Due to the late spring and summer sampling on SBI the removal of young of year individuals had little effect on the pseudo- R^2 or odds ratio.

Extensive sampling on SCI during the autumn resulted in numerous captures of neonates and associated adults. Inclusion of these samples biased LRDM results and impacted both the pseudo- R^2 and odds ratio for relatedness; however relatedness and relationship remained significant predictors even after removal of young of year. The continued association of relatives after the ca. 0.8 year mark suggests a level of previously undocumented sociality within the system, which may explain the strong signals of isolation by distance reported in Chapter 1.

Cryptic sociality and kin affiliation has been noted for the sister species *X. vagilis* on the mainland, in which fostering was demonstrated to effect philopatry and kin-affiliative behaviors through delayed dispersal (Davis et al. 2010; Davis 2011). The studies of Davis et al. (2010) highlight several similarities between the two species, including dense populations, low dispersal, and small home range sizes. Our findings suggest that island night lizards may also form kin groups through delayed juvenile dispersal and prolonged parent-offspring interactions. Some reclusive reptiles that are social also exhibit parental care, such as attendance of neonates in egg-guarding lizards (e.g. Huang 2006; Mateo and Cuadrado 2012) or maternal attendance of pre-ecdysis neonates in pit-vipers (e.g. Greene et al. 2002; Hoss et al. 2015). Given the frequent and prolonged association between adults and neonates, it is possible *X. riversiana* also exhibits parental care. Although predators on both islands are limited, attending parents could protect neonates from intra-specific aggression. Unsurprisingly, samples collected in autumn most frequently included neonates and associated adults as parturition occurs seasonally (Fellers and Drost 1991; Mautz 1993). However, the association of related

island night lizards beyond this parturition period warrants further investigation into the extent of their social structure and affiliative behaviors.

Conservation Implications

Our characterization of dispersal ecology of the island night lizard suggests scale dependent effects and supports the independent management of each island. On SBI, we found parent-offspring distances of approximately 14 m and spatial autocorrelation up to 375 m whereas dispersal distances on SCI were 41 m with spatial autocorrelation up to 1,813 m. These distance estimates will be useful for the management and monitoring (USFWS 2014) of populations on both islands. We suggest that management actions focus on maintaining population sizes and metapopulation connectivity, and that the spatial scales derived from our analyses be used to guide those actions. On SBI, a scale of 100 m to 375 m should be used as a focus for remediation efforts, such as direct-line connectivity between habitat patches. On SCI, management should focus at the scales of 1-2 km in efforts to connect remote patches through corridors of prime habitat, as opposed to replanting isolated or remote patches. Furthermore, these findings can inform the design and mitigation of increased infrastructure by identifying patches that would become disconnected at these scales under increased development.

Conclusions

Dispersal is a key factor in the life history of a species, and a key parameter affecting conservation and management decisions (Bowler and Benton 2005; Hawkes 2009). Although dispersal can be directly observed, it is often labor and time intensive. Indirect inference of dispersal based on genetic evidence is gaining in application but

lacks a framework for consistent and reliable inference. Studies utilizing both CMR and genetic inference methods have found that CMR methods generally underestimate dispersal distances, while assignment methods on genetic data can often overestimate dispersal and conflict with direct observations (e.g. Dussex et al. 2016). The application of genetic inference methods to estimate dispersal is likely to be a valuable tool for conservation management in understanding the scale of dispersal processes and the potential effects of management actions on connectivity. However, we have demonstrated that different inference methods may yield very different results which may lead to incorrect inferences and misspecification of parameters, rendering management actions ineffectual (Bowler and Benton 2005; Jackson and Fahrig 2014). Recent studies found parentage analyses to be the most accurate method for characterizing dispersal ecology, and our analyses of the island night lizard support this usage. Our findings suggest that natal dispersal parameters should not be derived from spatial autocorrelation or variogram analyses as the parameters inferred are highly variable and likely overestimate dispersal in the context of individual movement. However, these approaches may yield insight into the scale of fine-scale patterns relevant to conservation and suggest a minimum scale below which individuals are likely to be related and thus management actions may be confounded (e.g. Jackson and Fahrig 2014).

Literature Cited

- Bowler DE, Benton TG (2005) Causes and consequences of animal dispersal strategies: relating individual behavior to spatial dynamics. *Biological Reviews of the Cambridge Philosophical Society*, 80, 205-225.
- Broquet T, Petit EJ (2009) Molecular estimation of dispersal for ecology and population genetics. *Annual Review of Ecology, Evolution, and Systematics*, 40, 193-216.
- Davis AR (2010) Kin presence drives philopatry and social aggregation in juvenile Desert Night Lizards (*Xantusia vigilis*). *Behavioral Ecology*, 23(1), 18-24.
doi: 10.1093/beheco/arr144
- Davis AR, Corl A, Surget-Groba Y, Sinervo B (2011) Convergent evolution of kin-based sociality in a lizard. *Proceedings of the Royal Society B*, 278, 1507-1514.
doi:10.1098/rspb.2010.1703
- Do C, Waples RS, Peel D, Macbeth GM, Tillett BJ, Ovenden JR (2014) NeEstimator V2: re-implementation of software for the estimation of contemporary effective population size (N_e) from genetic data. *Molecular Ecology Resources*, 14, 209-214.
- Dussex N, Broquet T, Yearsley JM (2016) Contrasting dispersal inference methods for the greater white-toothed shrew. *The Journal of Wildlife Management*, 80, 812-823.
- Dutech C, Rossi JP, Fabreguettes O, Robin C (2008) Geostatistical genetic analysis for inferring the dispersal pattern of a partially clonal species: example of the chestnut blight fungus. *Molecular Ecology*, 17, 4597-4607.
- Epperson B, Li T (1997) Gene Dispersal and Spatial Genetic Structure. *Evolution*, 51(3), 672-681.
- Fellers GM, Drost CA (1991) Ecology of the island night lizard, *Xantusia riversiana*, on SBI, California. *Herpetological Monographs*, 5, 28-78.
- Goudet J, Perrin N, Waser P (2002) Tests for sex-biased dispersal using bi-parentally inherited genetic markers. *Molecular Ecology*, 11, 1103-1114.
- Goudet J, Jombart T (2015) R package 'hierfstat': estimation and tests of hierarchical F-statistics version 0.04-22
- Greene HW, May PGDL, Hardy S, Scituro JM, Farrell TM (2002) Parental behaviors by pit vipers. G.W. Schuett, M. Hoggren, M.E. Douglas, H.W. Greene (Eds.),

Biology of the Vipers, Eagle Mountain Publications, Eagle Mountain, Utah (2002), pp. 179–225.

Hardy OJ, Vekemans X (1999) Isolation by distance in a continuous population: reconciliation between spatial autocorrelation analysis and population genetics models. *Heredity*, 83, 145-154.

Hardy OJ, Vekemans X (2002) SPAGeDi: a versatile computer program to analyse spatial genetic structure at the individual or population levels. *Molecular Ecology Notes*, 2, 618-620.

Hardy OJ, Maggia L, Bandou E, Breyne P, Caron H, Chevallier MH, Doligez A, Dutech C, Kremer A, Latouche-Halle C, Troispoux V, Veron V, Degen B (2006) Fine-scale genetic structure and gene dispersal inferences in ten neotropical tree species. *Molecular Ecology*, 15, 559-571.

Hawkes C (2009) Linking movement behavior, dispersal, and population processes: is individual variation a key? *Journal of Animal Ecology*, 78, 894-906.

Hill WG (1981) Estimation of effective population size from data on linkage disequilibrium. *Genetical Research*, 38, 209-216.

Hothorn T, Hornik K, van de Wiel MA, Zeileis A (2006) A lego system for conditional inference. *The American Statistician*, 60, 257-263.

Hoss SK, Deutschman DH, Booth W, Clark RW (2015) Post-birth separation affects the affiliative behavior of kin in a pitviper with maternal attendance. *Biological Journal of the Linnean Society*, 116, 637-648.

Huang W (2006) parental care in the long-tailed skink, *Mabuya longicaudata*, on a tropical Asian island. *Animal Behaviour*, 72, 791-795.

Jackson ND, Fahrig L (2014) Landscape context affects genetic diversity at a much larger spatial extent than population abundance. *Ecology*, 95, 871-881.

Jombart T (2008) Adegnet: a R package for the multivariate analysis of genetic markers. *Bioinformatics*, 24, 1403-1405.

Jones OR, Wang J (2010) Colony: a program for parentage and sibship inference from multilocus genotype data. *Molecular Ecology Resources*, 10, 551-555.

Kalinowski ST, Taper ML, Marshall TC (2007) Revising how the computer program CERVUS accommodates genotyping error increases success in paternity assignment. *Molecular Ecology*, 16, 1099-1106.

- King JE (2007) Standardized Coefficients in Logistic Regression. Annual meeting of the Southwest Educational Research Association, San Antonio, Texas.
- Le Corre V, Roussel G, Zanetto A, Kremer A (1998). Geographical structure of gene diversity in *Quercus petraea* (Matt.) Liebl. III. Patterns of variation identified by geostatistical analyses. *Heredity*, 80, 464–473.
- Legendre P, Fortin MJ (1989) Spatial pattern and ecological analysis. *Vegetatio*, 80, 107-138.
- Manel S, Gaggiotti OE, Waples RS (2005) Assignment methods: matching biological questions with appropriate techniques. *Trends in Ecology and Evolution*, 20, 136-142.
- Mateo JA, Cuadrado M (2012) Communal nesting and parental care in Oudri's fan-footed gecko (*Ptyodactylus oudrii*): field and experimental evidence of an adaptive behavior. *Journal of Herpetology*, 46, 209-212.
- Mautz WJ (1993) Ecology and energetics of the island night lizard, *Xantusia riversiana*, on San Clemente Island, California. In: Third California Islands symposium: Recent advances in research on the California Islands (ed Hochberg FG), pp. 417-428. Santa Barbara Museum of Natural History, Santa Barbara, CA.
- Milligan BG (2003) Maximum-likelihood estimation of relatedness. *Genetics*, 163, 1153-1167.
- Moore JA, Draheim HM, Etter D, Winterstein S, Scribner KT (2014) Application of large-scale parentage analysis for investigating natal dispersal in highly vagile vertebrates: a case study of American black bears (*Ursus americanus*). *PLoS ONE* 9:e91168.
- Nakazawa M (2015) R package 'fmsb': functions for medical statistics book with some demographic data version 0.5.2.
- Pimm SL, Alibhai S, Bergl R, Dehgan A, Giri C, Jewell Z, Joppa L, Kays R, Loarie S (2015) Emerging technologies to conserve biodiversity. *Trends in Ecology and Evolution*, 30, 685-696.
- Prunier JG, Colyn M, Legendre X, Nimon KF, Flamand MC (2015) Multicollinearity in spatial genetics: separating the wheat from the chaff using commonality analyses. *Molecular Ecology*, 24, 263-283.

- R Core Team (2016) R: A language and environment for statistical computing. R Foundation for Statistical Computing, Vienna, Austria. Available online: <https://www.R-project.org/>.
- Rice SE, Beasley RR, Lance SL, Jones KL, Clark RW (2016) Development of 24 polymorphic microsatellite markers for the Island Night Lizard (*Xantusia riversiana*) in Microsatellite records for volume 8, issue 2. Conservation Genetic Resources, 8,169-196 doi: 10.1007/s12686-016-0549-4.
- Rossi RE, Mulla DJ, Journel AG, Franz EH (1992) Geostatistical tools for modeling and interpreting ecological spatial dependence. Ecological Monographs, 62, 277-314.
- Rousset F (2000) Genetic differentiation between individuals. Journal of Evolutionary Biology, 13, 58-62.
- Smith TJ, McKenna CM (2013) A comparison of logistic regression pseudo R² indices. Multiple Linear Regression Viewpoints, 39, 17–26.
- Tarroso P, Velo-Anton G, Carvalho SB (2015) phylin: an r package for phylogeographic interpolation. Molecular Ecology Resources, 15, 349-357.
- United States Fish and Wildlife Service (2014) Island night lizard (*Xantusia riversiana*) final Post-Delisting Monitoring Plan. U.S. Fish and Wildlife Service, Carlsbad Fish and Wildlife Office, Carlsbad, California.
- Wagner HH, Holderegger R, Werth S, Gugerli F, Hoebee SE, Scheidegger C (2005) Variogram analysis of the spatial genetic structure of continuous populations using multilocus microsatellite data. Genetics, 169:1739-1752.
- Wang J (2011) Coancestry: a program for simulating, estimating and analyzing relatedness and inbreeding coefficients. Molecular Ecology Resources, 11,141-145.
- Wright S (1946) Isolation by distance under diverse systems of mating. Genetics, 31, 39-59.
- Yaegashi S, Watanabe K, Monaghan MT, Omura T (2014) Fine-scale dispersal in a stream caddisfly inferred from spatial autocorrelation of microsatellite markers. Freshwater Science, 33, 172-180.

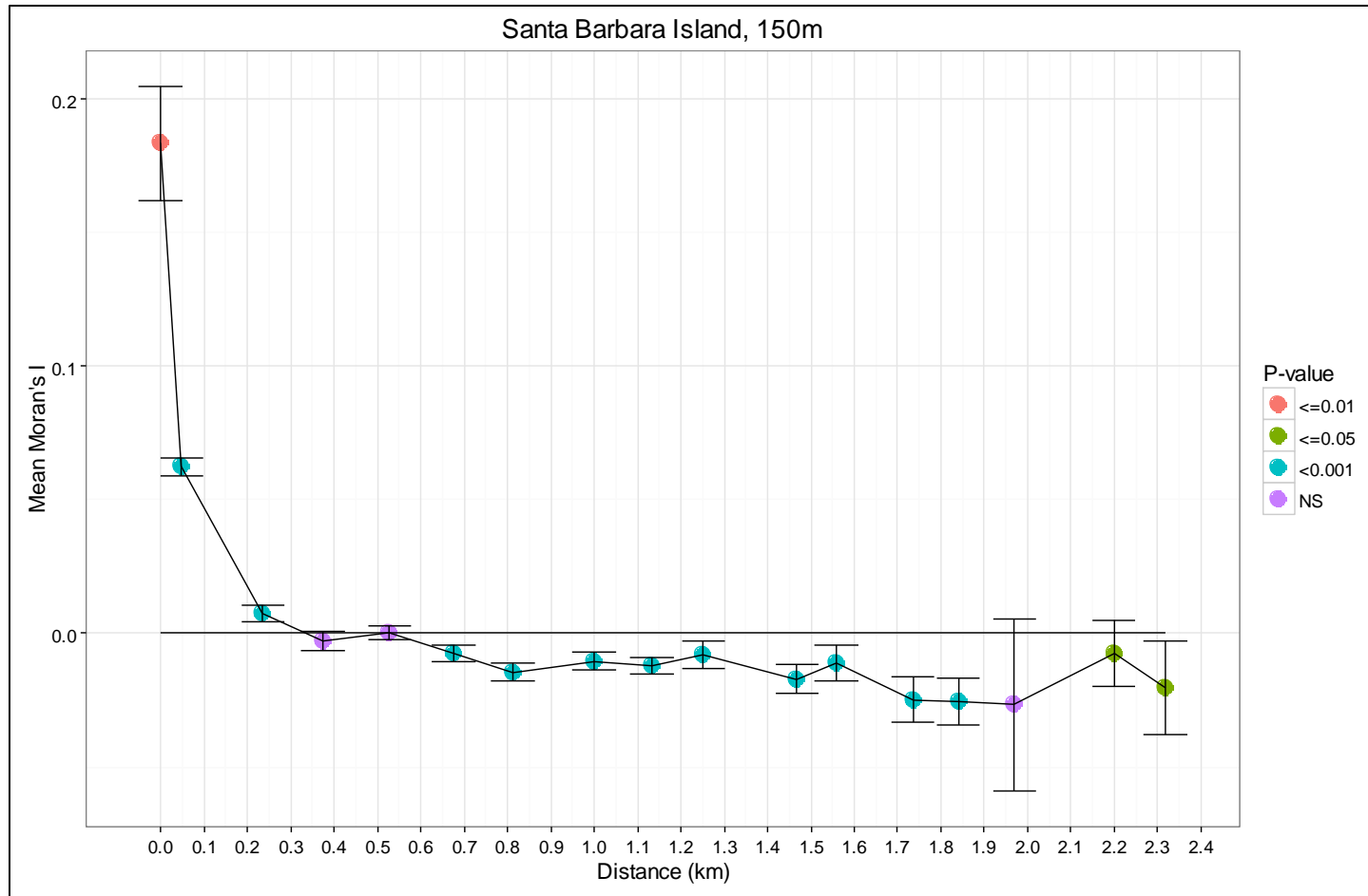


Figure 2.1. Correlogram of Moran's I on Santa Barbara Island. Moran's I was calculated for each distance bin and significance assessed through permutation. Points represent the value of Moran's I for the mean distance within each 150 m distance interval. Bars indicate standard error around the mean while each point color indicates significance of correlation within each point

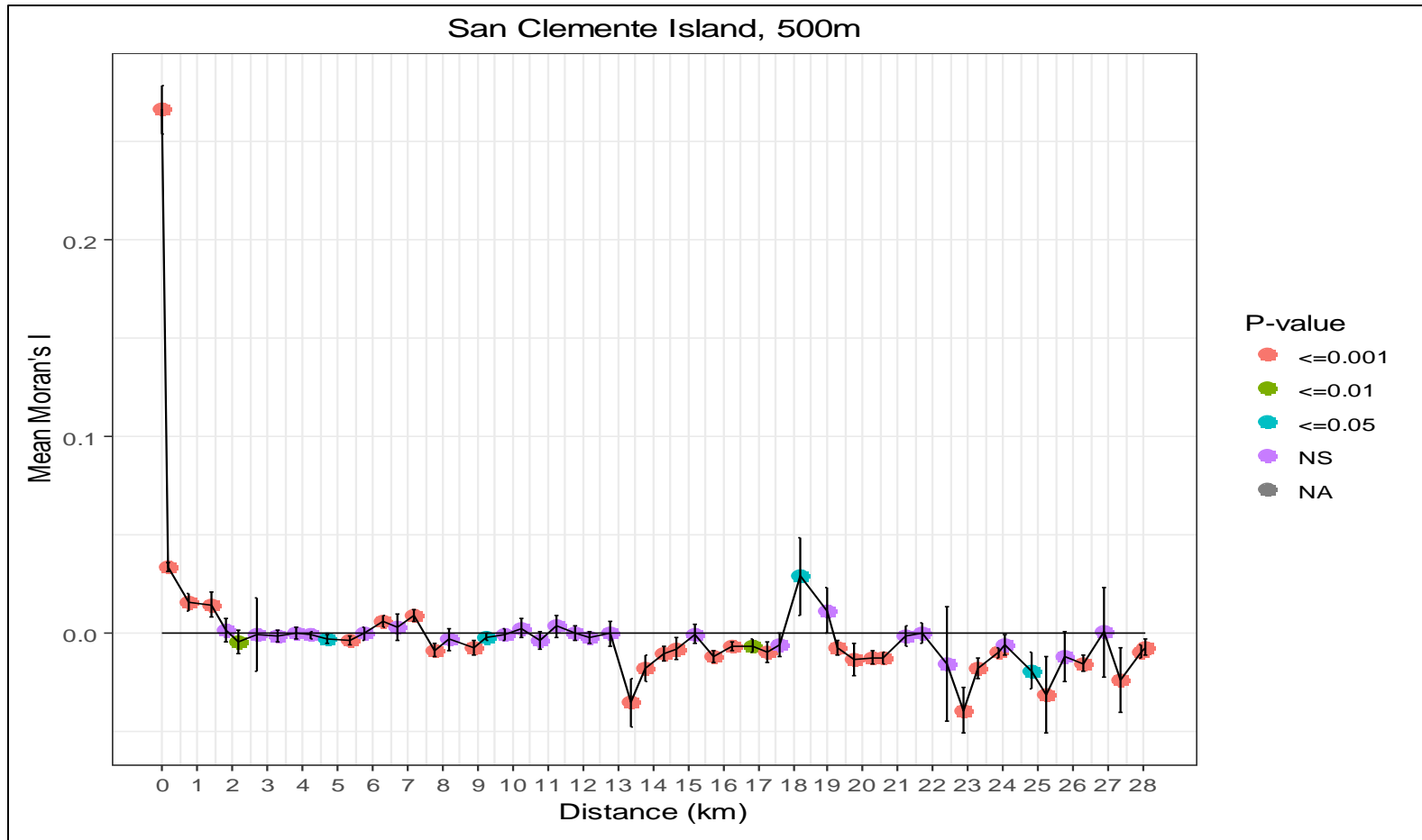


Figure 2.2. Correlogram of Moran's I on San Clemente Island. Moran's I was calculated for each distance bin and significance assess through permutation. Points represent the value of Moran's I for the mean distance within each 500 m distance interval. Bars indicate standard error around the mean while each point color indicates significance of correlation within each point.

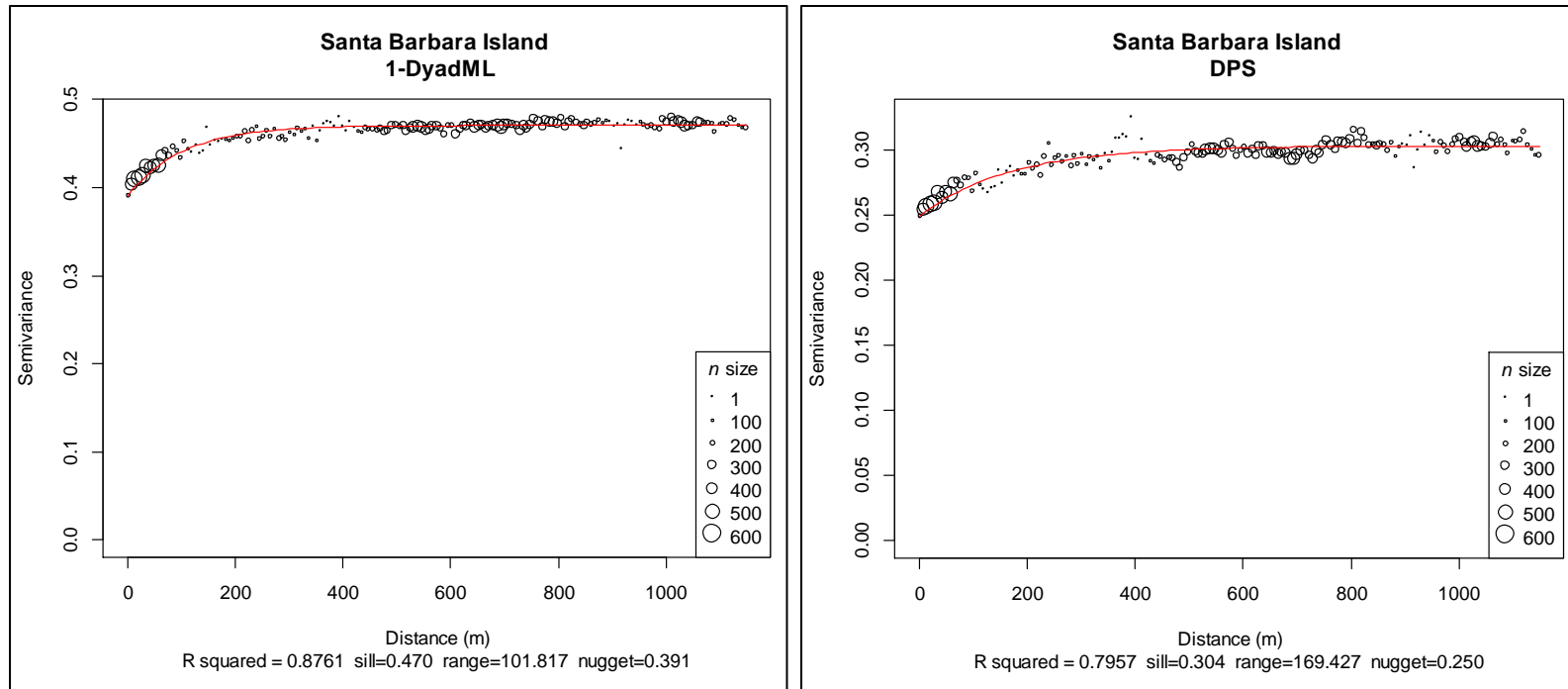


Figure 2.3. Variogram analyses for Santa Barbara Island. Empirical variograms (circles) were generated from two distance measures: left) 1-DyadML relatedness estimates, right) Inter-individual genetic distance DPS. Circle size denotes the number of pairwise comparisons within each distance class. Maximum distance evaluated was 1,100 m with a lag distance of 7 m for both variables. Theoretical variograms (red line) were fit as fixed-nugget models. Model R^2 values were used as a measure of model support and the point of spatial independence is denoted by the range.

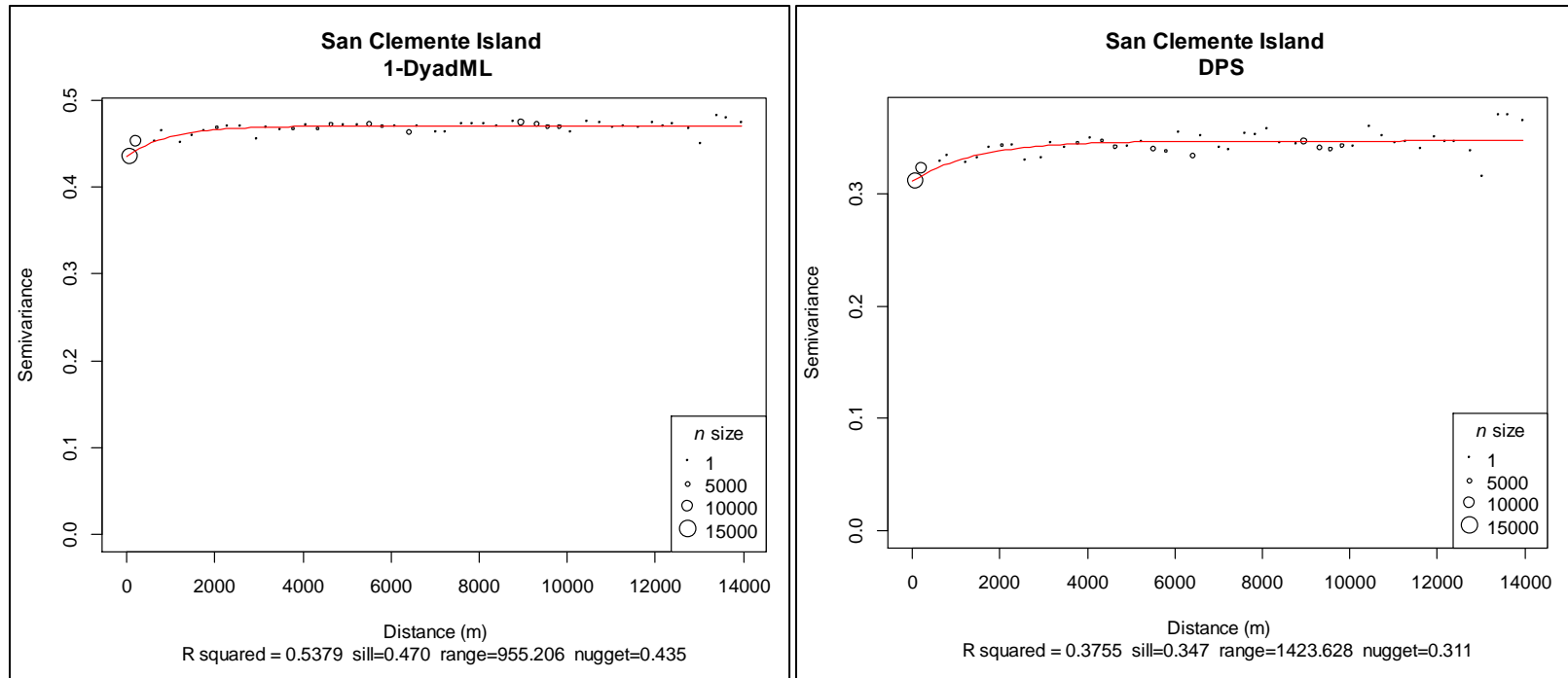


Figure 2.4. Variogram analyses for San Clemente Island. Empirical variograms (circles) were generated from two distance measures: left) 1-DyadML relatedness estimates, right) Inter-individual genetic distance DPS. Circle size denotes the number of pairwise comparisons within each distance class. Maximum distance evaluated was 14,000 m with a lag distance of 290 m for both variables. Theoretical variograms (red line) were fit as fixed-nugget models. Model R^2 values were used as a measure of model support and the point of spatial independence is denoted by the range.

Table 2.1. Isolation by distance model results. Results from the program SPAGEDI for estimation of Wright's σ . Islands were estimated independently (SBI=Santa Barbara Island, SCI=San Clemente Island). Density (De) was estimated as individuals/km² by considering the census population size (Nc) and island area, average for effective density across sampling locations (Ne) with 95% confidence intervals (Ne-LCI=lower, Ne-UCI=upper), and census population size over prime habitat area (Ncp). Lag distance refers to the increment of distance bins (m). SPAGEDI estimated the number of breeders (Nb) and σ (m); standard errors in parentheses for each parameter were estimated by jackknifing over loci. Two data sets were ran for each island, the full data set (All Individuals) and a data set in which the young of year were removed (>40 SVL Individuals).

Island	Density Method	De	Lag	All Individuals		>40 SVL Individuals	
				Nb	σ	Nb	σ
SBI	Nc	6795.37	25	79.52 (7.69)	30.5 (1.5)	79.44 (7.70)	30.5 (1.5)
	Ncp	167619.00	25	96.33 (48.17)	6.8 (1.7)	104.63 (44.95)	7.0 (1.5)
	Ne – LCI	19157.91	25	77.22 (14.06)	17.9 (1.6)	79.90 (12.04)	18.2 (1.4)
	Ne – UCI	33679.07	25	81.58 (12.24)	13.9 (1.0)	84.23 (16.04)	14.1 (1.3)
	Ne	24291.60	25	75.58 (11.87)	15.7 (1.2)	78.57 (16.44)	16.0 (1.7)
	Ne	24291.60	50	75.58 (11.87)	15.7 (1.2)	78.57 (16.44)	16.0 (1.7)
	Ne	24291.60	200	75.58 (11.87)	15.7 (1.2)	78.57 (16.44)	16.0 (1.7)
SCI	Nc	141490.60	50	151.03 (26.84)	9.2 (0.8)	142.58 (17.30)	9.0 (0.5)
	Ncp	267991.90	50	163.56 (37.09)	7.0 (0.8)	140.68 (23.15)	6.5 (0.5)
	Ne – LCI	23016.35	50	159.12 (54.55)	23.5 (4.0)	140.85 (61.86)	22.1 (4.8)
	Ne – UCI	182711.40	50	159.00 (22.51)	8.3 (0.6)	152.20 (26.53)	8.1 (0.7)
	Ne	34631.00	50	160.18 (44.80)	19.2 (2.7)	133.94 (44.96)	17.5 (2.9)
	Ne	34631.00	100	160.18 (44.80)	19.2 (2.7)	133.94 (44.96)	17.5 (2.9)
	Ne	34631.00	200	160.18 (44.80)	19.2 (2.7)	133.94 (44.96)	17.5 (2.9)

Table 2.2. Pairwise distances among relatives. Islands are indicated as Santa Barbara Island (SBI) or San Clemente Island (SCI). Relationships were first-order (FO, based on Rice and Clark (2016)), COLONY inferred relationships of parent-offspring (PO), full sibling (FS), half sibling (HS) or unrelated (U). For each relationship, the number of pairwise comparisons (N), mean (Mean), standard deviation (Sd), median (Median), and maximum (Max) distance values (m). The P column is the approximated p-value comparing the same Relationships between islands. The lower half of the table displays values for each island with young of year samples (>40mm SVL) removed.

	SBI					SCI					
Relationship	N	Mean	Sd	Median	Max	N	Mean	Sd	Median	Max	P
FO	44	16.55	25.25	10.14	158.63	74	21.82	36.61	2.91	156.75	0.4109
PO	20	13.93	13.24	9.50	42.49	52	20.64	40.44	1.00	156.75	0.4815
FS	14	24.90	39.70	12.93	158.63	33	22.42	30.00	4.55	95.29	0.8244
HS	418	243.25	404.76	38.86	1862.69	686	3480.46	5961.83	132.95	26465.22	<2.2e-16
U	48064	831.05	502.81	778.79	2368.02	171220	11285.37	8175.89	9670.69	28258.99	
	SBI > 40 mm SVL					SCI > 40 mm SVL					
Relationship	N	Mean	Sd	Median	Max	N	Mean	Sd	Median	Max	P
FO	44	16.55	25.25	10.14	158.63	43	37.18	41.86	16.90	156.75	0.0062
PO	20	13.93	13.24	9.50	42.49	26	40.68	49.99	12.79	156.75	0.0228
FS	14	24.90	39.70	12.93	158.63	19	38.01	31.51	25.61	95.29	0.3005
HS	391	236.72	402.38	37.31	1862.69	613	3447.68	5994.7	136.08	26465.22	<2.2e-16
U	45631	836.88	502.73	783.46	2368.02	141120	11193.78	7949.20	9667.75	28258.99	

Table 2.3. Logistic regression on distance matrices results. LRDM was conducted separately for each island (SBI=Santa Barbara Island, SCI=San Clemente Island) and for each data set with all individuals (All Samples) or controlled by removal of young of year (>40mm SVL). LRDM was conducted on each predictor variable (Model) independently to determine significance (p-value) through permutation and model support by Nagelkerke's R^2 (R^2). Odds-ratios (Odds-ratio) were computed from 3-variable models in which either the DyadML estimator (Dyad) or COLONY-inferred relationships were used (COLONY) due to the collinear nature of relatedness and relationship. Since the predictors of sex and maturity were used in 2 3-variable models both odds ratios are listed with the forward slash separating the DyadML model from the COLONY relationship model. The predictors of sex and maturity were categorical matches between male and female (sex) and sexually mature and immature individuals (Maturity).

Model	SBI						SCI					
	All Samples			>40mm SVL			All Samples			>40mm SVL		
	p-value	Odds-ratio	R^2	p-value	Odds-ratio	R^2	p-value	Odds-ratio	R^2	p-value	Odds-ratio	R^2
<i>Dyad</i>	0.0001	1.0644	0.112	0.0001	1.0659	0.112	0.0001	1.4373	0.339	0.0001	1.0307	0.081
<i>COLONY</i>	0.0001	1.7004	0.089	0.0001	1.7316	0.089	0.0001	0.9969	0.392	0.0001	0.9990	0.073
Sex	0.6845	1.3120/ 2.4283	0.008	0.7005	1.3265/ 2.4386	0.008	0.0001	1.0006/ 1.0003	0.018	0.3911	1.0003/ 1.0002	0.005
Maturity	0.9356	1.3259/ 1.2964	0.001	0.8512	1.3409/ 1.3139	0.001	0.0033	1.0005/ 0.9799	0.009	0.6900	1.0003/ 0.9959	0.001

Chapter 3: Demogenetic simulations reveal fragmenting effects of climate change on insular lizard populations.

Stephen E. Rice¹ and Rulon W. Clark¹

1. San Diego State University, Dept of Biology, 5500 Campanile Drive, San Diego, California, 92182

Abstract

The extinction risk of insular species with limited dispersal is expected to increase under global climate change as they may be unable to track habitat. Coupled niche-population models have become a fundamental tool for estimating extinction risk due to climate change, yet they do not include genetic patterns when evaluating these effects. Demogenetic simulations can extend coupled niche-population models to produce spatially-explicit genetic and demographic information for all simulated individuals and provide insight into the effects of climate change at demographic and population genetic levels. We used CDMETAPOP to simulate a population of island night lizards (*Xantusia riversiana*) on Santa Barbara Island to evaluate their sensitivity to climate change. We simulated climate change to the year 2100 with a total of 8 scenarios based on 2 climate models, 2 emissions pathways, and 2 connectivity models. We found that: 1) *X. riversiana* is predicted to lose approximately 93%-99% of suitable habitat by 2038, 2) population genetic structure is expected to increase drastically to 0.209-0.673 from a contemporary value of 0.0346, and 3) expected minimum abundance declined sharply between 2007 and 2038 with values of 0-1% of the 2007 population size in all scenarios by 2100. These model results suggest *X. riversiana* is sensitive to climate change which

may decrease census population size, fragment and isolate suitable habitat, and result in high levels of genetic divergence over short periods of time. These patterns may drive the Santa Barbara Island population to extinction under certain scenarios. Management plans should address methods to improve connectivity on the island and attempt to create refugial patches. Contingency plans, such as translocation, may be required to prevent population extirpation. This study highlights the utility of demogenetic simulations in evaluating population demographic and genetic patterns under climate change with suggestions on workflows for running simulations in a high-throughput manner.

Introduction

Global climate change may lead to rapid changes in environmental conditions, thus presenting unique challenges to species persistence. Climate change is expected to strongly affect species with restricted ranges, specialized niches, limited dispersal ability, and small effective population sizes (Oliver and Morecroft 2014), conditions intrinsic to many insular species. Populations may respond to climate change by tracking habitat shifts, coping through phenotypic plasticity or adaptation, or failing these, may go extinct (Penuelas et al. 2013). The persistence of populations is thereby directly related to organisms' abilities to track suitable habitat or cope with changing conditions. For insular species, climate change may shift suitable niche space outside of the dispersal threshold and may result in sharp population declines, increased selective pressures, or extinction.

Species sensitivity to climate change has been assessed through multiple modeling approaches, which range from species distribution models (SDMs) to stochastic simulations linking population demography to SDM predictions (e.g. Fordham et al.

2012; Swab et al. 2015). While effective tools for assessing population viability, these approaches do not incorporate genetic population structure, diversity estimates, and do not include scenarios for adaptation. Recent advances in individual-based simulations have led to landscape demogenetic models (Landguth et al. 2017a) which allow for a greater range of questions and scenarios to be investigated that incorporate demographic and genetic data.

Studies which use demogenetic models to investigate the effects of environmental change have been primarily focused on aquatic systems (e.g. Landguth et al. 2014; Piou et al. 2015). The use of detailed demogenetic models for climate change assessments in terrestrial systems remains largely unexplored. The flexibility of this modeling approach allows the coupling of population demography with SDM predictions to investigate the effects of climate change on population viability while also providing data to describe population genetic patterns. In addition to their flexibility, demogenetic models can simulate genetic data equivalent to empirical approaches which provide benchmarks for model parameterization (e.g. Row et al. 2014).

Islands provide exemplary systems for evaluating the use of demogenetic simulations in assessments of terrestrial systems due to their natural isolation and limited spatial extent. These attributes allow fine-scale simulations of closed populations to determine the sensitivity of insular species to climate change while simultaneously evaluating the practical constraints of demogenetic simulations. Chapters 1 and 2 characterized genetic patterns of an island endemic, the island night lizard (*Xantusia riversiana*) across two thirds of the species range. These studies found correlations of

landscape features with genetic structure and characterized dispersal patterns which provide empirical benchmarks for the parameterization of demogenetic models. Previous ecological research identified precipitation as an important variable in reproduction and calculated habitat-specific carrying capacities (Fellers and Drost 1991), suggesting a coupling of demography and climatic suitability. The island night lizard is one of the few reptiles endemic to the California Channel Islands; however, climate change sensitivity has yet to be assessed due to an expectation of limited effect on these locally abundant populations (United States Fish and Wildlife Service (USFWS) 2014). The combination of closed and well-characterized populations with the need for climate change sensitivity analyses presents a compelling opportunity to apply demogenetic simulations to this insular system.

We constructed demogenetic models in the program CDMETAPOPOP (Landguth et al. 2017a) for island night lizards on Santa Barbara Island (SBI) to determine the effects of climate change on expected minimum abundances (EMA), quasi-extinction risks, and population genetic structure. We used stochastic simulations which included demographic and environmental stochasticity to assess population sensitivity to climate change. We modeled the effects of climate change through annual changes in patch carrying capacity and evaluated the sensitivity of extinction risk and population genetic patterns to variability in the effective distances between patches due to climate change. Finally, we evaluated the practicality of using demogenetic models to conduct these analyses and identified approaches to improve these models in terrestrial systems.

Methods

Study Species

Xantusia riversiana is the only reptile endemic to three California Channel Islands: SBI, San Clemente Island (SCI), and San Nichols Island (SNI). Each island is a distinct evolutionary and management unit (USFWS 2014). Two subspecies were recognized by Smith (1946), with SBI and SCI populations grouped as *X. r. reticulata* and SNI recognized as *X. r. riversiana* based on morphology. In addition to morphology, the SNI population differs in habitat utilization, body size, and reproductive rates (Fellers et al. 1998). Island night lizards are habitat generalist on SBI and SCI with the greatest densities occurring in California boxthorn (*Lycium californicum*), prickly pear cactus (*Opuntia littoralis*), and rocky habitats (Fellers and Drost 1991; Mautz 1993). Population densities in prime habitat are estimated to be in excess of 3,200 individuals/ha with total population sizes on SCI estimated at 21.3 million and 17,600 on SBI (USFWS 2014). Individuals on SCI may live in excess of 23 years (Mautz 2015, pers. comm) with sexual maturity reached between 2 and 3 years (Goldberg and Bezy 1974; Fellers and Drost 1991). Reproduction is influenced by precipitation patterns and hypothesized to occur biennially for mature females (Fellers and Drost 1991). Chapter 1 demonstrated that geographic distance and landscape features were correlated with genetic distance on SBI and SCI. Landscape features included negative correlations with prime habitat and positive correlations with canyons, secondary roadways, and coastal cholla cactus (*Cylindropuntia prolifera*) on SCI and wooly seablite (*Suaeda taxifolia*), crystalline iceplant (*Mesembryanthemum crystallinum*), and barren ground on SBI. Estimates of

dispersal distance range from an average displacement of 3 m (Mautz 1993) to the genetically inferred dispersal distances from Chapter 2 which ranged from 14 m on SBI to 41 m on SCI. Island night lizards were delisted from threatened status under the Endangered Species Act in 2014, contingent on post-delistment monitoring. Climate change sensitivity has not been assessed for the species but is anticipated to be of minimal impact (USFWS 2014).

Habitat Suitability Models

We constructed SDMs in MAXENT (Phillips et al. 2006) to identify contemporary correlates of climatic niche with occurrences limited to SCI and SBI, due to shared ecological and life history patterns. We used occurrence data from capture data (Appendix B) and GBIF ([doi:10.15468/dl.rie3zo](https://doi.org/10.15468/dl.rie3zo)). We removed records without GPS coordinates, those that mapped outside of SBI and SCI, and those prior to 1959 to limit occurrence records to those which potentially overlap historic climate data. The occurrence data presented in Appendix B were spatially biased by distance to trails (SBI) and distance to roadways (SCI); therefore, we constructed bias maps using the distance of a cell to primary access route to assign probabilities of sampling a given cell. The probability of a given cell being sampled was the proportion of the cell's distance bin among all raster cells for each respective island.

Climatic predictors were the first 19 bioclim variables generated from 800 m² historical (1981-2010) PRISM precipitation and temperature data (PRISM 2012) using the R package DISMO (Hijmans et al. 2017). Terrain predictors of slope, aspect, terrain roughness, terrain ruggedness, and topographic position were constructed from a 10 m

resolution National Elevation Data set (United States Geological Survey 2017) and resampled to 100 m using the R package RASTER (Hijmans et al. 2016). Highly correlated predictors were removed through stepwise variance inflation factor (VIF) analysis in the R package USDM (Naimi 2015) with a threshold of 10. Cleaned occurrence data was used with retained predictors to construct SDMs using the autofeatures setting, duplicate occurrence records removed, and bootstrapped 1,000 times (Franklin 2010).

Two global climate models were chosen for the projection of SDMs to future time periods. The two models, CanESM and Miroc, are considered predictive for the Basic Characterization Model, which informs many California climate assessments (Flint et al. 2013). The CanESM and Miroc climate models, at representative concentration pathways (RCPs) of 4.5 and 8.5, were downscaled to 100 m resolution by Dr. Alan Flint (USGS) for monthly temperature and precipitation variables. We constructed bioclim variables for projections to the years 2038, 2069, and 2100 by averaging monthly variables over the 30 years prior to each time point. Terrain variables remained unchanged in all scenarios. The bootstrapped SDMs were projected to each time point and averaged to identify habitat suitability under climate change scenarios. We defined the contemporary habitat suitability map as the year 2007 for all downstream analyses and interpolations, which allowed consistent 30 year time spans for all endpoint projections.

Demogenetic Simulations

We modeled the effects of climate change on population viability and genetic structure using the demogenetic modeling approach of Landguth et al. (2017) with the program CDMETAPOP. Demogenetic models included climate change as a process which

modified the habitat suitability value of each raster cell. The effect of climate change on population viability was investigated by linking patch carrying capacities to habitat suitability values. Additionally, two resistance surface models were used to examine the effect of climate change on inter-patch connectivity: a static model based on geographic distance and a dynamic model based on habitat suitability. We linearly interpolated between each endpoint to produce annual SDMs ranging from 2007 through the year 2100 using RASTER. We modeled every 1 ha raster cell as a distinct patch with a constant relationship between carrying capacity and habitat suitability. The constant relationship between individuals and habitat suitability was determined by taking the census population size and dividing by the sum of contemporary habitat suitability. Populations on SBI were modeled with patch carrying capacities determined by habitat suitability multiplied by the constant of 117.76 individuals; populations on SCI were not modeled due to computational constraints.

Demographic parameters were drawn from the ecological literature of *X. riversiana* (Fellers and Drost 1991; Mautz 1993) and *X. vigilis* (Zweifel and Lowe 1966). *Xantusia riversiana* exist in age structured populations; however, there is insufficient data to estimate the survival parameters needed to model demography. We used a 4-stage model (Appendix E.1) of demography informed by survival estimates of a sister species, *X. vigilis*, which occur on the mainland. Both species display similar patterns of high juvenile survival (Mautz 1993) and reproductive potential (Goldberg and Bezy 1974). Fecundity values for *X. riversiana* from Fellers and Drost (1991) were used

as parameters (Appendix E.1) for reproductively active (4th stage) females which were modeled as seasonally monogamous with strict biennial reproduction.

All demogenetic models included environmental and demographic stochasticity. Stochasticity was incorporated through standard deviations in patch carrying capacity, standard deviations in vital rates, random removal of individuals in excess of patch carrying capacities, and probabilistic dispersal and mate-seeking distances. The standard deviation of each patch was the carrying capacity multiplied by 0.1415. This value was determined from empirical data as the proportion of the standard deviation to mean population density within a management area on San Clemente Island (Mautz 1993). Survival rate variability was modeled through the standard deviation in survival rates for each age group as estimated from Table 4 in Zweifel and Lowe (1966). Variability in fecundity was modeled by assigning the offspring number for each female from a normal distribution around the mean with standard deviation (Fellers and Drost 1991). Population dynamics for each patch were limited by carrying capacity wherein the initial population size for each time step was less than or equal to the carrying capacity in the preceding time step. Modeling variability in population size and demography in addition to temporal changes in carrying capacity resulted in stochastic genetic patterns which modeled the effect of drift and dispersal processes on population genetic patterns.

We used the same cost distance matrices, dispersal formula parameters, and thresholds for mating and movement for both sexes. The cost distance matrices for each time step consisted of the effective resistance distances between all patches as calculated by the program CIRCUITSCAPE (McRae and Beier 2007). The static model based on

geographic distance was constructed with a raster map with all terrestrial cells assigned a neutral value of 1, which constrained dispersal paths to land and has been shown to approximate log-transformed geographic distance (Lee-Yaw et al. 2009). Dynamic resistance maps, which assessed changes in connectivity, were produced for each time step with resistance set as the inverse of the habitat suitability for each raster cell. We modeled movements with a negative exponential function (scale =1.0, shape =0.75) and a maximum effective resistance distance threshold of 0.555 for geographic distance models and 1.25 for connectivity models. These values were chosen as they resulted in equilibrated global F_{st} estimates similar to the observed empirical value of 0.0346 reported in Chapter 1 when modeled on the contemporary suitability map for 450 years. In addition to the 4 climate change scenarios, we modeled a “no change” scenario in which contemporary habitat suitability remained the same throughout the simulation.

We simulated 17,600 individuals with 20 microsatellite loci each with 15 alleles and no mutation. Simulations began with a panmictic population and equilibrated on contemporary conditions for 450 years to produce a 2007 estimate of global F_{st} approximate to the empirical data. Changes in carrying capacity and effective resistance distance began at the 2008 time step. Populations were fully sampled at the years 2038, 2069, and 2100 and global F_{st} calculated in the R package DIVERSITY (Keenan et al. 2013). Full census data was extracted for each time step between 2007 and 2100 and was used to calculate proportional EMA, compared to 2007, and generate quasi-extinction graphs following McCarthy and Thompson (2001). All scenarios were replicated 100 times and ran on a high performance computational (HPC) cluster.

Results

Habitat Suitability

Seven bioclim variables and 3 terrain variables were retained by stepwise VIF (Table 3.1) resulting in a maximum correlation between Bio5 and Bio9 of 0.7706. Maximum temperature in the warmest month, Bio5, had the most useful information by itself and topographic position index (TPI) had the most information not present in other variables. The minimum observed habitat suitability value for any occupancy record was 0.1095, which was used as the threshold definition to visualize habitat patches and differentiate suitable from unsuitable habitat patches (Appendices E.2-E.13). All climate scenarios displayed striking decreases in suitable habitat availability and distribution. These models predicted 93.13%-99.81% reductions in suitable habitat on SBI and SCI from 2007 under all scenarios for the year 2038 (Figure 3.1), which results in a change from 7482 ha under current conditions to 514 - 14 ha under climate change. Habitat suitability for all scenarios declined through the year 2069 with a complete loss of suitable habitat under both CanESM scenarios and the Miroc 4.5 scenario by the year 2100. The Miroc 8.5 model retained the most suitable habitat and was the only scenario investigated which did not result in the complete elimination of suitable habitat. Suitable habitat expanded in all scenarios to on a nearby island to Santa Catalina Island, east of SBI and SCI, which is outside of the current and historic species distribution.

Demogenetic Simulations

All models equilibrated at global F_{st} values (Figure 3.2) which approximated the empirical value of 0.0346. The distance only models revealed sharp increases in global

Fst across all climate scenarios. Mean global Fst was 0.043 at the 2007 time step in equilibrated models and increased to a range of 0.209-0.330 by 2100 depending on the climate scenario (Figure 3.2, top). The CanESM 8.5 model could not be assessed at the year 2100 due to population extinction throughout the simulations. EMA revealed sharp population declines (Figures 3.3-3.5, top) at all time points with the Miroc 8.5 projection being the most optimistic with 1.76% of the 2007 population remaining by 2100 (Table 3.2). The CanESM 8.5 model resulted in complete extinction and the remaining models ended the century with $\leq 0.15\%$ of the 2007 population remaining. Quasi-extinction graphs (Figures 3.3-3.5, top) also show increased extinction risks at 2038 with sharp increases in extinction risk through the end of the century. Connectivity models equilibrated at a global mean Fst value of 0.037 by 2007 and revealed the same trends and model rankings in global Fst as distance models; however values were almost twice as great (Figure 3.2, bottom). Mean global Fst values for connectivity models ranged from 0.5318-0.6733 by 2100 with CanESM 8.5 absent due to extinction. EMA and quasi-extinction analyses for connectivity models returned the same trends as distance models at similar values with the CanESM 8.5 model again resulting in extinction (Table 3.2, Figures 3.3-3.5, bottom).

Discussion

SDMs can offer insight into the predicted shifts of suitable habitat for a species under climate change (Franklin 2010). When combined with demogenetic simulations, SDMs allow for a spatially-explicit investigation into the effects of climate change on population demographic and genetic patterns. The current monitoring framework for the

island night lizard suggests that climate change is not a concern for this species (USFWS 2014); however, our results indicate this species may be heavily impacted by climate change with >93% loss in suitable habitat, drastic increases in population genetic structure, and steep declines in population abundance. We investigated the sensitivity of *X. riversiana* to climate change on SBI following a coupled niche-population model framework to determine the effects of climate change on population abundance and population genetic structure. We found global F_{st} values increased from the 2007 time point by factors of 4.76-7.55 for models with only geographic distance and 14.23-18.31 for models where climate change modified the intervening matrix. EMA revealed stark decreases in abundances across all climate models by 2038 with population extinction for the CanESM 8.5 scenario and a maximum of 1.76% of the 2007 population under the most optimistic model, Miroc 8.5, with a distance only dispersal scenario. EMA values for other climate models were <1% by 2100 (Table 3.2).

Habitat Suitability

The SDMs for *X. riversiana* represent the first efforts to characterize changes in habitat suitability for reptiles on the California Channel Islands. These models were correlative models built with abiotic factors and thus do not include vegetation or soil characteristics which may be important for island night lizard populations (Fellers and Drost 1991; Mautz 1993). MAXENT is considered one of the most accurate SDM methods but may lead to more pessimistic projections than other methods (Conlisk et al. 2013). Even with these limitations, the contemporary SDM offered key insights into climatic factors which correlate with *X. riversiana* distributions on SBI and SCI. Precipitation is

positively correlated with reproduction and recruitment in island and mainland *Xantusia* species (Zweifel and Lowe 1966; Fellers and Drost 1991). Precipitation was incorporated in this SDM through the bioclim suite of variables which include interactions between temperature and precipitation. The largest contributing variable to these models was Bio9, the mean temperature in the driest quarter (Jun –Aug), which overlaps with the gestational period of *X. riversiana* (Goldberg and Bezy 1974). This variable may represent physiological constraints associated with gestation and realized climatic niche, as Fellers and Drost (1991) observed decreased reproductive output during drought. Further experimental research is needed to examine the hypothesis that reproductive physiology and environmental constraints on gestation limit this species climatic niche.

SDMs projected under the Miroc and CanESM climate models revealed similar trends across both RCPs. The greatest decline in suitable habitat occurred between the contemporary model and 2038. The steepness of this decline, a loss of approximately 93% - 99% of contemporary habitat, is jarring given the longevity of the species and recent delistment. While these values may be pessimistic, they offer a clear indication that climate change is projected to have much larger effects on insular species within the California Floristic Province than included in current management plans. We recommend that management and conservation efforts on the California Channel Islands incorporate habitat suitability forecasts as planning tools. Forecasting changes in habitat suitability may suggest regions and species in which habitat tracking may be an inviable option and alternatives such as translocation and assisted colonization may be needed to prevent extinction under climate change.

Demogenetic Simulations

Individual-based spatially explicit demogenetic models are a recent tool which gives insight into population level pattern-process relationships. Previous research with CDMETAPOP is limited due to the recent publication of the method (Landguth et al. 2017a) but has included evaluation of blister rust resistance scenarios in whitebark pine (Landguth et al. 2017b) and invasive species management (Landguth et al. 2017a). However, CDMETAPOP is built modularly to draw on previous individual-based spatially explicit models, such as CDPOP (Landguth and Cushman 2010), which have been utilized to explore topics ranging from climate change sensitivity in Lynx (Row et al. 2014) to experimental design (Rico 2017). Demogenetic simulations conducted with CDMETAPOP may be parameterized to yield coupled niche population models with genetic data which can enhance research into the effects of connectivity, population structure, or adaptation under changing climate. Demogenetic simulations may improve coupled niche population modeling efforts by providing greater insight into the genetic effects of climate change, but the tradeoffs of this approach include increased computational time and resources to parameterize and analyze.

We approached demogenetic simulations from the framework of coupled niche population models by linking habitat suitability values with patch carrying capacity and varying that carrying capacity at each time step. Additionally, we explored the effect of modeling effective resistance between patches as a function of annual habitat suitability and compared this approach to a more traditional approach based on geographic distance alone. We found demogenetic simulation to be a computationally expensive tool that

provided insight into population viability and genetic structure under multiple climate change and effective distance scenarios. This study was only possible through the use of a HPC cluster to increase model throughput during parameterization and simulation, and would have been intractable on a standard workstation due to processing time and the storage space required for simulations and analyses (>1 TB for this study). The ability to run independent instances of CDMETAPOP across multiple computer cores and use basic R scripts to adjust model parameters and analyze simulated data allowed model parameterization and simulations to occur in a high-throughput manner limited only by computer usage quotas. Demogenetic models constructed for SBI were 17,600 individuals spread across 247 1 ha patches for a time period 542 years. A single iteration could complete on a single processor with 2GB of memory in 8-12 hours. This partitioning of computational load across multiple cores allowed an increase in the number of model runs, but remained only a fraction of the number used in traditional coupled niche population models (e.g. Conlisk et al. 2013, Swab et al. 2015). However, the number was similar to other demogenetic approaches (e.g. Landguth et al. 2014; Piou et al. 2015). The parameterization and execution of simulations on a computer cluster is recommended to ensure robust examination of parameter space, and will be essential if modeling changes in genetic patterns from assumed equilibrium conditions.

Failure to validate equilibrium conditions for global F_{st} , and presumably other genetic metrics, when parameterizing models may lead to spurious and incorrect inferences. The current configuration of CDMETAPOP prevents parallelization and we found that the computational load becomes intractable for millions of individuals. Our

attempts to parameterize models of SCI revealed that even at 10% of the census population size (2.15 million) computer cores given 15 GB of RAM were unable to generate the initial population in a 24 hour period. Furthermore, we found that efforts to parameterize models based on reducing the modeled population to the effective population size at each collection site failed to reach equilibrium of global F_{st} values even when dispersal was set to the maximum threshold. While we could achieve values equivalent to empirical values, these values were not stable and continued to increase even as effective distance and carrying capacity remained stationary. Failure to validate the assumed pattern would have led to a serious inference error on the magnitude of change expected under climate change scenarios. In addition to validating equilibrium conditions when examining questions of genetic structure, researchers may be forced to examine various simulated population sizes or spatial extents based on computational constraints.

Implications for Conservation

The current distribution of *X. riversiana* will likely constrain its ability to cope with climate change through habitat tracking due to insular populations and mean dispersal distances less than 50 m on both SBI and SCI. The amount of habitat available to island night lizards based on SDM predictions is concerning due to the sharp declines in suitable habitat by 2038 in all scenarios and continued decline through the end of the century. Demogenetic simulations on SBI revealed populations are sensitive to climate change across all climate change scenarios when carrying capacity is linked to climatic suitability. We found that global F_{st} as a metric of intra-island patch isolation was more

sensitive to the resistance of the intervening matrix whereas demographic patterns, represented by EMA, were not. Even when the distance between patches is static, isolation of populations poses a major concern, with high levels of global population genetic structure (Figure 3.2). These findings suggest that populations may be threatened by climate change through habitat loss, habitat degradation, and isolation of suitable patches. Increased isolation of patches even within a small island may further increase the extinction risk of the species through inbreeding depression or Allee effects (reviewed in Courchamp et al. 1999).

Based on SDM and simulation predictions, management intervention may be required to prevent extinction of *X. riversiana* on SBI as early as 2038. While we were unable to model SCI in demogenetic simulations, we expect similar patterns to hold given the shared life history traits and prime habitat requirements. The census population size is greater on SCI than SBI, thus the risk of quasi-extinction is likely reduced but sharp declines in population abundance are anticipated based on the loss of suitable habitat indicated by SDMs (Appendix E).

Conservation efforts on both islands should focus on the creation of refugia/management areas in regions predicted to be the most suitable across climate predictions in an effort to ameliorate the anticipated loss of suitable habitat and patch isolation over the next 2 decades. As a generalist species, the simulated responses of *X. riversiana* on SBI may be indicative of increased threats to plant communities or endemic deer mouse populations from climate change and a lack of viable habitat tracking. This

study is specific to island night lizards, but highlights a need for further study among insular species for which climate change sensitivity analyses are lacking.

Conclusions

Island night lizards are at high risk from climate change. The effects of climate change over a range of emission and model scenarios are predicted to cause sharp population declines through decreased carrying capacities and sharp increases in population structure even when only geographic distance between patches is considered. We recommend that the Channel Islands National Park Service, the managing entity of SBI, and other agencies continue to monitor habitat and population sizes and key climatic variables to determine if populations begin to decline as predicted by our models. Additional factors may add to persistence of *X. riversiana* populations under climate change, such as responses of vegetation or soil characteristics necessary to maintain thermoregulation or unidentified plasticity within the species that could buffer against declines. These modeling results are also subject to the limitations of the method, chiefly that we assume the niche of island night lizards is well described by environmental variables, that contemporary relationships hold in future scenarios, and that population demography is monotonically coupled to habitat suitability. While these assumptions are likely violated, further research is needed into the sensitivity of model predictions to changes in population size, SDM construction, and parameters associated with vital rates. Additional research with demogenetic simulations within this system should also address hypotheses related to adaptive responses to heat and drought tolerance, which can be implemented within the demogenetic models.

Demogenetic models are a valuable tool for climate change sensitivity analyses, but their usage is constrained to populations consisting of tens to hundreds of thousands. Parameterization of models to yield genetic patterns which approximate empirical conditions under equilibrium settings can highlight model sensitivities to the spacing and densities of populations while providing benchmarks for model parameterization. We found stochastic simulations were informative to evaluate the sensitivity of an island population to environmental and demographic stochasticity as well as the permeability of the intervening matrix and provide insight into the genetic and demographic trajectories this species may face during the remainder of the century. While 100 stochastic simulations is fewer than used in traditional population viability analyses, it is equivalent to previous work with demogenetic simulations. Leveraging HPC clusters should alleviate some of the computational constraints for more robust simulation sizes. We recommend researchers interested in demogenetic simulations pursue HPC solutions to allow for increased numbers of simulations and robust model inferences. Secondary constraints are the computational load of analyzing simulated data and will vary with the research being conducted. Estimation of extinction risk and temporal trends in population size are easily extracted from summary tables within simulations; however metrics of population structure, such as global F_{st} , require more effort and considerably more time to extract. As demogenetic simulations grow in usage, dedicated workflows will need to emerge to reduce computational loads and provide an implementation to conduct thorough sensitivity analyses on the effect of model parameters.

Literature Cited

- Conlisk E, Syphard AD, Franklin J, Flint L, Flint A, Regan H (2013) Uncertainty in assessing the impacts of global change with coupled dynamic species distribution and population models. *Global Change Biology*, 19(3), 858–869.
<https://doi.org/10.1111/gcb.12090>
- Courchamp F, Clutton-Brock T, Grenfell B (1999) Inverse density dependence and the Allee effect. *Trends in Ecology and Evolution*, 14(10), 405-410.
- Fellers GM, Drost CA (1991) Ecology of the Island Night Lizard, *Xantusia riversiana*, on Santa Barbara Island, California. *Herpetological Monographs*, 5, 28.
<https://doi.org/10.2307/1466975>
- Fellers GM, Drost CA, Mautz WJ, Murphey TG (1998) Ecology of the Island Night Lizard, *Xantusia riversiana*, on San Nicolas Island, California (Report) (p. 80). Retrieved from <http://pubs.er.usgs.gov/publication/96678>
- Flint LE, Flint AL, Thorne JH, Boynton R (2013) Fine-scale hydrologic modeling for regional landscape applications: the California Basin Characterization Model development and performance. *Ecological Processes*, 2, 25. doi:10.1186/2192-1709-2-25
- Fordham DA, Watts MJ, Delean S, Brook WB, Heard LMB, Bull CM (2012) Managed relocation as an adaptation strategy for mitigating climate change threats to the persistence of an endangered lizard. *Global Change Biology*, 18, 2743-2755.
<http://10.1111/j/1365-2486.2012.02742.x>
- Franklin J (2010) Mapping species distributions: spatial inference and prediction. Cambridge; New York: Cambridge University Press. Retrieved from <http://dx.doi.org/10.1017/CBO9780511810602>
- Goldberg SR, Bezy RL (1974) Reproduction in the island night lizard, *Xantusia riversiana*. *Herpetologica*, 350–360.
- Hijmans RJ, Phillips S, Leathwick J, Elith J (2017) R package: "dismo": <https://cran.r-project.org/package=dismo>
- Hijmans RJ, van Etten J, Cheng J, Mattiuzzi M, Sumner M, Greenberg A, Lamigueiro OP, Bevan A, Racine EB, Shortridge A (2016) R package: "raster": <https://cran.r-project.org/package=raster>
- Keenan K, McGinnity P, Cross TF, Crozier WW, Prodohl PA (2013) An R package for the estimation of population genetics parameters and their associated errors.

- Methods in Ecology and Evolution, 4(8), 782-788. <https://doi.org/10.1111/2041-210X.12067>
- Landguth EL, Cushman SA (2010) CDPOP: a spatially explicit cost distance population genetics program. *Molecular Ecology Resources*, 10(1), 156-161. <https://doi.org/10.1111/j.1755-0998.2009.02719.x>
- Landguth EL, Bearlin A, Day CC, Dunham J (2017a) CDMetaPOP: an individual-based, eco-evolutionary model for spatially explicit simulation of landscape demogenetics. *Methods in Ecology and Evolution*, 8(1), 4–11. <https://doi.org/10.1111/2041-210X.12608>
- Landguth EL, Holden ZA, Mahalovich MF, Cushman SA (2017b) Using landscape genetics simulations for planting blister rust resistant whitebark pine in the US Northern Rocky Mountains. *Frontiers in Genetics*, 8, 9. <https://dx.doi.org/10.3389/fgene.2017.00009>
- Landguth EL, Muhlfeld CC, Waples RS, Jones L, Lowe WH, Whited D, Lucotch J, Neville H, Luikart G (2014) Combining demographic and genetic factors to assess population vulnerability in stream species. *Ecological Applications*, 24(6), 1505–1524.
- Lee-Yaw JA, Davidson A, Mcrae BH, Green DM (2009) Do landscape processes predict phylogeographic patterns in the wood frog? *Molecular Ecology*, 18(9), 1863–1874. <https://doi.org/10.1111/j.1365-294X.2009.04152.x>
- Mautz WJ (1993) Ecology and energetics of the island night lizard, *Xantusia riversiana*, on San Clemente Island, California. In F. Hochberg (Ed.), *Third California Islands symposium: Recent advances in research on the California Islands* (pp. 417–428). Santa Barbara, CA: Santa Barbara Museum of Natural History.
- McCarthy MA, Thompson C (2001) Expected minimum population size as a measure of threat. *Animal Conservation*, 4(4), 351–355.
- McRae BH, Beier P (2007) Circuit theory predicts gene flow in plant and animal populations. *Proceedings of the National Academy of Sciences*, 104(50), 19885–19890.
- Naimi B (2015) R package: "usdm": <https://cran.r-project.org/package=usdm>
- Oliver TH, Morecroft MD (2014) Interactions between climate change and land use change on biodiversity: attribution, problems, risks, and opportunities. *WIREs Climate Change*, 5, 317-335.

- Penuelas J, Sardans J, Estiarte M, Aogaya R, Carnicer J, Coll M, Barbeta A, Rivas-Ubach A, Jlusia J, Garbulsky M, Filella J, Jump AS (2013) Evidence of current impact of climate change on life: a walk from gene to the biosphere. *Global Change Biology*, 19, 2303-2338.
- Phillips SJ, Anderson RP, Schapire RE (2006) Maximum entropy modeling of species geographic distributions. *Ecological Modelling*, 190(3–4), 231–259.
<https://doi.org/10.1016/j.ecolmodel.2005.03.026>
- PRISM Climate Group. (2012) United States 30-yr Normals: precipitation, minimum temperature, maximum temperature 1981-2010. available online:
<http://prism.oregonstate.edu>. Oregon State University, Corvallis, OR, USA.
- Piou C, Taylor MH., Papaix J, Prévost E (2015) Modelling the interactive effects of selective fishing and environmental change on Atlantic salmon demogenetics. *Journal of Applied Ecology*, 52(6), 1629–1637.
<https://doi.org/10.1111/1365-2664.12512>
- Rico Y (2017) Using computer simulations to assess sampling effects on spatial genetic structure in forest tree species. *New Forests*, 48(2), 225-243.
<https://doi.org/10.1007/s11056-017-9571-y>
- Row JR, Wilson PJ, Gomez C, Koen EL, Bowman J, Thornton D, Murray DL (2014) The subtle role of climate change on population genetic structure in Canada lynx. *Global Change Biology*, 20(7), 2076–2086. <https://doi.org/10.1111/gcb.12526>
- Smith HM (1946) A subspecies of the lizard *Xantusia riversiana*. *Journal of the Washington Academy of Sciences*, 36(11), 392–393.
- Swab RM, Regan HM, Matthies D, Becker U, Bruun HH (2015) The role of demography, intra-species variation, and species distribution models in species' projections under climate change. *Ecography*, 38(3), 221–230.
<https://doi.org/10.1111/ecog.00585>
- United States Fish and Wildlife Service (2014) Island night lizard (*Xantusia riversiana*) final Post-Delisting Monitoring Plan. U.S. Fish and Wildlife Service, Carlsbad Fish and Wildlife Office, Carlsbad, California.
- United States Geological Survey (2017) 3D Elevation Program (3DEP). available online:
<https://nationalmap.gov/3DEP/index.html>
- Zweifel RG, Lowe CH (1966) The Ecology of a Population of *Xantusia vigilis*, the Desert Night Lizard. *American Museum Novitates*, 2247, 1–57.

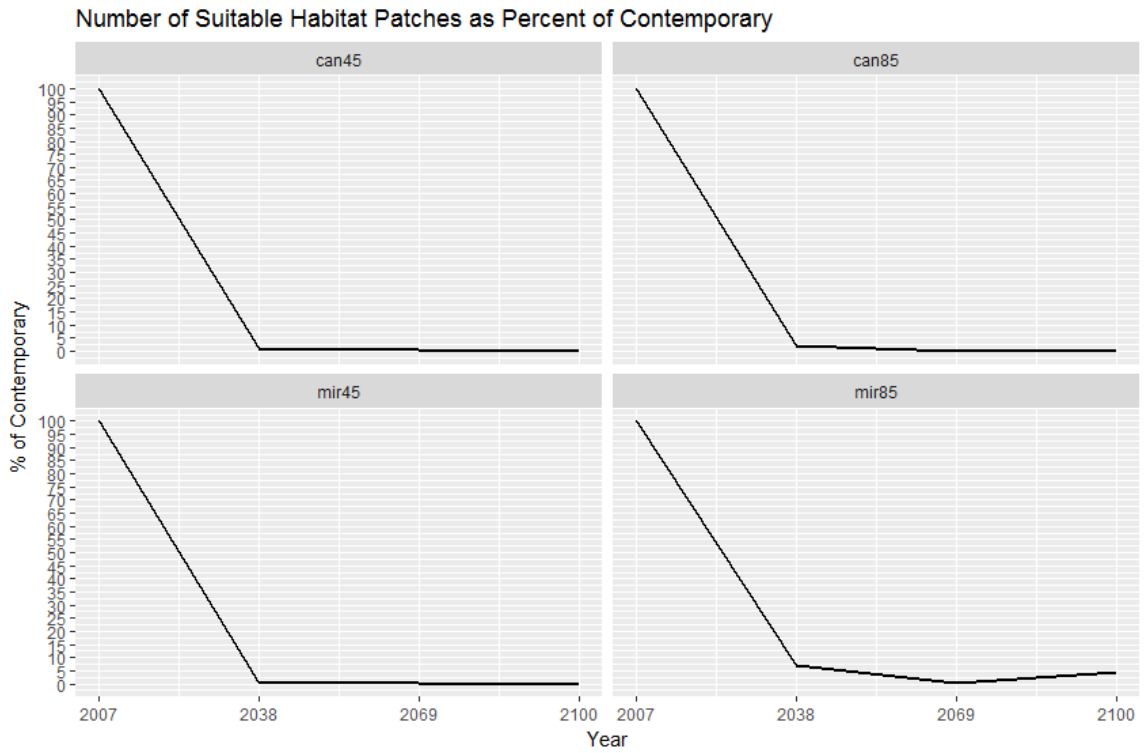


Figure 3.1. Percentage of contemporary suitable habitat patches remaining on both Santa Barbara Island and San Clemente Island. Habitat patches were defined based on an observed occupancy value of 0.1095 with the % of contemporary values representing the percentage of suitable 1 ha patches compared to the contemporary model.

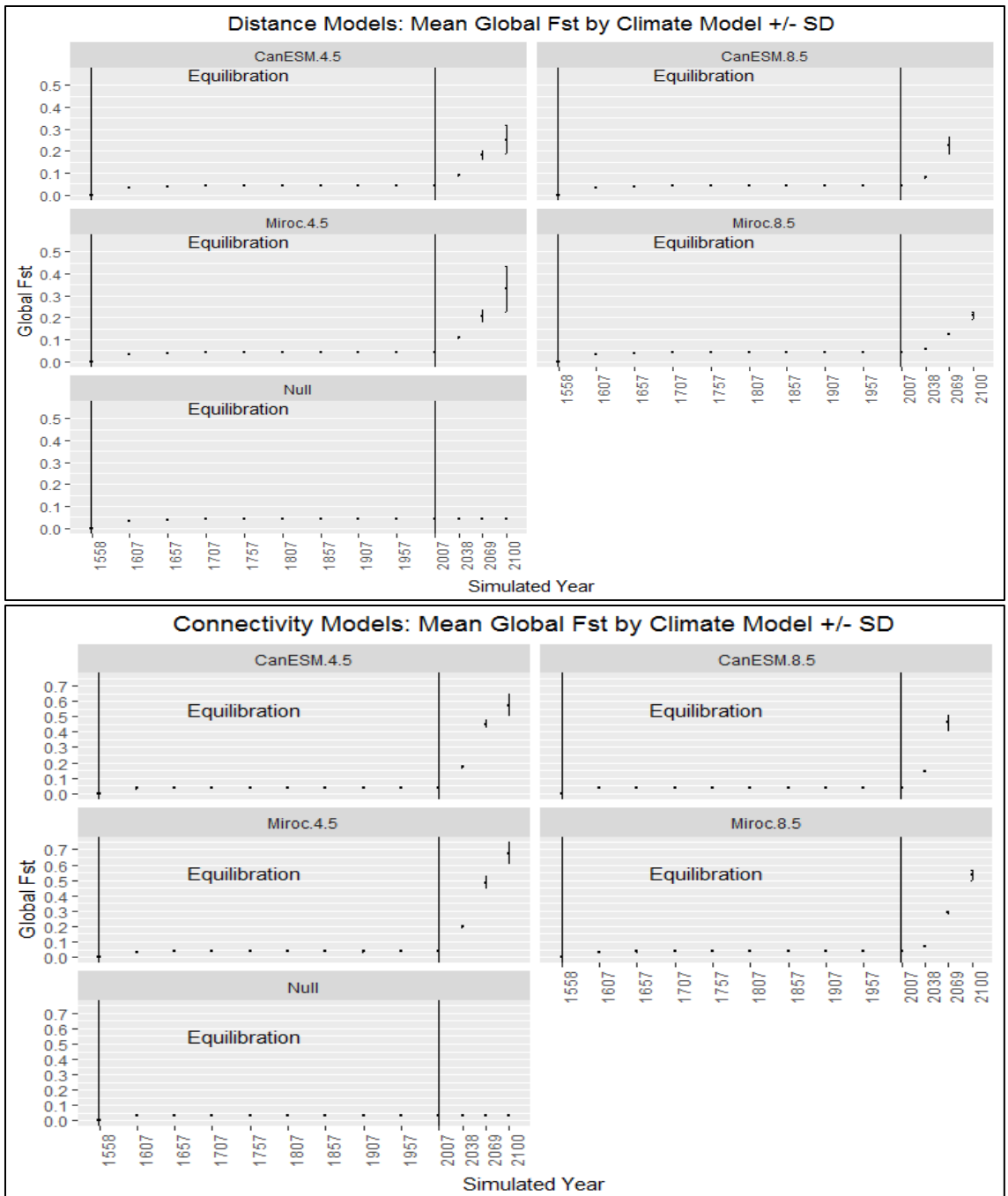


Figure 3.2. Mean global Fst with standard deviations. Distance-based models (top) and connectivity models (bottom) listed with climate model identification with RCP is given in the title. The Y-axis is global Fst averaged over all simulations for each model with error bars indicating standard deviation of the mean. Vertical lines denote the range considered for model equilibration. Mean Fst is denoted with +/- standard deviations plotted from point data from sampled time points (X-axis).

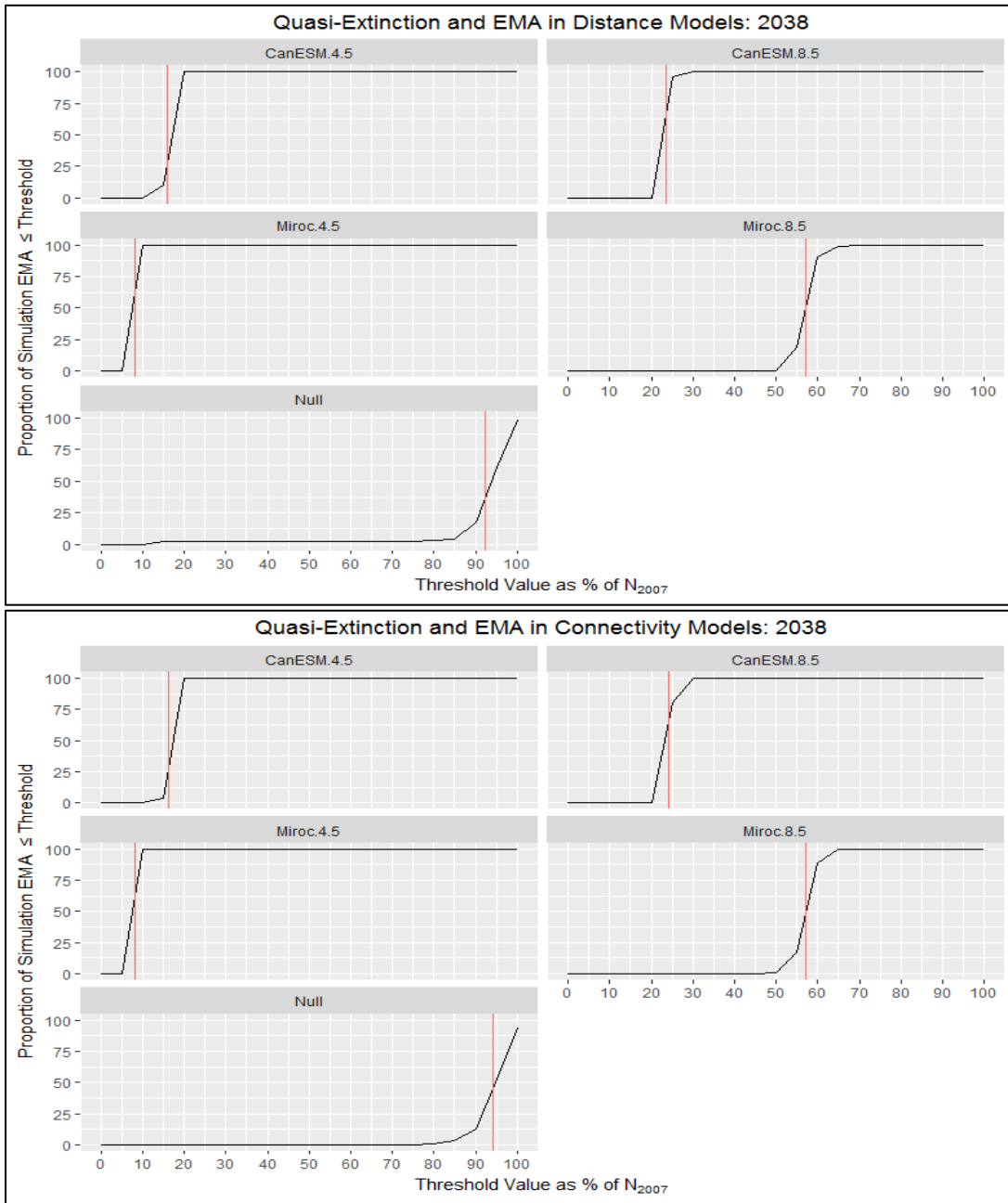


Figure 3.3. Quasi-extinction for distance and connectivity models 2007-2038. Distance-based models (top) and connectivity models (bottom) listed with climate model identification with RCP is given in the title. The Y-axis represents risk, defined as the proportion of models with a minimum size, represented as the proportion of the 2007 census population size remaining, less than or equal to the threshold value (X-axis). The red vertical line represents the proportional EMA averaged across all runs for a given model.

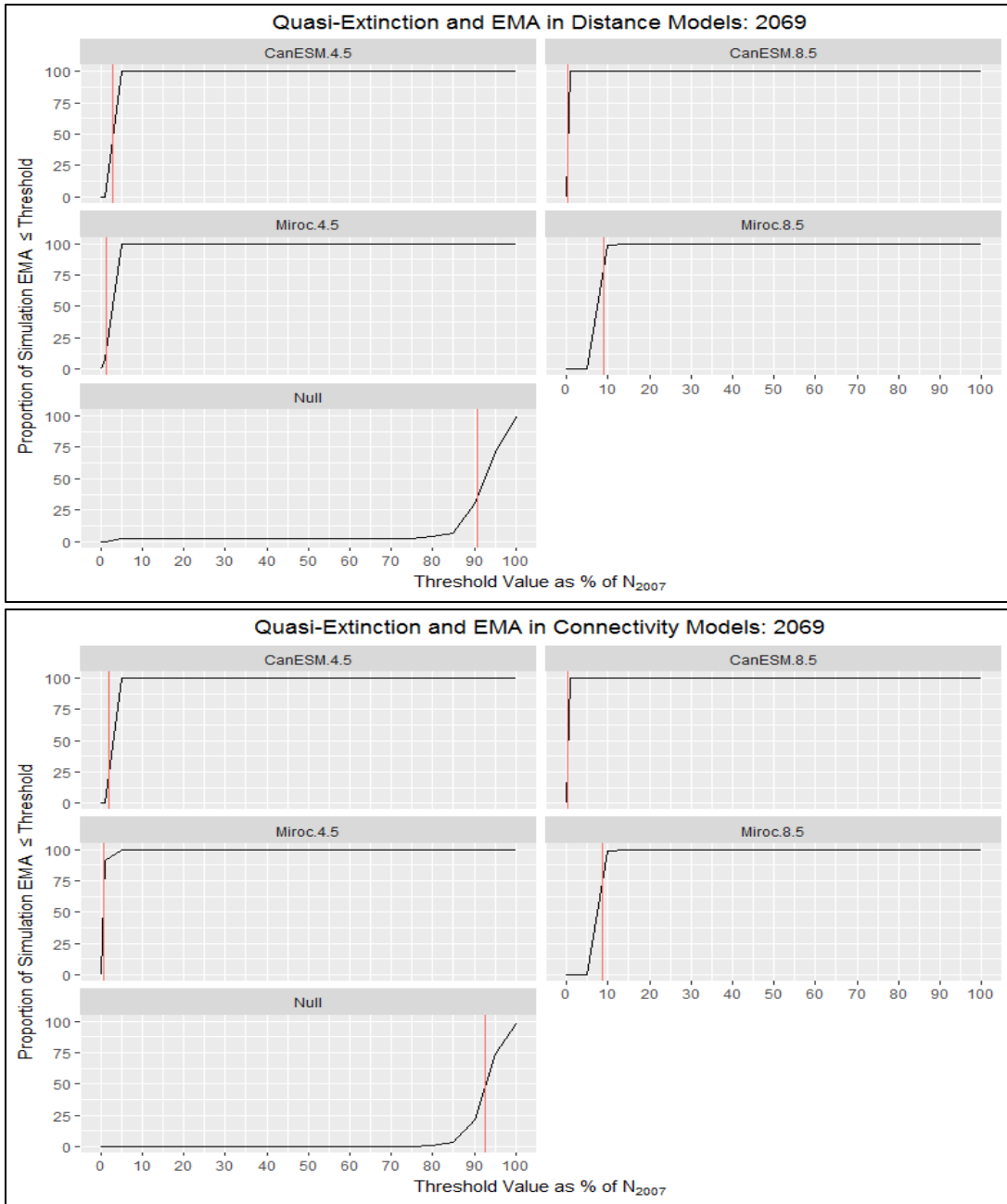


Figure 3.4. Quasi-extinction for connectivity models 2007-2069. Distance-based models (top) and connectivity models (bottom) listed with climate model identification with RCP is given in the title. The Y-axis represents risk, defined as the proportion of models with a minimum size, represented as the proportion of the 2007 census population size remaining, less than or equal to the threshold value (X-axis). The red vertical line represents the proportional EMA averaged across all runs for a given model.

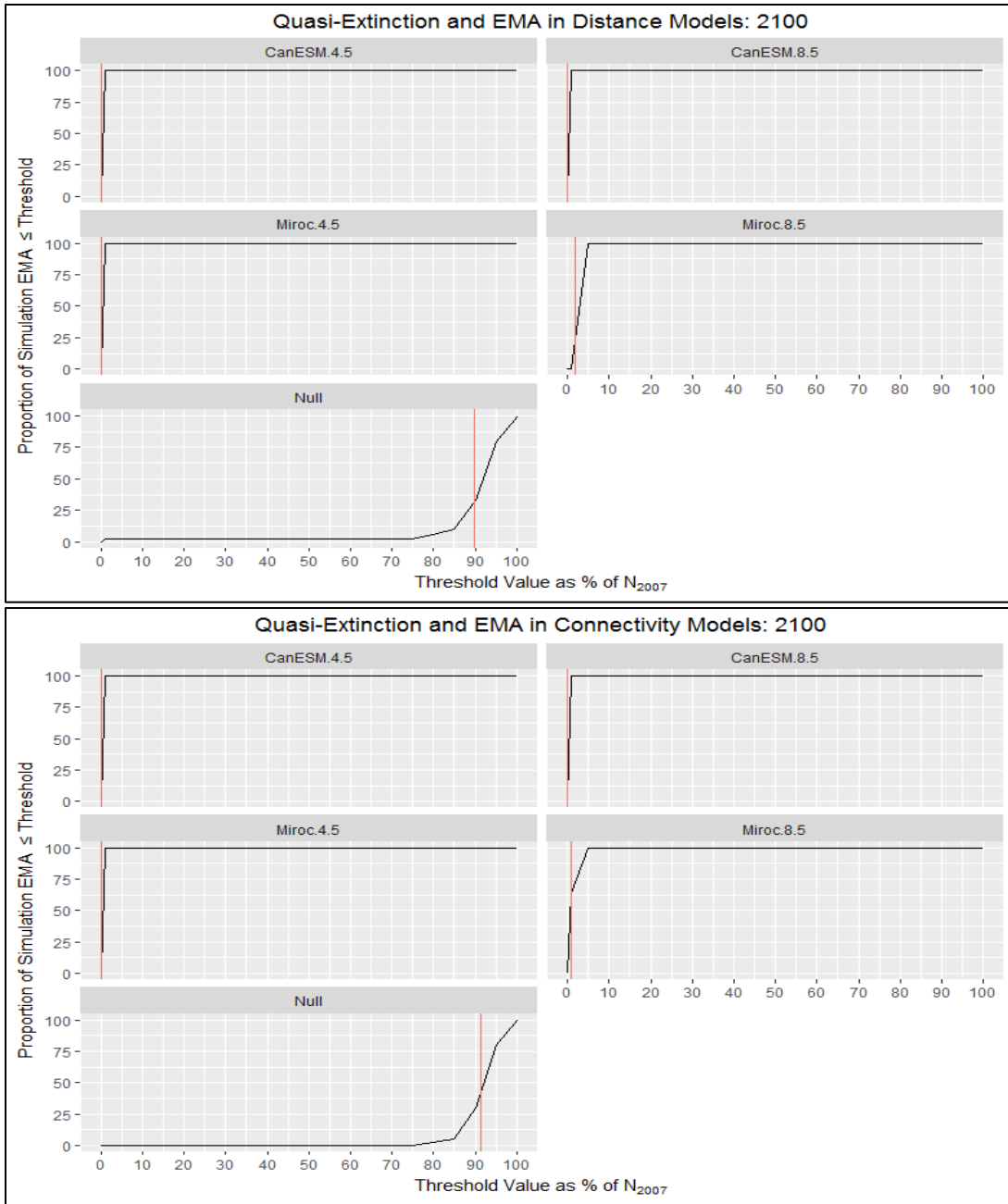


Figure 3.5. Quasi-extinction for connectivity models 2007-2100. Distance-based models (top) and connectivity models (bottom) listed with climate model identification with RCP is given in the title. The Y-axis represents risk, defined as the proportion of models with a minimum size, represented as the proportion of the 2007 census population size remaining, less than or equal to the threshold value (X-axis). The red vertical line represents the proportional EMA averaged across all runs for a given model.

Table 3.1. Environmental and topographic predictors. Predictors were retained for models of SBI and SCI based on stepwise VIF. MAXENT calculated percent contribution and permutation importance for each variable.

Variable	Description	Percent Contribution	Permutation Importance
Bio9	Mean temperature of driest quarter	26.6	30.8
Bio15	Precipitation seasonality	12.6	4.7
Bio3	Isothermality	11.9	15.2
Bio6	Minimum temperature of coldest month	9.2	6.1
Bio5	Maximum temperature of warmest month	8	8.5
TPI	Topographic position	7.8	5
Aspect	Direction slope faces	7.2	7.4
Bio14	Precipitation of driest month	6.5	11.3
Slope	Elevational steepness	5.1	4.9
Bio18	Precipitation of warmest quarter	5	6.1

Table 3.2. Proportional EMA by year, climate change scenario, and model.

Simulation averaged proportional EMA between the observed minimum abundance between the contemporary model (2007) and the endpoint, over 100 stochastic simulations. Climate models were CanESM and Miroc with 2 RCPS, 4.5 and 8.5, and a null model of stable contemporary conditions. The distance model refers to the stable geographic equivalent resistance model and connective model refers to variable effective distances between patches.

Climate Model	Distance Model			Connectivity Model		
	2038	2069	2100	2038	2069	2100
CanESM 4.5	15.790	2.819	0.150	16.181	1.961	0.082
CanESM 8.5	23.403	0.379	0.000	24.175	0.299	0.000
Miroc 4.5	8.065	1.354	0.094	8.269	0.747	0.044
Miroc 8.5	57.000	8.828	1.760	57.139	8.696	0.924
No Change	92.920	90.688	89.840	94.056	92.747	91.547

CONCLUSIONS

The goal of this dissertation was to integrate population genetics with coupled niche population models to conduct a conservation genetic assessment of the island night lizard under contemporary and future conditions. By quantifying contemporary genetic patterns and characterizing dispersal I was able to conduct stochastic simulations which determined the effect of climate change on extinction risks and population genetic structure on Santa Barbara Island. This dissertation presents the first application of demogenetic simulations to examine the effects of climate change on a terrestrial vertebrate and the first efforts to quantify the sensitivity and effects of climate change on a reptile endemic to the California Channel Islands. The approaches and results of this dissertation are applicable to conservation management and monitoring of island night lizard populations, other reptiles endemic to the California Channel Islands, and present a workflow for high-throughput demogenetic simulations.

The first chapter focused on quantifying contemporary population genetic patterns and identifying landscape factors correlated with intra-island genetic divergence between collection sites on Santa Barbara Island and San Clemente Island. I found that island night lizards have significant genetic structure with 2 populations on the northern and southern ends of San Clemente Island with strong admixture throughout the island. The landscape features positively correlated with genetic distance on San Clemente Island were coastal cholla, canyons, and secondary roadways. Santa Barbara Island populations were highly structured with 4 populations corresponding to the northern, western, south eastern, and mid-island regions. The landscape features correlated with genetic distance

were different from San Clemente Island and included mixed herbaceous cover of wooly seablite with crystalline iceplant and barren ground. Prime habitat of California boxthorn and prickly pear cactus were negatively correlated with genetic distance on both islands, supporting ecological research that shows these habitat types as vital resources for *Xantusia riversiana* (Fellers and Drost 1991; Mautz 1993). The landscape features positively correlated with genetic distance may disrupt connectivity between populations on each island and should be targeted for remediation and restorations efforts.

Furthermore, these results: 1) demonstrate that human modifications to insular habitats can disrupt genetic connectivity and range from hundreds of years for the introduction of crystalline iceplant or under a century for roads on San Clemente Island, 2) identify the best habitat for restoration, with a goal of improving connectivity among populations, are California boxthorn and prickly pear cactus leading to a shared management strategy across islands, and 3) suggest that habitat has an effect on carrying capacity (Fellers and Drost 1991; Mautz 1993) and connectivity between populations which can influence the overall population genetic structure and probability of recolonization patches which may be extirpated. Future research on the landscape genetics of *X. riversiana* should include the third island San Nicholas Island in comparative analyses and leverage field-based approaches, such as telemetry, to identify the true resistance values of habitat and develop resource selection functions to further guide conservation management.

While the ecology of the island night lizard has been studied for multiple years across all islands within the range (Fellers and Drost 1991; Mautz et al. 1992; Mautz 1993; Fellers et al. 1998) there were aspects of species biology which could not be

accurately described with capture-mark-recapture approaches. The second chapter of this dissertation leveraged the field and genetic data from Chapter 1 to characterize dispersal in *X. riversiana* on Santa Barbara Island and San Clemente Island. I found no evidence of sex-biased dispersal and indirect estimates of dispersal derived from parentage analyses were 14 m on Santa Barbara Island and 41 m on San Clemente Island; these findings were consistent with Wright's σ . Spatial autocorrelation analyses were incongruent with all other results, but offered insight into the scale of population genetic patterns on each island. Surprisingly, I detected kin-affiliative behavior through a permutation based logistic regression of relatedness, relationship, sex, and maturity on co-captured individuals. Pairs of individuals were 1.067 times more likely to be captured at the same point with a one standard deviation change in DyadML relatedness estimates on SBI and 1.031 times more likely on SCI. Kin-affiliative behavior and cryptic sociality have been reported for a sister species (Davis et al. 2010, Davis 2011), *X. vigilis*, and may be more common in lizards than currently appreciated. Further research to characterize dispersal patterns in Xantusiid lizards would benefit from the inclusion of detailed telemetry data paired with genetic data to further refine dispersal distance estimates and elucidate cryptic sociality and space use within the species.

The post-delisting plans for the island night lizard (United States Fish and Wildlife Service 2014) indicate that climate change is not expected to impact populations of island night lizards. The third and final chapter of my dissertation estimated the sensitivity of *X. riversiana* on Santa Barbara Island to climate change. I generated a contemporary species distribution model based on capture data and supplemented with

GBIF entries and found that >93% of suitable habitat is lost by 2038 on Santa Barbara and San Clemente Islands. I used demogenetic simulations informed by Chapter 2 to parameterize models which yielded estimates of population structure similar to the 0.0346 global F_{st} for Santa Barbara Island found in Chapter 1. These stochastic models were used to investigate the sensitivity of *X. riversiana* to climate change when carrying capacity was coupled to habitat suitability values in projected species distribution models. I found that island night lizards were highly sensitive to climate change induced reductions in carrying capacity, which resulted in 99%-100% population loss based on a comparison of expected minimum abundances under climate change to contemporary conditions. The genetic structure of island night lizards was also sensitive to the resistance of the intervening habitat with mean global F_{st} increasing more than 2 times for models where climate change modified habitat resistance values compared to distance-only models. There are caveats to model interpretation, as these models rely heavily on an assumed monotonic relationship between population carrying capacity and habitat suitability. However, the projected loss of suitable habitat due to climate change coupled with the severe population declines and sensitivity of genetic connectivity to habitat resistance indicates that climate change may have a more profound impact on insular reptile populations than previously thought. Future research should continue to monitor populations on Santa Barbara Island to determine the trajectory of populations while also assessing physiological thresholds and plasticity of responses to further refine expectations of species persistence under climate change. Additional research is also needed in developing demogenetic simulations into a more robust analytical tool capable

of being processed in parallel and parameterized to more readily conduct sensitivity analyses.

These research findings suggest that island night lizards, while exceedingly abundant on inhabited islands, are sensitive to habitat modifications and may show patterns of genetic divergence over short time spans when habitat quality and the intervening matrix are compromised. Island night lizards are expected to be at high risk from climate change over the next several decades, and management actions are likely needed to support species persistence. To support connectivity among populations, management actions should focus on remediation of poor habitat and revegetation with California boxthorn and prickly pear cactus. These habitat types will serve to increase local abundances which may buffer some of the early population losses due to climate change while reducing the effective distance between patches. The scale of these efforts should generally be smaller than 1 ha based on dispersal estimates and spatial scale of genetic autocorrelation. I suggest management actions specifically target regions on each island with the greatest habitat suitability in current and projected distribution models for early remediation efforts in order to increase population densities in these regions as micro-refugia for the species. In the event of captive breeding or translocation efforts are needed, attention should be paid to estimates of relatedness to maintain potentially important social structures while avoiding collections which may result in inbreeding.

Literature Cited

- Davis AR (2010) Kin presence drives philopatry and social aggregation in juvenile Desert Night Lizards (*Xantusia vigilis*). *Behavioral Ecology*, 23(1), 18-24.
doi: 10.1093/beheco/arr144
- Davis AR, Corl A, Surget-Groba Y, Sinervo B (2011) Convergent evolution of kin-based sociality in a lizard. *Proceedings of the Royal Society B*, 278, 1507-1514.
doi:10.1098/rspb.2010.1703
- Fellers GM, Drost CA (1991) Ecology of the island night lizard, *Xantusia riversiana*, on Santa Barbara Island, California. *Herpetological Monographs*, 5, 28-78.
- Fellers GM, Drost CA, Mautz WJ, Murphey T (1998) Ecology of the island night lizard, *Xantusia riversiana*, on San Nicolas Island, California. Prepared for the US Navy by the USGS, Western Ecological Research Center, Pt. Reyes Field Station, Pt. Reyes National Seashore, CA.
- Mautz WJ (1993). Ecology and energetics of the island night lizard, *Xantusia riversiana*, on San Clemente Island, California. Pp. 417-428, In: F. G. Hochberg (ed.), *Third California Islands symposium: Recent advances in research on the California Islands*. Santa Barbara Museum of Natural History, Santa Barbara, CA. 661 pp.
- Mautz WJ, Daniels CB, Bennett AF (1992) Thermal dependence of locomotion and aggression in a Xantusiid lizard. *Herpetologica*, 48, 271-279.
- United States Fish and Wildlife Service (2014) Island night lizard (*Xantusia riversiana*) final Post-Delisting Monitoring Plan. U.S. Fish and Wildlife Service, Carlsbad Fish and Wildlife Office, Carlsbad, California.

Appendix A: Microsatellite loci primers and replication files

Protocol A.1. DNA extractions and PCR conditions for microsatellite data.

DNA Extraction

We extracted DNA with a standard salt digestion of 10 mg of tissue with 300 μ l of lysis buffer (100 mM NaCl, 100 mM Tris-Cl, 25 mM EDTA, 0.5% SDS) with 1.5 μ l Proteinase K (20 mg/ml), followed by guanidine thiocyanate protein precipitation (4M guanidine thiocyanate, 0.1M Tris-Cl), 100% isopropanol precipitation of DNA, and 70% ethanol clean-up. Extracted DNA was eluted in low TE, quantified by Nanodrop (ND-1000) and used as template for polymerase chain reactions (PCR).

PCR Conditions

Twenty-three primer pairs (Rice et al. 2016, Appendix A.2) were optimized for PCR conditions through gradient PCRs and arranged into a combination of multiplexed reactions and post-pcr mixes (Appendix A.2) based on reaction conditions, amplicon size, and primer-primer interactions identified by the National Institute of Standards and Technology Primer tool (2005). Reverse primers were pigtailed (Brownstein et al. 1996) on the 5' end and fluorophores were added to the 5' end of the forward primers. All reactions were conducted using the same thermocycle protocol. Ten nanograms of extracted DNA was plated and dried overnight prior to PCR. Reactions were carried out in 10 μ l volumes (5 units Taq Polymerase, 1 μ l buffer, 1 μ l dNTPs, multiplexed primers, and MilliQ water to 10 μ l) under a thermocycler protocol of 94°C for 3 minutes followed by 33 cycles of 94°C for 35s, 63°C for 45s, and 72°C for 45s and the final extension at 72°C for 5 min.

Table A.2. Microsatellite primers and genotyping notes. Microsatellite loci used to generate genetic data (Appendix B) are listed by locus name with primer sequence for the forward (F) and reverse (R) primers, the repeat motif, and the observed size range (Size). The optimal molarity of magnesium chloride (Buffer) and fluorophore (Dye) are listed. The groupings of primers into multiplexes are denoted in the column MP, the value of which identifies grouped primers. The post-mix column identifies multiplexes that were mixed post-pcr to minimize primer-primer interactions or due to differences in optimal buffer. Markers included for analyses after quality control procedures are denoted with a “yes” under the island specific column (SCI = San Clemente Island, SBI = Santa Barbara Island) while those markers that were excluded at any point in the quality control process are identified by “no”. The panel assignments and bin files are provided in sections A.3. and A.4 respectively.

Locus name	Primer Sequence	Repeat Motif	Size	Buffer	Dye	MP	Post	SCI	SBI
Xari01	F:ATATCAGGTGCGGATTTGGG	AAAG	161-238	20mM	PET	4	YES	YES	YES
	R:AAAGGCTTCACTTGCCAGC								
Xari05	F:CACACTCAAGCTCTCTTACATATGGG	ATCT	145-258	20mM	NED	3	NO	YES	YES
	R:AAGGATGTCATTACTTCATGCCC								
Xari07	F:AACGCCAAGGATTATGGAGG	AACT	144-221	20mM	FAM	4	YES	YES	YES
	R:AGAATTTGGAAGGGCGGC								
Xari09	F:AATTGTCCTGTCCCAAAGGG	AAAG	204-307	20mM	FAM	1	NO	YES	YES
	R:AGCTTCCCATCTTCCACAGC								
Xari10	F:TTTGTGTGTGTGAAATTGATTGG	ATCT	119-213	20mM	NED	4	YES	YES	YES
	R:AGGGCTGTGGAGTTTCATGC								
Xari11	F:TTACTAGACCTGTGTTTCTCGGG	AAAG	308-392	20mM	HEX	1	NO	YES	YES
	R:CACTTTAGCCAAAGGAAGAGTGC								
Xari13	F:TTATGGAGAGCCCATTCACG	AAAG	190-288	20mM	NED	1	NO	YES	YES
	R:CATCTTCAAGGTGGTACAATATCTTCC								
Xari18	F:AGAGCTGGCTCACAAGGAGG	AAAG	140-245	20mM	HEX	1	NO	YES	NO
	R:CTCCAATCAAAGCAAAGCCC								
Xari20	F:GTGAAGGCTGCAGTTCGG	ATCT	164-236	20mM	PET	5	NO	YES	YES
	R:CTGTGTGGGTCCAGAAGTGG								

Xari21	F:GTTTAGTTCAGAACAAGCCAGGG	AAAG	160-231	20mM	HEX	4	YES	YES	YES
	R:CTGTAAACATTTACCATTCACGC								
Xari22	F:TCTTTCCTTTCACACCCACCC	AAAG	180-316	20mM	FAM	3	NO	NO	YES
	R:GAAGACAAGCGCCCTTCC								
Xari30	F:TTGGTGGAAACGTGCCTGG	TTCC	135-261	20mM	FAM	5	NO	YES	NO
	R:GCTCTTTCTCACCTGCCTGG								
Xari31	F:CAGGAATGTACACTGATACAGAATATGG	ATCT	140-258	20mM	NED	5	NO	YES	YES
	R:GCTTCTATCTTTACATCCTGTGATCC								
Xari33	F:TCAGAACAAATAATTAACATGTGGC	ATCT	105-198	20mM	FAM	2	YES	NO	YES
	R:GGCTAGTACCATCTCCCTCCC								
Xari35	F:CAAATTGTGAGTGTTATGCAAATAGC	AAAG	168-240	30mM	PET	2	YES	YES	YES
	R:TCCAGAATAAGGATTCGCCC								
Xari38	F:TGCATGTTATGTGAAGCAGCC	AAAG	114-237	20mM	HEX	2	YES	YES	YES
	R:TGCATGCATGGAATCAAGC								
Xari41	F:TCTGTATGTAGTGCTTTGACTATGCC	AAAG	102-200	20mM	NED	2	YES	YES	YES
	R:TGGTTACCTATCCCAAAGGAGC								
Xari42	F:TAAGCCTGTGGGAAGAGTGG	ATCT	325-380	20mM	FAM	2	YES	YES	YES
	R:TTATAAATTGAGGAAAGTCTCTAAACTAGG								
Xari44	F:TGCCTCCACTTATGTTCTACAAGG	ATCT	134-230	20mM	PET	3	NO	NO	YES
	R:TTGCACACTCTCCACATCCC								
Xari45	F:TTGCAGTGTTAAGGTGTCATAGG	AAAG	146-237	20mM	HEX	5	NO	YES	YES
	R:TTCCCTTCTTGGCTTGTGG								
Xari46	F:GACCCTCCTCTTTCTACAGTGC	AAAG	105-187	20mM	FAM	1	NO	YES	YES
	R:TTTCTGAACTACACGGAAATGC								
Xari47	F:TTAAGCAGAAATGCACCCTCC	AAAG	156-275	20mM	HEX	3	NO	YES	YES
	R:TTTGCAGAAAGTAGCAAATGC								
Xari48	F:GCAATAATATCAAACCAACAAGCC	ATCT	192-256	20mM	PET	1	NO	YES	YES
	R:TTTGGCACTTGCTGACG								

File A.3. Microsatellite loci panel file. Microsatellite loci panel file in the tab delimited ABI file format. File lists locus name, fluorophore color, allele bin range, and motif size from development.

Version	GM v 4.1								
Kit type:	MICROSATELLITE								
Chemistry Kit	Xari	none							
Panel	MP1	none							
XARI46	blue	100.0	200.0	-	4	0.0	none	none	false
XARI09	blue	200.0	320.0	-	4	0.0	none	none	false
XARI18	green	120.0	250.0	-	4	0.0	none	none	false
XARI11	green	300.0	400.0	-	4	0.0	none	none	false
XARI13	yellow	190.0	290.0	-	4	0.0	none	none	false
XARI48	red	190.0	300.0	-	4	0.0	none	none	false
Panel	MP2	none							
XARI33	blue	100.0	200.0	-	4	0.0	none	none	false
XARI42	blue	300.0	400.0	-	4	0.0	none	none	false
XARI38	green	110.0	250.0	-	4	0.0	none	none	false
XARI41	yellow	100.0	200.0	-	4	0.0	none	none	false
XARI35	red	150.0	250.0	-	4	0.0	none	none	false
Panel	MP3	none							
XARI22	blue	170.0	320.0	-	4	0.0	none	none	false
XARI47	green	140.0	280.0	-	4	0.0	none	none	false
XARI05	yellow	140.0	270.0	-	4	0.0	none	none	false
XARI44	red	130.0	240.0	-	4	0.0	none	none	false
Panel	MP4	none							
XARI07	blue	140.0	240.0	-	4	0.0	none	none	false
XARI21	green	160.0	260.0	-	4	0.0	none	none	false
XARI10	yellow	110.0	240.0	-	4	0.0	none	none	false
XARI01	red	150.0	250.0	-	4	0.0	none	none	false
Panel	MP5	none							
XARI30	blue	130.0	275.0	-	4	0.0	none	none	false
XARI45	green	130.0	240.0	-	4	0.0	none	none	false
XARI31	yellow	140.0	260.0	-	4	0.0	none	none	false
XARI20	red	150.0	250.0	-	4	0.0	none	none	false

File A.4. Microsatellite loci bin file. Microsatellite loci bin file in the tab delimited ABI file format. File lists locus name, followed by allele name, mean bin size (in base pairs) and the range (in base pairs) for the bin with bin color.

```

Version      GM v 4.1
Chemistry Kit Xari
BinSet Name  MP1
Panel Name   MP1
Marker Name  XARI46
105  105.5  0.6  0.6  dark gray
110  109.6  0.4  0.4  dark gray
114  113.7  0.4  0.4  dark gray
118  117.9  0.4  0.4  dark gray
120  119.7  0.6  0.6  dark gray
122  121.8  0.4  0.4  dark gray
126  126.0  0.4  0.4  dark gray
130  130.3  0.4  0.4  dark gray
133  132.5  0.5  0.5  dark gray
134  134.5  0.4  0.4  dark gray
139  138.7  0.4  0.4  dark gray
141  140.9  0.5  0.5  dark gray
143  143.3  0.4  0.4  dark gray
148  148.0  0.4  0.4  dark gray
152  152.6  0.4  0.4  dark gray
156  156.7  0.6  0.6  dark gray
161  160.9  0.4  0.4  dark gray
165  164.9  0.4  0.4  dark gray
169  169.2  0.4  0.4  dark gray
173  173.3  0.4  0.4  dark gray
177  177.3  0.4  0.4  dark gray
181  181.0  0.5  0.5  dark gray
187  187.2  0.5  0.5  dark gray
Marker Name  XARI09
204  203.6  0.5  0.5  dark gray
210  209.6  0.4  0.4  dark gray
212  211.7  0.5  0.5  dark gray
221  221.3  0.5  0.5  dark gray
223  223.2  0.5  0.5  dark gray
228  227.8  0.5  0.5  dark gray
244  243.5  0.5  0.5  dark gray
251  251.2  0.4  0.4  dark gray
254  254.1  0.4  0.4  dark gray
255  255.0  0.4  0.4  dark gray
258  258.0  0.5  0.5  dark gray

```

259	258.8	0.2	0.2	dark gray
262	261.8	0.5	0.5	dark gray
266	266.0	0.5	0.5	dark gray
268	267.6	0.2	0.2	dark gray
269	269.4	0.5	0.5	dark gray
273	273.2	0.5	0.5	dark gray
277	277.0	0.5	0.5	dark gray
279	278.5	0.5	0.5	dark gray
281	280.8	0.5	0.5	dark gray
285	284.7	0.5	0.5	dark gray
289	288.5	0.5	0.5	dark gray
293	292.4	0.5	0.5	dark gray
296	296.2	0.4	0.4	dark gray
300	299.9	0.5	0.5	dark gray
304	304.0	0.5	0.5	dark gray
307	307.1	0.5	0.5	dark gray
Marker Name XARI18				
140	139.5	0.5	0.5	dark gray
144	143.9	0.5	0.5	dark gray
152	152.0	0.5	0.5	dark gray
156	155.9	0.5	0.5	dark gray
160	159.7	0.5	0.5	dark gray
164	163.5	0.5	0.5	dark gray
167	167.3	0.5	0.5	dark gray
169	169.3	0.5	0.5	dark gray
171	171.3	0.5	0.5	dark gray
173	173.0	0.5	0.5	dark gray
175	175.0	0.5	0.5	dark gray
177	176.8	0.5	0.5	dark gray
179	178.9	0.5	0.5	dark gray
181	180.7	0.5	0.5	dark gray
183	182.7	0.5	0.5	dark gray
185	185.0	0.5	0.5	dark gray
186	186.4	0.5	0.5	dark gray
189	189.2	0.5	0.5	dark gray
190	190.2	0.5	0.5	dark gray
193	193.0	0.5	0.5	dark gray
194	194.1	0.5	0.5	dark gray
198	197.8	0.5	0.5	dark gray
202	201.6	0.5	0.5	dark gray
203	203.5	0.5	0.5	dark gray
205	205.4	0.5	0.5	dark gray
209	208.9	0.5	0.5	dark gray
213	212.5	0.5	0.5	dark gray

216	216.5	0.5	0.5	dark gray
221	221.2	0.5	0.5	dark gray
224	224.1	0.5	0.5	dark gray
229	229.3	0.5	0.5	dark gray
240	239.5	0.5	0.5	dark gray
245	245.5	0.5	0.5	dark gray
Marker Name XARI11				
308	308.5	0.5	0.5	dark gray
310	310.2	0.4	0.4	dark gray
314	314.2	0.5	0.5	dark gray
318	318.2	0.5	0.5	dark gray
322	322.0	0.5	0.5	dark gray
324	324.2	0.4	0.4	dark gray
326	326.1	0.5	0.5	dark gray
328	328.0	0.4	0.4	dark gray
330	330.0	0.5	0.5	dark gray
332	332.0	0.4	0.4	dark gray
334	333.9	0.4	0.4	dark gray
336	335.9	0.4	0.4	dark gray
338	337.9	0.5	0.5	dark gray
340	339.9	0.4	0.4	dark gray
342	341.7	0.4	0.4	dark gray
344	343.7	0.4	0.4	dark gray
346	345.6	0.4	0.4	dark gray
347	347.5	0.4	0.4	dark gray
349	349.4	0.5	0.5	dark gray
351	351.3	0.5	0.5	dark gray
353	353.2	0.5	0.5	dark gray
355	355.0	0.5	0.5	dark gray
357	356.9	0.5	0.5	dark gray
359	358.7	0.5	0.5	dark gray
361	360.6	0.5	0.5	dark gray
363	362.5	0.5	0.5	dark gray
364	364.3	0.5	0.5	dark gray
366	366.1	0.5	0.5	dark gray
368	368.0	0.5	0.5	dark gray
370	369.8	0.5	0.5	dark gray
372	371.7	0.5	0.5	dark gray
373	373.6	0.5	0.5	dark gray
375	375.3	0.5	0.5	dark gray
377	377.3	0.5	0.5	dark gray
379	379.2	0.5	0.5	dark gray
381	380.7	0.5	0.5	dark gray
383	382.9	0.4	0.4	dark gray

388	388.2	0.5	0.5	dark gray
392	391.6	0.5	0.5	dark gray
Marker Name XARI13				
190	190.3	0.3	0.3	dark gray
194	194.0	0.5	0.5	dark gray
201	200.8	0.5	0.5	dark gray
205	204.5	0.5	0.5	dark gray
208	208.3	0.4	0.4	dark gray
212	212.2	0.4	0.4	dark gray
216	215.9	0.4	0.4	dark gray
220	219.7	0.4	0.4	dark gray
221	221.4	0.5	0.5	dark gray
223	223.5	0.4	0.4	dark gray
227	227.3	0.4	0.4	dark gray
229	229.2	0.4	0.4	dark gray
231	231.0	0.4	0.4	dark gray
233	233.0	0.4	0.4	dark gray
235	234.8	0.5	0.5	dark gray
237	236.9	0.4	0.4	dark gray
239	238.6	0.4	0.4	dark gray
240	240.5	0.5	0.5	dark gray
242	242.4	0.4	0.4	dark gray
244	244.4	0.5	0.5	dark gray
246	246.2	0.4	0.4	dark gray
250	250.0	0.4	0.4	dark gray
254	253.7	0.4	0.4	dark gray
258	257.5	0.5	0.5	dark gray
260	259.6	0.4	0.4	dark gray
262	261.4	0.4	0.4	dark gray
264	263.6	0.4	0.4	dark gray
265	265.2	0.4	0.4	dark gray
267	267.3	0.5	0.5	dark gray
269	269.0	0.4	0.4	dark gray
273	272.7	0.5	0.5	dark gray
277	276.6	0.5	0.5	dark gray
281	280.4	0.5	0.5	dark gray
285	284.5	0.5	0.5	dark gray
288	288.2	0.5	0.5	dark gray
Marker Name XARI48				
192	191.9	0.5	0.5	dark gray
197	196.6	0.5	0.5	dark gray
200	200.5	0.2	0.2	dark gray
204	204.4	0.4	0.4	dark gray
208	208.2	0.4	0.4	dark gray

212	212.3	0.4	0.4	dark gray
216	216.1	0.4	0.4	dark gray
220	220.1	0.4	0.4	dark gray
224	223.9	0.4	0.4	dark gray
228	227.8	0.4	0.4	dark gray
230	229.9	0.4	0.4	dark gray
232	231.8	0.4	0.4	dark gray
236	235.8	0.4	0.4	dark gray
240	239.8	0.4	0.4	dark gray
244	243.6	0.4	0.4	dark gray
247	247.5	0.4	0.4	dark gray
256	255.7	0.4	0.4	dark gray

Panel Name MP2

Marker Name XARI33

105	105.0	0.5	0.5	dark gray
107	106.7	0.5	0.5	dark gray
110	110.2	0.5	0.5	dark gray
118	117.7	0.5	0.5	dark gray
121	121.3	0.5	0.5	dark gray
126	126.4	0.5	0.5	dark gray
129	128.7	0.5	0.5	dark gray
132	131.5	0.5	0.5	dark gray
135	134.8	0.5	0.5	dark gray
138	137.6	0.4	0.4	dark gray
140	139.0	0.5	0.5	dark gray
141	141.3	0.5	0.5	dark gray
144	144.1	0.5	0.5	dark gray
149	148.6	0.5	0.5	dark gray
153	152.5	0.5	0.5	dark gray
157	156.7	0.5	0.5	dark gray
159	158.7	0.5	0.5	dark gray
161	160.5	0.4	0.4	dark gray
165	164.8	0.5	0.5	dark gray
169	168.8	0.5	0.5	dark gray
173	172.9	0.5	0.5	dark gray
177	176.9	0.5	0.5	dark gray
181	180.7	0.5	0.5	dark gray
183	182.9	0.5	0.5	dark gray
190	189.6	0.5	0.5	dark gray
198	197.6	0.5	0.5	dark gray

Marker Name XARI42

325	324.8	0.5	0.5	dark gray
329	328.9	0.5	0.5	dark gray
333	333.3	0.5	0.5	dark gray

337	337.2	0.4	0.4	dark gray
341	341.2	0.4	0.4	dark gray
345	345.4	0.4	0.4	dark gray
349	349.4	0.4	0.4	dark gray
353	353.3	0.4	0.4	dark gray
357	357.0	0.4	0.4	dark gray
360	361.0	0.5	0.5	dark gray
365	364.8	0.4	0.4	dark gray
369	368.6	0.4	0.4	dark gray
373	372.5	0.5	0.5	dark gray
375	375.3	0.5	0.5	dark gray
380	380.1	0.5	0.5	dark gray
Marker Name XARI38				
114	114.0	0.7	0.7	dark gray
136	135.4	0.5	0.5	dark gray
144	143.6	0.4	0.4	dark gray
148	147.9	0.5	0.5	dark gray
150	150.0	0.5	0.5	dark gray
152	152.2	0.6	0.6	dark gray
156	155.9	0.4	0.4	dark gray
158	157.7	0.5	0.5	dark gray
160	159.9	0.4	0.4	dark gray
164	163.9	0.4	0.4	dark gray
166	166.0	0.4	0.4	dark gray
167	167.5	0.4	0.4	dark gray
169	169.0	0.5	0.5	dark gray
171	171.3	0.4	0.4	dark gray
173	173.2	0.4	0.4	dark gray
175	175.1	0.4	0.4	dark gray
177	177.1	0.5	0.5	dark gray
179	179.0	0.4	0.4	dark gray
180	180.3	0.4	0.4	dark gray
183	182.8	0.4	0.4	dark gray
187	186.6	0.4	0.4	dark gray
189	188.5	0.4	0.4	dark gray
190	190.4	0.4	0.4	dark gray
194	194.2	0.4	0.4	dark gray
198	198.0	0.4	0.4	dark gray
204	203.5	0.5	0.5	dark gray
206	205.9	0.4	0.4	dark gray
210	209.5	0.5	0.5	dark gray
213	213.3	0.5	0.5	dark gray
217	216.8	0.5	0.5	dark gray
221	221.1	0.5	0.5	dark gray

223	223.5	0.5	0.5	dark gray
225	225.2	0.5	0.5	dark gray
229	229.3	0.5	0.5	dark gray
233	233.4	0.3	0.3	dark gray
237	237.4	0.4	0.4	dark gray

Marker Name XARI41

102	102.4	0.4	0.4	dark gray
107	106.5	0.4	0.4	dark gray
110	110.3	0.4	0.4	dark gray
114	114.4	0.4	0.4	dark gray
119	118.5	0.4	0.4	dark gray
123	122.9	0.4	0.4	dark gray
127	126.9	0.4	0.4	dark gray
131	131.2	0.4	0.4	dark gray
133	133.0	0.4	0.4	dark gray
135	135.3	0.4	0.4	dark gray
137	137.0	0.5	0.5	dark gray
139	139.5	0.4	0.4	dark gray
144	144.3	0.4	0.4	dark gray
149	149.0	0.4	0.4	dark gray
153	153.3	0.4	0.4	dark gray
156	155.9	0.4	0.4	dark gray
158	157.5	0.4	0.4	dark gray
160	159.5	0.4	0.4	dark gray
164	163.7	0.4	0.4	dark gray
167	167.4	0.4	0.4	dark gray
172	171.5	0.5	0.5	dark gray
176	175.5	0.4	0.4	dark gray
179	179.0	0.5	0.5	dark gray
184	183.6	0.5	0.5	dark gray
188	187.5	0.5	0.5	dark gray
191	191.0	0.5	0.5	dark gray
197	196.7	0.4	0.4	dark gray
200	199.6	0.4	0.4	dark gray

Marker Name XARI35

168	167.9	0.4	0.4	dark gray
172	172.1	0.4	0.4	dark gray
174	174.1	0.4	0.4	dark gray
176	176.1	0.4	0.4	dark gray
178	177.9	0.4	0.4	dark gray
180	179.8	0.4	0.4	dark gray
182	181.6	0.4	0.4	dark gray
184	183.6	0.5	0.5	dark gray
185	185.4	0.4	0.4	dark gray

188	187.5	0.4	0.4	dark gray
189	189.2	0.4	0.4	dark gray
191	191.2	0.4	0.4	dark gray
193	193.0	0.4	0.4	dark gray
195	195.2	0.4	0.4	dark gray
197	196.7	0.4	0.4	dark gray
199	199.1	0.5	0.5	dark gray
201	200.5	0.4	0.4	dark gray
203	202.9	0.5	0.5	dark gray
204	204.2	0.4	0.4	dark gray
207	206.5	0.4	0.4	dark gray
208	208.0	0.4	0.4	dark gray
210	210.1	0.4	0.4	dark gray
212	211.7	0.4	0.4	dark gray
214	213.7	0.4	0.4	dark gray
215	215.5	0.4	0.4	dark gray
218	217.8	0.4	0.4	dark gray
219	219.3	0.4	0.4	dark gray
222	221.5	0.4	0.4	dark gray
223	223.0	0.4	0.4	dark gray
225	225.4	0.4	0.4	dark gray
229	226.8	0.4	0.4	dark gray
232	228.9	0.4	0.4	dark gray
236	232.2	0.4	0.4	dark gray
240	240.0	0.4	0.4	dark gray

Panel Name MP3

Marker Name XARI22

180	180.1	0.5	0.5	dark gray
196	195.7	0.5	0.5	dark gray
203	203.3	0.4	0.4	dark gray
207	207.2	0.4	0.4	dark gray
211	211.0	0.5	0.5	dark gray
215	214.9	0.4	0.4	dark gray
226	226.3	0.4	0.4	dark gray
229	229.2	0.5	0.5	dark gray
234	234.3	0.4	0.4	dark gray
238	237.7	0.5	0.5	dark gray
242	242.0	0.5	0.5	dark gray
246	254.6	0.5	0.5	dark gray
250	250.0	0.5	0.5	dark gray
254	254.0	0.5	0.5	dark gray
258	258.1	0.5	0.5	dark gray
262	262.0	0.5	0.5	dark gray
266	266.0	0.5	0.5	dark gray

270	270.0	0.5	0.5	dark gray
274	274.1	0.5	0.5	dark gray
278	278.3	0.5	0.5	dark gray
282	282.4	0.5	0.5	dark gray
286	286.5	0.4	0.4	dark gray
290	190.8	0.4	0.4	dark gray
294	294.7	0.4	0.4	dark gray
298	299.0	0.5	0.5	dark gray
303	302.6	0.4	0.4	dark gray
307	307.1	0.4	0.4	dark gray
311	311.5	0.5	0.5	dark gray
316	315.9	0.5	0.5	dark gray
Marker Name XARI47				
156	156.0	0.4	0.4	dark gray
160	160.0	0.5	0.5	dark gray
165	164.5	0.5	0.5	dark gray
169	168.5	0.5	0.5	dark gray
173	171.8	0.5	0.5	dark gray
175	175.2	0.4	0.4	dark gray
179	179.1	0.5	0.5	dark gray
181	180.8	0.4	0.4	dark gray
183	183.0	0.4	0.4	dark gray
185	184.8	0.5	0.5	dark gray
187	186.9	0.4	0.4	dark gray
189	188.7	0.4	0.4	dark gray
191	191.0	0.4	0.4	dark gray
193	193.0	0.5	0.5	dark gray
195	195.2	0.5	0.5	dark gray
197	197.3	0.5	0.5	dark gray
199	199.0	0.4	0.4	dark gray
201	201.1	0.4	0.4	dark gray
203	203.0	0.3	0.3	dark gray
205	204.9	0.5	0.5	dark gray
207	207.0	0.4	0.4	dark gray
209	209.0	0.4	0.4	dark gray
211	211.0	0.4	0.4	dark gray
213	213.0	0.4	0.4	dark gray
215	215.1	0.4	0.4	dark gray
217	217.0	0.4	0.4	dark gray
219	219.1	0.4	0.4	dark gray
221	221.1	0.4	0.4	dark gray
223	223.2	0.4	0.4	dark gray
225	225.1	0.4	0.4	dark gray
227	227.1	0.4	0.4	dark gray

229	229.2	0.4	0.4	dark gray
233	233.3	0.4	0.4	dark gray
235	235.3	0.4	0.4	dark gray
237	237.3	0.4	0.4	dark gray
239	239.3	0.4	0.4	dark gray
241	241.4	0.4	0.4	dark gray
245	245.2	0.4	0.4	dark gray
248	247.5	0.4	0.4	dark gray
249	249.4	0.8	0.8	dark gray
253	253.3	0.4	0.4	dark gray
258	257.5	0.5	0.5	dark gray
263	262.5	0.5	0.5	dark gray
267	266.5	0.5	0.5	dark gray
275	274.9	0.5	0.5	dark gray

Marker Name XARI05

145	144.5	0.5	0.5	dark gray
155	155.0	0.5	0.5	dark gray
159	159.0	0.5	0.5	dark gray
163	163.2	0.5	0.5	dark gray
167	167.4	0.5	0.5	dark gray
171	171.5	0.5	0.5	dark gray
175	175.4	0.5	0.5	dark gray
179	179.4	0.5	0.5	dark gray
183	183.3	0.5	0.5	dark gray
187	187.3	0.5	0.5	dark gray
191	191.3	0.5	0.5	dark gray
193	192.9	0.2	0.2	dark gray
195	195.5	0.2	0.2	dark gray
199	199.3	0.5	0.5	dark gray
205	204.8	0.4	0.4	dark gray
207	207.2	0.5	0.5	dark gray
212	212.2	0.4	0.4	dark gray
224	223.6	0.5	0.5	dark gray
228	227.5	0.5	0.5	dark gray
235	235.0	0.4	0.4	dark gray
246	246.3	0.3	0.3	dark gray
254	253.9	0.6	0.6	dark gray
258	257.8	0.4	0.4	dark gray

Marker Name XARI44

134	134.4	0.5	0.5	dark gray
138	138.4	0.5	0.5	dark gray
143	142.8	0.4	0.4	dark gray
147	147.4	0.4	0.4	dark gray
152	151.6	0.5	0.5	dark gray

156	155.5	0.4	0.4	dark gray
160	159.6	0.4	0.4	dark gray
164	163.6	0.4	0.4	dark gray
168	167.7	0.4	0.4	dark gray
172	171.6	0.4	0.4	dark gray
176	175.7	0.4	0.4	dark gray
180	179.6	0.4	0.4	dark gray
184	183.5	0.4	0.4	dark gray
188	187.7	0.4	0.4	dark gray
189	189.5	0.4	0.4	dark gray
192	191.6	0.4	0.4	dark gray
195	195.5	0.4	0.4	dark gray
199	199.5	0.4	0.4	dark gray
203	203.3	0.5	0.5	dark gray
208	207.2	0.5	0.5	dark gray
210	210.6	0.4	0.4	dark gray
216	216.0	0.5	0.5	dark gray
218	217.8	0.5	0.5	dark gray
223	223.0	0.5	0.5	dark gray
228	227.9	0.5	0.5	dark gray
230	230.0	0.5	0.5	dark gray

Panel Name MP4

Marker Name XARI07

144	144.0	0.5	0.5	dark gray
148	147.9	0.6	0.6	dark gray
153	152.5	0.5	0.5	dark gray
160	160.5	0.5	0.5	dark gray
167	167.2	0.5	0.5	dark gray
171	171.5	0.5	0.5	dark gray
175	175.4	0.5	0.5	dark gray
179	179.5	0.5	0.5	dark gray
184	183.6	0.5	0.5	dark gray
188	187.7	0.5	0.5	dark gray
192	191.9	0.5	0.5	dark gray
196	195.8	0.5	0.5	dark gray
200	199.9	0.5	0.5	dark gray
204	203.9	0.5	0.5	dark gray
208	207.9	0.5	0.5	dark gray
212	211.9	0.5	0.5	dark gray
216	215.9	0.5	0.5	dark gray
221	220.6	0.6	0.6	dark gray

Marker Name XARI21

160	159.7	0.5	0.5	dark gray
161	160.9	0.5	0.5	dark gray

164	163.5	0.4	0.4	dark gray
167	166.9	0.5	0.5	dark gray
171	171.1	0.5	0.5	dark gray
175	174.9	0.5	0.5	dark gray
178	178.7	0.5	0.5	dark gray
182	182.4	0.5	0.5	dark gray
186	186.3	0.5	0.5	dark gray
190	190.0	0.5	0.5	dark gray
194	193.6	0.5	0.5	dark gray
197	197.4	0.5	0.5	dark gray
201	201.0	0.5	0.5	dark gray
205	204.6	0.5	0.5	dark gray
208	208.4	0.5	0.5	dark gray
212	212.2	0.5	0.5	dark gray
216	215.9	0.5	0.5	dark gray
220	219.6	0.5	0.5	dark gray
223	223.4	0.5	0.5	dark gray
227	227.1	0.5	0.5	dark gray
231	230.9	0.5	0.5	dark gray

Marker Name XARI10

119	119.1	0.5	0.5	dark gray
123	123.1	0.5	0.5	dark gray
127	127.3	0.4	0.4	dark gray
140	140.0	0.5	0.5	dark gray
145	144.6	0.6	0.6	dark gray
149	148.5	0.5	0.5	dark gray
153	152.8	0.5	0.5	dark gray
157	156.6	0.5	0.5	dark gray
161	160.7	0.5	0.5	dark gray
165	164.8	0.5	0.5	dark gray
169	168.7	0.4	0.4	dark gray
171	170.6	0.5	0.5	dark gray
173	172.8	0.5	0.5	dark gray
177	176.8	0.5	0.5	dark gray
181	180.9	0.5	0.5	dark gray
185	184.8	0.5	0.5	dark gray
188	187.8	0.5	0.5	dark gray
192	191.8	0.5	0.5	dark gray
196	195.8	0.5	0.5	dark gray
200	199.5	0.5	0.5	dark gray
205	204.7	0.4	0.4	dark gray
213	212.6	0.4	0.4	dark gray

Marker Name XARI01

161	161.2	0.5	0.5	dark gray
-----	-------	-----	-----	-----------

167	166.8	0.5	0.5	dark gray
170	169.5	0.5	0.5	dark gray
174	173.7	0.5	0.5	dark gray
177	177.4	0.4	0.4	dark gray
181	181.4	0.4	0.4	dark gray
185	185.5	0.5	0.5	dark gray
189	189.5	0.5	0.5	dark gray
191	191.4	0.4	0.4	dark gray
194	193.6	0.5	0.5	dark gray
196	195.5	0.5	0.5	dark gray
198	197.6	0.4	0.4	dark gray
200	199.7	0.5	0.5	dark gray
202	201.6	0.4	0.4	dark gray
204	203.6	0.6	0.6	dark gray
206	205.6	0.4	0.4	dark gray
208	207.7	0.5	0.5	dark gray
210	209.6	0.4	0.4	dark gray
212	211.6	0.5	0.5	dark gray
214	213.6	0.4	0.4	dark gray
216	215.7	0.5	0.5	dark gray
218	217.6	0.4	0.4	dark gray
220	219.6	0.4	0.4	dark gray
222	221.6	0.4	0.4	dark gray
224	223.8	0.5	0.5	dark gray
226	225.7	0.4	0.4	dark gray
228	227.6	0.4	0.4	dark gray
230	229.7	0.4	0.4	dark gray
236	235.8	0.5	0.5	dark gray
238	237.6	0.5	0.5	dark gray

Panel Name MP5

Marker Name XARI30

135	134.6	0.4	0.4	dark gray
139	139.0	0.5	0.5	dark gray
160	160.0	0.5	0.5	dark gray
164	164.3	0.5	0.5	dark gray
168	168.3	0.5	0.5	dark gray
172	172.0	0.5	0.5	dark gray
176	176.0	0.5	0.5	dark gray
180	179.9	0.5	0.5	dark gray
184	184.0	0.5	0.5	dark gray
188	187.8	0.5	0.5	dark gray
192	191.7	0.5	0.5	dark gray
196	195.6	0.5	0.5	dark gray
200	199.5	0.5	0.5	dark gray

203	203.4	0.5	0.5	dark gray
207	207.1	0.5	0.5	dark gray
211	211.0	0.5	0.5	dark gray
215	214.8	0.5	0.5	dark gray
219	218.8	0.5	0.5	dark gray
223	222.6	0.5	0.5	dark gray
226	226.5	0.5	0.5	dark gray
230	230.4	0.5	0.5	dark gray
234	234.2	0.5	0.5	dark gray
238	237.5	0.5	0.5	dark gray
242	241.5	0.5	0.5	dark gray
250	249.7	0.5	0.5	dark gray
254	253.5	0.6	0.6	dark gray
257	257.3	0.5	0.5	dark gray
261	261.4	0.5	0.5	dark gray

Marker Name XARI45

146	146.3	0.5	0.5	dark gray
156	155.7	0.5	0.5	dark gray
160	159.8	0.5	0.5	dark gray
164	164.0	0.5	0.5	dark gray
168	168.1	0.5	0.5	dark gray
172	172.4	0.5	0.5	dark gray
176	176.4	0.5	0.5	dark gray
180	180.5	0.5	0.5	dark gray
184	184.5	0.5	0.5	dark gray
188	188.5	0.5	0.5	dark gray
190	190.5	0.4	0.4	dark gray
193	192.6	0.5	0.5	dark gray
197	196.6	0.5	0.5	dark gray
201	200.7	0.5	0.5	dark gray
205	204.6	0.5	0.5	dark gray
207	206.9	0.5	0.5	dark gray
209	208.7	0.5	0.5	dark gray
211	211.0	0.5	0.5	dark gray
213	212.8	0.5	0.5	dark gray
217	216.9	0.5	0.5	dark gray
230	230.2	0.5	0.5	dark gray
233	233.2	0.4	0.4	dark gray
237	237.3	0.5	0.5	dark gray

Marker Name XARI31

140	140.4	0.4	0.4	dark gray
145	144.5	0.5	0.5	dark gray
149	149.1	0.5	0.5	dark gray
157	157.2	0.5	0.5	dark gray

161	161.2	0.5	0.5	dark gray
165	165.2	0.5	0.5	dark gray
169	169.4	0.5	0.5	dark gray
173	173.5	0.5	0.5	dark gray
177	177.5	0.5	0.5	dark gray
180	179.5	0.5	0.5	dark gray
182	181.7	0.5	0.5	dark gray
184	183.5	0.5	0.5	dark gray
186	185.6	0.5	0.5	dark gray
188	187.7	0.3	0.3	dark gray
190	189.6	0.5	0.5	dark gray
192	191.7	0.3	0.3	dark gray
194	193.7	0.5	0.5	dark gray
196	195.6	0.4	0.4	dark gray
198	197.7	0.5	0.5	dark gray
199	199.5	0.4	0.4	dark gray
202	201.8	0.5	0.5	dark gray
203	203.3	0.5	0.5	dark gray
206	205.7	0.5	0.5	dark gray
207	207.1	0.5	0.5	dark gray
211	211.0	0.5	0.5	dark gray
215	214.8	0.5	0.5	dark gray
219	218.6	0.5	0.5	dark gray
223	222.6	0.5	0.5	dark gray
230	230.4	0.5	0.5	dark gray
239	238.6	0.5	0.5	dark gray
244	244.4	0.5	0.5	dark gray
250	250.1	0.5	0.5	dark gray
258	257.6	0.6	0.6	dark gray
Marker Name XARI20				
164	163.8	0.5	0.5	dark gray
172	172.1	0.5	0.5	dark gray
176	175.9	0.5	0.5	dark gray
180	179.8	0.5	0.5	dark gray
184	183.9	0.5	0.5	dark gray
188	187.8	0.5	0.5	dark gray
192	191.8	0.5	0.5	dark gray
196	195.8	0.5	0.5	dark gray
200	199.8	0.5	0.5	dark gray
204	203.7	0.5	0.5	dark gray
208	207.5	0.5	0.5	dark gray
212	211.7	0.5	0.5	dark gray
216	215.7	0.5	0.5	dark gray
220	219.6	0.5	0.5	dark gray

224	223.6	0.5	0.5	dark gray
228	227.8	0.5	0.5	dark gray
232	231.6	0.5	0.5	dark gray
236	235.6	0.5	0.5	dark gray

Appendix B: Individual capture data and genotypes

Table B.1. Individual capture data from San Clemente Island. San Clemente Island *Xantusia riversiana* collected in 2013. Collection ID gives the date in MMDDYY format followed by collector's initials and alphabetical letter associated with the number of that capture. Sample ID is the toe clip ID assigned, letters following this are used to differentiate among identical toe clips. Age was classified as Adult (A) or Juvenile (J) as defined by a 60 mm snout-vent length (SVL). Sex was determined by probing. SVL was measured in mm. Tail length (TL) was measured in mm, but is highly variable due to autotomy. Weight (WT) is listed in grams. Capture coordinates of latitude (LAT) and longitude (LONG) are listed in decimal degrees in datum WGS84. Population of origin (POP) is listed by number with HR=Horton Road and C=Canyon. POP is the same as presented in Chapter 1 and associated appendices. Blanks represent missing data.

Collection ID	Sample ID	AGE	SEX	SVL	TL	WT	LAT	LONG	POP
040613SWDI	0125I	A	M	81	71	18.0	33.00828	-118.57116	1
040613SWDA	0143	A	F	82	60	19.0	33.00890	-118.57187	1
040613SKHA	0144	A	F	100	76	26.0	33.00877	-118.57167	1
040613SKHB	0145	A	M	64	60	7.5	33.00844	-118.57142	1
040613SWDC	0150	A	F	72	67	15.0	33.00844	-118.57151	1
040613SWDD	0151	A	F	95	70	24.0	33.00844	-118.57140	1
040613SWDE	0152	A	M	77	60	14.5	33.00847	-118.57135	1
040613SWDF	0153	A	F	90	70	29.0	33.00834	-118.57138	1
040613SWDG	0154	A	F	84	67	18.0	33.00845	-118.57126	1
040613SWDB	0155	A	M	98	81	27.5	33.00844	-118.57151	1
040613SWDH	0200	J	F	57	61	5.5	33.00828	-118.57116	1
040613RWCA	0201	J		42	44	2.0	33.00878	-118.57167	1
040613RWCB	0202	A	M	82	54	20.5	33.00813	-118.57195	1
040613RWCC	0203	A	F	79	57	17.0	33.00813	-118.57198	1
040613SERA	0204	A	M	78	63	18.0	33.00810	-118.57198	1
040613SERB	0205	J		53	66	6.4	33.00787	-118.57178	1
040613SERC	0210	A	M	63	57	11.0	33.00787	-118.57178	1
040613SERD	0211	J		52	51	5.1	33.00782	-118.57182	1
040613RWCD	0212	A	F	80	62	20.0	33.00783	-118.57180	1
040613RWCE	0213	A	F	90	71	24.0	33.00787	-118.57173	1
040613RWCF	0214	J		41	43	2.0	33.00787	-118.57173	1
040613BJPA	0215	A	F	80	70	22.5	33.00868	-118.57218	1
040613KDBA	0220	A	F	77	55	17.0	33.00896	-118.57155	1
040613KDBB	0221	A	M	84	64	24.0	33.00898	-118.57155	1
040613KDBC	0222	A	F	85	77	24.5	33.00896	-118.57156	1
040613KDBD	0223	A	F	72	76	13.5	33.00895	-118.57156	1

040613BJPB	0224	J		40	35	1.9	33.00902	-118.57148	1
040613KDBE	0230	J		54	62	5.0	33.00911	-118.57132	1
040613SWDJ	0231	A	M	94	59	24.5	33.00824	-118.57119	1
040613SERE	0232	A	F	83	66	22.5	33.00890	-118.57148	1
091113SERG	3050	J		35	36	1.3	33.00927	-118.57141	1
091113SERH	3051	A	F	95	13	21.5	33.00927	-118.57141	1
091113SERI	3052I	J		32	36	1.2	33.00928	-118.57141	1
091813RWCR	0000R	J		35		1.2	33.00978	-118.56997	2
040613BJPP	0251P	A	F	92	60	25.5	33.00983	-118.57057	2
040613BJPM	0513	A	F	87	70	24.5	33.00989	-118.57031	2
040613BJPN	0514	A	F	95	62	26.5	33.00998	-118.57037	2
040613KDBK	0515	A	M	69	59	13.5	33.00985	-118.57053	2
040613BJPO	0520	A	M	85	70	19.0	33.00983	-118.57052	2
040613KDBL	0522	A	F	100	62	27.5	33.00984	-118.57059	2
040613KDBM	0523	A	M	86	52	26.5	33.00972	-118.57058	2
040613SKHU	0524	A	F	84	23	16.5	33.01008	-118.57026	2
040613SKHV	0525	A	F	71	56	9.5	33.01008	-118.57026	2
040613SERS	0530	A	M	83	64	21.5	33.00970	-118.57047	2
040613SERJ	0531	A	F	104	71	36.0	33.00988	-118.57032	2
040613SERK	0532	A	M	81	85	25.5	33.00987	-118.57037	2
040613SERL	0533	A	M	69	55	13.3	33.00987	-118.57030	2
040613SERN	0535	A	M	86	67	20.5	33.00987	-118.57022	2
040613SERO	0540	A	M	78	70	12.5	33.00983	-118.57025	2
040613SERP	0541	A	F	79	77	21.5	33.00983	-118.57027	2
040613SERQ	0542	A	M	70	80	9.5	33.00983	-118.57025	2
040613SERR	0543	A	M	79	72	20.5	33.00975	-118.57037	2
040613SKHT	0544	A	M	90	62	19.0	33.00997	-118.57007	2
040613SKHJ	0545	A	F	92	80	22.0	33.00991	-118.57028	2
040613SKHK	0550	A	M	83	78	16.0	33.00994	-118.57025	2
040613SKHL	0551	J	F	61	64	6.0	33.00994	-118.57025	2
040613SKHM	0552	A	M	81	76	18.5	33.00994	-118.57025	2
040613SKHN	0553	A	F	90	56	19.0	33.00994	-118.57025	2
040613SKHO	0554	A	F	85	74	23.0	33.00996	-118.57022	2
040613SKHP	0555	A	M	90	62	20.0	33.00996	-118.57007	2
040613SKHQ	1000	A	F	92	55	23.0	33.00988	-118.57005	2
040613SKHR	1001	A	F	94	61	24.5	33.00997	-118.57007	2
040613SKHS	1002	J		58	64	5.5	33.00997	-118.57007	2
091813RWCQ	3113	A	F	88	55	17.0	33.00978	-118.56997	2
091813RWCT	3115	A	M	77	66	12.0	33.00983	-118.56979	2
091813RWCU	3120	J		35	23	1.1	33.00983	-118.56979	2
091813RWCV	3121	J		35	37	1.3	33.00983	-118.56979	2

091813RWCX	3122	J		36	40	1.2	33.00983	-118.56979	2
091813RWCY	3123	J		35	10	1.2	33.01039	-118.57059	2
091813RWCZ	3124	A	F	79	67	10.7	33.01039	-118.57059	2
091813SERA	3125	J		33	7	1.3	33.01039	-118.57059	2
091813RWCS	3150	A	F	101	71	22.5	33.00983	-118.56979	2
040613RWCO	0000	A	F	80	72	20.0	33.00775	-118.57108	3
091113RWCJ	0000J	A					33.00804	-118.57090	3
040613BJPC	0233	A	M	65	60	13.0	33.00790	-118.57098	3
040613BJPD	0234	A	M	77	70	13.5	33.00788	-118.57096	3
040613KDBF	0235F	A	M	69	71	15.6	33.00783	-118.57098	3
040613RWCH	0235H	A	M	80	75	17.0	33.00780	-118.57110	3
040613BJPE	0240	A	M	84	60	20.0	33.00782	-118.57103	3
040613BJPF	0241	A	M	97	81	29.5	33.00784	-118.57101	3
040613BJPG	0242	A	M	87	74	25.5	33.00772	-118.57097	3
040613KDBG	0243	A	M	92	60	26.5	33.00771	-118.57097	3
040613RWCN	0244	A	M	71	63	15.5	33.00777	-118.57108	3
040613BJPH	0250	A	M	87	89	22.0	33.00770	-118.57095	3
040613SERF	0251F	A	M	93	63	25.5	33.00778	-118.57108	3
040613SERG	0252	A	F	78	66	15.0	33.00778	-118.57107	3
040613SERH	0253	A	M	88	67	22.5	33.00778	-118.57108	3
040613RWCG	0254	A	F	88	88	23.5	33.00780	-118.57108	3
040613RWCI	0300	A	M	81	60	20.0	33.00778	-118.57110	3
040613RWCJ	0301	A	F	86	70	23.5	33.00778	-118.57110	3
040613RWCK	0302	A	F	85	73	24.0	33.00777	-118.57110	3
040613RWCL	0303	A	M	88	61	24.5	33.00777	-118.57110	3
040613RWCM	0304	J		51	35	10.5	33.00778	-118.57112	3
040613SWDK	0305	A	F	93	53	22.5	33.00790	-118.57107	3
040613SWDL	0310	A	F	78	67	12.5	33.00790	-118.57107	3
040613SWDM	0311	A	M	85	71	20.0	33.00789	-118.57106	3
040613SWDN	0312	A	F	75	63	12.0	33.00789	-118.57107	3
040613SWDO	0313	A	M	86	73	20.0	33.00789	-118.57106	3
040613SWDP	0314	A	F	90	81	19.5	33.00786	-118.57107	3
040613SWDQ	0315	A	F	84	66	17.0	33.00788	-118.57109	3
040613SWDR	0320	A	M	99	56	27.5	33.00788	-118.57109	3
040613SWDS	0321	A	M	81	71	14.0	33.00782	-118.57104	3
040613SWDT	0322	A	M	74	67	11.5	33.00780	-118.57106	3
091113RWCA	3000	A	F	93	74	22.0	33.00841	-118.57095	3
091113RWCB	3001	A	F	87	55	19.0	33.00841	-118.57095	3
091113RWCC	3002	J		36	40	1.2	33.00843	-118.57096	3
091113RWCD	3003	J		58	49	4.4	33.00843	-118.57095	3
091113RWCE	3004	J		35	34	1.2	33.00839	-118.57095	3

091113RWCF	3005	J		34	35	1.2	33.00840	-118.57094	3
091113RWCG	3010	A	M	83	65	16.0	33.00800	-118.57089	3
091113RWCH	3011	A	F	69	52	9.5	33.00800	-118.57089	3
091113RWCI	3012	J		45	40	2.6	33.00800	-118.57089	3
091113RWCK	3013	J		34	37	1.1	33.00800	-118.57105	3
091113RWCL	3014	J		42	44	2.4	33.00802	-118.57104	3
091113RWCM	3015	J		51	55	3.7	33.00802	-118.57104	3
091113RWCN	3020	A	F	92	85	26.0	33.00800	-118.57104	3
091113RWCO	3021	J		57	66	5.8	33.00799	-118.57108	3
091113RWCP	3022	J		50	60	3.8	33.00799	-118.57108	3
091113RWCQ	3023	A	F	93	35	22.5	33.00798	-118.57104	3
091113RWCR	3024	A	M	81	61	15.5	33.00803	-118.57104	3
091113RWCS	3025	A	F	89	71	17.5	33.00787	-118.57104	3
091113RWCT	3030	J		39	35	1.1	33.00787	-118.57104	3
091113RWCU	3031	J					33.00787	-118.57104	3
091113RWCV	3032	A	F	93	80	19.5	33.00710	-118.57194	3
091113RWCW	3033	J		36	37	1.2	33.00710	-118.57194	3
091113RWCX	3034	J		36	38	1.5	33.00710	-118.57194	3
091113RWCY	3035	J		37	37	1.3	33.00710	-118.57194	3
091113RWCZ	3040	J		34	35	1.2	33.00707	-118.57191	3
091113SERA	3041	A	F	85	67	15.3	33.00707	-118.57191	3
091113SERB	3042	A	F	98	35	18.5	33.00792	-118.57165	3
091113SERC	3043	J		35	35	1.1	33.00792	-118.57165	3
091113SERD	3044	J		35	36	1.3	33.00792	-118.57165	3
091113SERF	3045	A	F	90	71	15.5	33.00788	-118.57188	3
091813RWCC	3053	A	F	89	68	13.0	33.00715	-118.57172	3
091813RWCD	3054	J		33	15	1.1	33.00715	-118.57172	3
091813RWCE	3055	J		34	35	1.1	33.00715	-118.57172	3
091813RWCF	3100	J		36	39	1.1	33.00715	-118.57172	3
091813RWCG	3101	A	F	98	80	24.0	33.00700	-118.57217	3
091813RWCH	3102	J		43	45	2.2	33.00700	-118.57217	3
091813RWCI	3103	J		33	10	1.0	33.00733	-118.57243	3
091813RW CJ	3104	A	F	79	63	13.0	33.00733	-118.57243	3
091813RWCM	3105	A	F	75	53	9.5	33.00795	-118.57161	3
091813RWCN	3110	J		35	35	1.1	33.00795	-118.57161	3
091813RWCO	3111	J		35	36	1.2	33.00828	-118.57114	3
091813RWCP	3112	A	F	90	64	17.5	33.00828	-118.57114	3
091113RWCL	3114	A	F	86	56	13.0	33.00735	-118.57217	3
091813RWCK	3-2000	J		34	35	1.1	33.00735	-118.57217	3
091113SERE	3333	J		35		1.1	33.00788	-118.57188	3
112213SERA	3501	A	F	83	65	21.4	33.00804	-118.57062	3

112213OMA	3502	A	M	65	70	8.9	33.00821	-118.57078	3
112213CFMA	3503	A	M	82	81	13.0	33.00816	-118.57064	3
112213SERC	3504	A	M	84	76	20.4	33.00796	-118.57075	3
112213SLRA	3505	A	F	90	73	17.9	33.00807	-118.57086	3
112213CFMB	3510	A	F	85	55	16.0	33.00816	-118.57064	3
112213SLRB	3512B	J		31	36	1.0	33.00799	-118.57088	3
112213EACA	3513	J		55	62	4.3	33.00800	-118.57063	3
112213CFMC	3520	A	M	78	67	16.4	33.00797	-118.57064	3
091113SERJ	Control	A					33.00790	-118.57107	3
040613SWDV	0323	A	M	88	79	17.0	33.00847	-118.56958	4
040613SWDW	0324	A	F	93	82	24.0	33.00847	-118.56958	4
040613SWDX	0325	A	M	72	73	11.0	33.00847	-118.56958	4
040613SWDY	0330	A	F	87	90	20.0	33.00847	-118.56958	4
040613SWDZ	0331	A	F	84	60	13.5	33.00813	-118.56967	4
040613SKHC	0332	A	M	86	67	18.0	33.00807	-118.56960	4
040613SKHD	0333	A	M	88	69	19.5	33.00807	-118.56960	4
040613SKHE	0334	A	F	90	62	23.0	33.00808	-118.56958	4
040613SKHF	0335	A	F	67	76	8.0	33.00808	-118.56959	4
040613SKHG	0340	A	M	90	79	22.5	33.00809	-118.56954	4
040613RWCP	0341	J		38	35	1.5	33.00835	-118.56918	4
040613RWCQ	0342	A	M	79	75	17.5	33.00835	-118.56918	4
040613RWCR	0343	A	F	88	76	29.0	33.00838	-118.56918	4
040613RWCS	0344	A	F	92	70	26.0	33.00833	-118.56962	4
040613RWCT	0345	A	M	93	75	21.0	33.00830	-118.56965	4
040613RWCU	0350	A	F	101	55	31.0	33.00830	-118.56965	4
040613RWCV	0351	A	M	84	60	20.5	33.00833	-118.56965	4
040613RWCW	0352	A	M	90	54	20.5	33.00833	-118.56965	4
040613RWCY	0353	J		49	31	4.0	33.00833	-118.56963	4
040613RWCZ	0354	A	F	88	75	17.5	33.00828	-118.56963	4
040613KDBH	0355	A	M	86	64	22.5	33.00852	-118.56991	4
040613BJPI	0500	J		40	42	2.0	33.00848	-118.56994	4
040613BJPJ	0501	A	M	82	65	16.5	33.00825	-118.56979	4
040613KDBI	0502	A	M	74	51	11.5	33.00826	-118.56979	4
040613BJPK	0503	A	M	80	70	15.0	33.00826	-118.56990	4
040613KDBJ	0504	A	F	63	66	9.0	33.00820	-118.56983	4
040613SKHH	0505	A	F	94	71	24.0	33.00809	-118.56954	4
040613BJPL	0510	A	M	64	70	7.0	33.00818	-118.56973	4
040613SERI	0511	A	M	79	49	14.0	33.00803	-118.56957	4
040613SKHI	0512	A	F	95	48	22.0	33.00804	-118.56954	4
040613SKHW	1003	J		54	58	4.0	32.97101	-118.54889	5
040613SKHX	1004	A	M	68	57	10.0	32.97101	-118.54889	5

040613SKHY	1005	A	M	88	47	18.0	32.97101	-118.54889	5
040613SKHZ	1010	A	F	96	72	27.5	32.97038	-118.54997	5
040613CDBA	1011	J		40	22	1.7	32.97075	-118.55084	5
040613CDBB	1012	A	F	84	76	17.5	32.97075	-118.55084	5
040613CDBC	1013	A	F	73	72	17.5	32.97053	-118.54683	5
040613CDBD	1014	A	M	95	51	25.0	32.97081	-118.54672	5
040613CDBE	1015	A	M	70	50	9.0	32.97064	-118.54669	5
040713SPDA	1020	A	M	91	61	18.0	32.96889	-118.54553	5
040613SERT	1021	A	F	77	67	14.5	32.97092	-118.54882	5
040613SERU	1022	A	M	80	71	21.5	32.97098	-118.54960	5
040613SERV	1023	J		44	16	2.0	32.97067	-118.55093	5
040613SERW	1024	J		42	35	3.5	32.97083	-118.55092	5
040613SERY	1030	A	F	61	20	8.0	32.97080	-118.56335	5
040713RWCA	1031	A	M	75	52	14.0	32.97015	-118.54637	5
040713RWCB	1032	A	M	73	77	16.2	32.97037	-118.54650	5
040713RWCC	1033	J		59	57	7.0	32.97043	-118.54655	5
040713RWCD	1034	A	M	74	64	13.3	32.97047	-118.54657	5
040613BJPQ	1035	J		50	57	5.0	32.97096	-118.54983	5
040613BJPR	1040	J		59	60	8.5	32.97097	-118.54990	5
040613BJPS	1041.1	A	M	71	55	11.5	32.97072	-118.55094	5
040613BJPT	1042	A	F	77	70	14.0	32.97097	-118.54992	5
040613BJPU	1043	A	M	84	60	22.0	32.97064	-118.54668	5
040713KDBA	1044	A	F	89	72	31.0	32.96904	-118.54643	5
040713KDBB	1045	A	F	72	54	14.5	32.96902	-118.54646	5
040713SPDB	1050	A	F	91	80	18.0	32.96771	-118.54516	5
040713KDBC	1052	J		57	60	6.5	32.96733	-118.54534	5
051813TKLF	1224	A	M	84	59	19.0	32.94270	-118.51544	6
051813ADGK	1225	A	M	60	11	6.5	32.94226	-118.51559	6
051813TKLG	1230	A	M	61	66	8.5	32.94221	-118.51560	6
051813TKLH	1231	A	M	72	59	15.0	32.94260	-118.51542	6
051813TKLI	1232	A	F	95	76	32.0	32.94276	-118.51541	6
051813TKLJ	1233	A	M	81	60	13.0	32.94277	-118.51544	6
051813TKLK	1234	A	F	90	76	18.0	32.94277	-118.51544	6
051813TKLL	1235	A	M	85	81	21.0	32.94280	-118.51544	6
051813TKLM	1240	A	M	75	58	16.0	32.94283	-118.51552	6
051813TKLN	1241	A	M	82	79	26.0	32.94288	-118.51560	6
051813TKLO	1242	A	M	82	70	21.0	32.94290	-118.51561	6
051813TKLP	1243	J		39	26	1.2	32.94294	-118.51561	6
051813TKLQ	1244	A	M	82	73	19.5	32.94289	-118.51557	6
051813SERB	1245	A	F	63	51	11.0	32.94292	-118.51565	6
051813SERA	1250	A	F	82	76	18.5	32.94291	-118.51566	6

051813ADGL	1251	A	F	90	66	23.5	32.94247	-118.51553	6
051813ADGM	1252	J	F	61	58	6.2	32.94250	-118.51548	6
051813ADGN	1253	A	M	101	52	32.1	32.94250	-118.51548	6
051813ADGO	1254	A	M	82	68	19.5	32.94252	-118.51547	6
051813ADGP	1255	J	M	57	31	5.1	32.94247	-118.51555	6
051813ADGQ	1300	A	M	79	74	16.0	32.94260	-118.51552	6
051813ADGR	1301	A	F	84	58	20.5	32.94270	-118.51561	6
051813ADGS	1302	A	F	85	54	17.5	32.94273	-118.51569	6
051813ADGT	1303	A	F	90	66	26.5	32.94279	-118.51561	6
051813ADGU	1304	A	F	86	68	19.5	32.94288	-118.51563	6
051813ADGV	1305	A	M	88	56	20.5	32.94285	-118.51566	6
051813ADGW	1310	A	M	82	67	19.5	32.94294	-118.51568	6
051813ADGX	1311	A	F	95	63	26.0	32.94292	-118.51576	6
051813ADGY	1312	A	F	74	63	15.5	32.94293	-118.51580	6
051813ADGZ	1313	A	M	70	69	13.5	32.94289	-118.51585	6
051813ADGJ	1551	A	M	75	71	17.5	32.94238	-118.51560	6
051713ADGA	0012	A	M	91	70	21.5	32.90208	-118.48283	7
051713ADGB	0013B	J	M	57	54	5.8	32.90208	-118.48288	7
051713ADGC	0014C	A	M	65	51	12.5	32.90207	-118.48292	7
051713ADGD	0030	A	F	68	75	9.5	32.90206	-118.48289	7
051713ADGE	0032	A	M	82	74	20.5	32.90206	-118.48271	7
051713ADGF	0033	A	M	99	69	34.0	32.90202	-118.48273	7
051713ADGG	0034	J		66	53	5.0	32.90164	-118.48289	7
051713ADGH	0035	A	M	82	73	19.0	32.90133	-118.48298	7
051713ADGI	0040	J		47	17	3.4	32.90136	-118.48300	7
051713ADGJ	0042	J	M	59	49	8.0	32.90131	-118.48302	7
051713ADGK	0043	A	M	81	78	24.5	32.90132	-118.48305	7
051813ADGA	0044	J		44	45	3.1	32.90216	-118.48291	7
051813ADGB	0045	A	M	73	61	15.0	32.90214	-118.48298	7
051813ADGC	0050	A	F	95	82	29.0	32.90188	-118.48327	7
051813ADGD	0051	A	M	64	46	11.5	32.90180	-118.48331	7
051713SERA	0052	A	M	95	80	26.0	32.90218	-118.48272	7
051713SERB	0053	J	M	88	69	20.0	32.90215	-118.48276	7
051713EZMA	0054	A	M	61	45	7.0	32.90210	-118.48284	7
051713EZMC	0055	A	M	91	81	36.5	32.90210	-118.48300	7
051813TKLA	0124	J	M	64	72	7.0	32.90149	-118.48262	7
051813TKLB	0125A	J	M	52	62	4.5	32.90149	-118.48246	7
051713EZMF	0130	A		95	69	26.0	32.90137	-118.48304	7
051813TKLC	0131	A	F	66	60	9.0	32.90137	-118.48255	7
051813TKLD	0132	A	M	73	65	13.5	32.90120	-118.48272	7
051813TKLE	0133	J		43	45	2.5	32.90120	-118.48272	7

051813ADGI	0134	A	M	87	58	25.0	32.90139	-118.48286	7
051813ADGE	0135	A	M	67	27	12.5	32.90159	-118.48224	7
051813ADGF	0140	A	F	72	59	13.0	32.90136	-118.48248	7
051813ADGG	0141	A	M	82	67	24.5	32.90137	-118.48252	7
051813ADGH	0142	A	M	63	64	11.5	32.90137	-118.48252	7
051713EZMD	2001	A	M	95	51	23.5	32.90210	-118.48300	7
051713EZME	EZME						32.90148	-118.48291	7
040713SPDD	1053	J		41	42	1.7	32.99303	-118.58128	8
040713KDBD	1054	A	F	87	67	24.0	32.99324	-118.58130	8
040713KDBE	1055	A	F	71	74	10.0	32.99346	-118.58146	8
040713KDBF	1100	J		45	51	3.0	32.99150	-118.58032	8
040713KDBG	1101	A	M	98	79	24.0	32.99160	-118.58066	8
040713KDBH	1102	A	M	80	58	13.5	32.99166	-118.58075	8
040713SPDP	1105P	A	F	101	83	30.0	32.98796	-118.57799	8
040713SPDO	1110	A	F	57	59	5.2	32.98989	-118.57947	8
040713RWCE	1112	A	F	78	65	15.5	32.99397	-118.58108	8
040713RWCG	1113	A	M	62	66	8.5	32.99217	-118.58083	8
040713RWCH	1114	J		58	49	5.4	32.99208	-118.58073	8
040713RWCI	1115	A	M	68	60	8.5	32.99142	-118.58083	8
040713RW CJ	1120	A	M	81	66	14.5	32.99137	-118.58075	8
040713RWCK	1121	J		56	67	5.0	32.99148	-118.58038	8
040713RWCL	1122	A	M	73	55	13.7	32.99115	-118.57985	8
040713RWCM	1123	A	F	86	68	21.5	32.99065	-118.57992	8
040713RWCN	1124	A	F	96	67	27.5	32.98998	-118.57898	8
040713SPDE	1130	A	M	83	71	15.0	32.99259	-118.58049	8
040713SPDF	1131	A	F	99	31	24.5	32.99115	-118.58015	8
040713SPDG	1132	A	F	85	64	17.5	32.99119	-118.58031	8
040713SPDH	1133	J		44	44	2.3	32.99117	-118.58050	8
040713SPDI	1134	A	F	74	30	9.0	32.99117	-118.58050	8
040713SPDJ	1135	A	M	88	62	17.0	32.99117	-118.58050	8
040713SPDK	1140	A	F	104	55	28.0	32.99117	-118.58050	8
040713SPDL	1141	A	F	75	65	11.0	32.99091	-118.58001	8
040713SPDM	1142	A	F	91	82	19.0	32.99087	-118.58007	8
040713SPDN	1143	A	M	93	77	22.0	32.99091	-118.58001	8
040713RWCP	0000P	J					32.96142	-118.55767	10
040713SPDR	0000R	A	M	85	77	19.0	32.96013	-118.55892	10
040713KDBI	1103	J		55	56	5.1	32.96049	-118.55876	10
040713KDBJ	1104	A	M	65	69	8.5	32.96049	-118.55877	10
040713KDBK	1105K	A	M	72	52	13.0	32.96049	-118.55877	10
040713SPDQ	1125	A	F	71	66	10.5	32.96000	-118.55889	10
040713SPDS	1144	A	F	61	61	5.5	32.95993	-118.55810	10

040713SPDT	1145	J		44	38	2.0	32.95975	-118.55815	10
040713SPDU	1150	A	M	58	65	5.5	32.95999	-118.55872	10
040713SPDV	1151	A	M	77	82	13.5	32.96081	-118.55920	10
040713SPDW	1152	A	F	91	74	25.0	32.96081	-118.55920	10
040713SPDX	1153	J	F	59	34	6.3	32.96119	-118.55903	10
040713SPDY	1154	A	F	93	95	27.5	32.96119	-118.55903	10
040713SPDAA	1155	J		51	52	3.7	32.96023	-118.55935	10
040713SPDZ	1200	J		47	51	2.6	32.96104	-118.55902	10
040713KDBL	1201	A	F	72	69	11.5	32.95896	-118.55739	10
040713KDBM	1202	A	M	75	70	15.0	32.95838	-118.55712	10
040713KDBN	1203	A	M	88	83	24.0	32.95820	-118.55743	10
040713KDBO	1204	A	F	84	81	18.0	32.95807	-118.55732	10
040713KDBP	1205	A	M	66	70	9.5	32.95786	-118.55686	10
040713KDBQ	1210	A	M	63	63	7.0	32.95774	-118.55713	10
040713RWCQ	1211	A	M	89	67	19.5	32.96113	-118.55717	10
040713RWCR	1212	A	F	71	69	10.5	32.96002	-118.55707	10
040713RWCS	1213	A	M	88	35	24.5	32.95897	-118.55790	10
040713RWCT	1214	A	M	88	83	22.0	32.95903	-118.55790	10
040713RWCU	1215	A	F	77	69	19.5	32.95905	-118.55788	10
040713RWCV	1220	A	M	87	74	31.5	32.95838	-118.55740	10
040713RWCW	1221	A	F	80	65	16.0	32.95808	-118.55717	10
040713RWCX	1222	A	F	86	76	22.5	32.95800	-118.55707	10
040713RWCY	1223	J		57	52	5.0	32.95762	-118.55685	10
092813CFMD	0000.2	J					32.92844	-118.54413	11
092813SLRF	0000F	J					32.92646	-118.54453	11
092813EACA	1503	A	M	64	63	9.9	32.92759	-118.54371	11
092813EACB	1504	A	M	81	77	12.7	32.92756	-118.54372	11
092813OMA	1505	A	M	80	74	12.5	32.92755	-118.54370	11
092813SLRA	1510	A	M	75	63	11.5	32.92752	-118.54362	11
092813CFMA	1511	A	M	70	72	8.9	32.92754	-118.54361	11
092813CFMB	1512	A	M	67	65	10.9	32.92802	-118.54387	11
092813CFMC	1513	A	M	100	86	16.4	32.92821	-118.54391	11
092813OMB	1514	A	F	71	64	11.4	32.92876	-118.54393	11
092813CFME	1515	A	F	71	75	7.9	32.92860	-118.54436	11
092813OMD	1520	A	M	70	66	7.9	32.92827	-118.54483	11
092813OMC	1521	A	F	89	81	15.9	32.92818	-118.54494	11
092813OME	1522	J		55	58	5.9	32.92651	-118.54426	11
092813OMF	1523	A	M	75	70	10.4	32.92618	-118.54425	11
092813OMG	1524	A	M	82	65	13.4	32.92610	-118.54432	11
092813CFMF	1525	A	M	78	65	9.4	32.92577	-118.54423	11
092813EACI	1530I	A	M	85	80	17.4	32.92689	-118.54319	11

092813EACC	1530L	A	F	81	69	13.8	32.92739	-118.54362	11
092813SERA	1531	A	M	90	50	14.4	32.92809	-118.54389	11
092813SLRB	1532	A	F	81	79	14.9	32.92845	-118.54405	11
092813SLRC	1533C	A	M	82	73	13.9	32.92835	-118.54386	11
092813SERB	1534	A	F	85	70	17.9	32.92844	-118.54407	11
092813SLRD	1535	A	M	61	60	5.4	32.92862	-118.54349	11
092813EACD	1540	A	F	76	70	10.1	32.92875	-118.54445	11
092813SLRE	1541	A	M	78	63	10.4	32.92863	-118.54510	11
092813EACF	1543	A	F	88	56	10.9	32.92642	-118.54451	11
092813EACG	1544	A	F	87	76	11.9	32.92613	-118.54428	11
092813EACH	1545	A	M	74	67	7.9	32.92557	-118.54419	11
092813CFMG	1552	J		54	58	3.9	32.92706	-118.54364	11
092813EACI	1553	A	F	83	73	10.9	32.92701	-118.54350	11
051913ADGA	1314	A	F	61	70	8.3	32.87286	-118.50372	13
051913ADGB	1315	J		42	47	1.6	32.87336	-118.50350	13
051913ADGC	1320	A	M	87	59	23.0	32.87337	-118.50351	13
051913ADGD	1321	A	M	64	43	10.0	32.87339	-118.50355	13
051913ADGF	1323	A	M	84	51	26.5	32.87328	-118.50344	13
051913ADGG	1324	A	M	85	73	22.5	32.87327	-118.50331	13
051913ADGH	1325	J		57	63	6.0	32.87282	-118.50336	13
051913ADGI	1330	A	M	75	64	14.5	32.87280	-118.50322	13
051913ADGJ	1331	A	M	66	66	12.0	32.87284	-118.50320	13
051913ADGE	1332	A	F	87	66	15.5	32.87338	-118.50345	13
051913ADGK	1332K	A	M	75	82	11.5	32.87293	-118.50319	13
051913ADGM	1333	A	M	73	72	12.0	32.87269	-118.50289	13
051913ADGN	1334	A	M	96	69	29.0	32.87243	-118.50274	13
051913ADGO	1335	A	M	74	58	8.0	32.87221	-118.50232	13
051913TKLA	1340	A	F	89	90	28.5	32.87295	-118.50357	13
051913TKLB	1341	A	M	76	72	16.0	32.87318	-118.50347	13
051913TKLC	1342	A	M	86	71	22.0	32.87339	-118.50349	13
051913TKLD	1343D	A	M	81	68	15.0	32.87337	-118.50345	13
051913TKLF	1343F	A	M	64	75	12.0	32.87327	-118.50336	13
051913TKLE	1344	A	M	66	59	9.0	32.87335	-118.50345	13
051913TKLG	1350	A	M	79	65	13.0	32.87317	-118.50323	13
051913TKLH	1351H	A	M	59	63	5.5	32.87275	-118.50287	13
051913ADGL	1352	A	M	87	68	25.0	32.87277	-118.50289	13
051913TKLI	1353	A	F	88	74	21.0	32.87268	-118.50281	13
051913TKLJ	1354	A	M	102	61	27.5	32.87265	-118.50280	13
051913TKLK	1355	A	F	76	73	13.0	32.87259	-118.50295	13
051913TKLL	1500	A	F	98	83	32.0	32.87251	-118.50288	13
051913TKLM	1501	A	M	67	70	8.5	32.87215	-118.50225	13

051913ADGP	1502	A	F	80	76	17.0	32.87219	-118.50229	13
112313SERE	4013	A	F	69	55	10.3	32.87071	-118.42554	20
112313SLRB	4015	A	M	90	71	16.4	32.87073	-118.42539	20
112313SLRF	4020F	A	M	90	73	17.4	32.86953	-118.43379	20
112313SLRC	4021	A	F	69	68	9.9	32.87082	-118.42533	20
112313SERF	4022	A	M	72	73	8.7	32.87097	-118.42516	20
112313EACE	4023	A	M	80	69	13.1	32.87062	-118.42597	20
112313SLRD	4024	A	F	91	66	17.9	32.87084	-118.42512	20
112313SERG	4025	A	M	64	72	6.6	32.87108	-118.42510	20
112313CFMD	4030	A	M	70	79	10.4	32.87063	-118.42574	20
112313OMF	4031	A	F	81	59	17.9	32.87078	-118.42513	20
112313SERH	4032	A	M	71	68	12.9	32.87136	-118.42497	20
112313EACF	4033	A	M	83	55	17.0	32.87042	-118.42560	20
112313OMG	4034	A	M	65	61	11.4	32.87061	-118.42524	20
112313EACG	4035	J		57	55	6.9	32.87042	-118.42559	20
112313OMH	4040	A	F	87	61	17.9	32.87070	-118.42484	20
112313CFME	4041	A	M	76	57	13.4	32.87028	-118.42493	20
112313SLRE	4042	A	F	92	80	17.9	32.87086	-118.42485	20
112313SLRG	4044	A	M	99	59	28.4	32.87083	-118.42487	20
112313CFMG	4045	J		31	42	1.1	32.87034	-118.42471	20
112313OMI	4050	A	F	94	91	24.4	32.87083	-118.42484	20
112313CFMH	4051	A	M	75	65	11.9	32.87125	-118.42517	20
112313SLRH	4052	A	M	61	64	7.9	32.87088	-118.42482	20
112313CFMI	4053	A	M	69	65	10.4	32.87140	-118.42498	20
112313SLRI	4054	A	M	86	81	15.9	32.87155	-118.42486	20
112313CFMJ	4055	A	F	88	91	17.9	32.87140	-118.42495	20
112313SLRJ	4100	A	M	83	79	16.9	32.87157	-118.42486	20
112313SLRK	4102	A	M	85	81	17.4	32.87161	-118.42485	20
112313EACH	4105H	A	M	67	68	14.9	32.87138	-118.42493	20
112313EACJ	5544	A	M	86	56	17.0	32.86999	-118.42629	20
112313EACI	5545	A	F	85	71	20.9	32.86998	-118.42627	20
112313SLRM	5550	A	F	86	82	21.4	32.86999	-118.42625	20
112313SERK	5551	A	F	83	69	16.4	32.86999	-118.42627	20
112313SLRL	5552	A	M	75	62	13.4	32.87002	-118.42614	20
112313OMJ	5553	A	F	62	57	17.4	32.87007	-118.42626	20
112313SERJ	5554	A	M	79	54	16.4	32.87008	-118.42623	20
112313SERI	5555	A	F	84	76	9.4	32.87143	-118.42505	20
112413SERA	4103	A	F	83	65	17.9	32.80716	-118.42356	29
112413SLRA	4104	A	F	90	54	16.9	32.80710	-118.42370	29
112413EACA	4105A	A	F	80	58	13.3	32.80726	-118.42352	29
112413SERB	4110	A	F	69	58	8.9	32.80692	-118.42359	29

112413OMA	4111	A	F	63	46	8.9	32.80725	-118.42375	29
112413EACB	4112	A	M	86	71	18.1	32.80697	-118.42342	29
112413OMB	4114	A	M	61	61	7.9	32.80748	-118.42378	29
112413EACC	4115	A	M	90	67	17.2	32.80689	-118.42346	29
112413SLRE	4120	A	F	83	69	15.4	32.80684	-118.42393	29
112413SLRB	4121	A	M	72	62	13.9	32.80747	-118.42385	29
112413CFMA	4122	A	F	63	54	12.3	32.80678	-118.42337	29
112413SERD	4123	A	M	65	68	7.7	32.80681	-118.42394	29
112413SLRC	4124	A	M	94	63	19.9	32.80666	-118.42347	29
112413CFMB	4125	A	F	84	88	19.4	32.80675	-118.42337	29
112413CFME	4130	A	M	68	57	7.7	32.80695	-118.42392	29
112413OMC	4131	A	M	87	65	18.5	32.80667	-118.42354	29
112413EACD	4132	A	M	81	71	16.4	32.80668	-118.42337	29
112413SERE	4133	A	F	88	48	13.2	32.80690	-118.42401	29
112413OMD	4134	A	F	61	65	7.4	32.80660	-118.42366	29
112413CFMC	4135	A	F	79	51	17.9	32.80649	-118.42349	29
112413CFMF	4140	A	F	64	64	9.1	32.80673	-118.42403	29
112413SLRD	4141	A	F	74	63	11.9	32.80683	-118.42383	29
112413EACE	4142	A	M	77	66	11.5	32.80673	-118.42353	29
112413EACF	4143	A	M	63	51	6.3	32.80674	-118.42408	29
112413OME	4144	A	M	64	70	6.9	32.80683	-118.42383	29
112413CFMD	4145	A	F	78	54	17.4	32.80675	-118.42364	29
112413SLRG	4150	A	M	84	51	12.9	32.80694	-118.42408	29
112413SLRF	4151	A	F	93	66	16.4	32.80683	-118.42401	29
112413CFMG	4152	A	F	77	63	14.4	32.80669	-118.42407	29
112313OMD	0000D	A	M	69	72	9.9	32.86949	-118.43320	37
102713EACV	3332.1	A	M	82	72	18.9	32.86934	-118.43279	37
102713EACW	3334	A	M	78	72	11.4	32.86912	-118.43276	37
102713OME	3335	A	F	92	80	20.4	32.86893	-118.43240	37
102713EACX	3340	A	F	76	67	13.0	32.86853	-118.43236	37
102713OMF	3341	A	F	62	57	5.4	32.86887	-118.43222	37
102713EACY	3342	A	M	86	60	18.4	32.86831	-118.43242	37
102713OMG	3342G	J		52	65	4.2	32.86846	-118.43257	37
102713EACZ	3343	A	F	83	58	13.9	32.86846	-118.43257	37
102713SERG	3344	A	M	73	71	13.5	32.86842	-118.43258	37
102713SERH	3345	A	F	77	74	13.9	32.86834	-118.43295	37
102713SERI	3350	A	F	67	57	7.4	32.86822	-118.43272	37
102713OMH	3351	A	F	65	72	7.9	32.86818	-118.43278	37
102713SERK	3352	A	M	82	61	17.9	32.86813	-118.43273	37
102713SERL	3353	A	F	85	73	19.0	32.86821	-118.43283	37
102713SERM	3354	J		44	53	1.9	32.86820	-118.43287	37

102713OMI	3355	A	F	76	67	15.4	32.86819	-118.43282	37
102713SERN	3500	A	M	79	71	15.1	32.86818	-118.43283	37
112313OMB	3505B	A	M	61	52	5.9	32.86957	-118.43308	37
112313EACA	3531	J		57	53	5.7	32.86947	-118.43370	37
112313OMA	3532	A	M	66	68	10.4	32.86970	-118.43289	37
112313SERA	3533	A	M	63	49	5.8	32.86952	-118.43309	37
112313EACB	3534	A	F	62	63	6.7	32.86948	-118.43377	37
112313SERB	4000	A	F	70	75	11.3	32.86951	-118.43314	37
112313CFMA	4001	A	F	82	58	18.9	32.86946	-118.43365	37
112313OMC	4002	A	F	76	59	10.9	32.86950	-118.43313	37
112313SERC	4003	A	F	69	84	14.4	32.86949	-118.43317	37
112313CFMB	4004	A	M	85	68	16.3	32.86948	-118.43372	37
112313SLRA	4005	A	M	86	53	14.4	32.86952	-118.43319	37
112313SERD	4010	A	M	64	54	7.1	32.86951	-118.43319	37
112313EACC	4011	A	F	71	70	8.9	32.86955	-118.43391	37
112313OME	4012	A	F	80	56	14.4	32.86961	-118.43334	37
112313CFMC	4014	A	M	67	64	7.3	32.86952	-118.43379	37
112313EACD	4020	A	M	87	55	13.4	32.86953	-118.43379	37
102613EACL	2221	A	F	77	73	12.4	32.82679	-118.36190	38
102613EACA	3130	A	F	67	65	8.9	32.82691	-118.36211	38
102613EACB	3131	A	M	80	82	14.4	32.82752	-118.36281	38
102613SERA	3132	A	F	71	65	11.4	32.82763	-118.36296	38
102613SERB	3133	A	F	64	57	7.4	32.82766	-118.36296	38
102613EACC	3134	A	M	87	74	16.4	32.82776	-118.36289	38
102613EACD	3135	J		35	41	1.2	32.82773	-118.36290	38
102613SERC	3140	A	M	71	74	10.9	32.82772	-118.36315	38
102613OMC	3141	A	M	65	64	7.4	32.82674	-118.36197	38
102613EACE	3142	J		55	61	4.0	32.82752	-118.36282	38
102613SERD	3143	A	F	93	62	15.1	32.82671	-118.36200	38
102613SERE	3144	J		32	36	2.0	32.82667	-118.36196	38
102613EACF	3145F	J		40	49	1.8	32.82673	-118.36200	38
102613OMD	3151	A	F	90	68	16.0	32.82673	-118.36202	38
102613EACG	3152	J		42	45	2.0	32.82673	-118.36202	38
102613SERF	3153	J		36	34	1.1	32.82680	-118.36200	38
102613EACH	3154	A	F	84	74	17.6	32.82681	-118.36206	38
102613SERG	3155	J		51	48	3.0	32.82683	-118.36206	38
102613OME	3205.1	A	M	91	67	18.4	32.82691	-118.36213	38
102613OMF	3210	J		35	30	0.8	32.82738	-118.36240	38
102613SERH	3211	J		52	58	1.1	32.82733	-118.36254	38
102613EACJ	3213	J		54	55	4.2	32.82756	-118.36278	38
102613EACK	3214	J		35	36	1.2	32.82769	-118.36303	38

102613SERJ	3215	A	F	67	74	9.4	32.82743	-118.36247	38
102613SERK	3220	A	M	71	63	10.4	32.82690	-118.36193	38
102613EACM	3222	J		47	48	2.9	32.82679	-118.36190	38
102613EACN	3235	J		53	58	5.0	32.82671	-118.36185	38
102613OMA	3310	J		56	53	5.5	32.82722	-118.36245	38
102613EACI	3312I	J		34	32	0.9	32.82736	-118.36256	38
102613OMB	OMBDT	A					32.82766	-118.36301	38
102713EACC	3145C	A	M	84	83	15.5	32.84860	-118.40021	39
102713EACG	3201G	A	F	76	28	10.9	32.84848	-118.39953	39
102713OMB	3204B	A	M	69	56	11.6	32.84866	-118.39952	39
102713SERA	3240	A	M	82	72	15.9	32.84876	-118.40090	39
102713EACA	3241	A	F	67	67	8.0	32.84867	-118.40108	39
102713SERB	3242	A	F	76	61	13.9	32.84859	-118.40102	39
102713SERC	3243	A	F	72	53	11.4	32.84918	-118.40053	39
102713EACB	3244	A	M	87	80	13.8	32.84861	-118.40025	39
102713SERD	3250	A	M	62	59	7.0	32.84886	-118.39999	39
102713EACD	3251	A	M	86	72	13.6	32.84859	-118.40021	39
102713SERE	3252	A	M	71	51	7.9	32.84856	-118.39985	39
102713SERF	3253.1	A	M	62	61	6.3	32.84863	-118.39991	39
102713EACE	3254	A	M	77	69	10.6	32.84854	-118.39976	39
102713OMA	3255	A	F	80	71	15.4	32.84855	-118.39975	39
102713EACF	3300	A	F	68	57	7.9	32.84852	-118.39953	39
102713EACH	3302	A	M	79	47	12.9	32.84847	-118.39953	39
102713EACI	3303	A	M	67	67	7.1	32.84846	-118.39943	39
102713EACJ	3305	J		36	34	1.5	32.84843	-118.39929	39
102713EACK	3311	A	F	80	70	17.9	32.84843	-118.39931	39
102713EACL	3312L	A	M	79	51	13.9	32.84843	-118.39930	39
102713OMC	3313C	A	F	71	65	12.2	32.84862	-118.39954	39
102713EACM	3314	A	M	74	68	8.5	32.84877	-118.39941	39
102713EACN	3315	A		78	53	12.0	32.84871	-118.39920	39
102713EACO	3320	A	M	91	78	21.0	32.84832	-118.39957	39
102713OMD	3321	A	F	86	75	18.5	32.84829	-118.39939	39
102713EACP	3322	A	F	63	59	10.4	32.84831	-118.39936	39
102713EACQ	3323	A	F	68	71	10.4	32.84817	-118.39958	39
102713EACR	3324	A	F	78	61	17.5	32.84819	-118.39963	39
102713EACS	3325	A	F	67	76	14.0	32.84823	-118.39969	39
102713EACT	3330	A	M	82	58	14.4	32.84815	-118.39970	39
102713EACU	3331	A	M	74	62	14.6	32.84814	-118.39968	39
092913EACA	3200	J		37	37	1.2	32.86840	-118.50082	C
092913EACB	3201B	A	M	62	69	7.4	32.86792	-118.50137	C
092913OMB	3202	A	M	91	80	31.4	32.86764	-118.50132	C

092913OMD	3203	A	F	92	64	22.4	32.86671	-118.50210	C
092913OME	3204E	A	M	64	68	7.0	32.86592	-118.50334	C
092913OMA	3223	J		41	40	1.6	32.86830	-118.50062	C
092913SERA	3224	A	F	66	74	8.9	32.86836	-118.50063	C
092913SERB	3225	J		38	42	1.4	32.86831	-118.50063	C
092913SERC	3230	A	M	74	63	11.4	32.86781	-118.50126	C
092913CFMA	3231	A	F	90	65	20.4	32.86761	-118.50120	C
092913CFMB	3232	J		32	34	0.8	32.86742	-118.50162	C
092913OMC	3233	A	F	95	21	22.4	32.86728	-118.50190	C
092913SLRA	3234	A	F	90	78	17.4	32.86584	-118.50355	C
021313RWCT	0000T	A		65	30	-	32.90269	-118.48262	HR
021313RWCA	0001	J		44	53	3.5	32.90238	-118.48284	HR
021313RWCB	0002	A		72	54	12.1	32.90244	-118.48287	HR
021313RWCC	0003	A		83	75	14.1	32.90247	-118.48279	HR
021313RWCD	0004	A		71	69	10.9	32.90246	-118.48276	HR
021313RWCE	0005	A		84	81	>20	32.90248	-118.48271	HR
021313RWCF	0010	A		86	84	>20	32.90248	-118.48261	HR
021313RWCG	0011	A		75	66	11.3	32.90246	-118.48258	HR
021313RWCH	0012H	J		35	23	1.2	32.90248	-118.48258	HR
021313RWCI	0013	A		86	62	14.9	32.90246	-118.48258	HR
021313RW CJ	0014J	A		99	82	>20	32.90248	-118.48254	HR
021313RWCK	0015	A		74	82	15.1			HR
021313RWCY	0020	A		77	78	16.9	32.90277	-118.48262	HR
021313RW CZ	0021	A		94	84	>20	32.90282	-118.48267	HR
021313SERA	0022	A		74	65	14.9	32.90281	-118.48265	HR
021313SERC	0023	A		59	55	6.5	32.90286	-118.48261	HR
021313SERD	0024	A		65	55	10.2	32.90286	-118.48260	HR
021313SERF	0025	A		95	43	>20	32.90293	-118.48353	HR
021313RW CX	0100	A		73	75	12.2	32.90276	-118.48262	HR
021313RW CL	0101	A		78	59	12.4	32.90254	-118.48254	HR
021313RW CM	0102	A		65	54	7.9	32.90257	-118.48255	HR
021313RW CN	0103	J		69	36	8.7	32.90260	-118.48256	HR
021313RW CO	0104	J		44	25	2.4	32.90261	-118.48260	HR
021313RW CP	0105	A		84	84	>20	32.90260	-118.48259	HR
021313RW CQ	0110	J		45	47	3.4	32.90263	-118.48267	HR
021313RW CR	0111	J		64	51	5.8	32.90262	-118.48267	HR
021313RW CS	0112	A		69	67	11.1	32.90264	-118.48267	HR
021313RW CU	0113	A		75	62	10.2	32.90267	-118.48264	HR
021313RW CV	0114	A		77	76	>20	32.90269	-118.48264	HR
021313RW CW	0115	J		41	39	1.5	32.90276	-118.48261	HR
021313SERG	0120	A		90	52	>20	32.90272	-118.48399	HR

021313SERH	0121	A		80	68	16.4	32.90275	-118.48399	HR
021313SERJ	0123	A		66	65	9.6	32.90278	-118.48413	HR
021313SERE	1111	A		87	60	>20	32.90285	-118.48260	HR
091813RWCA	3051A	A	F	97	65	24.0	32.90305	-118.48256	HR
091813RWCB	3052B	J		35	36	1.1	32.90305	-118.48256	HR

Table B.2. Individual capture data from Santa Barbara Island. Santa Barbara Island *Xantusia riversiana* collected in 2015. Collection ID gives the date in MMDDYY format followed by collector's initials and alphabetical letter associated with the number of that capture. Sample ID is the toe clip ID assigned, letters following this are used to differentiate among identical toe clips. Age was classified as Adult (A) or Juvenile (J) as defined by a 60 mm snout-vent length (SVL). Sex was determined by probing. SVL was measured in mm. Tail length (TL) was measured in mm, but is highly variable due to autotomy. Weight (WT) is listed in grams. Capture coordinates of latitude (LAT) and longitude (LONG) are listed in decimal degrees in datum WGS84. Population of origin (POP) is listed by site initials. POP is the same as presented in Chapter 1 and associated appendices. Blanks represent missing data.

Collection ID	Sample ID	AGE	SEX	SVL	TL	WT	LAT	LONG	POP
071115SERD	1104	A	M	72	75	12.5	33.48551	-119.03078	AP
071115SERE	1105	A	F	80	71	18.5	33.48551	-119.03078	AP
071215SERA	1110	A	M	68	49	7.5	33.4855	-119.03071	AP
071415SERA	1111	A	M	80	69	13	33.48549	-119.03078	AP
083115SERA	1112	A	M	81	72	15.5	33.48521	-119.03001	AP
071415SERB	1112.2	A		65	68	8	33.48584	-119.03078	AP
090315SERA	1224	A	M	66	64	7.8	33.48551	-119.03076	AP
090315SERB	1225	A	M	65	66	10	33.48505	-119.03132	AP
090315SERC	1230	A	F	72	65	9.3	33.48516	-119.03104	AP
090315SERD	1231	A	M	88	59	19.3	33.48515	-119.03101	AP
090315SERE	1232	A	F	98	75	24	33.48515	-119.03101	AP
090315SERF	1233	A	M	84	56	15.8	33.48516	-119.03071	AP
090315SERG	1234	A	M	65	70	7.5	33.48508	-119.03028	AP
090515SERA	1235	A	M	88	47	20.8	33.48518	-119.03119	AP
090515SERB	1240	A	F	96	54	19.8	33.4851	-119.03133	AP
090515SERC	1241	A	M	63	70	5.5	33.48534	-119.03081	AP
090515SERJ	1252	A	M	70	67	9.2	33.48685	-119.0322	AP
090515SERK	1253	J		48	60	3	33.48666	-119.03196	AP
090515SERL	1254	J		56	61	4.3	33.4852	-119.03085	AP
090615SERA	1255	A	M	93	81	18.7	33.48511	-119.0313	AP
090615SERB	1300	A	M	91	78	20.5	33.48513	-119.0313	AP
090615SERC	1301	A	F	101	57	32.7	33.48515	-119.03122	AP
090615SERD	1302	A	F	88	76	21	33.48534	-119.03083	AP
090615SERE	1303	A	M	65	74	7.2	33.48519	-119.03086	AP
090615SERF	1304	A	M	76	81	13.8	33.48516	-119.03027	AP
090615SERJ	1312	A	F	75	78	11	33.48544	-119.03078	AP
090715SERA	1313	A	M	78	75	11.2	33.48533	-119.03064	AP
090715SERB	1314	A	M	64	72	4.2	33.48544	-119.03064	AP

090515SERE	1243	A	M	79	51	13.3	33.4747	-119.03593	CB
090515SERF	1244	A	M	74	57	14.5	33.47469	-119.03589	CB
090515SERG	1245	A	F	82	63	19.8	33.47475	-119.03586	CB
090515SERH	1250	A	F	61	53	8.5	33.47476	-119.03589	CB
090515SERI	1251	A	F	88	15	18.7	33.47486	-119.03592	CB
090615SERG	1305	A	M	83	47	16	33.47488	-119.0359	CB
090615SERH	1310	A	F	82	65	17.5	33.47496	-119.03587	CB
090615SERI	1311	A	F	81	68	16.3	33.47504	-119.03578	CB
062515SERA	0500	A	M	74	82	15	33.46601	-119.0365	CC
062515SERB	0501	A	F	82	73	19	33.46601	-119.0365	CC
062515SERC	0502	A	M	94	79	28	33.46605	-119.03635	CC
062515SERD	0503	J	M	57	59	6.1	33.46605	-119.03635	CC
062515SERE	0504	A	M	100	67	31.2	33.4662	-119.03633	CC
062515SERF	0505	A	M	92	84	23.5	33.46611	-119.03691	CC
062515SERG	0510	A	M	62	60	8.3	33.46613	-119.0369	CC
062515SERH	0511	A	M	82	75	17.3	33.46613	-119.0369	CC
062515SERI	0512	A	F	81	72	16.5	33.46613	-119.03692	CC
062515SERJ	0513	A	F	92	82	25.8	33.46616	-119.03673	CC
062515SERK	0514	A	F	61	44	6.2	33.46622	-119.03664	CC
062515SERM	0515	A	M	60	61	6.7	33.46618	-119.03662	CC
062515SERN	0520	A	M	73	76	13	33.46615	-119.03671	CC
062515SERO	0521	A	F	96	61	28	33.46607	-119.03639	CC
062515SERP	0522	A	M	69	44	11.3	33.46626	-119.03631	CC
062515SERQ	0523	A	F	94	63	30.2	33.46611	-119.03687	CC
062515SERR	0524	J		44	41	2.2	33.46605	-119.03688	CC
062515SERS	0525	A	M	89	81	23	33.46609	-119.03638	CC
062515SERT	0530	A	F	86	70	19.5	33.46597	-119.03667	CC
062515SERV	0531	J		47	56	3.8	33.46616	-119.0363	CC
062615SERA	0532	A	M	86	78	20.5	33.46619	-119.03617	CC
062615SERB	0533	A	F	103	82	34.7	33.46616	-119.03692	CC
062615SERC	0534	A	M	80	74	18.7	33.46598	-119.03683	CC
062615SERD	0535	A	M	93	86	25	33.466	-119.03687	CC
062515SERU	0540	A	F	103	84	33.7	33.46616	-119.0363	CC
062615SERE	0541	A	F	92	82	23	33.466	-119.03687	CC
062615SERF	0542	A	M	91	64	20.8	33.46597	-119.0365	CC
062615SERG	0543	A	F	93	86	24.5	33.46591	-119.03669	CC
062615SERH	0544	A	F	84	66	19.5	33.46596	-119.03673	CC
062615SERI	0545	J		41	43	2.2	33.466	-119.03636	CC
062615SERJ	escaped2	A					33.46619	-119.03635	CC
053115SERD	0140	J		42	50	2.4	33.47767	-119.03333	GC
053115SERE	0141	A	M	60	71	8.3	33.47676	-119.03159	GC

060115SERA	0150	A		84	87	19.7	33.47673	-119.03221	GC
060115SERB	0151	J		46	36	2.9	33.47675	-119.03124	GC
060115SERC	0152	A	M	72	65	11.7	33.47674	-119.03127	GC
060115SERD	0153	J		58	53	5.7	33.47673	-119.0313	GC
060115SERE	0154	J		51	63	4.5	33.47633	-119.03473	GC
060215SERL	0221	A	F	90	46	21.7	33.47723	-119.03229	GC
060215SERM	0222	A	M	67	72	8.1	33.4762	-119.03146	GC
060215SERN	0223	A	M	85	70	21.8	33.47725	-119.03229	GC
061315SERB	0255	A	M	94	79	29.2	33.47626	-119.0315	GC
061315SERC	0300	A	M	87	76	21	33.4762	-119.03142	GC
061315SERD	0301	A	F	66	57	10.2	33.47601	-119.03201	GC
061315SERE	0302	J		56	56	6	33.47601	-119.03201	GC
061315SERO	0314	A	M	85	71	22.7	33.47615	-119.0321	GC
061315SERP	0315	A	M	68	70	10.5	33.47604	-119.03196	GC
061315SERQ	0320	A	M	87	54	19.7	33.47592	-119.03197	GC
061415SERA	0321	A	M	78	73	18	33.47589	-119.03201	GC
061515SERA	0322	A	M	101	58	29.7	33.47546	-119.03165	GC
061515SERB	0323	A	M	84	69	20.5	33.47591	-119.03201	GC
061515SERC	0324	A	M	84	60	18	33.47588	-119.03201	GC
061515SERD	0325	A	M	82	62	18.7	33.4759	-119.03185	GC
061515SERE	0330	A	M	64	58	9.5	33.47596	-119.03193	GC
061515SERF	0331	A	M	63	58	9.2	33.47614	-119.03229	GC
061515SERH	0332	A	F	97	82	26.7	33.47605	-119.03208	GC
061515SERI	0333	A	M	62	64	7.7	33.4761	-119.0321	GC
061515SERJ	0334	A	M	67	64	11.7	33.47599	-119.0323	GC
061615SERA	0335	A	F	94	66	25.7	33.47809	-119.03199	GC
061515SERB	0340	A	M	72	70	12	33.47607	-119.0325	GC
061515SERC	0341	A	M	68	54	10.2	33.47603	-119.03245	GC
061515SERD	0342	A	F	89	82	22.5	33.476	-119.03227	GC
061515SERE	0343	A	M	88	76	22.5	33.476	-119.03227	GC
061515SERF	0344	A	M	86	59	22.7	33.476	-119.03219	GC
061515SERG	0345	A	M	99	67	27.5	33.47608	-119.032	GC
061515SERH	0350	A	M	87	71	18.2	33.47609	-119.03207	GC
061515SERI	0351	A	M	83	73	19.7	33.47608	-119.03207	GC
061515SERJ	0352	A	M	73	82	13.5	33.47596	-119.03216	GC
061315SERN	3314	J	M	59	62	8.5	33.47618	-119.03142	GC
061315SERA	3331	A	F	94	26	25.5	33.47718	-119.03218	GC
063015SERJ	0000.2	J	M	57	23	4	33.47879	-119.03377	LC
052015SERA	0001	A	M	60	74	5.2	33.48077	-119.02953	LC
053115SERB	0134	A	F	70	63	15.7	33.47916	-119.03286	LC
053115SERC	0135	A	F	84	78	23.7	33.48073	-119.0298	LC

053115SERF	0142	A	F	63	56	8.2	33.47984	-119.03114	LC
053115SERG	0143	A	M	92	66	28.5	33.47985	-119.03108	LC
053115SERH	0144	A	M	62	60	9.7	33.47984	-119.03107	LC
053115SERI	0145	A	M	73	75	14	33.47984	-119.03107	LC
070115SERA	1041	A	M	85	83	20.8	33.48051	-119.02955	LC
052715SERA	0002	A	M	64.2	68.4	8.2	33.47607	-119.03743	NP
052715SERB	0003	J		51	57	3.5	33.47607	-119.03745	NP
052815SERA	0004	J		40	45	2.5	33.4781	-119.03735	NP
052815SERB	0005	A	M	61	67	5.8	33.4777	-119.03728	NP
052815SERC	0010	A	F	78	63.5	16.2	33.47767	-119.03728	NP
052815SERD	0011	A	F	80	63.2	21.2	33.47773	-119.0369	NP
052815SERE	0012	A	M	60	67	6.2	33.47776	-119.0368	NP
052815SERF	0013	A	F	73	52	12.2	33.47776	-119.0368	NP
052815SERG	0014	A	M	75	72	14.7	33.47771	-119.03684	NP
052815SERH	0015	A	M	66	55	10.2	33.4777	-119.03682	NP
052815SERI	0020	A	M	58.5	66	5.6	33.47765	-119.03677	NP
052815SERJ	0022	A	M	72	41	10.2	33.47775	-119.0373	NP
052815SERO	0031	A	M	62	75	8.7	33.47698	-119.03714	NP
052815SERQ	0033	A	M	81	66	17.2	33.47739	-119.03708	NP
052815SERR	0034	A	M	76	67	12.2	33.47735	-119.03694	NP
052815SERS	0035	J	M	56	64	4.9	33.47734	-119.03709	NP
052815SERT	0040	A	F	78	69	19.3	33.47707	-119.037	NP
052815SERU	0041	A	M	76	50	15	33.47705	-119.03716	NP
052915SERA	0043	J	M	56	62	6.3	33.47762	-119.03745	NP
052915SERB	0044	A	F	62	43	9.5	33.47763	-119.03751	NP
052915SERC	0045	J	M	55	55	6.1	33.47721	-119.03737	NP
052915SERE	0050	J		42	50	2.7	33.47725	-119.03748	NP
052915SERF	0051	A	M	60	45	7.6	33.47722	-119.03748	NP
052915SERG	0052	J		48	58	4.1	33.47702	-119.03714	NP
052915SERH	0053	A	M	61	71	7.2	33.47705	-119.03713	NP
052915SERI	0054	A	F	74	73	14.7	33.47698	-119.03716	NP
052915SERJ	0055	J		39	50	2.2	33.47697	-119.03716	NP
052915SERK	0100	J		47	30	3.4	33.47773	-119.03708	NP
052915SERL	0101	A	F	73	48	14.2	33.47727	-119.03632	NP
052915SERO	0103	J		40	40	2.2	33.47688	-119.03696	NP
052915SERP	0104	A	F	87	60	19.5	33.47691	-119.03693	NP
052915SERR	0105	A	M	73	50	12.2	33.47679	-119.03685	NP
052915SERS	0110	A	M	77	67	16.2	33.47683	-119.0369	NP
052915SERT	0111	A	M	85	38	18.2	33.47679	-119.03687	NP
053015SERA	0112	J		46	48	3.7	33.47677	-119.03687	NP
053015SERB	0113	A	M	62	73	10.2	33.47675	-119.03705	NP

053015SERC	0114	J		52	50	5.6	33.47673	-119.03748	NP
053015SERD	0115	A	F	86	53	17.7	33.47645	-119.03706	NP
053015SERE	0120	A	F	67	59	10.2	33.47647	-119.03719	NP
053015SERF	0121	J	F	57	61	4.9	33.47662	-119.03745	NP
053115SERA	0133	A	M	64	57	10	33.47701	-119.03634	NP
060115SERH	0201	J	F	59	39	5	33.47548	-119.03763	NP
061015SERC	0230	A	M	68	56	11.7	33.47902	-119.03744	NP
061015SERE	0231	A	F	76	75	14.2	33.4775	-119.03701	NP
061015SERF	0232	A	M	85	64	21.6	33.47745	-119.03691	NP
061015SERG	0233	A	M	84	68	17.7	33.47743	-119.03693	NP
062815SERA	1000	A	F	68	50	9	33.4766	-119.03712	NP
062815SERB	1001	J		55	65	5.3	33.47656	-119.03692	NP
062815SERC	1002	J		53	52	4.5	33.47676	-119.03696	NP
062815SERD	1003	A	M	62	58	7.3	33.47678	-119.03692	NP
062815SERE	1004	A	M	77	62	14	33.47692	-119.03683	NP
062815SERF	1005	J		57	55	4.2	33.47705	-119.03712	NP
090815SERA	1315	A	M	63	64	9.5	33.47604	-119.03741	NP
090815SERB	1320	J		39	27	1.4	33.47767	-119.03727	NP
090815SERC	1321	A	M	67	65	7.5	33.47766	-119.03727	NP
090815SERD	1322	J	M	51	42	3.8	33.47773	-119.03709	NP
090815SERE	1323	A	F	64	48	8.7	33.47763	-119.0368	NP
090815SERF	1324	A	F	77	46	14.5	33.47758	-119.03663	NP
090815SERG	1325	J		57	54	4	33.47693	-119.03718	NP
090815SERH	1330	A	F	70	65	11.2	33.47704	-119.03712	NP
090815SERI	1331	A	M	71	60	10	33.47733	-119.03706	NP
090815SERJ	1332	A	M	76	78	9.8	33.47743	-119.037	NP
090815SERK	1334	A	M	76	61	12.2	33.47743	-119.03692	NP
090815SERL	1335	A	F	75	78	16	33.47745	-119.03687	NP
090815SERM	1340	A	M	85	77	18	33.47741	-119.03684	NP
090815SERN	1341	A	M	63	70	6.2	33.47738	-119.03678	NP
052915SERM	3133	A	M	69	14	10.2	33.47724	-119.03635	NP
061015SERD	3333	A	F	83	39	19.5	33.47754	-119.03705	NP
052915SERQ	3334	A	M	79	11	13.2	33.47695	-119.03695	NP
061115SERC	0000	A					33.47932	-119.03675	PP
052815SERK	0023	A	M	81	72	15.2	33.47919	-119.03638	PP
052815SERL	0024	A	M	71.5	61	10.2	33.47931	-119.03632	PP
052815SERM	0025	J		49.5	54.4	3.4	33.47932	-119.03629	PP
052815SERN	0030	A	F	81	72	23.2	33.47927	-119.0363	PP
052815SERP	0032	A	M	79	73	15.2	33.47932	-119.03658	PP
052815SERV	0042	A	F	88	77	21	33.4798	-119.03672	PP
052915SERN	0102	J		47	57	4.2	33.47972	-119.03677	PP

053015SERG	0122	A	M	74	80	12.3	33.47932	-119.0363	PP
053015SERH	0123	J		55	63	5.3	33.47936	-119.03642	PP
053015SERI	0124	A	M	72	61	12.5	33.47932	-119.03642	PP
053015SERJ	0125	A	M	89	74	21.2	33.47932	-119.03642	PP
053015SERK	0130	A	F	72	62	12.5	33.47965	-119.03618	PP
053015SERL	0131	A	M	92	75	30.2	33.47984	-119.03599	PP
053015SERM	0132	A	M	76	75	15.2	33.47937	-119.03634	PP
061015SERA	0224	A	M	75	74	17.7	33.47927	-119.03641	PP
061015SERB	0225	J		37	31	1.9	33.47926	-119.03642	PP
061115SERA	0234	A	M	86	58	22.7	33.47926	-119.03613	PP
061115SERB	0235	A	M	68	75	9.2	33.47957	-119.03615	PP
061115SERD	0240	A	M	87	57	25.2	33.47927	-119.03653	PP
061115SERE	0241	J		51	42	6	33.47947	-119.03636	PP
061115SERF	0242	A	M	86	82	24.7	33.47952	-119.03634	PP
061115SERG	0243	A	F	88	66	24.5	33.47947	-119.03641	PP
061115SERH	0244	A	F	87	53	24.2	33.47935	-119.03629	PP
061115SERI	0245	A	F	91	68	23.7	33.47952	-119.03619	PP
061215SERA	0250	A	F	90	69	23.5	33.47964	-119.036	PP
061215SERB	0251	A	M	83	75	22	33.47951	-119.03618	PP
061215SERC	0252	A	M	65	62	10.3	33.47943	-119.03626	PP
061215SERD	0253	A	M	60	65	7	33.47953	-119.03618	PP
061215SERE	0254	A	M	69	73	12.2	33.47979	-119.03643	PP
061315SERF	0303	A	M	93	63	25.2	33.47935	-119.03616	PP
061315SERG	0304	A	M	79	77	15.7	33.47955	-119.0362	PP
061315SERH	0305	A	M	71	70	13.5	33.47935	-119.03616	PP
061315SERI	0310	A	M	64	68	9.7	33.47941	-119.03627	PP
061315SERJ	0311	J	M	59	57	6.6	33.47951	-119.03613	PP
061315SERK	0312	A	M	92	98	28.7	33.47951	-119.03616	PP
061315SERM	0313	A	M	61	55	8.7	33.47953	-119.03617	PP
060115SERF	0155	A	M	88	85	21.7	33.47038	-119.04023	S
060115SERG	0200	J		58	51	5.8	33.47042	-119.04026	S
060215SERA	0202	A	M	64	66	12	33.47197	-119.04153	S
060215SERB	0203	A	M	90	62	20.5	33.47199	-119.04152	S
060215SERC	0204	A	F	84	84	20	33.47031	-119.04021	S
060215SERD	0205	A	M	82	83	18.7	33.47037	-119.04021	S
060215SERE	0210	A	M	84	81	18.5	33.47039	-119.04022	S
060215SERF	0211	A	M	76	83	18	33.47044	-119.0403	S
060215SERG	0212	A	M	64	55	5.9	33.47068	-119.04038	S
060215SERH	0213	J	M	57	42	5.7	33.47075	-119.04042	S
060215SERI	0214	A	F	88	71	19.5	33.47104	-119.04054	S
060215SERJ	0215	A	F	95	74	26	33.47102	-119.04058	S

060215SERK	0220	A	M	84	79	17.2	33.47107	-119.04057	S
062915SERA	1010	A	M	64	65	7	33.47049	-119.03368	SE
062915SERB	1011	A	F	61	50	5.5	33.47045	-119.03368	SE
062915SERC	1012	A	M	80	75	13.8	33.47049	-119.03366	SE
062915SERE	1013	A	M	63	48	6.5	33.47063	-119.0331	SE
063015SERA	1014	A	M	61	64	8	33.4707	-119.03362	SE
063015SERB	1015	J		49	52	3.3	33.4705	-119.03368	SE
063015SERC	1020	A	F	91	77	24.3	33.47029	-119.03365	SE
063015SERD	1021	A	M	85	50	14.3	33.4703	-119.03363	SE
063015SERE	1022	A	M	78	70	12.5	33.47029	-119.03365	SE
063015SERG	1023	A	M	89	65	19.5	33.47058	-119.03368	SE
063015SERH	1024	A	M	77	65	12.5	33.47058	-119.03368	SE
063015SERI	1025	A	M	65	67	7.5	33.47067	-119.03307	SE
063015SERK	1030	A	F	80	56	13	33.4708	-119.03349	SE
063015SERL	1031	A	M	61	51	6.5	33.47058	-119.03369	SE
063015SERM	1032	A	M	68	51	8	33.47058	-119.03371	SE
063015SERN	1033	A	M	72	53	10.5	33.47063	-119.03313	SE
063015SERO	1034	A	M	90	52	20	33.47058	-119.0337	SE
063015SERP	1035	A	M	92	82	24	33.47029	-119.03365	SE
063015SERQ	1040	J		47	45	1.3	33.47032	-119.03367	SE
070915SERA	1042	A	M	78	62	13	33.47026	-119.03368	SE
071015SERA	1043	A	M	79	65	10	33.47061	-119.0331	SE
071015SERB	1044	A	M	69	67	8.5	33.47056	-119.03305	SE
071015SERC	1045	A	F	86	57	18	33.47054	-119.0336	SE
071015SERD	1050	A	M	84	60	14	33.47051	-119.0336	SE
071015SERE	1051	A	M	95	77	26	33.47051	-119.0336	SE
071015SERF	1052	A	M	87	70	16.5	33.47026	-119.03368	SE
071015SERG	1053	J	M	58	51	5.4	33.47043	-119.03303	SE
071015SERH	1054	A	M	78	71	17.5	33.47043	-119.03303	SE
071015SERI	1055	A	F	62	48	6.5	33.47048	-119.03369	SE
071015SERJ	1100	A	F	75	62	10.3	33.47031	-119.03362	SE
071115SERA	1101	A	M	85	60	17	33.47038	-119.03361	SE
071115SERB	1102	A	M	84	56	18.5	33.47047	-119.03366	SE
071115SERC	1103	A	M	95	62	20.5	33.47028	-119.03362	SE
063015SERF	1333	J		55	15	6	33.47038	-119.03362	SE
062915SERD	1500	J	M	59	50	5	33.47048	-119.03369	SE
083115SERB	1113	A	M	80	81	13.5	33.48087	-119.04344	WP
090115SERA	1114	J		47	47	2.7	33.48103	-119.04372	WP
090115SERB	1115	A	M	62	66	5.9	33.4812	-119.04343	WP
090115SERC	1120	A	M	78	53	10.5	33.48117	-119.04353	WP
090115SERD	1121	J		55	64	4.7	33.48102	-119.04356	WP

090115SERE	1122	J		55	47	4.1	33.48104	-119.04355	WP
090115SERF	1123	A	M	74	76	11.3	33.48104	-119.04353	WP
090115SERG	1124	A	F	73	48	10	33.48103	-119.04351	WP
090115SERH	1125	A	F	86	56	21	33.48104	-119.04349	WP
090115SERI	1130	A	M	62	62	7.3	33.48141	-119.04329	WP
090115SERJ	1131	J		57	58	5.5	33.48141	-119.0434	WP
090115SERK	1132	J		58	46	5.5	33.4814	-119.04337	WP
090115SERL	1133	J		58	59	3.9	33.48143	-119.04329	WP
090115SERM	1134	A	M	93	81	23.5	33.48106	-119.04343	WP
090115SERN	1135	J		51	57	3.1	33.48096	-119.04345	WP
090115SERO	1140	A	F	76	68	11.5	33.48136	-119.04319	WP
090115SERP	1141	A	M	72	67	8	33.48101	-119.0434	WP
090115SERQ	1142	A	M	83	56	16.8	33.48092	-119.04346	WP
090115SERR	1143	J		53	60	4	33.48094	-119.04347	WP
090115SERS	1144	A	F	81	56	16.5	33.48093	-119.04346	WP
090115SERT	1145	J		56	51	4.3	33.4809	-119.04346	WP
090115SERU	1150	A	M	71	50	8	33.48093	-119.04338	WP
090115SERV	1151	A	F	84	58	20	33.48095	-119.04335	WP
090115SERW	1152	A	F	90	66	23	33.48095	-119.04334	WP
090115SERX	1153	J		40	42	1.9	33.48083	-119.04343	WP
090115SERY	1154	A	F	71	72	14.8	33.48097	-119.04316	WP
090115SERZ	1155	J		43	45	2	33.48097	-119.04316	WP
090215SERA	1200	J		56	61	4	33.48084	-119.0433	WP
090215SERB	1201	A	M	80	53	16	33.48084	-119.0433	WP
090215SERC	1202	A	M	76	72	13.3	33.48086	-119.04319	WP
090215SERD	1203	A	M	75	49	10.3	33.48085	-119.04321	WP
090215SERE	1204	J		51	56	3.8	33.48084	-119.04316	WP
090215SERF	1205	A	F	84	68	17	33.48086	-119.04315	WP
090215SERG	1210	A	M	67	33	6.9	33.48081	-119.0432	WP
090215SERH	1211	J		52	47	3.6	33.48079	-119.04311	WP
090215SERI	1212	A	M	77	58	13.5	33.48038	-119.04309	WP
090215SERJ	1213	J		51	60	5.2	33.4809	-119.04303	WP
090215SERK	1214	A	M	72	66	9.3	33.48093	-119.04303	WP
090215SERL	1215	A	M	62	68	5.2	33.48087	-119.04311	WP
090215SERM	1220	A	F	73	69	13.5	33.48117	-119.04298	WP
090215SERN	1221	A	M	64	39	6.4	33.48064	-119.04337	WP
090215SERO	1222	A	M	75	66	11	33.48053	-119.04328	WP
090215SERP	1223	A	F	84	76	23.3	33.48053	-119.04328	WP

0 4		0	8	1	1	6	4	3	7	4	2	8	1	7	5	5	9	1	4	9	3	3	3	6	0	3	3	5	5	8	6	6	4	8	1			0	2	2	3	0	4	0	8	0	4				
3 0 0 5		1	1	2	2	1	1	2	2	2	2	3	3			1	1	1	1	1	1	2	3	3	2	2	2	2	1	1	1	1	2	1	1	2	2	2	2	2	1	1	1	1	2	2	2	2			
5	3	2	0	1	1	4	0	2	6	4	0	6	7	0	0	4	7	3	9	7	1	9	0	8	2	7	5	1	5	2					1	1	2	2	0	1	0	3	5	8	4	0	4	0	2		
3 1 0		1	1	2	2	1	1	2	2	2	2	3	3	1	1	1	1	1	1	1	2	2	3	3	2	2	2	2	1	1	1	1	2					1	2	1	2	1	1	1	1	2	2	2	2		
0	3	3	2	1	9	6	0	5	6	4	8	8	6	5	3	5	7	3	9	4	4	7	0	2	0	5	9	5	9	9	0	0			9	9	8	0	0	8	0	6	3	6	4	3	2	4	8		
3 0 1 1		1	1	2	2	1	2	2	2	2	2	3	3	1	1	1	1	1	1	1	2	3	3	2	3	1	2	1	1	1	1	2	3	1	2	1	1	2	2	1	2	1	1	1	1	1	1	2	2	2	2
1	3	0	2	1	2	3	2	2	8	4	4	2	3	1	1	1	0	7	5	9	8	7	7	0	3	7	1	5	9	6			7	8	5	8	0	0	1	7	8	0	1	9	0	5	9	8	9	9	0
3 0 1 2		1	1	2	2	1	1	2	2	2	2	3	3	1	1	1	1	1	1	2	2	3	3	2	2	2	2	1	1	1	1	2	2	1	2	2	2	2	2	2	1	2	1	1	1	1	2	1	2	2	2
0	3	6	8	1	1	3	5	5	6	6	8	4	8	1	5	5	9	4	9	4	8	3	0	0	3	5	9	7	2			7	8	4	5	9	0	0	6	0	0	1	8	3	6	0	0	5	4	8	
3 0 1 3		1	1	2	2	1	1	2	2	2	2	3	3			1	1	1	1	1	1	3	3	2	2	2	2	1	1	1	1	2	2	1	2	1	1	2	2	2	2	1	2	1	1	1	2	1	2	2	2
1	3	3	5	1	1	4	3	3	4	6	4	4	8	0	0	7	0	4	9	9	7	9	9	0	0	1	5	9	5			9	8	5	8	0	0	6	8	0	1	9	0	6	8	0	4	8	0	4	
3 0 1 4		1	1	2	2	1	1	2	2	2	2	3	3	1	1	1	1	1	1	2	3	3	2	2	2	2	2	1	1	1	1	2	2	1	2	1	1	2	2	2	2	1	2	1	1	1	2	2	2	2	
4	3	4	3	1	5	0	3	2	2	6	6	8	3	3	7	7	1	9	9	3	4	9	0	8	4	9	7	7	9			6	6	6	7	9	0	0	2	2	1	2	2	6	8	3	6	2	2	2	
3 0 1 5		1	1	2	2	1	2	2	2	2	2	3	3	1	1	1	1	1	1	2	3	3	2	2	2	2	2	1	1	1	1	2	2	1	2	1	1	2	2	2	2	1	2	1	1	1	2	1	2	2	
0	3	8	2	1	1	6	2	5	4	8	2	8	3	5	9	4	0	4	9	7	7	3	7	0	0	5	9	3			5	5	9	0	0	6	7	7	8	0	0	1	7	7	8	5	6	2	2		
3 0 2 2		1	1	2	2	1	2	2	2	2	2	3	3			1	1	1	1	2	3	3	2	2	2	2	2	1	1	1	1	2	2	1	2	1	1	2	2	2	2	1	2	1	1	1	2	2	2	2	
0	3	8	3	1	9	8	2	0	2	0	4	9	4	0	0	7	7	4	4	5	9	5	0	8	8	9	3	5			6	8	4	0	0	1	7	9	0	0	2	6	6	2	5	0	4	2	0	0	
3 0 2 1		1	1	2	2	1	2	2	2	2	2	3	3	1	1	1	1	1	2	2	3	3	2	2	2	2	2	1	1	1	1	2	2	1	2	1	1	2	2	2	2	2	2	1	1	1	2	1	2	2	2
2	3	0	4	1	1	3	5	3	0	2	8	9	7	1	5	7	5	4	9	4	8	5	3	8	8	1	5	9			6	8	4	0	0	6	8	4	0	0	2	2	0	3	7	8	3	6	0	0	
3 0 2 2		1	1	2	2	1	1	2	2	2	2	3	3	1	1	1	1	1	2	2	3	3	2	2	2	2	2	1	1	1	1	2	2	1	2	1	1	2	2	2	2	1	2	1	1	1	2	1	2	2	
0	3	4	1	1	5	4	9	3	2	6	4	7	7	1	9	4	5	4	1	8	2	5	5	8	2	5	7			6	6	8	0	0	3	9	8	1	1	2	1	1	1	1	2	1	1	1	1	1	
3 0 2 3		1	1	2	2	1	1	2	2	2	2	3	3	1	1	1	1	1	1	2	3	3	2	2	2	2	2	1	1	1	1	2	2	1	2	1	1	2	2	2	2	1	2	1	1	1	2	2	2	2	
0	3	2	9	1	9	4	7	6	0	8	2	4	2	5	7	4	7	3	1	3	7	3	0	0	1	3	1			6	7	4	0	0	3	9	9	5	5	7	7	0	3	7	7	6	9	9	0	0	
2	3	2	9	1	9	4	7	6	0	8	2	4	2	5	7	4	7	3	1	3	7	3	0	0	1	3	1			6	7	4	0	0	3	9	9	5	5	7	7	0	3	7	7	6	9	9	0	0	
3 0 2 3		1	1	2	2	1	1	2	2	2	2	3	3	1	1	1	1	1	1	2	3	3	2	2	2	2	2	1	1	1	1	2	2	1	2	1	1	2	2	2	2	1	2	1	1	1	2	2	2	2	
0	3	2	9	1	9	4	7	6	0	8	2	4	2	5	7	4	7	3	1	3	7	3	0	0	1	3	1			6	7	4	0	0	3	9	9	5	5	7	7	0	3	7	7	6	9	9	0	0	

304	3	143	169	251	260	171	227	223	224	220	330	364	00	175	179	176	179	179	229	353	365	258	262	193	217	187	180	192	206	177	200	210	184	188	168	180	199	194	184	
3025	3	134	139	251	255	185	239	225	221	224	334	346	165	165	177	177	172	173	239	315	355	255	255	211	213	166	167	177	190	200	204	219	188	188	211	219	177	217	176	210
3030	3	134	144	251	255	199	235	222	222	224	334	364	165	173	174	177	179	199	211	355	366	255	255	211	217	168	177	180	200	208	211	220	188	180	211	217	210	211	188	
3031	3	139	148	251	255	195	235	222	222	224	334	364	165	177	179	179	199	211	355	379	255	255	211	217	168	177	180	200	204	211	219	188	180	211	217	210	211	188		
3032	3	156	169	251	255	203	227	222	222	224	334	344	164	166	183	189	199	211	228	345	355	255	255	211	217	168	177	177	200	204	211	219	188	180	211	217	210	211	188	
3033	3	144	166	251	255	202	227	222	222	224	336	366	00	00	179	183	199	211	228	349	373	255	255	211	217	168	177	177	200	208	211	219	188	180	211	217	210	211	188	
3034	3	144	169	251	255	202	227	222	222	224	336	366	00	00	179	183	199	211	228	349	373	255	255	211	217	168	177	177	200	208	211	219	188	180	211	217	210	211	188	
3035	3	149	168	251	255	209	227	222	222	224	336	366	00	00	188	199	199	211	228	349	373	255	255	211	217	168	177	177	200	208	211	219	188	180	211	217	210	211	188	
3040	3	139	169	251	255	204	227	222	222	224	336	364	153	166	188	199	199	211	228	349	373	255	255	211	217	168	177	177	200	208	211	219	188	180	211	217	210	211	188	
3041	3	134	169	251	255	202	227	222	222	224	336	366	00	00	179	183	199	211	228	349	373	255	255	211	217	168	177	177	200	208	211	219	188	180	211	217	210	211	188	
3042	3	146	169	251	255	207	227	222	222	224	336	366	00	00	178	173	199	211	228	377	375	255	255	211	217	168	177	177	200	208	211	219	188	180	211	217	210	211	188	
3043	3	134	145	251	255	207	227	222	222	224	336	366	00	00	179	173	199	211	228	349	373	255	255	211	217	168	177	177	200	208	211	219	188	180	211	217	210	211	188	
3044	3	146	169	251	255	207	227	222	222	224	336	366	00	00	178	173	199	211	228	377	375	255	255	211	217	168	177	177	200	208	211	219	188	180	211	217	210	211	188	
3045	3	134	145	251	255	207	227	222	222	224	336	366	00	00	179	173	199	211	228	349	373	255	255	211	217	168	177	177	200	208	211	219	188	180	211	217	210	211	188	

3 2		9	3	1	8	1	6	3	9	6	4	2	3			1	3	9	4	3	7	3	0	6	8	1	5	3	1	6	6	9	8	1	5	3	1	8	2	2	0	2	7	3	4	0	4		
0						1	1	2	2	2	2	3	3	1	1	1	1	1	1	1	2	3	3	2	2	2	2	1	1	1	1	1	2	2	1	1	2	2	2	2	2	1	1	1	1	1	2	2	
3 3 3	4	0				7	7	4	6	0	2	6	6	5	6	7	7	2	3	9	0	5	5	5	5	0	2	6	7	6	7	2	2	1	1	2	2	0	0	0	0	0	6	6	8	9	0	0	
0						1	2	2	2	2	2	3	3	1	1	1	1	1	1	2	3	3	2	2	2	2	1	1	1	1	1	2	2	1	1	2	2	1	2	1	2	1	1	1	1	2	2		
3 3 4	4	4	4	1	3	6	2	9	2	4	4	3	4	5	9	7	3	7	9	7	8	5	3	0	0	1	9	1	9	2	6	6	4	7	5	1	2	2	0	0	7	0	6	6	8	9	0	2	
0						1	1	2	2	2	2	3	3	1	1	1	1	1	1	2	3	3	2	2	2	2	1	1	1	1	1	2	2	1	1	1	1	1	1	2	1	1	1	1	1	2	1		
3 3 5	4	0				3	7	8	2	6	0	6	6	5	6	7	8	1	4	9	0	5	6	5	7	2	3	6	7	6	7	9	8	2	6	1	3	4	6	2	7	8	2	4	8	8	6	4	
0						1	1	2	2	2	2	3	3			1	1	1	1	2	2	3	3	2	2	2	2	1	1	1	1	2	2	1	1	2	2	1	1	1	1	1	1	1	2	1	1		
3 3 4	4	4	3	1	1	3	6	4	5	2	2	3	5	0	0	2	7	7	1	1	1	2	1	5	6	5	0	1	6	7	7	9	5	6	8	1	1	2	2	1	1	1	1	1	1	2	1		
0						1	1	2	2	2	2	3	3	1	1	1	1	1	1	2	3	3	2	2	2	2	1	1	1	1	1	2	2	1	1	1	1	1	1	2	2	2	2	1	1	1	1		
3 4 1	4	4	4	1	7	7	4	2	4	6	7	3	1	3	5	0	0	5	6	6	6	3	3	2	2	1	1	1	1	1	2	2	1	1	1	1	1	1	2	2	2	2	1	1	1	1	2	2	
0						1	1					3	3			1	1			1	1		2	2		1	1	1	1	1	1	1	1	1	1	1	1	1	1	1	1	1	1	1	1	1	1		
3 4 4	4	0	0	0	0	8	9	0	0	0	0	4	5	0	0	3	4	0	0	3	7	0	8	8	0	0	3	9	8	6	7	7	6	8	8	2	6	0	0	0	0	0	0	0	0	0	0	0	0
0						1	1	2	2	2	2	3	3	1	1	1	1	1	1	2	3	3	2	2	2	2	1	1	1	1	1	2	2	1	1	2	2	1	1	2	2	2	2	1	1	1	1	1	2
3 4 4	4	0				3	3	3	3	2	0	3	3	3	7	1	9	1	5	3	1	7	0	8	4	9	9	9	1	2	8	8	6	6	7	1	1	3	8	2	2	3	4	7	6	8	0	0	
0						1	1	2	2	2	2	3	3	1	1	1	1	1	1	2	3	3	2	2	2	2	1	1	1	1	1	2	2	1	1	1	1	2	2	1	2	1	1	1	1	1	1	2	
3 4 5	4	9	9	0	0	7	8	2	4	0	0	4	4	6	7	4	1	7	4	9	0	4	5	4	4	0	0	7	7	7	8	8	1	8	9			2	2	1	2	6	0	8	9	9	8	0	
0						1	1	2	2	2	2	3	3	1	1	1	1	1	1	2	3	3	2	2	2	2	1	1	1	1	1	2	2	1	1	1	1	1	1	2	2	1	2	1	1	1	1	2	
3 5 0	4	4	3	1	9	6	7	9	6	4	8	2	1	7	1	5	8	4	7	3	2	7	0	6	4	7	9	0	6	7	6	8	8	1	8	1	8	4	0	0	1	8	0	7	0	6	6	9	0
0						1	1	2	2	2	2	3	3	1	1	1	1	1	2	2	3	3	2	2	1	1	1	1	1	1	2	2	1	1	1	1	2	2	2	2	2	2	1	1	1	1	1	1	1
3 5 1	4	0				3	4	5	5	6	8	2	3	5	6	7	5	3	9	0	4	6	4	6	9	9	7	7	7	7	7	0	0	1	6	6	1	2	2	2	0	0	7	7	9	9	9	9	6

3		4	4			3	6	1	9	0	0	8	4	3	1	0	3	3	1	9	9	3	5	2	6	1	9	7	9	8	0	4	2	5	5	5	8	2	0	4	0	6	0	3	6	0	0							
0		1	1	2	2	1	1	2	2	2	2	3	3			1	1	1	1			3	3	2	2	1	2	1	1	1	1	1	1	2	1	1	2	2	2	2	2	1	1	1	1	1	2							
4	7	3	3	5	7	9	9	3	6	2	3	3	8	8	0	0	6	8	3	3	0	0	3	5	5	5	9	9	3	6	7	6	4	0	8	8	0	0	0	0	0	0	1	7	8	8	9	8	0					
0		1	1			1	1	2	2	2	2	3	3	1	1	1	1	1	1	2	2	3	3	2	2	1	1	1	1	1	1	1	1	1	2	2	2	2	2	2	2	2	1	1	1	1	2	2						
4	7	3	4			8	9	3	3	2	2	3	4	4	4	6	8	3	3	1	2	2	5	5	6	7	9	9	7	7	6	4	6	7	9	2	8	8	7	5	0	2	0	3	3	7	9	9	0	0				
0		1	1			1	1	2	2	2	2	3	3	1	1	1	1	1	1	2	2	3	3	2	2	1	2	1	1	1	1	1	1	1	2	2	2	2	2	2	2	2	1	1	1	1	2	2						
4	7	5	6			8	9	3	4	1	3	3	3	5	5	7	9	2	3	9	0	5	6	7	8	8	0	7	7	6	4	8	9	0	9	9	8	8	0	1	0	3	9	7	2	8	8	0	4					
0		1	1	2	2	1	1	2	2	2	2	3	3	1	1	1	1	1	1	1	1	3	3	2	2	1	2	1	1	1	1	1	1	1	2	2	2	2	2	2	2	2	1	1	1	1	1	1						
4	7	1	3	5	8	8	9	2	4	2	3	2	4	5	5	6	7	3	3	8	8	5	6	6	9	9	0	6	7	8	8	0	0	2	0	9	0	9	0	6	8	0	0	0	1	6	7	9	9	9				
0		1	1			1	1	2	2	2	2	3	3	1	1	1	1	1	1	2	2	3	3	2	2	2	2	1	1	1	1	1	1	1	2	2	2	2	2	2	2	2	2	1	1	1	1	1	1					
4	7	0	4			5	9	3	5	2	3	3	5	4	4	6	7	5	3	9	2	5	6	5	8	2	3	6	7	6	8	8	1	1	2	2	2	2	2	2	2	2	1	1	1	1	1	1						
0		1	1			1	1	2	2	2	2	3	3	1	1	1	1	1	1	2	2	3	3	2	2	1	2	1	1	1	1	1	1	1	2	2	2	2	2	2	2	2	2	1	1	1	1	1	1					
4	7	3	3			7	9	3	3	3	3	4	4	6	6	6	6	6	3	3	0	2	5	5	6	9	3	6	7	7	8	8	9	0	0	6	7	8	1	1	1	1	1	1	1	1	1	1						
0		1	1	2	2	1	1	2	2	2	2	3	3	1	1	1	1	1	1	2	2	3	3	2	2	1	2	1	1	1	1	1	1	2	2	2	2	2	2	2	2	2	2	1	1	1	1	2	2					
5	7	3	3	5	7	7	8	2	3	1	3	4	4	5	6	7	8	1	1	9	1	4	5	6	6	0	0	6	9	7	8	8	0	1	4	5	9	0	9	0	8	8	0	2	7	1	7	8	9	0	4			
0		1	1	2	2	1	1	2	2	2	2	3	3	1	1	1	1	1	1	2	2	3	3	2	2	1	2	1	1	1	1	1	1	2	2	2	2	2	2	2	2	2	2	2	1	1	1	1	2	2				
5	7	3	5	5	6	7	9	2	5	2	2	2	5	5	6	7	8	1	1	4	4	1	5	6	6	9	2	6	7	7	8	8	0	1	4	5	9	0	9	0	7	7	8	9	9	0	0	0	0					
0		1	1			1	1	2	2	2	2	3	3	1	1	1	1	1	2	2	3	3	2	2	2	2	1	1	1	1	1	1	1	2	2	2	2	2	2	2	2	2	2	2	1	1	1	1	1	1				
0		1	1			1	1	2	2	2	2	3	3	1	1	1	1	1	2	2	3	3	2	2	2	2	1	1	1	1	1	1	1	2	2	2	2	2	2	2	2	2	2	2	1	1	1	1	1	1				
5	7	6	0			7	8	2	5	2	2	5	5	5	6	7	7	2	3	2	3	5	5	6	7	0	3	5	7	6	8	0	2	4	0	1	7	8	0	2	4	0	1	1	1	1	2	2	1	2	1	1	1	1
0		1	1	2	2	1	1	2	2	2	2	3	3	1	1	1	1	1	2	2	3	3	2	2	1	2	1	1	1	1	1	1	2	2	2	2	2	2	2	2	2	2	2	2	1	1	1	1	1	2				
5	7	3	6	5	8	6	7	3	4	1	4	4	4	5	6	6	7	2	3	8	0	4	5	6	9	9	0	6	6	7	7	2	8	9	0	9	7	9	0	7	8	0	1	9	0	8	9	9	9	0	4			
0		1	1			1	1	2	2	2	2	3	3			1	1	1	1	1	2	3	3	2	2	1	1	1	1			1	1	1	1	1	1	2	2	1	2	1	1	1	1	1	1	1	1	1	1			
5	7	0	4			7	9	2	2	2	2	5	5	0	0	5	5	1	1	9	2	5	5	6	6	9	5	9	0	0	0	2	5	6	6	9	7	9	0	0	6	6	1	7	8	8	9	9	0	0				

2001	7	126	134	00	171	186	223	224	223	234	334	353	00	167	171	113	113	182	201	357	357	266	268	201	221	167	175	184	192	179	200	190	206	00	202	206	200	200	172	176	190	190	200	200		
EME	7	134	156	00	183	186	231	234	233	242	324	336	161	166	188	180	113	222	222	357	365	282	289	202	225	168	186	177	179	192	205	217	177	200	202	203	207	106	176	182	188	188	196	196		
1053	8	130	139	11	183	183	216	224	224	244	334	344	144	155	177	170	118	119	393	366	254	270	193	279	177	177	177	177	190	188	188	188	194	184	200	106	166	199	199	00	00	00	00	00	00	
1054	8	143	140	00	199	199	223	224	244	334	344	354	155	177	179	144	118	119	393	355	255	255	223	277	188	199	199	199	188	188	194	228	188	188	204	106	166	199	199	200	200	200	200	200	200	
1055	8	130	145	11	190	199	216	224	224	249	336	344	00	00	169	144	118	119	200	366	235	235	193	277	188	199	199	188	188	194	205	188	188	199	200	209	166	199	199	199	199	199	199	199		
1100	8	118	118	21	183	202	226	228	233	334	349	157	165	179	173	118	118	133	337	235	235	203	225	179	195	177	180	199	186	200	188	199	208	201	209	189	199	201	189	199	199	199	200	200	200	200
1101	8	139	139	21	199	190	226	223	244	337	357	157	157	179	183	119	119	366	366	277	277	229	227	179	179	177	180	199	180	200	188	199	199	204	188	199	199	199	199	199	199	199	199	199	199	
1102	8	139	145	11	193	190	225	224	249	339	349	157	157	174	170	119	119	399	360	000	000	000	000	000	000	000	000	144	161	161	170	144	200	218	196	196	196	196	196	196	196	196	196	196	196	
1105	8	155	155	21	193	208	223	222	248	335	355	156	168	189	180	119	118	399	364	245	245	193	229	177	177	177	199	188	188	199	208	200	200	200	200	200	200	200	200	200	200	200	200	200	200	200
1110	8	145	155	21	195	199	222	222	255	335	355	00	00	199	199	113	113	235	335	266	267	224	223	199	177	177	177	185	177	188	199	188	199	208	198	199	203	200	203	204	198	199	199	199	199	199
1111	8	133	145	21	195	199	222	222	248	334	349	00	00	199	199	113	113	355	355	230	230	224	224	199	177	177	177	185	177	188	199	188	199	208	198	199	203	200	203	204	198	199	199	199	199	199
1112	8	133	145	21	195	199	222	222	248	334	349	157	155	179	170	113	113	355	355	238	230	224	224	199	177	177	177	185	177	188	199	188	199	208	198	199	203	200	203	204	198	199	199	199	199	199

33		9	9	1	9	3	0	5	5	4	4	2	9	7	7	5	9	7	1	9	1	7	0	8	0	1	5	9	9	8	2	0	0	5	5	1	5	4	8	6	0	4	4	4	4	0	6						
1134		1	1	2	2	1	1	2	2	2	2	3	3	1	1	1	1	1	1	1	1	1	3	3	2	2	2	2	1	1	1	1	1	1	1	1	1	2	1	1	1	1	1	1	1	2	0						
1135	8	0	0	1	5	8	7	8	1	3	2	2	4	5	5	7	7	3	4	8	0	5	6	7	0	2	2	7	7	7	9	9	2	2	6	0	7	8	8	8	1	3	9	0	6	0	4	0	0				
1140	8	3	3	1	1	9	3	5	5	4	4	9	7	0	0	9	9	7	4	8	9	9	0	0	0	0	9	9	9	9	8	8	8	8	0	5	5	1	5	8	8	1	1	9	9	6	6	4	4	4	8	0	0
1141	8	0	3	0	0	4	8	6	5	4	4	7	7	0	0	5	0	1	1	1	1	1	2	3	3	2	3	2	2	1	1	1	1	1	1	1	2	2	1	3	6	0	8	0	4	0	6	8	9	9	8	1	2
1142	8	0	5	1	1	3	8	5	5	4	2	7	7	7	7	4	1	7	0	3	8	9	4	6	3	5	2	2	7	7	7	6	8	8	0	0	9	9	6	8	9	3	9	9	6	8	8	9	0	0	0		
1143	8	0	3	1	9	3	9	5	5	4	4	7	7	7	7	4	9	7	4	3	9	0	6	6	3	7	2	2	7	7	8	8	0	0	5	5	1	5	4	8	9	1	9	0	6	6	9	9	1	1	2	2	
0000P		1	1	2	2	1	2	2	2	2	2	3	3			1	1	1	1	1	1	2	3	3	2	2	2	2	1	1	1	1	1	1	2	2	1	1	2	2	1	1	1	1	1	2	2	2	2	2	2	0	
0000R		1	1	2	2	1	1	2	2	2	2	3	3			1	1	1	1	1	1	2	3	3	2	2	2	2	1	1	1	1	1	1	2	2	1	1	2	2	1	1	2	2	1	1	1	1	1	2	2	2	0
1103		1	1	2	2	1	1	2	2	2	2	3	3			1	1	1	1	1	1	2	3	3	2	2	2	2	1	1	1	1	1	1	2	2	1	1	2	2	1	1	2	2	1	1	1	1	2	2	2	0	
1104		1	1	2	2	1	1	2	2	2	2	3	3	1	1	1	1	1	1	1	1	2	3	3	2	2	2	2	1	1	1	1	1	1	2	2	1	1	2	2	1	1	2	2	1	1	1	1	2	2	2	0	
1104		1	1	2	2	1	1	2	2	2	2	3	3	1	1	1	1	1	1	1	1	2	3	3	2	2	2	2	1	1	1	1	1	1	2	2	1	1	2	2	1	1	2	2	1	1	1	1	2	2	2	0	
1104		1	1	2	2	1	1	2	2	2	2	3	3	1	1	1	1	1	1	1	1	2	3	3	2	2	2	2	1	1	1	1	1	1	2	2	1	1	2	2	1	1	2	2	1	1	1	1	2	2	2	0	

00		8	2	1	9	9	9	3	2	8	0	7	9			1	5	7	9	5	9	0	7	4	4	3	3	1	1	0	0	8	6	7	5	9	7	9	0	6	0	2	3	0	4	6	8							
4102		1	1	2	2	1	1	2	2	2	2	3	3			1	1	1	1	1	2	3	3	2	2	1	2	1	1	1	1	1	1	1	1	1	1	1	1	2	1	1	1	1	1	1	2							
20		3	4	5	8	7	7	2	4	1	2	4	5	0	0	6	6	2	3	8	1	5	7	9	9	0	0	2	7	7	8	0	5	6	6	6	4	6	5	8	8	5	8	9	9	0	6	3	4	6	0	8	6	4
4105H		1	1			1	1	2	2	2	2	3	3	1	1	1	1	1	1	1	2	3	3	2	2	2	2	1	2	1	1	1	1	1	1	1	1	1	1	2	1	1	1	1	2	1	1	1	1	2				
00		4	9	0	0	7	1	7	4	1	8	0	1	9	5	1	3	1	9	3	0	9	8	6	6	5	7	3	3	0	4	2	0	4	8	3	3	7	0	6	6	4	9	7	4	6	8							
5544		1	1			1	1	2	2	2	2	3	3	1	1	1	1	1	1	1	2	3	3	2	2	1	2	1	1	1	1	1	1	1	1	1	1	2	1	2	1	1	1	1	2	1	2							
40		1	2			7	7	2	2	2	2	4	5	7	7	1	4	2	9	1	4	5	6	6	6	9	0	7	8	8	0	7	8	5	0	5	7	8	2	9	0	9	0	6	3	4	8	6	2	6	4			
5545		1	1			8	2	3	5	2	3	4	4	5	5	6	7	2	3	9	1	4	5	8	8	1	2	8	8	6	7	8	6	4	4	5	8	8	9	8	3	1	0	6	7	7	8	9	9	6	2	6		
5550		1	1	2	2	1	1	2	2	2	2	3	3	1	1	1	1	1	1	1	1	3	3	2	2	1	2	1	1	1	1	1	1	1	1	1	1	1	2	2	1	1	1	1	1	1	2	1	2					
00		2	4	8	8	6	7	3	3	2	3	5	5	5	6	6	7	3	9	9	4	5	6	7	9	1	6	8	6	6	9	0	9	9	8	8	8	9	8	4	0	0	6	7	8	0	9	0	8					
5551		1	1	2	2	1	1	2	2	2	2	3	3			1	1	1	1	1	1	1	1	1	1	1	1	1	1	1	1	1	1	1	1	1	1	1	2	1	1	1	1	1	1	1	1	1	1	0				
00		2	2	5	5	7	8	2	2	2	2	3	4	0	0	6	7	0	3	8	9	4	5	6	6	0	0	7	8	8	4	9	2	4	4	5	8	8	8	7	1	7	9	6	6	4	4	7	4	0	0			
5552		1	1	2	2	1	1	2	2	2	2	3	3	1	1	1	1	1	1	2	2	3	3	2	2	2	2	1	2	1	1	1	1	1	1	1	1	1	1	2	1	1	1	1	1	1	1	1	1	1	1			
00		2	3	5	8	7	7	2	3	2	2	5	5	5	6	9	0	4	2	1	1	5	5	4	5	0	0	7	7	6	6	7	9	5	5	8	6	6	2	9	9	8	2	9	9	0	3	7	9	9	6			
5553		1	1	2	2	1	1	2	2	2	2	3	3	1	1	1	1	1	1	2	3	3	2	2	1	2	1	1	1	1	1	1	1	1	1	1	1	1	1	2	1	1	1	1	1	1	1	1	1	1	1			
00		4	5	6	6	7	2	2	2	2	4	4	5	5	6	8	3	3	8	1	4	5	6	7	9	0	5	5	8	9	7	6	6	0	7	7	5	5	4	2	9	0	7	7	8	2	9	9	0	6				
5554		1	1	2	2	1	1	2	2	2	2	3	3			1	1	1	1	1	2	3	3	2	2	2	2	1	2	1	1	1	1	1	1	1	1	1	1	1	1	1	1	1	1	1	1	1	1	1	2			
00		2	4	5	8	6	7	0	2	2	3	3	4	0	0	5	5	3	4	9	1	4	6	6	7	0	1	7	7	7	8	0	9	6	0	5	0	0	4	4	8	9	9	0	0	4	8	8	9	1	1			
5555		1	1			1	1	2	2	2	2	3	3			1	1	1	1	1	2	3	3	2	2	1	2	1	1	1	1	1	1	1	1	1	1	1	1	1	1	1	1	1	1	1	1	1	1	1	1	2		
00		2	3	0	0	7	8	0	2	3	4	4	6	0	0	6	6	2	3	9	1	5	5	6	7	9	2	7	7	6	8	8	8	8	4	4	6	1	7	0	0	0	0	0	9	0	7	2	9	0	4	4	6	
4100		1	1	2	2	1	1	2	2	2	2	3	3	1	1	1	1	1	1	1	1	3	3	2	2	2	2	1	2	1	1	1	1	1	1	1	1	1	1	1	1	1	1	1	1	1	1	1	1	1	1	2		
09		3	4	5	8	6	8	2	3	1	2	4	4	4	6	7	8	2	3	8	9	4	5	4	7	2	3	7	7	8	9	9	0	9	2	6	8	8	9	1	1	6	6	7	8	9	0	6	2	0				

3 2 3 5		1 2 2	1 2 2	2 5 1	2 5 1	1 9 4	1 9 4	2 6	2 5	2 6	2 6	2 3	2 3	3 5	3 6	1 5	1 7	1 7	1 8	1 3	1 3	1 3	1 3	2 0	2 2	3 5	3 6	2 8	2 8	2 3	2 3	1 6	1 7	1 8	2 1	2 1	1 8	2 0	2 0	2 6	2 6	1 5	1 8	1 8	2 1	2 0	2 0	1 8	1 8	1 9	1 9	2 0	2 0	2 4	2 4	1 8	1 8	1 0	1 0	2 0	2 0	2 4	2 4	1 8	1 8	1 0	1 0	2 0	2 0
3 1 0	3 8	1 3	1 3	2 4	2 6	1 9	1 9	2 0	2 3	2 2	2 2	2 2	2 3	3 3	1 4	1 6	1 6	1 9	1 4	1 4	1 9	1 4	1 4	2 0	2 0	3 5	3 5	0 0	0 0	2 5	2 5	1 6	1 6	1 8	1 9	2 0	2 0	2 0	2 0	2 7	2 7	1 8	1 8	2 0	2 0	2 6	2 6	1 1	1 1	2 2	2 2	2 3	2 3	1 8	1 8	1 6	1 6	2 0	2 0	2 3	2 3	1 8	1 8	1 6	1 6	2 0	2 0		
3 1 2 1	3 8	1 4	1 5			1 8	2 3	2 6	2 5	2 0	2 8	2 6	2 3	3 6	1 0	1 4	1 4	1 6	1 8	1 3	1 3	1 3	1 3	1 8	2 0	3 4	3 5	2 7	2 7	1 9	2 2	1 6	1 7	1 7	1 8	1 8	2 0	2 0	2 4	2 4	1 9	1 9	2 1	2 1	2 5	2 5	1 7	1 7	1 9	1 9	1 6	1 6	1 9	1 9	1 4	1 4	2 9	2 9	1 8	1 8	1 6	1 6	2 0	2 0					
O M B D T	3 8	1 3	1 3	2 5	2 8	2 0	2 1	2 5	2 5	2 0	2 4	2 0	2 3	3 4	1 6	1 7	1 6	1 7	1 7	1 1	1 3	1 3	1 8	2 1	3 2	3 4	2 5	2 1	2 2	2 2	2 6	2 7	1 8	1 8	1 8	1 9	1 8	2 0	2 0	2 3	2 3	2 6	2 6	1 7	1 7	2 0	2 0	2 3	2 3	1 8	1 8	1 6	1 6	2 0	2 0														
3 1 4 5 C	3 9	1 4	1 8	2 5	2 3	1 9	1 0	2 2	2 1	2 2	2 2	2 3	3 5	3 7	1 5	1 7	1 4	1 7	1 1	1 1	1 1	1 1	1 9	2 7	2 5	3 4	3 1	2 0	2 0	1 9	2 2	1 3	1 3	1 8	1 8	1 8	1 9	1 9	1 9	1 9	2 7	2 7	1 8	1 8	2 0	2 0	2 4	2 4	1 9	1 9	1 6	1 6	2 0	2 0															
3 2 0 1 G	3 9	1 2	1 4	2 6	2 7	1 8	1 9	2 0	2 1	2 2	2 2	2 3	3 4	3 7	1 6	1 7	1 7	1 8	1 1	1 3	1 3	1 9	2 7	2 4	3 5	3 6	2 6	2 6	1 9	2 2	1 3	1 3	1 6	1 6	1 7	1 7	2 0	2 0	2 4	2 4	1 8	1 8	2 0	2 0	2 3	2 3	1 6	1 6	2 0	2 0																			
3 2 0 4 B	3 9	1 2	1 3	2 5	2 5	1 6	1 8	2 1	2 2	2 2	2 2	2 3	3 4	3 7	1 5	1 6	1 6	1 7	1 1	1 3	1 3	1 9	2 1	2 2	3 4	3 4	2 4	2 4	1 9	2 2	1 1	1 1	1 6	1 6	1 8	1 8	2 0	2 0	2 4	2 4	1 8	1 8	2 0	2 0	2 3	2 3	1 6	1 6	2 0	2 0																			
3 2 4 0	3 9	1 2	1 3	2 5	2 7	1 9	2 2	2 0	2 1	2 2	2 2	2 3	3 4	3 7	1 4	1 6	1 7	1 8	1 1	1 3	1 3	1 9	2 8	2 5	3 4	3 1	2 0	2 0	1 9	2 2	1 3	1 3	1 6	1 6	1 7	1 7	2 0	2 0	2 4	2 4	1 8	1 8	2 0	2 0	2 3	2 3	1 6	1 6	2 0	2 0																			
3 2 4 1	3 9	1 2	1 3	2 6	2 7	1 9	1 4	2 2	2 2	2 2	2 2	2 3	3 4	3 5	1 6	1 6	1 6	1 6	1 2	1 2	1 2	1 4	2 0	2 1	3 4	3 6	2 0	2 0	1 5	2 2	1 1	1 1	1 6	1 6	1 8	1 8	2 0	2 0	2 4	2 4	1 8	1 8	2 0	2 0	2 3	2 3	1 6	1 6	2 0	2 0																			
3 2 4 2	3 9	1 4	1 6	2 5	2 8	1 7	1 7	2 0	2 1	2 2	2 2	2 3	3 7	3 6	1 5	1 6	1 6	1 7	1 1	1 2	1 2	1 4	2 0	2 1	3 5	3 6	2 4	2 4	1 9	2 2	1 3	1 3	1 6	1 6	1 7	1 7	2 0	2 0	2 4	2 4	1 8	1 8	2 0	2 0	2 3	2 3	1 6	1 6	2 0	2 0																			

3 2 3 0	C	1 4 8	1 5 2	2 5 1	2 5 1	1 7 5	1 7 9	2 1 6	2 2 7	2 1 6	2 2 4	3 3 6	3 8 3	0	0	1 6 4	1 7 1	1 1 9	1 3 1	1 8 9	1 8 9	3 4 5	3 4 9	2 3 8	2 8 2	1 9 3	2 0 1	1 6 7	1 5 5	1 6 9	1 9 8	2 1 4	1 9 2	1 7 0	2 0 2	1 7 7	1 9 0	1 9 0	1 9 4	0	0						
3 2 3 1	C	1 1 4	1 3 9	2 5 1	2 6 2	1 7 5	1 7 9	2 1 6	2 2 7	2 2 4	2 2 8	2 4 0	3 4 2	3 4 4	1 5 3	1 5 3	1 6 4	1 7 1	1 2 3	1 3 1	2 2 9	2 2 4	3 5 7	3 5 7	2 7 0	2 8 2	2 0 7	2 0 0	1 9 4	1 8 8	1 8 8	1 9 9	1 9 8	1 7 9	1 7 2	2 0 0	2 0 0	1 9 0	2 0 0	1 9 0	1 9 0	2 0 0	2 0 0				
3 2 3 2	C	1 2 2	1 3 0	2 5 1	2 6 9	1 7 5	1 8 3	2 1 9	2 2 4	2 2 8	2 2 4	2 3 2	3 3 8	3 3 3	1 5 7	1 5 7	1 6 7	1 8 7	1 3 3	1 3 3	2 0 0	2 0 3	3 3 8	2 5 4	2 7 8	1 9 3	2 0 9	1 5 9	1 6 7	1 7 9	1 9 4	1 9 9	1 9 9	1 6 6	1 7 7	1 7 6	2 0 0	2 0 0	1 9 0	2 0 0	1 9 0	1 9 0	2 0 0	2 0 0			
3 2 3 3	C	1 2 6	1 3 0	2 5 1	2 6 6	1 8 3	1 8 6	2 1 9	2 2 4	2 2 8	2 2 4	2 3 1	3 5 3	3 5 3	1 5 3	1 6 5	1 7 1	1 7 5	1 3 5	1 3 5	2 2 9	2 2 2	3 5 6	3 6 6	2 6 0	2 8 3	1 9 0	2 6 1	1 8 8	1 8 8	1 9 9	1 9 9	1 6 6	1 7 7	1 7 6	2 0 0	2 0 0	1 9 0	2 0 0	1 9 0	1 9 0	2 0 0	2 0 0				
3 2 3 4	C	1 2 2	1 3 4	0	0	0	0	0	0	0	0	0	0	0	0	0	0	0	0	0	0	0	0	0	0	0	0	0	0	0	0	0	0	0	0	0	0	0	0	0	0	0	0	0	0		
0 0 0 0 0 0	H R	1 5 2	1 5 6	0	0	1 7 1	1 7 9	2 2 7	2 4 4	2 1 6	2 2 8	2 2 4	3 4 2	3 5 3	0	0	1 6 9	1 7 3	0	0	1 9 7	2 0 1	0	0	0	0	0	0	0	0	0	0	0	0	0	0	0	0	0	0	0	0	0	0	0	0	0
0 0 0 1	H R	1 3 9	1 5 6	2 6 6	2 7 9	1 7 1	1 8 6	2 1 6	2 2 9	2 2 4	2 2 8	2 3 0	3 4 6	3 4 6	0	0	1 8 3	1 8 3	1 9 9	1 9 9	2 7 8	3 0 9	3 4 7	2 5 9	2 6 7	1 8 5	2 9 5	1 6 6	1 8 8	2 8 6	2 0 6	2 0 6	2 2 6	2 2 6	2 0 0	2 0 0	1 7 5	2 0 6	2 0 6	1 7 3	1 8 8	1 9 8	2 0 4	2 0 4			
0 0 0 2	H R	1 3 9	1 3 9	2 5 1	2 5 3	1 8 3	1 8 3	2 5 0	2 5 2	2 2 8	2 2 4	2 3 2	3 4 9	3 9 2	0	0	2 1 3	2 3 2	1 7 4	1 8 4	1 9 6	1 9 6	0	0	0	0	0	0	0	0	0	0	0	0	0	0	0	0	0	0	0	0	0	0	0	0	
0 0 0 3	H R	1 2 6	1 3 0	0	0	1 7 1	1 8 6	2 2 7	2 2 4	2 2 8	2 2 4	2 3 0	3 4 4	3 4 4	0	0	1 6 4	1 7 5	1 1 1	1 1 1	2 9 1	0 0 1	5 5 3	5 5 4	2 2 2	2 2 3	1 9 0	2 7 8	1 8 8	1 8 8	1 9 6	2 0 0	2 0 0	2 1 0	2 1 0	1 7 2	1 7 2	1 6 6	1 7 6	1 8 8	1 9 8	2 0 0	2 0 0				
0 0 0 4	H R	1 3 0	1 5 2	0	0	0	0	0	0	0	0	0	0	0	0	0	1 7 1	1 7 5	1 2 3	1 2 3	1 9 1	1 9 1	0	0	0	0	0	0	0	0	0	0	0	0	0	0	0	0	0	0	0	0	0	0	0	0	
0 0 0 5	H R	1 3 0	1 3 4	2 7 9	2 8 6	1 8 0	1 9 7	2 2 7	2 3 9	2 1 6	2 2 8	2 2 4	3 4 9	3 4 9	1 4 5	1 6 4	1 7 5	1 7 5	1 1 1	1 1 1	2 9 7	2 1 2	3 5 2	3 5 3	2 3 8	2 3 3	2 2 1	2 2 5	1 7 5	1 7 6	2 0 4	2 1 5	2 1 5	1 7 0	2 1 7	2 1 7	1 9 0	2 0 0	2 0 0	1 8 8	1 8 8	1 9 0	1 9 0	2 0 0	2 0 0		

000	H	130	139	255	279	171	190	246	269	220	228	233	330	330	157	157	160	183	183	111	111	208	208	234	234	220	220	175	175	198	198	217	217	226	226	192	192	207	207	178	178	173	173	190	190	196	196	
001	H	134	143			183	186	227	230	223	238	347	376	166	166	164	166	167	168	139	139	211	214	235	253	234	226	223	177	188	155	180			200	200	200	200	219	219	178	178	199	199	199	199	200	200
002	H	126	134	266	281	183	183	211	235	226	226	344	344	164	168	188	183	133	133	200	214	222	345	360	226	224	199	200	167	188	200	206	200	206	200	206	200	209	200	160	168	173	179	200	200	200	200	
003	H	134	156	279	279	188	188	255	261	222	223	378	385	166	177	188	183	133	133	200	211	224	345	358	226	228	199	200	167	177	188	188	200	206	200	206	200	209	200	160	168	177	190	200	200	200	200	
004	H	134	156			188	188	211	235	226	226	344	344	164	168	188	183	133	133	200	214	222	345	357	226	224	199	200	167	188	200	206	200	206	200	206	200	209	200	160	168	173	179	200	200	200	200	
005	H	122	137	299	281	186	186	222	223	222	222	344	344	164	168	188	183	133	133	200	211	224	345	356	226	222	199	200	167	177	188	188	200	206	200	206	200	209	200	160	168	177	190	200	200	200	200	
006	H	126	136	265	288	189	188	211	222	222	222	344	344	166	167	177	172	133	133	200	211	224	345	366	226	224	199	200	167	177	188	188	200	206	200	206	200	209	200	160	168	177	190	200	200	200	200	
007	H	130	139			179	188	222	222	222	222	333	333	159	166	166	166	133	133	200	211	224	333	333	226	224	199	200	167	177	188	188	200	206	200	206	200	209	200	160	168	173	179	200	200	200	200	
008	H	122	125			189	184	222	222	222	222	344	344	166	187	177	173	133	133	200	211	224	345	360	226	222	199	200	167	177	188	188	200	206	200	206	200	209	200	160	168	173	179	200	200	200	200	
009	H	134	152			178	184	222	222	222	222	333	333	165	166	166	166	133	133	200	211	224	345	357	226	222	199	200	167	177	188	188	200	206	200	206	200	209	200	160	168	173	179	200	200	200	200	

0 0 2 5	H R	1 2 2	1 4 3	0 0	1 7 1	1 9 4	2 3 1	2 4 2	2 2 4	2 2 8	3 3 9	3 7 7	0 0	1 4 4	1 6 7	1 3 1	1 3 1	1 9 7	2 0 1	3 4 5	3 4 5	2 6 2	2 7 4	1 9 3	1 9 3	1 6 3	1 7 5	1 8 8	1 9 2	1 8 4	1 8 8	2 0 5	2 1 2	0 0	2 1 0	2 1 4	1 6 4	1 9 6	1 4 7	1 8 0	1 8 6	1 9 0	0 0	
0 1 0 0	H R	1 2 6	1 3 9	2 6 2	2 6 1	1 7 5	2 2 3	2 4 4	2 1 2	2 1 6	3 3 4	3 4 0	1 5 7	1 6 1	1 7 3	1 8 9	1 3 4	1 4 3	1 9 7	1 9 9	3 5 3	3 6 6	2 6 6	2 8 7	1 9 9	1 9 7	1 7 6	1 7 8	2 0 0	2 0 5	2 0 8	1 1 1	1 1 8	2 2 6	2 2 8	1 8 8	2 1 5	2 1 8	1 8 4	1 8 8	1 9 0	1 9 4	1 9 2	2 0 4
0 1 0 1	H R	1 2 6	1 3 0	2 5 1	2 5 3	1 8 3	2 8 5	2 3 9	2 1 6	2 2 8	3 2 9	3 6 1	0 0	1 7 5	1 8 3	1 1 9	1 3 9	1 3 3	2 9 9	2 2 7	3 5 3	3 6 6	2 6 2	2 6 7	2 2 1	2 2 6	1 6 6	1 8 8	2 0 0	2 0 8	2 6 7	1 7 7	2 0 6	2 1 4	2 2 1	2 2 9	1 9 0	2 0 8	2 1 7	2 1 9	1 7 3	1 9 8	1 9 6	2 0 0
0 1 0 2	H R	1 3 4	1 4 8	2 5 1	2 7 9	1 8 6	2 3 9	2 2 2	2 2 8	2 3 6	3 2 4	3 4 9	1 6 5	1 6 9	1 7 0	1 8 1	1 3 1	1 3 1	2 9 1	2 9 4	3 5 3	3 6 6	2 4 2	2 8 9	2 2 1	2 2 6	1 7 7	1 7 7	1 7 7	2 0 8	2 0 8	1 6 9	1 8 5	2 2 6	2 2 4	2 1 4	2 1 9	1 9 0	2 0 6	2 1 4	2 1 8	1 9 9	2 0 4	
0 1 0 3	H R	1 3 0	1 3 9	2 5 5	2 6 0	1 8 3	2 5 7	2 2 2	2 2 2	2 3 2	3 2 2	3 4 2	1 7 7	1 6 1	1 7 1	1 8 1	1 3 1	1 3 1	2 9 1	2 4 5	3 5 6	3 6 6	2 4 6	2 8 7	2 2 1	2 2 6	1 7 7	1 7 7	1 7 7	2 0 8	2 0 8	1 6 9	1 8 5	2 2 4	2 2 4	2 1 4	2 1 9	1 9 0	2 0 6	2 1 4	2 1 8	1 9 9	2 0 4	
0 1 0 4	H R	1 2 6	1 4 8	2 5 1	2 8 9	1 7 6	2 3 9	2 2 2	2 2 2	2 3 6	3 4 4	3 4 0	1 4 4	1 5 7	1 8 3	1 3 1	1 3 1	2 9 7	2 0 8	3 6 0	3 6 6	2 4 2	2 4 6	2 2 1	2 2 6	2 2 1	1 6 6	1 8 8	2 0 0	2 0 8	1 6 9	1 8 5	2 2 6	2 2 0	2 1 8	2 2 8	2 1 4	2 1 9	1 8 8	1 9 9	2 0 4			
0 1 0 5	H R	1 3 0	1 3 9	2 5 1	2 5 3	1 8 6	2 2 7	2 2 2	2 2 2	2 3 8	3 4 4	3 4 9	1 5 3	1 6 9	1 7 0	1 8 5	1 3 9	1 3 9	2 9 2	2 3 3	3 5 5	3 5 8	2 8 2	2 2 5	2 2 7	1 6 3	1 7 7	1 7 7	2 0 9	2 0 9	1 7 6	1 8 5	2 2 4	2 2 4	2 1 6	2 1 7	1 9 0	2 0 7	2 1 6	2 1 8	1 9 9	2 0 2		
0 1 1 0	H R	1 3 4	1 5 6	2 5 1	2 9 3	1 8 6	2 6 9	2 2 6	2 2 6	2 3 2	3 4 4	3 4 4	1 6 1	1 6 9	1 8 3	1 8 3	1 3 5	2 0 8	2 1 5	3 6 0	3 6 6	2 4 2	2 4 6	2 2 4	2 2 1	2 2 6	1 6 6	1 8 8	2 0 0	2 0 8	1 6 9	1 8 5	2 2 5	2 2 0	2 1 8	2 2 8	2 1 4	2 2 8	2 1 7	2 1 9	1 8 9	2 0 0		
0 1 1 1	H R	1 3 4	1 4 3	2 7 9	2 8 9	1 7 6	2 3 1	2 2 2	2 2 2	2 3 6	3 3 4	3 4 0	1 4 0	1 4 0	1 6 9	1 3 1	1 3 4	2 0 1	2 1 2	3 0 4	3 5 7	3 6 4	2 4 0	2 4 6	2 2 1	2 2 6	1 6 6	1 7 7	1 7 7	2 0 1	2 0 1	1 6 7	1 7 2	2 2 4	2 2 4	2 2 0	2 2 0	2 1 7	2 1 8	1 9 9	2 0 0			
0 1 1 2	H R	1 2 2	1 3 4	2 5 1	2 7 9	1 8 3	2 4 2	2 2 2	2 2 2	2 3 6	3 3 4	3 4 0	1 5 4	1 5 4	1 7 5	1 3 1	1 4 1	2 0 4	2 1 4	3 5 3	3 6 7	3 6 4	2 4 0	2 4 6	2 2 1	2 2 6	1 6 6	1 7 7	1 7 7	2 0 1	2 0 1	1 6 7	1 7 2	2 2 4	2 2 4	2 2 0	2 2 0	2 1 7	2 1 8	1 9 9	2 0 0			
0 1 1 3	H R	1 3 4	1 3 3	2 7 3	2 7 5	1 8 1	2 4 2	2 2 8	2 2 2	2 3 3	3 3 4	3 3 6	1 6 1	1 6 5	1 7 8	1 3 1	1 3 1	2 0 7	2 1 5	3 5 7	3 6 0	3 6 4	2 4 6	2 4 6	2 2 1	2 2 6	1 6 7	1 7 8	2 0 1	2 0 1	1 6 2	1 7 0	2 2 5	2 2 0	2 1 8	2 2 0	2 1 6	2 1 7	1 9 0	2 0 4	2 0 8			
0 1 1 4	H R	1 3 3	1 3 3	2 7 3	2 7 5	1 8 1	2 4 2	2 2 2	2 2 2	2 3 3	3 3 4	3 3 6	1 6 1	1 6 5	1 7 8	1 3 1	1 3 1	2 0 7	2 1 5	3 5 7	3 6 0	3 6 4	2 4 6	2 4 6	2 2 1	2 2 6	1 6 7	1 7 8	2 0 1	2 0 1	1 6 2	1 7 0	2 2 5	2 2 0	2 1 8	2 2 0	2 1 7	2 1 8	1 9 9	2 0 0				

Table B.4. Individual genetic data from Santa Barbara Island. Microsatellite genotypes from captured individuals on Santa Barbara Island. Sample ID and order match Table B.1. Locus ID is the microsatellite locus number (e.g. Xari46 = 46 below). Columns A and B represent the allele calls for each locus. Allele calls of 0 denote missing data, all other entries are allele called based on size in base pairs.

S a m p l e I D	P O P	46		09		18		13		48		11		33		38		41		35		42		22		47		05		44		7		21		10		1		30		45		31		20							
		A	B	A	B	A	B	A	B	A	B	A	B	A	B	A	B	A	B	A	B	A	B	A	B	A	B	A	B	A	B	A	B	A	B	A	B	A	B	A	B	A	B										
1104	P	134	156	277	285	188	183	250	262	208	206	344	366	166	165	177	179	133	133	211	219	236	238	224	224	220	220	199	199	166	168	189	184	211	218	188	188	199	198	220	220	217	217	188	180	211	217	188	180	226	226	226	226
1105	P	126	134	277	273	188	183	250	262	208	206	344	366	166	165	177	179	133	133	211	219	236	238	224	224	220	220	199	199	166	168	189	184	211	218	188	188	199	198	220	220	217	217	188	180	211	217	188	180	226	226	226	226
1110	P	156	173	288	281	199	190	293	290	220	220	366	373	166	165	188	180	133	133	211	219	236	238	224	224	220	220	199	199	166	168	189	184	211	218	188	188	199	198	220	220	217	217	188	180	211	217	188	180	226	226	226	226
1111	P	134	148	281	286	199	190	293	290	220	220	366	373	166	165	188	180	133	133	211	219	236	238	224	224	220	220	199	199	166	168	189	184	211	218	188	188	199	198	220	220	217	217	188	180	211	217	188	180	226	226	226	226
1112	P	134	148	281	286	199	190	293	290	220	220	366	373	166	165	188	180	133	133	211	219	236	238	224	224	220	220	199	199	166	168	189	184	211	218	188	188	199	198	220	220	217	217	188	180	211	217	188	180	226	226	226	226
1122	P	147	178	288	288	188	180	293	292	220	220	366	373	166	165	188	180	133	133	211	219	236	238	224	224	220	220	199	199	166	168	189	184	211	218	188	188	199	198	220	220	217	217	188	180	211	217	188	180	226	226	226	226
1222	P	135	177	288	283	188	183	293	290	220	220	366	373	166	165	188	180	133	133	211	219	236	238	224	224	220	220	199	199	166	168	189	184	211	218	188	188	199	198	220	220	217	217	188	180	211	217	188	180	226	226	226	226

4		6	3	7	9	5	3	5	6	6	4	6	6	1	5	3	3	1	9	0	7	3	3	0	8	7	9	7	5	8	0	0	4	1	8	1	5	2	6	0	7	2	6	8	6	6	6					
4																																																				
1		1	1	2	2	1	2	2	2	2	2	3	3	1	1	1	1	1	1	2	2	3	3	2	2	2	2	1	1	1	2	2	2	2	2	2	2	2	2	2	2	2	1	1	1	2	1	2				
2	C	1	4	7	9	9	0	3	5	0	2	4	4	6	6	8	8	4	5	0	0	4	6	7	8	0	3	6	6	7	2	0	0	0	0	5	0	0	0	0	0	0	0	7	7	8	0	9	1			
5	B	8	3	3	3	4	5	5	8	4	0	0	7	5	5	3	3	4	3	7	8	1	0	0	2	9	3	3	7	2	2	8	5	8	7	0	2	2	2	2	2	2	7	6	2	2	6	6				
1		1	1	2	2	1	1	2	2	2	2	3	3	1	1	1	1	1	1	2	2	3	3	2	2	1	2	1	1	1	2	2	2	2	2	2	2	2	2	2	2	2	1	1	1	1	2	2				
2	C	2	4	8	8	7	8	3	5	2	4	4	6	6	6	7	8	3	3	8	1	5	6	6	7	9	3	6	7	7	8	0	0	9	1	5	6	9	0	0	0	0	7	7	8	9	0	0				
0	B	6	3	1	9	9	3	5	8	4	4	7	6	5	5	9	3	5	9	9	7	0	6	4	3	3	7	9	2	0	0	4	7	6	7	5	8	6	0	0	7	2	2	2	8	8	8					
1		1	1	2	2	1	1	2	2	2	2	3	3	1	1	1	1	1	1	2	2	3	3	2	2	1	1	1	1	1	2	2	2	2	2	2	2	2	2	2	2	1	1	1	1	2	2	2				
2	C	5	5	7	9	8	9	3	3	2	2	6	7	6	6	7	8	2	4	0	1	5	6	7	8	9	9	8	8	8	8	0	1	6	0	7	8	0	1	0	0	7	8	9	1	0	1					
1	B	2	2	7	3	3	8	1	9	0	8	3	3	1	5	9	7	7	4	1	2	7	0	0	6	3	3	3	7	4	8	8	2	1	5	7	1	2	0	3	7	2	4	4	0	8	2					
1		1	1	2	2	1	1	2	2	2	2	3	3	1	1	1	1	1	1	2	2	3	3	2	2	1	1	1	1	1	2	2	2	2	2	2	2	2	2	2	2	2	1	1	1	2	1	2				
3	C	4	5	7	8	7	9	5	5	2	4	7	7	6	6	8	9	3	3	0	1	4	5	7	8	9	9	6	7	7	8	0	1	1	1	2	2	2	2	2	2	2	2	2	2	2	2	2				
0	B	3	2	7	1	5	4	0	8	8	0	0	3	1	1	7	0	1	9	7	2	1	8	6	3	7	7	5	2	4	4	2	2	2	2	2	2	2	2	2	2	1	1	1	2	1	9	0	4			
1		1	1	2	2	1	1	2	2	2	2	3	3	1	1	1	1	1	1	2	2	3	3	3	3	1	2	1	1	1	2	2	2	2	2	2	2	2	2	2	2	2	2	2	1	1	1	2	2			
3	C	4	6	7	8	8	8	3	4	2	2	4	4	6	6	6	8	5	5	0	2	5	5	1	1	9	2	8	8	8	9	0	0	7	0	6	8	0	0	0	0	7	8	9	0	0	0					
1	B	3	5	3	1	3	3	5	6	4	8	0	4	5	5	7	7	3	8	1	3	3	7	1	1	3	1	7	7	0	2	0	4	1	8	5	8	8	6	6	3	7	2	8	0	2	8	8				
1		1	1	2	2	1	1	2	2	2	2	3	3	1	1	1	1	1	1	2	2	3	3	2	2	1	1	1	1	2	2	2	2	2	2	2	2	2	2	2	2	2	2	2	2	2	2	2				
3	C	3	4	7	9	7	8	5	6	2	4	4	5	6	6	7	7	1	5	8	0	5	6	7	8	9	9	7	7	0	0	8	8	8	8	8	8	8	8	8	8	8	8	8	8	8	8	8	8			
1	B	4	8	3	3	9	3	8	5	0	0	4	9	5	5	1	1	9	3	9	1	7	0	0	2	3	3	1	1	8	8	8	8	7	2	7	6	2	2	2	2	2	2	2	2	2	2	2				
0		1	1	2	2	2	2	2	2	2	2	3	3	1	1	1	1	1	1	2	2	3	3	2	2	1	2	1	1	1	2	2	2	2	2	2	2	2	2	2	2	2	2	2	2	2	2					
5	C	4	7	7	7	0	0	3	5	1	1	6	7	5	6	7	8	3	3	0	1	5	5	7	9	9	3	8	8	8	8	8	8	8	8	8	8	8	8	8	8	8	8	8	8	8	8	8				
0	C	8	3	3	7	2	7	9	8	6	6	6	3	7	5	9	7	5	9	8	2	7	4	4	7	3	3	3	4	5	4	4	8	0	4	8	0	5	2	2	2	2	2	2	2	2	2	2				
0		1	1	2	2	1	1	2	2	2	2	3	3	1	1	1	1	1	1	2	2	3	3	2	2	1	1	1	1	2	2	2	2	2	2	2	2	2	2	2	2	2	2	2	2	2	2					
5	C	7	7	7	8	7	8	3	5	1	3	6	8	5	6	7	9	4	4	1	1	4	5	7	7	9	9	7	7	8	9	0	0	9	9	9	9	9	9	9	9	9	9	9	9	9	9	9				
0	C	3	3	3	9	9	6	1	0	6	2	6	1	7	1	1	8	9	9	2	5	1	7	4	4	3	7	1	1	8	5	2	4	7	7	7	7	7	7	7	7	7	7	7	7	7	7					
0		1	1	2	2	1	1	2	2	2	2	3	3	1	1	1	1	1	1	2	2	3	3	2	2	1	1	1	1	2	2	2	2	2	2	2	2	2	2	2	2	2	2	2	2	2	2					
5	C	3	4	7	0	9	9	3	5	2	3	5	6	6	7	6	7	3	5	0	1	4	5	5	6	9	9	6	7	8	9	0	0	9	0	8	0	9	9	9	9	9	9	9	9	9	9	9				
0	C	0	3	7	0	0	4	5	4	8	2	5	6	5	3	0	9	9	8	8	0	5	7	8	6	7	7	7	1	0	2	4	8	7	1	1	5	4	8	0	3	8	8	0	2	6	0	0				
0		1	1	2	2	1	1	2	2	2	2	3	3	1	1	1	1	1	1	2	2	3	3	2	2	1	1	1	1	2	2	2	2	2	2	2	2	2	2	2	2	2	2	2	2	2	2					
5	C	4	7	8	8	8	9	2	5	2	4	5	7	6	6	7	7	3	5	1	4	4	5	7	8	9	9	6	7	8	9	0	0	2	6	0	0	0	0	8	1	6	8	9	0	0	0					
4	C	3	3	1	9	3	0	7	4	0	0	1	0	5	5	1	5	9	3	5	0	5	7	4	2	3	7	7	9	8	5	8	4	1	0	5	5	2	2	2	2	8	5	8	4	8	2	0	8			

0011	NP	126	143	273	285	179	183	242	258	212	222	232	359	366	169	173	175	183	111	115	222	223	360	360	274	276	193	223	163	174	189	204	217	181	189	211	211	172	176	202	204	208
0012	NP	143	148	285	293	199	198	242	254	224	224	355	370	165	166	167	171	113	115	117	199	215	353	374	274	274	193	223	163	174	189	204	217	181	189	211	211	172	176	202	204	208
0013	NP	126	143	277	281	199	198	242	254	224	224	355	370	165	166	167	171	113	115	117	199	215	353	374	274	274	193	223	163	174	189	204	217	181	189	211	211	172	176	202	204	208
0014	NP	118	126	00	00	183	194	246	236	226	232	345	355	165	167	166	171	115	119	119	222	223	393	366	270	270	193	223	163	174	189	204	217	181	189	211	211	172	176	202	204	208
0015	NP	126	148	273	289	198	202	242	258	228	228	352	375	165	166	168	183	114	119	117	200	215	353	370	270	270	193	223	163	174	189	204	217	181	189	211	211	172	176	202	204	208
0020	NP	144	148	279	289	202	205	246	256	226	226	337	373	165	166	171	115	119	119	222	223	393	366	270	270	193	223	163	174	189	204	217	181	189	211	211	172	176	202	204	208	
0022	NP	144	143	273	285	199	202	246	256	226	226	366	366	165	163	163	183	114	119	117	200	215	353	370	270	270	193	223	163	174	189	204	217	181	189	211	211	172	176	202	204	208
0031	NP	126	143	285	285	199	194	246	256	226	226	363	377	165	166	167	171	113	119	119	222	223	393	366	270	270	193	223	163	174	189	204	217	181	189	211	211	172	176	202	204	208
0033	NP	135	146	273	277	195	194	242	252	228	228	355	373	165	166	166	174	118	118	117	200	215	353	370	270	270	193	223	163	174	189	204	217	181	189	211	211	172	176	202	204	208
0034	NP	144	143	273	289	196	198	242	254	224	224	356	373	165	166	166	174	118	118	117	200	215	353	370	270	270	193	223	163	174	189	204	217	181	189	211	211	172	176	202	204	208
0035	NP	134	143	273	285	199	200	242	252	228	228	357	373	166	166	168	173	118	118	117	200	215	353	370	270	270	193	223	163	174	189	204	217	181	189	211	211	172	176	202	204	208
0040	NP	135	148	288	288	198	203	242	252	228	228	357	374	166	166	167	173	118	118	117	200	215	353	370	270	270	193	223	163	174	189	204	217	181	189	211	211	172	176	202	204	208

40		4	2	1	9	6	3	5	5	8	2	0	0	9	3	0	1	1	9	4	3	5	9	6	4	1	5	7	5	8	8	4	8	7	0	7	5	2	4	0	5	6	6	6	0	0	8					
00		1	1	2	2	1	2	2	2	2	2	3	3	1	1	1	1	1	1	1	2	3	3	2	2	2	2	1	1	1	1	2	2	2	2	2	2	2	2	2	1	1	1	2	2	2	2	2				
41	N	4	4	7	9	9	0	5	6	1	3	7	7	6	7	7	1	1	4	5	9	0	5	6	5	8	0	1	7	7	8	4	4	0	0	0	1	8	8	1	2	0	0	7	8	8	0	0	8			
00		1	1	2	2	1	1	2	2	2	2	3	3	1	1	1	1	1	1	2	2	3	3	2	2	2	2	1	1	1	1	2	2	2	2	2	2	2	2	2	2	2	1	1	1	1	2	2	2			
43	N	3	4	7	9	7	7	4	5	0	4	4	0	1	5	4	1	9	9	4	8	0	6	6	6	7	1	2	8	8	7	2	4	2	4	7	5	7	7	9	2	0	0	7	8	8	9	0	0	8		
00		1	1	2	2	1	1	2	2	2	2	3	3	1	1	1	1	1	1	2	3	3	2	2	1	2	1	1	1	1	2	2	2	2	2	2	2	2	2	2	2	2	1	1	1	1	2	2	2			
44	N	2	4	8	9	7	8	3	3	3	3	7	7	5	6	7	7	3	4	8	1	5	6	7	8	9	0	6	9	8	4	4	2	8	0	7	8	8	0	0	1	1	7	8	8	9	0	0	8			
00		1	1	2	2	1	1	2	2	2	2	3	3	1	1	1	1	1	1	2	3	3	2	2	1	2	1	1	1	1	2	2	2	2	2	2	2	2	2	2	2	2	1	1	1	1	2	2	2			
45	N	1	2	8	9	9	9	3	3	3	3	4	7	5	6	6	8	4	5	9	2	5	5	7	7	9	0	7	7	8	4	6	6	6	0	7	7	8	8	0	1	1	7	7	8	8	0	0	0			
00		1	1	2	2	1	1	2	2	2	2	3	3	1	1	1	1	1	1	2	3	3	2	2	1	2	1	1	1	1	2	2	2	2	2	2	2	2	2	2	2	2	2	1	1	1	1	2	2	2		
50	N	5	5	7	8	7	9	3	5	1	2	5	6	6	6	7	7	3	5	9	2	5	6	6	6	1	2	6	7	8	5	8	8	8	9	9	1	1	8	9	1	0	1	7	8	1	1	0	0	0		
00		1	1	2	2	1	1	2	2	2	2	3	3	1	1	1	1	1	1	2	3	3	2	2	2	2	1	1	1	1	2	2	2	2	2	2	2	2	2	2	2	2	2	2	1	1	1	1	2	2	2	
51	N	2	3	8	8	7	8	6	6	1	1	5	6	6	6	7	7	3	4	1	2	6	6	6	9	2	2	6	8	8	0	9	0	0	0	5	7	0	2	2	0	1	7	8	8	8	9	0	0	8		
00		1	1	2	2	1	1	2	2	2	2	3	3	1	1	1	1	1	1	2	3	3	2	2	1	2	1	1	1	1	2	2	2	2	2	2	2	2	2	2	2	2	2	2	1	1	1	1	2	2	2	
52	N	2	4	9	9	9	9	5	5	2	3	7	7	6	6	7	7	3	4	9	0	5	6	7	8	9	1	7	7	8	8	0	0	1	2	3	9	9	1	1	0	1	7	7	8	0	0	2	2	2		
00		1	1	2	2	1	1	2	2	2	2	3	3	1	1	1	1	1	1	2	3	3	2	2	1	2	1	1	1	1	2	2	2	2	2	2	2	2	2	2	2	2	2	2	1	1	1	1	2	2	2	
53	N	3	4	8	8	7	7	6	6	2	3	7	7	6	6	7	7	3	4	1	4	4	4	7	7	9	4	7	8	8	4	8	8	8	9	0	7	7	7	2	2	0	0	5	2	6	6	8	0	0	8	
00		1	1	2	2	1	1	2	2	2	2	3	3	1	1	1	1	1	1	2	3	3	2	2	1	2	1	1	1	1	2	2	2	2	2	2	2	2	2	2	2	2	2	2	2	1	1	1	1	2	2	2
54	N	1	4	7	8	9	0	3	5	1	3	5	6	5	6	6	8	3	4	0	0	5	6	5	7	9	2	6	7	8	8	0	0	9	1	5	0	9	0	9	0	8	6	1	7	7	8	0	0	4		
00		1	1	2	2	1	1	2	2	2	2	3	3	1	1	1	1	1	1	2	3	3	2	2	1	2	1	1	1	1	2	2	2	2	2	2	2	2	2	2	2	2	2	2	2	1	1	1	1	2	2	2
55	N	2	4	8	8	0	0	4	4	0	4	4	5	6	7	7	8	4	4	0	1	4	6	5	6	1	1	7	8	8	0	0	8	9	7	8	0	2	0	0	0	0	7	8	8	1	0	1	2	2		
01		1	1	2	2	1	1	2	2	2	2	3	3	1	1	1	1	1	1	2	3	3	2	2	2	2	1	1	1	1	2	2	2	2	2	2	2	2	2	2	2	2	2	2	2	1	1	1	1	2	2	2
00	N	2	4	8	8	9	9	5	5	0	1	5	7	6	6	8	8	4	4	0	0	5	6	7	7	1	1	7	8	6	6	9	0	9	2	7	9	8	1	0	0	7	8	8	8	0	0	4	4			
00		1	1	2	2	1	1	2	2	2	2	3	3	1	1	1	1	1	1	2	3	3	2	2	1	2	1	1	1	1	2	2	2	2	2	2	2	2	2	2	2	2	2	2	2	1	1	1	1	2	2	2

0101	NP	143	148	277	289	175	186	235	242	204	232	363	366	161	169	171	179	144	149	207	208	353	357	270	274	197	245	163	167	188	188	188	212	210	219	216	177	185	206	204	200	203	176	184	186	210	213	178	220	212			
0103	NP	126	126	273	273	175	183	234	221	211	226	347	337	169	173	171	174	144	149	297	297	341	360	262	268	213	220	187	188	188	219	220	222	216	210	226	220	220	227	160	206	207	207	207	176	188	188	199	200	204	204		
0104	NP	143	143	277	277	180	194	226	220	223	234	347	337	166	166	166	174	144	145	200	223	355	360	258	262	219	221	177	177	178	210	220	222	217	218	211	215	219	200	226	220	220	211	178	180	220	220	212	226	220	201	222	
0105	NP	148	156	273	281	202	238	229	228	224	247	363	337	165	165	171	173	145	149	228	224	349	349	262	268	223	223	188	188	177	218	220	224	217	217	219	200	226	219	220	220	217	176	188	186	200	209	200	212	220	221		
0110	NP	126	143	273	273	202	225	228	224	225	245	366	356	166	167	166	173	145	149	223	223	349	349	258	262	223	223	188	188	177	218	220	222	217	217	219	200	226	220	220	220	217	176	188	186	200	209	200	212	220	221		
0111	NP	148	156	273	273	202	225	228	224	225	245	366	356	166	167	166	173	145	149	223	223	349	349	258	262	223	223	188	188	177	218	220	222	217	217	219	200	226	220	220	220	217	176	188	186	200	209	200	212	220	221		
0112	NP	130	133	288	288	202	230	222	224	224	240	366	366	169	169	175	173	145	149	224	224	349	349	262	262	222	222	188	188	177	218	220	222	217	218	219	200	226	224	220	220	220	220	217	188	188	188	200	209	200	212	220	221
0114	NP	126	143	273	273	202	225	228	224	225	245	366	356	166	167	166	173	145	149	223	223	349	349	258	262	223	223	188	188	177	218	220	222	217	217	219	200	226	220	220	220	217	176	188	186	200	209	200	212	220	221		
0115	NP	138	139	281	288	200	234	222	224	224	240	366	366	166	166	166	173	145	149	224	224	349	349	262	262	222	222	188	188	177	218	220	222	217	217	219	200	226	224	220	220	220	220	217	188	188	188	200	209	200	212	220	221
0120	NP	118	127	281	281	202	234	222	222	223	266	377	360	165	169	177	173	145	149	220	220	356	366	264	266	219	221	188	188	188	219	220	222	217	217	219	200	226	224	220	220	220	220	217	188	188	188	200	209	200	212	220	221
0121	NP	114	116	281	281	202	234	222	222	223	266	377	360	165	169	177	173	145	149	220	220	356	366	264	266	219	221	188	188	188	219	220	222	217	217	219	200	226	224	220	220	220	220	217	188	188	188	200	209	200	212	220	221

1 0 0 5	N P	1 2 7 8 9	1 7 8 9 3	2 2 9 3	2 1 7 8 3	2 2 8 3 5	2 2 4 4 2	2 2 4 4 0	2 2 4 4 6	3 6 6 6	3 6 6 6	1 6 9 3	1 7 4 5	1 6 7 5	1 7 3 1	1 4 9 7	2 0 7 3	2 2 3 7	3 5 6 9	3 6 6 2	2 6 8 2	2 8 2 3	1 9 7 1	2 1 7 1	1 7 8 3	1 8 8 0	1 8 8 4	1 8 4 0	2 0 9 7	1 9 7 2	2 1 8 5	1 8 8 6	2 0 6 6	2 2 5 5	2 1 7 8	1 8 8 2	1 7 8 2	1 8 8 6	2 0 6 0	2 0 6 0	2 1 2		
1 3 1 5	N P	1 1 8 3	1 4 7 3	2 7 3	2 8 1	2 0 2	2 0 4	2 4 6	2 4 7	3 4 7	3 4 7	1 5 7	1 7 7	1 7 1	1 7 1	1 3 9	1 5 8	2 0 1	2 0 0	3 6 6	3 6 7	2 7 8	2 7 4	2 4 4	1 7 7	1 8 8	1 8 9	2 0 7	1 7 7	1 7 8	1 8 8	2 0 0	2 0 2	2 0 3	2 1 1	2 1 2	1 7 6	1 7 6	1 8 6	1 8 6	1 9 6	1 9 6	1 9 6
1 3 2 0	N P	1 1 8 8	1 1 8 7	2 7 5	2 8 3	1 8 5	2 0 5	2 6 2	2 4 2	2 3 7	3 4 3	1 6 5	1 6 5	1 7 5	1 8 3	1 3 9	1 4 4	2 0 1	2 2 3	3 5 7	3 6 5	2 8 6	2 8 1	2 0 1	1 7 7	1 8 8	1 9 8	1 9 6	1 7 8	2 0 8	1 8 8	2 0 6	2 1 1	2 1 1	2 1 1	1 7 6	1 8 4	1 8 6	2 0 2	2 0 0	2 0 8		
1 3 2 1	N P	1 1 8 6	1 2 6 1	2 8 9	2 8 3	1 8 2	2 0 1	2 6 9	2 4 2	2 3 0	3 4 9	3 5 1	1 6 5	1 6 0	1 6 4	1 3 4	1 4 3	2 2 3	2 3 4	3 5 9	3 8 2	2 8 8	2 7 3	2 3 3	1 3 7	1 8 8	1 9 9	1 9 0	2 0 1	2 2 6	1 5 9	1 9 9	1 9 1	2 0 0	2 1 1	2 1 1	2 1 1	1 8 4	1 8 4	1 8 6	2 0 0	1 9 6	2 0 4
1 3 2 2	N P	1 2 6 4	1 3 3	2 7 3	2 9 0	1 9 8	2 1 5	2 2 5	2 2 2	2 3 6	3 7 7	3 6 5	1 6 5	1 6 1	1 7 3	1 8 9	1 4 4	2 9 7	3 5 7	3 5 7	2 8 8	2 8 8	1 9 3	1 9 9	1 7 9	1 8 8	1 9 8	2 0 2	2 2 0	2 2 7	1 8 8	1 8 8	1 9 0	2 1 1	2 1 1	2 1 1	1 6 8	1 8 9	1 8 9	2 0 0	1 9 0	2 0 0	
1 3 2 3	N P	1 1 8 3	1 4 3	2 7 3	2 8 9	1 7 5	2 0 2	2 6 4	2 4 0	2 3 9	3 6 6	3 6 5	1 6 9	1 6 7	1 8 3	1 3 1	1 4 4	2 9 1	3 5 7	3 5 7	2 8 8	2 8 8	1 9 3	1 9 9	1 7 9	1 8 8	1 9 8	2 0 2	2 2 6	1 5 9	1 9 9	1 9 1	2 0 0	2 1 1	2 1 1	2 1 1	1 7 6	1 8 4	1 8 6	2 0 0	1 9 6	2 0 8	
1 3 2 4	N P	1 1 8 3	1 4 5	2 8 9	2 9 8	1 8 2	2 0 9	2 6 4	2 4 8	2 3 4	3 4 9	3 5 5	1 6 5	1 6 1	1 7 3	1 8 1	1 4 5	2 9 0	3 5 7	3 5 7	2 8 8	2 8 8	1 9 3	1 9 9	1 7 9	1 8 8	1 9 8	2 0 2	2 2 7	1 8 8	1 8 8	1 9 0	2 1 1	2 1 1	2 1 1	1 7 6	1 8 4	1 8 6	2 0 0	1 9 6	2 0 0		
1 3 2 5	N P	1 3 9	1 4 3	2 7 3	2 8 0	1 9 5	2 0 4	2 6 8	2 4 0	2 3 6	3 6 0	3 6 5	1 6 3	1 6 3	1 8 3	1 3 5	1 4 5	2 9 1	3 5 7	3 5 7	2 8 8	2 8 8	1 9 0	1 9 9	1 7 9	1 8 8	1 9 8	2 0 2	2 2 6	1 5 9	1 9 9	1 9 1	2 0 0	2 1 1	2 1 1	2 1 1	1 7 6	1 8 4	1 8 6	2 0 0	1 9 6	2 0 0	
1 3 3 0	N P	1 4 3	1 5 6	2 8 5	2 9 0	1 9 5	2 0 6	2 6 8	2 4 2	2 3 7	3 4 3	3 6 7	1 6 9	1 6 4	1 7 1	1 8 9	1 4 5	2 9 7	3 5 7	3 5 7	2 8 8	2 8 8	1 9 3	1 9 9	1 7 9	1 8 8	1 9 8	2 0 2	2 2 6	1 5 9	1 9 9	1 9 1	2 0 0	2 1 1	2 1 1	2 1 1	1 7 6	1 8 4	1 8 6	2 0 0	1 9 6	2 0 0	
1 3 3 1	N P	1 1 8	1 2 6	2 7 7	2 9 0	1 9 9	2 0 9	2 6 8	2 4 0	2 3 4	3 4 7	3 6 6	1 6 5	1 6 1	1 7 3	1 8 9	1 4 4	2 9 9	3 5 7	3 5 7	2 8 8	2 8 8	1 9 3	1 9 9	1 7 9	1 8 8	1 9 8	2 0 2	2 2 7	1 8 8	1 8 8	1 9 0	2 1 1	2 1 1	2 1 1	1 7 6	1 8 4	1 8 6	2 0 0	1 9 6	2 0 0		
1 3 3 2	N P	1 1 8	1 4 3	2 7 3	2 7 3	1 9 9	2 0 1	2 6 4	2 4 6	2 3 4	3 6 6	3 6 7	1 6 3	1 6 4	1 7 8	1 3 5	1 4 9	2 9 1	3 5 7	3 5 7	2 8 8	2 8 8	1 9 0	1 9 9	1 7 9	1 8 8	1 9 8	2 0 2	2 2 6	1 5 9	1 9 9	1 9 1	2 0 0	2 1 1	2 1 1	2 1 1	1 7 6	1 8 4	1 8 6	2 0 0	1 9 6	2 0 0	
1 3 3	N P	1 1 4	1 1 8	2 2 8	2 1 8	2 2 9	2 0 3	2 6 4	2 4 0	2 3 6	3 4 7	3 6 7	1 6 3	1 6 4	1 7 8	1 3 5	1 4 9	2 9 1	3 5 7	3 5 7	2 8 8	2 8 8	1 9 0	1 9 9	1 7 9	1 8 8	1 9 8	2 0 2	2 2 7	1 8 8	1 8 8	1 9 0	2 1 1	2 1 1	2 1 1	1 7 6	1 8 4	1 8 6	2 0 0	1 9 6	2 0 0		

34		8	3	1	5	3	8	9	9	8	2	6	0	5	5	7	1	9	4	7	0	3	0	4	8	1	1	9	5	0	8	0	0	8	4	1	5	6	0	0	7	6	6	4	2	0	8
1335	NP	18	13	29	29	19	18	26	26	20	20	35	36	16	16	16	16	14	15	21	21	31	30	28	28	13	13	18	18	17	17	20	19	22	22	21	21	22	22	20	19	17	17	19	20	20	4
1340	NP	18	13	27	28	17	23	24	22	23	24	37	37	15	16	17	18	14	14	29	29	31	30	26	26	13	13	16	16	17	17	20	19	22	22	21	21	22	22	20	19	17	17	19	20	20	4
1341	NP	26	23	33	33	19	20	24	22	23	36	36	15	17	17	18	14	14	29	29	31	30	26	26	13	13	16	16	17	17	20	19	22	22	21	21	22	22	20	19	17	17	19	20	20	4	
3133	NP	18	13	21	21	13	13	20	22	22	33	33	15	15	14	14	11	11	29	29	31	31	22	22	13	13	11	11	11	11	20	19	22	22	21	21	22	22	20	19	17	17	19	20	20	4	
3333	NP	26	23	35	35	19	20	24	22	23	36	36	15	17	17	18	14	14	29	29	31	30	26	26	13	13	16	16	17	17	20	19	22	22	21	21	22	22	20	19	17	17	19	20	20	4	
3334	NP	28	28	39	39	13	13	20	22	22	33	33	15	15	14	14	11	11	29	29	31	31	22	22	13	13	11	11	11	11	20	19	22	22	21	21	22	22	20	19	17	17	19	20	20	4	
0000	PP	43	43	33	33	44	44	19	22	22	33	33	16	17	16	16	13	13	29	29	31	31	22	22	13	13	11	11	11	11	20	19	22	22	21	21	22	22	20	19	17	17	19	20	20	4	
0023	PP	26	23	33	33	19	20	24	22	23	36	36	15	17	17	18	14	14	29	29	31	30	26	26	13	13	16	16	17	17	20	19	22	22	21	21	22	22	20	19	17	17	19	20	20	4	
0024	PP	44	43	37	35	9	9	0	5	7	2	2	9	3	5	3	1	1	29	29	31	31	22	22	13	13	11	11	11	11	20	19	22	22	21	21	22	22	20	19	17	17	19	20	20	4	
0025	PP	43	35	56	69	79	90	2	2	2	3	3	16	17	16	16	13	13	29	29	31	31	22	22	13	13	11	11	11	11	20	19	22	22	21	21	22	22	20	19	17	17	19	20	20	4	
0030	PP	43	36	11	21	22	22	22	22	23	34	34	15	16	15	15	12	12	30	30	32	32	23	23	14	14	12	12	12	12	21	20	23	23	22	22	23	23	21	20	18	18	20	21	21	4	

2		3	6	6	6	1	5	9	3	2	2	7	5	5	5	4	1	1	4	8	8	9	7	4	6	7	1	7	5	0	8	8	6	4	1	7	7	6	0	6	0	4	4	2	0	2	2													
5																																																												
0		1	1	2	2	1	2	2	2	2	2	3	3	1	1	1	1	1	1	2	2	3	3	2	2	1	2	1	1	1	1	1	1	2	2	2	2	2	2	2	2	1	1	1	2	1	2													
2	P	4	4	7	9	8	0	3	5	0	3	5	7	5	6	7	9	2	4	0	1	4	5	6	9	9	1	7	7	7	7	7	8	4	2	1	2	2	2	2	2	2	1	1	1	2	1	2												
3	P	3	3	3	6	3	9	1	4	8	6	5	0	7	5	1	0	7	9	1	9	9	3	2	8	3	7	1	9	6	4	2	4	7	5	7	1	1	2	0	0	0	0	0	7	6	4	0	2	6	0									
4	P	3	3	3	6	3	9	1	4	8	6	5	0	7	5	1	0	7	9	1	9	9	3	2	8	3	7	1	9	6	4	2	4	7	5	7	1	1	2	0	0	0	0	7	6	4	0	2	6	0										
0		1	1	2	2	1	2	2	2	2	2	3	3	1	1	1	1	1	1	2	2	3	3	2	3	2	2	1	1	1	1	1	2	2	3	3	2	2	2	2	2	2	2	1	1	1	2	2	2											
2	P	3	6	8	9	9	2	4	5	1	3	4	6	6	7	7	7	3	4	0	1	4	5	9	1	1	2	6	7	9	8	5	8	8	4	8	7	5	2	2	2	2	2	1	1	1	2	2	0	4										
3	P	9	5	5	6	0	8	2	0	2	6	0	3	9	3	1	5	5	9	8	2	9	3	4	6	7	5	7	9	8	5	8	8	4	8	7	5	2	2	2	2	2	1	1	1	2	2	0	4											
0		1	1	2	2	1	2	2	2	2	2	3	3	1	1	1	1	1	1	2	2	3	3	2	3	1	2	1	1	1	1	2	2	3	3	2	3	1	2	1	1	1	2	2	1	1	1	2	2											
2	P	5	5	8	8	9	0	4	5	1	2	4	7	6	6	6	6	4	4	0	1	5	6	9	1	9	0	7	9	9	8	9	4	6	7	1	1	1	1	1	2	1	1	1	1	2	2	0	1											
4	P	6	6	5	9	8	5	2	8	6	4	7	0	5	9	4	7	4	9	8	9	3	9	4	6	7	1	1	5	9	4	2	8	1	1	5	9	6	6	4	6	0	1	9	0	7	7	8	8	0	1									
0		1	1	2	2	1	2	2	2	2	2	3	3	1	1	1	1	1	1	2	2	3	3	2	3	2	2	1	1	1	1	2	2	3	3	2	3	2	2	2	2	2	2	2	1	1	1	2	2	2										
2	P	4	4	8	8	9	0	1	5	1	3	6	7	6	7	7	7	4	4	0	1	5	5	9	1	1	2	6	8	8	9	0	0	9	1	1	2	6	8	8	9	0	0	0	0	7	8	8	0	0	1									
4	P	3	3	3	5	0	5	2	0	2	2	6	3	5	3	9	9	4	9	1	5	3	7	0	6	7	5	7	7	0	5	8	8	4	8	7	7	7	0	1	1	1	2	2	2	1	1	1	2	2	0	1								
0		1	1	2	2	1	2	2	2	2	2	3	3	1	1	1	1	1	1	2	2	3	3	2	2	1	1	1	1	1	2	2	3	3	2	2	2	2	2	2	2	2	2	2	2	1	1	1	2	2	2									
2	P	4	4	8	8	9	0	1	5	1	3	6	7	6	7	7	7	4	4	0	1	5	5	9	1	1	2	6	8	8	9	0	0	9	1	1	2	6	8	8	9	0	0	0	0	7	8	8	0	0	1									
4	P	3	3	3	5	0	5	2	0	2	2	6	3	5	3	9	9	4	9	1	5	3	7	0	6	7	5	7	7	0	5	8	8	4	8	7	7	7	0	1	1	1	2	2	2	1	1	1	2	2	0	1								
0		1	1	2	2	1	2	2	2	2	2	3	3	1	1	1	1	1	1	2	2	3	3	2	2	1	1	1	1	1	2	2	3	3	2	2	2	2	2	2	2	2	2	2	2	2	2	1	1	1	2	2	2							
2	P	4	4	8	8	9	0	1	5	1	3	6	7	6	7	7	7	4	4	0	1	5	5	9	1	1	2	6	8	8	9	0	0	9	1	1	2	6	8	8	9	0	0	0	0	7	8	8	0	0	1									
4	P	3	3	3	5	0	5	2	0	2	2	6	3	5	3	9	9	4	9	1	5	3	7	0	6	7	5	7	7	0	5	8	8	4	8	7	7	7	0	1	1	1	2	2	2	1	1	1	2	2	0	1								
0		1	1	2	2	1	2	2	2	2	2	3	3	1	1	1	1	1	1	2	2	3	3	2	2	1	1	1	1	1	2	2	3	3	2	2	2	2	2	2	2	2	2	2	2	2	2	2	2	1	1	1	2	2	2					
2	P	4	4	8	8	9	0	1	5	1	3	6	7	6	7	7	7	4	4	0	1	5	5	9	1	1	2	6	8	8	9	0	0	9	1	1	2	6	8	8	9	0	0	0	0	7	8	8	0	0	1									
4	P	3	3	3	5	0	5	2	0	2	2	6	3	5	3	9	9	4	9	1	5	3	7	0	6	7	5	7	7	0	5	8	8	4	8	7	7	7	0	1	1	1	2	2	2	1	1	1	2	2	0	1								
0		1	1	2	2	1	2	2	2	2	2	3	3	1	1	1	1	1	1	2	2	3	3	2	2	1	1	1	1	1	2	2	3	3	2	2	2	2	2	2	2	2	2	2	2	2	2	2	2	2	1	1	1	2	2	2				
2	P	4	4	8	8	9	0	1	5	1	3	6	7	6	7	7	7	4	4	0	1	5	5	9	1	1	2	6	8	8	9	0	0	9	1	1	2	6	8	8	9	0	0	0	0	7	8	8	0	0	1									
4	P	3	3	3	5	0	5	2	0	2	2	6	3	5	3	9	9	4	9	1	5	3	7	0	6	7	5	7	7	0	5	8	8	4	8	7	7	7	0	1	1	1	2	2	2	1	1	1	2	2	0	1								
0		1	1	2	2	1	2	2	2	2	2	3	3	1	1	1	1	1	1	2	2	3	3	2	2	1	1	1	1	1	2	2	3	3	2	2	2	2	2	2	2	2	2	2	2	2	2	2	2	2	2	2	1	1	1	2	2	2		
2	P	4	4	8	8	9	0	1	5	1	3	6	7	6	7	7	7	4	4	0	1	5	5	9	1	1	2	6	8	8	9	0	0	9	1	1	2	6	8	8	9	0	0	0	0	7	8	8	0	0	1									
4	P	3	3	3	5	0	5	2	0	2	2	6	3	5	3	9	9	4	9	1	5	3	7	0	6	7	5	7	7	0	5	8	8	4	8	7	7	7	0	1	1	1	2	2	2	1	1	1	2	2	0	1								
0		1	1	2	2	1	2	2	2	2	2	3	3	1	1	1	1	1	1	2	2	3	3	2	2	1	1	1	1	1	2	2	3	3	2	2	2	2	2	2	2	2	2	2	2	2	2	2	2	2	2	2	2	1	1	1	2	2	2	
2	P	4	4	8	8	9	0	1	5	1	3	6	7	6	7	7	7	4	4	0	1	5	5	9	1	1	2	6	8	8	9	0	0	9	1	1	2	6	8	8	9	0	0	0	0	7	8	8	0	0	1									
4	P	3	3	3	5	0	5	2	0	2	2	6	3	5	3	9	9	4	9	1	5	3	7	0	6	7	5	7	7	0	5	8	8	4	8	7	7	7	0	1	1	1	2	2	2	1	1	1	2	2	0	1								
0		1	1	2	2	1	2	2	2	2	2	3	3	1	1	1	1	1	1	2	2	3	3	2	2	1	1	1	1	1	2	2	3	3	2	2	2	2	2	2	2	2	2	2	2	2	2	2	2	2	2	2	2	2	1	1	1	2	2	2
2	P	4	4	8	8	9	0	1	5	1	3	6	7	6	7	7	7	4	4	0	1	5	5	9	1	1	2	6	8	8	9	0	0	9	1	1	2	6	8	8	9	0	0	0	0	7	8	8	0	0	1									
4	P	3	3	3	5	0	5	2	0	2	2	6	3	5	3	9	9	4	9	1	5	3	7	0	6	7	5	7	7	0	5	8	8	4	8	7	7	7	0	1	1	1	2	2	2	1	1	1	2	2	0	1								
0		1	1	2	2	1	2	2	2	2	2	3	3	1	1	1	1	1	1	2	2	3	3	2	2	1	1	1	1	1	2	2	3	3	2	2	2	2	2	2	2	2	2	2	2	2	2	2	2	2	2	2	2	2	1	1	1	2	2	2
2	P	4	4	8	8	9	0	1	5	1	3	6	7	6	7	7	7	4	4	0	1	5	5	9	1	1	2	6	8	8	9	0	0	9	1	1	2	6	8	8	9	0	0	0	0	7	8	8	0	0	1									
4	P	3	3	3	5	0	5	2	0	2	2	6	3	5	3	9	9	4	9	1	5	3	7	0	6	7	5	7	7	0	5	8	8	4	8	7	7																							

30		4	9	1	9	3	6	5	9	8	8	0	3	9	3	7	0	8	8	7	7	3	7	8	2	3	3	3	5	8	8	0	4	6	5	7	1	9	4	6	6	8	6	4	8	6	0																
1031		S	E	1	1	2	2	1	1	2	2	2	2	2	3	3	1	1	1	1	1	1	1	2	2	3	3	2	2	1	1	1	1	1	2	2	1	1	1	1	2	1	1	1	1	2	1	1	1	2	1	1	9	9	6								
1032		S	E	1	1	2	2	1	1	2	2	2	2	2	3	3	1	1	1	1	1	1	1	2	2	3	3	2	2	1	1	1	1	1	2	2	1	1	1	2	2	1	1	2	2	2	2	1	1	1	1	2	2	2	1	1	9	9	6				
1033		S	E	1	1	2	2	1	1	2	2	2	2	2	3	3	1	1	1	1	1	1	1	2	2	3	3	2	2	2	2	1	1	1	1	1	2	2	1	1	1	2	2	1	1	2	2	2	2	1	1	1	1	2	2	2	1	1	9	9	6		
1034		S	E	1	1	2	2	1	1	2	2	2	2	2	3	3	1	1	1	1	1	1	1	2	2	3	3	2	2	2	2	1	1	1	1	1	2	2	1	1	1	2	2	1	1	2	2	2	2	1	1	1	1	2	2	2	1	1	9	9	6		
1035		S	E	1	1	2	2	1	1	2	2	2	2	2	3	3	1	1	1	1	1	1	1	2	2	3	3	2	2	2	2	1	1	1	1	1	2	2	1	1	1	2	2	1	1	2	2	2	2	1	1	1	1	2	2	2	1	1	9	9	6		
1040		S	E	1	1	2	2	1	1	2	2	2	2	2	3	3	1	1	1	1	1	1	1	2	2	3	3	2	2	1	1	1	1	1	2	2	1	1	1	2	2	1	1	2	2	2	2	1	1	1	1	2	2	2	1	1	9	9	6				
1042		S	E	1	1	2	2	1	1	2	2	2	2	2	3	3	1	1	1	1	1	1	1	2	2	3	3	2	2	2	2	1	1	1	1	1	2	2	1	1	1	2	2	1	1	2	2	2	2	1	1	1	1	2	2	2	1	1	9	9	6		
1043		S	E	1	1	2	2	1	1	2	2	2	2	2	3	3	1	1	1	1	1	1	1	2	2	3	3	2	2	1	1	1	1	1	2	2	1	1	1	2	2	1	1	2	2	2	2	1	1	1	1	2	2	2	1	1	9	9	6				
1044		S	E	1	1	2	2	1	1	2	2	2	2	2	3	3	1	1	1	1	1	1	1	2	2	3	3	2	2	1	1	1	1	1	2	2	1	1	1	2	2	1	1	2	2	2	2	1	1	1	1	2	2	2	1	1	9	9	6				
1045		S	E	1	1	2	2	1	1	2	2	2	2	2	3	3	1	1	1	1	1	1	1	2	2	3	3	2	2	2	2	1	1	1	1	1	2	2	1	1	1	2	2	2	2	1	1	2	2	2	2	1	1	1	1	2	2	2	1	1	9	9	6
1050		S	E	1	1	2	2	1	1	2	2	2	2	2	3	3	1	1	1	1	1	1	1	2	2	3	3	2	2	1	1	1	1	1	2	2	1	1	1	2	2	1	1	2	2	2	2	1	1	1	1	2	2	2	1	1	9	9	6				

1 3		4	6	9	3	2	0	5	0	6	2	5	3	5	5	1	9	5	3	8	2	3	3	2	3	7	3	1	9	0	0	8	4	8	7	7	2	4	8	7	1	8	6	6	0	2	6	
1 1 1 4	W P	1 8	1 8	2 3	2 6	1 9	2 0	2 5	2 7	2 0	2 3	3 5	3 5	1 6	1 6	1 7	1 9	1 3	1 3	1 0	2 2	3 5	3 7	2 0	2 2	1 9	2 1	1 6	1 6	1 7	1 8	2 0	2 0	2 0	2 7	1 7	2 1	2 1	2 0	2 0	2 0	1 7	1 7	1 8	1 8	1 9	1 9	1 6
1 1 5	W P	1 3	1 8	2 7	2 9	1 8	2 0	2 3	2 5	2 0	2 8	3 4	3 5	1 6	1 6	1 9	1 9	1 3	1 3	1 1	2 2	3 6	3 0	2 2	2 2	1 9	2 1	1 6	1 8	1 7	1 9	1 9	1 0	1 7	1 9	2 0	2 0	2 0	2 1	2 0	2 1	1 7	1 7	1 8	0 0	2 9	0 0	
1 1 2 0	W P	1 3	1 3	2 9	2 9	1 1	1 1	2 2	2 8	2 8	2 2	3 3	3 6	1 6	1 5	1 8	1 8	1 5	1 5	1 4	2 5	3 7	3 7	2 2	2 2	2 7	2 7	1 9	1 1	1 8	1 9	1 0	1 2	1 7	1 7	1 7	1 7	2 0	2 0	2 0	2 1	1 7	1 7	1 8	8 9	1 9	0 8	
1 1 2 1	W P	1 3	1 5	2 5	2 9	1 5	1 6	2 0	2 8	2 8	2 7	3 3	3 6	1 5	1 5	1 9	1 9	1 3	1 3	1 1	2 2	3 3	3 7	2 2	2 2	2 1	2 2	1 9	1 7	1 8	1 9	1 0	1 8	1 8	1 8	1 8	1 2	2 2	2 2	2 2	2 2	1 7	1 7	1 9	0 0	2 0	0 0	
1 1 2 2	W P	1 3	1 3	2 6	2 8	1 7	1 8	2 5	2 5	2 0	2 8	3 4	3 5	1 6	1 6	1 7	1 7	1 3	1 3	1 0	2 2	3 5	3 5	2 9	3 0	2 9	1 8	1 8	1 7	1 7	1 8	1 8	1 9	1 9	1 9	1 8	1 8	2 0	2 0	2 0	2 0	2 1	1 7	1 7	1 9	9 9	9 9	0 8
1 1 2 3	W P	1 3	1 3	2 7	2 3	2 0	2 1	2 3	2 3	2 4	2 6	3 6	3 7	1 6	1 5	1 5	1 4	1 5	1 4	1 4	2 0	2 0	3 5	3 6	2 5	2 6	1 2	1 6	1 8	1 6	1 9	1 8	1 8	1 8	2 0	2 0	2 0	2 0	2 0	2 1	1 7	1 7	1 9	0 0	2 4	0 0	2 4	
1 1 2 4	W P	1 8	1 5	2 5	2 9	1 6	1 6	2 0	2 4	2 8	2 2	3 5	3 3	1 6	1 5	1 5	1 8	1 9	1 9	1 2	2 5	3 3	3 3	2 2	2 6	2 7	1 9	1 9	1 7	1 8	1 8	1 2	1 9	1 9	1 9	1 2	2 2	2 2	2 2	2 2	2 1	1 7	1 7	1 8	0 0	2 4	0 0	
1 1 2 5	W P	1 3	1 3	2 9	2 6	1 8	1 9	2 5	2 4	2 8	2 2	3 7	3 3	1 5	1 9	1 7	1 1	1 4	1 3	1 2	2 3	3 3	3 3	2 2	2 4	1 1	1 9	1 7	1 7	1 8	1 8	1 8	1 8	1 6	1 9	1 9	1 9	2 0	2 0	2 0	2 0	2 1	1 8	1 8	1 9	9 9	0 8	2 1
1 1 3 0	W P	1 6	1 5	2 9	2 9	1 8	2 0	2 3	2 5	2 8	2 6	3 5	3 6	1 5	1 9	1 4	1 4	1 9	1 9	1 8	2 3	3 5	3 6	2 0	2 6	1 7	1 7	1 6	1 8	1 8	1 8	1 8	1 8	2 0	2 0	2 0	2 0	2 0	2 1	1 8	1 8	1 9	9 9	0 8	2 1	1 1	2 2	
1 1 3 1	W P	1 3	1 3	2 9	2 3	1 6	1 8	2 5	2 4	2 8	2 6	3 1	3 7	1 5	1 9	1 9	1 8	1 5	1 5	1 7	2 0	3 6	3 0	2 0	2 0	1 2	2 1	1 6	1 6	1 9	1 8	1 8	1 0	2 0	2 0	2 0	2 0	2 1	1 7	1 7	1 9	1 1	2 5	0 0	2 0	2 0		
1 1 3 2	W P	1 3	1 8	2 3	2 6	1 1	1 6	2 0	2 4	2 8	2 6	3 4	3 4	1 5	1 9	1 7	1 1	1 9	1 9	1 5	2 2	3 4	3 4	2 2	2 2	1 3	2 1	1 6	1 7	1 8	1 8	1 8	1 4	1 5	1 7	2 2	2 2	2 2	2 2	2 2	2 1	1 8	1 8	1 9	0 0	2 8	0 0	2 0

5 2		0	4	9	3	3	6	5	9	6	6	4	6	1	9	9	9	5	4	7	4	7	7	2	6	9	3	5	5	2	6	8	8	4	8	7	7	6	2	0	7	2	2	4	8	4	4
1 5 3		1 4 3	1 4 8	2 9 3	2 9 3	1 7 5	1 8 6	2 5 0	2 5 0	2 2 0	2 3 2	3 4 4	3 4 7	1 6 5	1 6 9	1 7 1	1 9 8	1 3 5	1 3 5	2 1 5	2 2 5	3 3 3	3 3 3	2 2 0	2 8 2	2 8 7	2 1 1	2 2 6	1 9 9	1 8 0	2 0 2	2 9 4	1 0 8	2 1 0	2 7 5	1 8 6	2 0 0	2 0 0	2 0 7	1 0 7	1 8 2	1 9 8	1 9 8	1 9 8	2 0 0		
1 5 4		1 4 8	1 5 6	2 8 5	2 8 9	1 8 3	1 8 3	2 3 5	2 4 6	2 0 8	2 1 5	3 5 0	3 7 0	1 6 5	1 6 5	1 7 1	1 7 5	1 3 5	1 3 5	2 0 7	2 1 5	3 3 3	3 3 0	2 2 9	2 8 7	2 2 7	1 9 7	2 1 7	1 6 7	1 6 7	1 7 6	1 7 6	1 7 6	1 7 6	1 7 6	2 0 0	2 1 9	2 0 6	2 0 0	2 0 0	2 1 0	2 1 0	1 7 6	1 7 6	1 8 4	1 9 0	2 0 4
1 5 5		1 4 8	1 5 6	2 8 9	2 8 9	1 8 3	1 8 3	2 3 5	2 4 6	2 0 8	2 1 5	3 5 0	3 7 0	1 6 5	1 6 5	1 7 1	1 7 5	1 3 5	1 3 5	2 0 7	2 1 5	3 3 3	3 3 0	2 2 9	2 8 7	2 2 7	1 9 7	2 1 7	1 6 7	1 6 7	1 7 6	1 7 6	1 7 6	2 0 0	2 1 9	2 0 6	2 0 0	2 0 3	2 0 0	2 1 0	2 1 0	1 7 6	1 7 6	1 8 4	1 9 0	2 0 4	
1 2 0 0		1 4 8	1 4 8	2 8 1	2 8 9	1 7 1	1 7 2	2 0 6	2 2 8	2 3 2	2 3 6	3 4 7	3 7 0	1 6 5	1 6 5	1 7 1	1 7 5	1 3 5	1 3 5	2 0 9	2 1 5	3 3 3	3 3 1	2 2 3	2 5 7	2 6 7	2 8 7	1 9 7	2 1 7	1 7 7	1 7 7	1 8 2	1 7 2	1 7 2	1 9 5	1 9 2	2 0 6	2 0 6	2 1 6	2 0 6	2 0 6	2 1 7	2 1 7	1 8 6	1 8 6	2 0 8	2 0 8
1 2 0 1		1 4 3	1 4 8	2 8 9	2 8 9	1 7 1	1 7 5	2 0 8	2 2 8	2 3 8	2 3 8	3 4 6	3 6 6	1 6 5	1 6 5	1 7 1	1 7 5	1 3 5	1 3 5	2 0 9	2 1 5	3 3 3	3 3 1	2 2 3	2 5 7	2 6 7	2 8 7	1 9 7	2 1 7	1 7 7	1 7 7	1 8 2	1 7 2	1 7 2	1 9 5	1 9 2	2 0 6	2 0 6	2 1 6	2 0 6	2 0 6	2 1 7	2 1 7	1 8 6	1 8 6	2 0 8	2 0 8
1 2 0 2		1 3 0	1 5 6	2 8 5	2 8 5	1 9 0	1 9 5	2 0 8	2 2 9	2 3 2	2 3 4	3 4 5	3 6 6	1 6 5	1 6 5	1 7 1	1 7 5	1 3 5	1 3 5	2 0 9	2 1 5	3 3 3	3 3 1	2 2 3	2 5 7	2 6 7	2 8 7	1 9 7	2 1 7	1 7 7	1 7 7	1 8 2	1 7 2	1 7 2	1 9 5	1 9 2	2 0 6	2 0 6	2 1 6	2 0 6	2 0 6	2 1 7	2 1 7	1 8 6	1 8 6	2 0 8	2 0 8
1 2 0 3		1 4 8	1 6 5	2 8 9	2 8 9	1 9 0	1 9 2	2 0 6	2 2 9	2 3 0	2 3 2	3 4 5	3 6 6	1 6 5	1 6 5	1 7 1	1 7 5	1 3 5	1 3 5	2 0 9	2 1 5	3 3 3	3 3 1	2 2 3	2 5 7	2 6 7	2 8 7	1 9 7	2 1 7	1 7 7	1 7 7	1 8 2	1 7 2	1 7 2	1 9 5	1 9 2	2 0 6	2 0 6	2 1 6	2 0 6	2 0 6	2 1 7	2 1 7	1 8 6	1 8 6	2 0 8	2 0 8
1 2 0 4		1 3 3	1 4 8	2 8 7	2 8 9	1 7 3	1 7 5	2 0 6	2 2 9	2 3 0	2 3 2	3 4 5	3 6 6	1 6 5	1 6 5	1 7 1	1 7 5	1 3 5	1 3 5	2 0 9	2 1 5	3 3 3	3 3 1	2 2 3	2 5 7	2 6 7	2 8 7	1 9 7	2 1 7	1 7 7	1 7 7	1 8 2	1 7 2	1 7 2	1 9 5	1 9 2	2 0 6	2 0 6	2 1 6	2 0 6	2 0 6	2 1 7	2 1 7	1 8 6	1 8 6	2 0 8	2 0 8
1 2 0 5		1 3 0	1 5 6	2 8 1	2 8 5	1 9 0	1 9 2	2 0 6	2 2 9	2 3 8	2 3 2	3 4 5	3 6 6	1 6 5	1 6 5	1 7 1	1 7 5	1 3 5	1 3 5	2 0 9	2 1 5	3 3 3	3 3 1	2 2 3	2 5 7	2 6 7	2 8 7	1 9 7	2 1 7	1 7 7	1 7 7	1 8 2	1 7 2	1 7 2	1 9 5	1 9 2	2 0 6	2 0 6	2 1 6	2 0 6	2 0 6	2 1 7	2 1 7	1 8 6	1 8 6	2 0 8	2 0 8
1 2 1 0		1 4 3	1 4 8	2 8 9	2 8 9	1 9 6	1 9 8	2 0 1	2 2 8	2 3 0	2 3 2	3 4 5	3 6 6	1 6 5	1 6 5	1 7 1	1 7 5	1 3 5	1 3 5	2 0 9	2 1 5	3 3 3	3 3 0	2 2 3	2 5 7	2 6 7	2 8 7	1 9 7	2 1 7	1 7 7	1 7 7	1 8 2	1 7 2	1 7 2	1 9 5	1 9 2	2 0 6	2 0 6	2 1 6	2 0 6	2 0 6	2 1 7	2 1 7	1 8 6	1 8 6	2 0 8	2 0 8
1 2 1 1		1 4 3	1 4 8	2 8 9	2 8 9	1 9 6	1 9 8	2 0 1	2 2 8	2 3 0	2 3 2	3 4 5	3 6 6	1 6 5	1 6 5	1 7 1	1 7 5	1 3 5	1 3 5	2 0 9	2 1 5	3 3 3	3 3 0	2 2 3	2 5 7	2 6 7	2 8 7	1 9 7	2 1 7	1 7 7	1 7 7	1 8 2	1 7 2	1 7 2	1 9 5	1 9 2	2 0 6	2 0 6	2 1 6	2 0 6	2 0 6	2 1 7	2 1 7	1 8 6	1 8 6	2 0 8	2 0 8
1 2 1 1		1 4 3	1 4 8	2 8 9	2 8 9	1 9 6	1 9 8	2 0 1	2 2 8	2 3 0	2 3 2	3 4 5	3 6 6	1 6 5	1 6 5	1 7 1	1 7 5	1 3 5	1 3 5	2 0 9	2 1 5	3 3 3	3 3 0	2 2 3	2 5 7	2 6 7	2 8 7	1 9 7	2 1 7	1 7 7	1 7 7	1 8 2	1 7 2	1 7 2	1 9 5	1 9 2	2 0 6	2 0 6	2 1 6	2 0 6	2 0 6	2 1 7	2 1 7	1 8 6	1 8 6	2 0 8	2 0 8

Appendix C: Chapter 1 supplementary material

C.1. IBR model construction and MRDM analyses

All categorical features were evaluated at all resistance values in models consisting of the focal categorical feature with all non-focal features given resistance values of 1, which approximates scaled geographic distance (Lee-Yaw et al. 2009), and non-terrestrial habitat masked from analyses. Single-variable resistance rasters were analyzed with a focal region layer that consisted of the minimum-spanning convex hulls formed by all sampling points within a sampling site. The focal region layer excluded collection sites with less than 20 samples represented in the relatives-removed data set. The pairwise resistance distance matrix was analyzed with non-parametric rank-based MRDM and 10,000 permutations to assess the significance and coefficient of determination for the given resistance value and habitat type. The MRDM analyses contained pairwise F_{st} for the included focal regions as the response matrix and only the resistance-distance matrix as the predictor matrix. The MRDM outputs were compared to a null model in which all included terrestrial raster-cells within the map extent were given a resistance value of 1. Landscape variables were included in further analyses if MRDM resulted in a significant model at $p \leq 0.05$ and the coefficient of determination was greater than that of the null model.

Due to the potential parameter space available to search after parameterization, we used the single-variable resistance distances to construct the expected significance and coefficient of determination for 2-variable to full models with MRDM for each GIS layer using the resistance values best-supported by single-variable parameterization

process as the predictor. The best 10% of models for each layer, as determined by significance and coefficient of determination of MRDM, were constructed as rasters and ran with Circuitscape using the focal regions. Final models were composed of two groupings, the best model(s) for each layer from single-variable or combined-variable analyses and those constructed in an additive fashion, with included features summed at points of overlap for the best models of each layer. If no feature was present in a layer that exceeded the single-variable optimization, that layer was dropped from final model construction and analyses.

C.2. R code usage

MRDM Regression Effect Estimation

Assumes a genetic distance matrix has been loaded (e.g. pairwise Fst) as well as single-factor pairwise resistance-distance matrices from Circuitscape. MRDM result is a rank-based non-parametric regression on 10000 permutations.

```
#Begin Code
```

```
library(ecodist)
```

```
four.var = MRM(as.dist(Fst)~as.dist(variable 1) + as.dist(variable 2) + as.dist(variable 3)  
+ as.dist(variable 4) , nperm = 10000 , mrank = T)
```

```
#End Code
```

MLPE Model Construction, AICc calculation, and R^2_β calculation

Assumes that pairwise matrices of interest have been centered and placed in a 3 column format within a single data frame. The null model refers to the null IBR model (see text).

```
#Begin Code
```

```
library(reshape2)
```

```
library(lme4)
```

```
library(MuMIn)
```

```
library(pbkrtest)
```

```
#Matrix manipulations, assume genetic distance = fst matrix
```

```
fst.melted = melt(fst, na.rm = T)
```

```
fst.center = fst - mean(fst.melted[,3])
```

```

fst.melted.center = melt(fst.center, na.rm = T)
colnames(fst.melted.center)=c("P1", "P2", "fst")
#Centers variable and provides 3 column format
data=fst.melted.center

null.melted = melt(null, na.rm = T)
null.center = null - mean(null.melted[,3])
null.melted.center = melt(null.center, na.rm = T)
colnames(null.melted.center)=c("P1", "P2", "null")
data = merge(data, null.melted.center)

ibr.melted = melt(ibr, na.rm = T)
ibr.center = ibr - mean(ibr.melted[,3])
ibr.melted.center = melt(ibr.center, na.rm = T)
colnames(ibr.melted.center)=c("P1", "P2", "ibr")
data = merge(data, ibr.melted.center)

#End results is data frame with P1, P2, Fst, Null, IBR columns

#MLPE Model Construction for AICc

null.lmer = lmer(fst~null + (1|P1) + (1|P2), data=data, REML=FALSE)
ibr.lmer = lmer(fst~null + ibr + (1|P1) + (1|P2), data=data, REML=FALSE)

#AICc calculation

AICc(null.lmer)

AICc(ibr.lmer)

```



```

#MLPE Model Construction for  $R_{\beta}^2$ 

small.model = lmer(fst~1+(1|P1)+(1|P2), data=data, REML = TRUE)

null.lmer = lmer(fst~null + (1|P1) + (1|P2), data=data, REML=TRUE)

ibr.lmer = lmer(fst~null + ibr + (1|P1) + (1|P2), data=data, REML=TRUE)

# $R_{\beta}^2$  Calculation

k1 = KRmodcomp(null.lmer, small.model)

k1.r=(((1)*((k1$stat$ddf)^-1)*k1$stat$Fstat)/(1+((1)*((k1$stat$ddf)^-1)*k1$stat$Fstat)))

k2 = KRmodcomp(ibr.lmer, small.model)

k2.r=(((1)*((k2$stat$ddf)^-1)*k2$stat$Fstat)/(1+((1)*((k2$stat$ddf)^-1)*k2$stat$Fstat)))

#END CODE

```

Table C.3. Summary statistics for each island and collection site. Statistics were generated with the `divBasic` function in the R package `diveRsimity`. Collection sites for each island are listed under each island with the total samples for that location (N), the samples retained in the relatives removed data set (Nrr). Summary statistics include the rarified allelic richness for all collection sites (Ar (all sites)) and for only those sites with more than 20 individuals in the relatives removed data set (Ar (>20)), expected heterozygosity (He) and observed heterozygosity (Ho). The Island-level comparisons were generated by grouping all samples indicated in Nrr into two groups (San Clemente Island and Santa Barbara Island) analyzed at the 18 shared loci. NA within a cell denotes not applicable due to removal from analyses. HWE probabilities were calculated in GENEPOP with probabilities <0.0001 set to 0.0001 at the locus level. Fis as calculated by allele identity within GENEPOP is given overall and for each site.

Site	N	Nrr	Ar (all sites)	Ar (>20)	He	Ho	HWE	Fis
San Clemente Island	609	534	21.47	NA	0.89	0.84	0.00e0	0.0459
1	33	31	8.98	10.35	0.86	0.87	0.8981	0.0137
2	39	33	8.78	10.08	0.86	0.86	0.2835	0.0148
3	86	71	9.31	11.0	0.86	0.87	0.1168	0.0027
4	30	25	8.53	9.77	0.86	0.87	0.6173	0.0019
5	28	24	8.59	9.92	0.86	0.88	0.3311	0.0018
6	31	29	8.24	9.50	0.84	0.86	0.4165	0.0044
Horton Road	36	28	8.07	9.25	0.84	0.86	0.3063	-0.0008
7	32	30	8.21	9.49	0.84	0.83	0.2200	0.0317
8	27	20	5.46	6.28	0.69	0.62	0.0005	0.1157
10	30	30	9.20	10.80	0.86	0.87	0.1464	-0.0022
11	31	28	8.55	9.94	0.85	0.82	0.0089	0.0508
13	29	28	9.07	10.69	0.87	0.88	0.1188	0.0089
Canyon	13	12	7.34	NA	0.82	0.86	0.4647	-0.0056
20	36	34	8.27	9.57	0.84	0.85	0.0838	0.0023
29	29	27	8.17	9.28	0.85	0.86	0.0488	0.0062
37	34	27	8.26	9.63	0.84	0.83	0.3470	0.0319
38	30	28	9.21	10.83	0.87	0.86	0.9637	0.0275
39	31	29	8.31	9.65	0.84	0.85	0.2572	0.0097
Santa Barbara Island	312	271	13.82	NA	0.86	0.82	2.47e-09	0.0473
AP	28	21	5.85	7.20	0.80	0.80	0.2612	0.0292
CB	8	8	5.62	NA	0.79	0.83	0.8888	-0.0051
CC	31	24	6.44	8.18	0.83	0.83	0.3197	0.0086
GC	39	38	6.65	8.65	0.83	0.84	0.6265	0.0134
LC	9	8	5.97	NA	0.81	0.89	0.9830	-0.0208
NP	69	60	6.49	8.42	0.82	0.82	0.0227	0.0134

PP	37	33	6.28	7.87	0.82	0.81	0.1433	0.0251
S	13	12	5.92	NA	0.79	0.77	0.1239	0.0581
SE	35	31	6.56	8.36	0.83	0.85	0.6892	0.0026
WP	43	36	5.67	7.17	0.78	0.76	0.1836	0.0453
Aggregate LC+GC	48	46	6.77	8.88	0.84	0.84	0.3103	0.0089

Table C.4. San Clemente Island collection site pairwise Fsts with 95% confidence intervals. Fst values on the lower triangle were calculated using diveRsimy. Confidence interval ranges calculated in diveRsimy are on the upper triangle, those overlapping 0 are in italics. Collection site names are in the first row and column; HR = Horton Road

	1	2	3	4	5	6	HR	7	8	10	11	13	20	29	37	38	39
1		<i>-0.0030-0.0130</i>	<i>-0.0031-0.0091</i>	0.0010-0.0203	0.0106-0.0288	0.0176-0.0365	0.0224-0.0472	0.0193-0.0399	0.0714-0.1250	0.0062-0.0229	0.0076-0.0277	0.0100-0.0293	0.0176-0.0376	0.0269-0.0474	0.0165-0.0390	0.0145-0.0343	0.0224-0.0444
2	0.0043		0.0013-0.0145	0.0030-0.0218	0.0102-0.0287	0.0186-0.0373	0.0262-0.0502	0.0209-0.0432	0.0720-0.1232	0.0124-0.0299	0.0126-0.0342	0.0135-0.0313	0.0242-0.0429	0.0340-0.0545	0.0187-0.0416	0.0205-0.0389	0.0238-0.0438
3	0.0022	0.0073		0.0002-0.0166	0.0119-0.0288	0.0220-0.0387	0.0296-0.0518	0.0250-0.0409	0.0661-0.1120	0.0086-0.0203	0.0139-0.0299	0.0124-0.0273	0.0211-0.0380	0.0335-0.0512	0.0252-0.0446	0.0194-0.0354	0.0265-0.0448
4	0.0092	0.0116	0.0076		0.0124-0.0353	0.0245-0.0475	0.0230-0.0474	0.0203-0.0429	0.0692-0.1199	0.0093-0.0308	0.0138-0.0359	0.0135-0.0363	0.0248-0.0478	0.0309-0.0536	0.0255-0.0516	0.0236-0.0456	0.0238-0.0491
5	0.0188	0.0184	0.0189	0.0232		0.0160-0.0389	0.0207-0.0459	0.0181-0.0403	0.0776-0.1314	0.0002-0.0214	0.0119-0.0356	0.0041-0.0252	0.0210-0.0429	0.0262-0.0493	0.0228-0.0469	0.0191-0.0418	0.0199-0.0437
6	0.0261	0.0267	0.0295	0.0351	0.0261		0.0319-0.0571	0.0318-0.0558	0.0806-0.1315	0.0091-0.0288	0.0196-0.0427	0.0186-0.0419	0.0237-0.0448	0.0351-0.0586	0.0239-0.0492	0.0260-0.0489	0.0295-0.0538
HR	0.0342	0.0375	0.0396	0.0343	0.0324	0.0437		<i>-0.0024-0.0188</i>	0.0953-0.1523	0.0224-0.0470	0.0206-0.0457	0.0211-0.0496	0.0271-0.0517	0.0405-0.0667	0.0257-0.0531	0.0324-0.0579	0.0286-0.0575
7	0.0279	0.031	0.0322	0.0302	0.0277	0.0421	0.0074		0.0966-0.1557	0.0188-0.0408	0.0148-0.0345	0.0173-0.0399	0.0235-0.0463	0.0309-0.0545	0.0246-0.0504	0.0285-0.0515	0.0275-0.0520
8	0.0975	0.0965	0.0886	0.0929	0.1034	0.1043	0.1215	0.1253		0.0801-0.1325	0.0868-0.1462	0.0668-0.1160	0.0887-0.1410	0.1036-0.1554	0.0835-0.1417	0.0843-0.1403	0.0972-0.1514
10	0.0136	0.0195	0.0137	0.0188	0.0097	0.0179	0.0338	0.0288	0.1048		0.0062-0.0256	0.0104-0.0301	0.0180-0.0361	0.0210-0.0425	0.0163-0.0397	0.0150-0.0363	0.0204-0.0430
11	0.0165	0.0221	0.0208	0.0236	0.0226	0.0303	0.0326	0.0232	0.1145	0.0147		0.0065-0.0301	0.0164-0.0367	0.0254-0.0489	0.0176-0.0446	0.0170-0.0374	0.0235-0.0490
13	0.019	0.0215	0.0189	0.0236	0.0135	0.0288	0.0338	0.0272	0.0896	0.0193	0.0166		0.0137-0.0356	0.0251-0.0484	0.0159-0.0384	0.0105-0.0325	0.0138-0.0384
20	0.027	0.0324	0.0288	0.0352	0.0309	0.0333	0.0385	0.0337	0.1145	0.026	0.0254	0.0233		0.0250-0.0462	0.0179-0.0413	0.0202-0.0418	0.0247-0.0466
29	0.0368	0.0436	0.0417	0.0413	0.0361	0.0461	0.0527	0.0413	0.1278	0.0305	0.036	0.0356	0.0347		0.0256-0.0511	0.0254-0.0467	0.0369-0.0612
37	0.0267	0.0291	0.0338	0.0367	0.0332	0.035	0.0383	0.0364	0.1116	0.0271	0.0293	0.0262	0.028	0.037		0.0180-0.0398	0.0150-0.0442
38	0.0232	0.0287	0.0264	0.0335	0.0291	0.0362	0.0442	0.0387	0.1114	0.0249	0.0263	0.0206	0.0304	0.0355	0.0282		0.0230-0.0467
39	0.0324	0.0327	0.0351	0.0348	0.0302	0.0406	0.0424	0.0387	0.1227	0.0306	0.035	0.0249	0.035	0.0479	0.0285	0.0337	

Table C.5. Santa Barbara Island collection site pairwise Fst values with 95% confidence intervals Fst values on the lower triangle were calculated using diveRcity. Confidence interval ranges calculated in diveRcity are on the upper triangle, those overlapping 0 are in italics. Collection site names are in the first row and column.

	AP	CC	GC	NP	PP	SE	WP
AP	-	0.0283- 0.0654	0.0182- 0.0495	0.0289- 0.0559	0.0336- 0.0630	0.0270- 0.0550	0.0363- 0.0684
CC	0.0454	-	0.0202- 0.0417	0.0276- 0.0485	0.0202- 0.0450	0.0132- 0.0344	0.0466- 0.0741
GC	0.0320	0.0300	-	0.0138- 0.0303	0.0121- 0.0324	0.0108- 0.0309	0.0318- 0.0556
NP	0.0408	0.0369	0.0213	-	0.0116- 0.0302	0.0241- 0.0415	0.0359- 0.0568
PP	0.0465	0.0314	0.0216	0.0201	-	0.0216- 0.0429	0.0288- 0.0549
SE	0.0394	0.0231	0.0199	0.0318	0.0314	-	0.0371- 0.0634
WP	0.0503	0.0590	0.0422	0.0457	0.0396	0.0499	-

Table C.6. San Clemente Island single-variable multiple regression on distance matrices results. The assigned values are denoted in the first row with “c” denoting conductance and “r” denoting resistance. Potential factors for inclusion in models are listed in the first column. The associated p-value (p) and coefficient of determination for non-parametric rank-based regressions (R^2) are given for each value. Values were compared against the R^2 of the null model for further inclusion (see text).

	100c		50c		2c		2r		50r		100r	
	p	R^2	p	R^2	p	R^2	p	R^2	p	R^2	p	R^2
Canyon shrubland/woodland	0.0008	0.2447	0.0012	0.2447	0.0008	0.2527	0.0004	0.2666	0.0003	0.2940	0.0002	0.2956
Coastal salt marsh	0.0007	0.2602	0.0002	0.2602	0.0004	0.2602	0.0004	0.2601	0.0009	0.2601	0.0001	0.2601
Disturbed/developed	0.0030	0.2657	0.0002	0.2657	0.0005	0.2625	0.0005	0.2587	0.0004	0.2512	0.0010	0.2511
Grasslands	0.0027	0.2999	0.0016	0.3001	0.0005	0.2782	0.003	0.2532	0.0211	0.1663	0.0500	0.1374
Maritime desert scrub - Cholla phase	0.0039	0.1960	0.0027	0.1978	0.0011	0.2441	0.0001	0.2846	0.0001	0.4323	0.0001	0.4351
Maritime desert scrub - Lycium phase	0.0001	0.5490	0.0001	0.5372	0.0001	0.3158	0.0019	0.2171	0.1245	0.0976	0.1569	0.0886
Maritime desert scrub - Prickly pear phase	0.0003	0.3363	0.0005	0.3186	0.0005	0.2640	0.0003	0.2557	0.0014	0.1927	0.0037	0.1650
Maritime desert scrub - prickly pear/cholla phase	0.0012	0.2071	0.0010	0.2084	0.0008	0.2493	0.001	0.2750	0.0003	0.3107	0.0006	0.3103
Maritime sage scrub	0.0006	0.2602	0.0002	0.2602	0.0007	0.2602	0.0005	0.2602	0.0009	0.2602	0.0004	0.2602
None/Unvegetated	0.0002	0.2140	0.0006	0.2152	0.0003	0.2541	0.0005	0.2590	0.0009	0.2513	0.0009	0.2506
Primary Roads - 5m buffer	0.0006	0.3772	0.0003	0.3831	0.0004	0.2709	0.0006	0.2526	0.1077	0.0813	0.1815	0.0611
Secondary Roads - 5m buffer	0.0001	0.3439	0.0001	0.3195	0.0002	0.2580	0.0010	0.2555	0.0034	0.2862	0.0060	0.2767
Canyons <500 ft	0.0006	0.2588	0.0005	0.2587	0.0003	0.2609	0.0009	0.2649	0.0012	0.2204	0.0002	0.2179
Canyons 500-1000 ft	0.0018	0.2216	0.0015	0.2287	0.0007	0.2544	0.0003	0.2728	0.0006	0.3075	0.0016	0.2880
Canyons >1000 ft	0.0007	0.2422	0.0006	0.2472	0.0008	0.2574	0.0007	0.2656	0.0001	0.2968	0.0001	0.3007

Table C.7. Santa Barbara Island single-variable multiple regression on distance matrices results. The assigned values are denoted in the first row with “c” denoting conductance and “r” denoting resistance. Potential factors for inclusion in models are listed in the first column. The associated p-value (p) and coefficient of determination for non-parametric rank-based regressions (R^2) are given for each value. Values were compared against the R^2 of the null model for further inclusion (see text).

	100c		50c		2c		2r		50r		100r	
	p	R^2	p	R^2	p	R^2	p	R^2	p	R^2	p	R^2
Barren	0.0929	0.2508	0.0679	0.3128	0.0290	0.4485	0.0229	0.4804	0.0198	0.5397	0.0211	0.5397
Brome	0.0199	0.4858	0.0209	0.4858	0.0190	0.4804	0.023	0.4670	0.0246	0.4572	0.0234	0.4572
California boxthorn	0.0004	0.7850	0.0010	0.7724	0.0047	0.5796	0.1107	0.30772	0.5484	0.0559	0.5976	0.0416
California grassland	0.0036	0.5369	0.0033	0.5388	0.0196	0.4804	0.0453	0.4330	0.0799	0.3697	0.1072	0.3372
Coastal cholla	0.0090	0.5590	0.0072	0.5590	0.0200	0.4804	0.036	0.4459	0.0794	0.3824	0.0826	0.3824
Common fiddleneck	0.0654	0.3872	0.0661	0.3872	0.0183	0.4849	0.0155	0.4958	0.0261	0.5115	0.0262	0.4967
Giant coreopsis	0.0826	0.3921	0.0788	0.3921	0.0158	0.4894	0.0234	0.4831	0.0289	0.4572	0.0351	0.4433
Goldfields	0.0211	0.4590	0.0199	0.4678	0.0177	0.4894	0.0212	0.4804	0.0172	0.5397	0.0175	0.5397
Island tarplant	0.0116	0.4661	0.0178	0.4502	0.0261	0.4529	0.0370	0.4459	0.0395	0.4502	0.0430	0.4502
Oatgrass	0.0038	0.6477	0.0087	0.6015	0.0269	0.4750	0.0243	0.4840	0.7422	0.0223	0.7828	0.0159
Prickly pear cactus	0.0060	0.5687	0.0057	0.5687	0.0154	0.4894	0.0447	0.4194	0.0605	0.3848	0.0728	0.3556
Structure	0.0209	0.4804	0.0205	0.4804	0.0229	0.4804	0.0180	0.4804	0.0245	0.4804	0.0200	0.4804
Woolly seablite + Crystalline iceplant	0.4018	0.1167	0.4081	0.1167	0.1835	0.2292	0.0030	0.6332	0.0055	0.6045	0.0054	0.5786
Woolly sunflower	0.0204	0.4804	0.0197	0.4804	0.0189	0.4804	0.0194	0.4804	0.0193	0.4858	0.0197	0.4858
Western Gull	0.5862	0.0403	0.5177	0.0612	0.1066	0.3077	0.0018	0.6498	0.0012	0.6945	0.0011	0.6924
Barn Owl	0.8512	0.0065	0.7329	0.0201	0.2525	0.1755	0.0101	0.6249	0.1844	0.2373	0.1811	0.2373

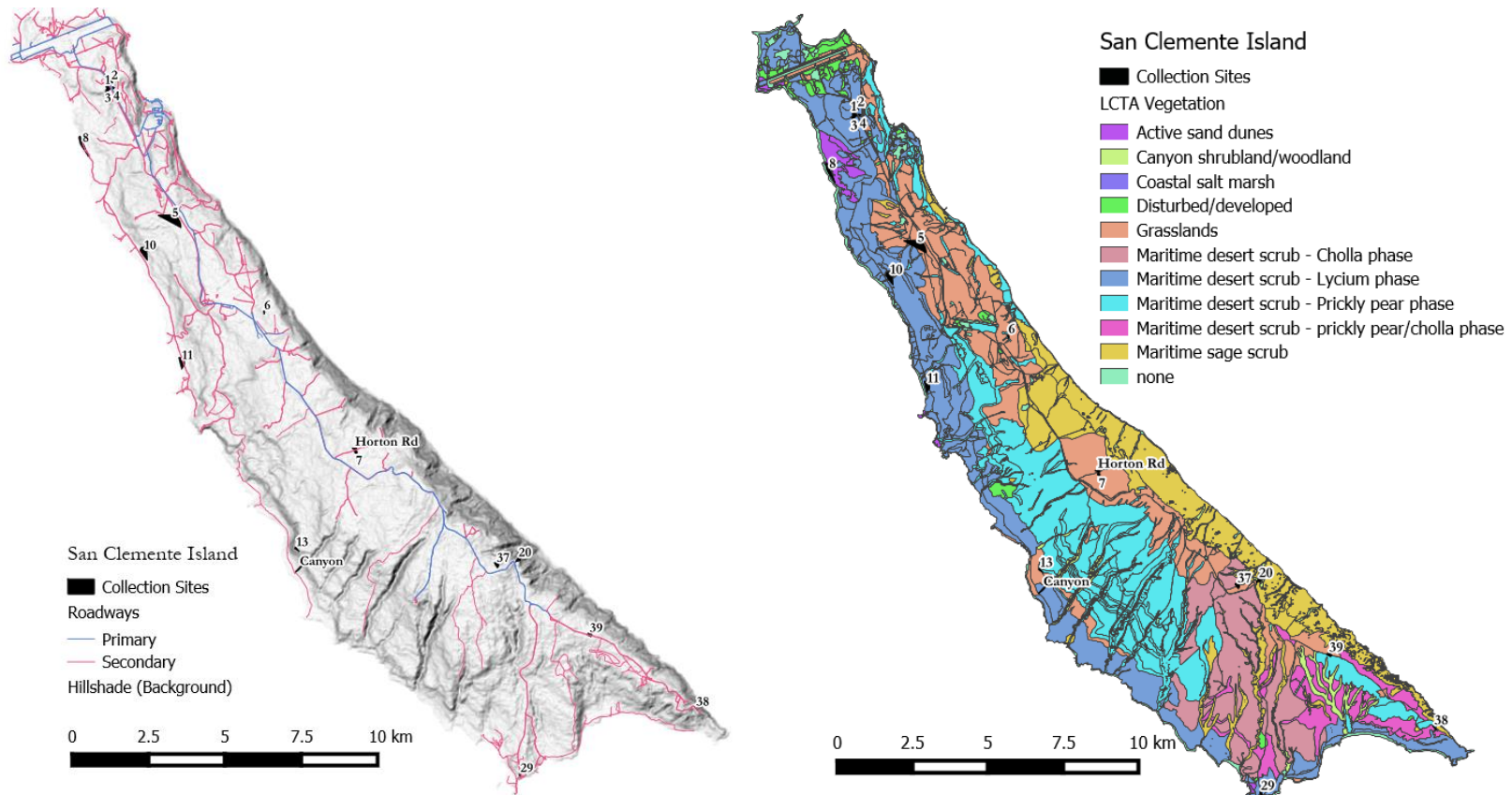


Figure C.8. Collection sites on San Clemente Island and associated habitat. Collection sites are shown as the minimum spanning convex hull for all captures within an area with the associated site name. Left: primary (blue) and secondary (pink) roadways are shown on a background hillshade (Mapsurfer). Right: LCTA Habitat types utilized in IBR analyses. The Canyon collection site was at the mouth of a canyon with 13 individuals sampled.

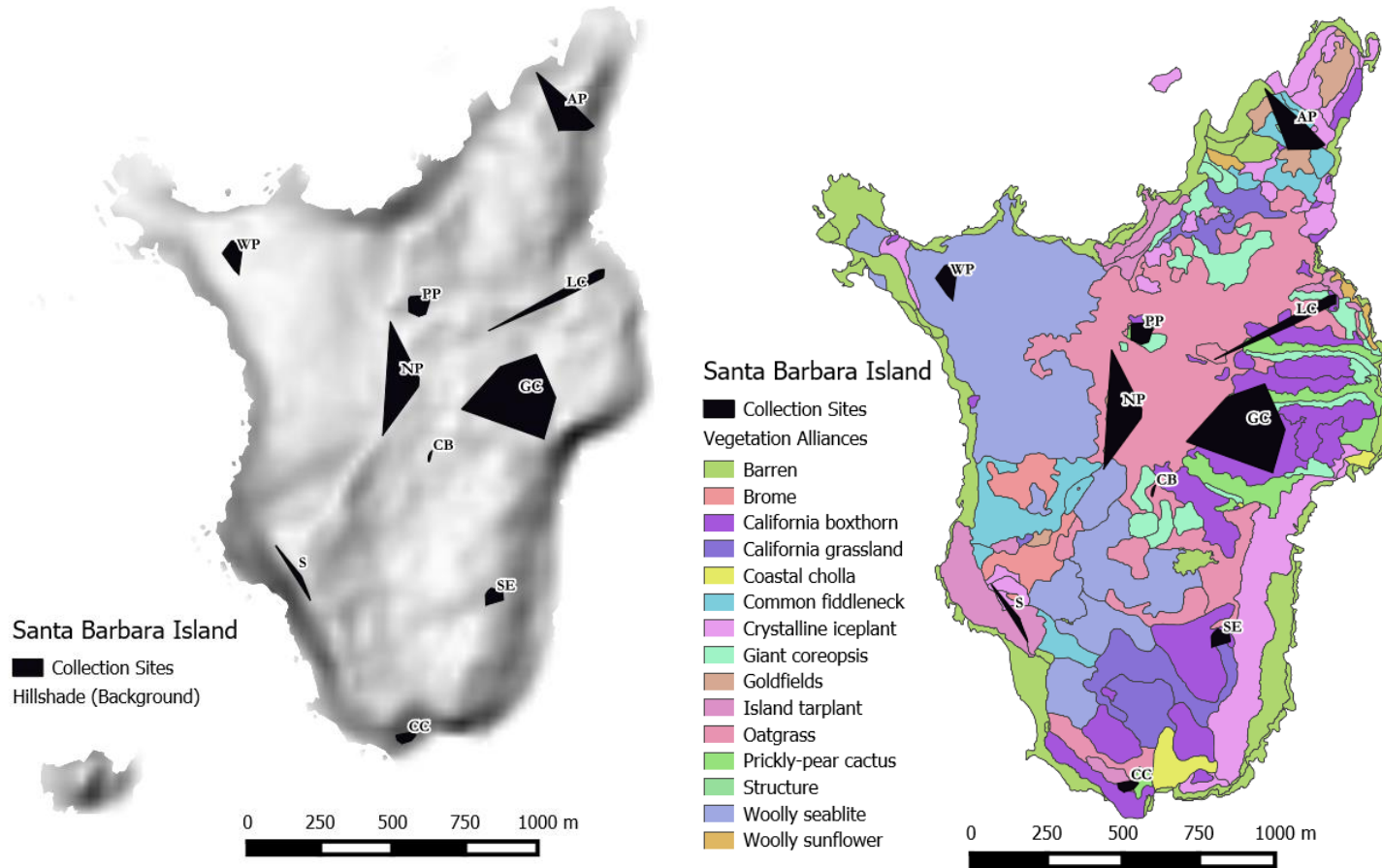


Figure C.9. Collection sites on Santa Barbara Island and associated habitat. Collection sites are shown as the minimum spanning convex hull for all captures within an area with the associated site name. Collection sites CB, LC, and S were opportunistic captures with 13 or fewer captures. Sutil islet off of the south-western coast was not sampled. Left: collection sites shown on a background hillshade (Mapsurfer). Right: Vegetation alliance used to define habitat types utilized in IBR analyses

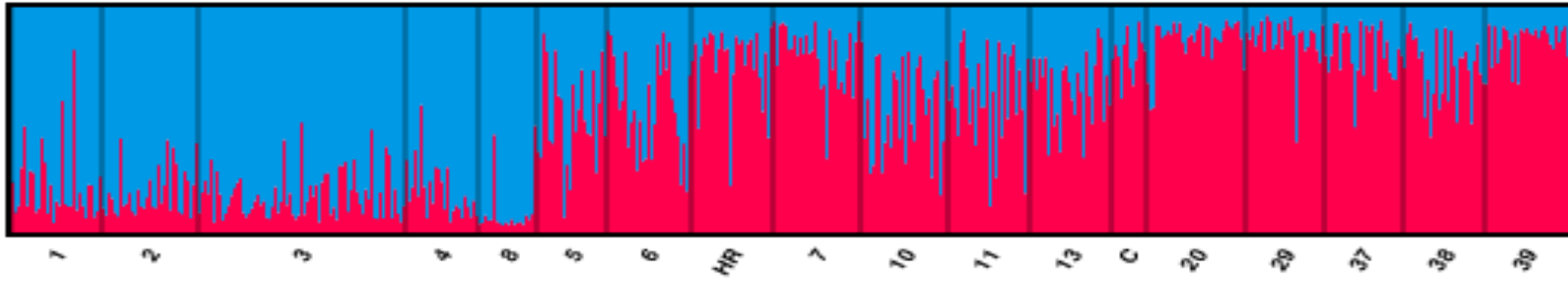


Figure C.10: San Clemente Island barplot for the Structure 2-cluster solution. Barplot showing individual coancestry proportions for the 2-cluster solution selected using the Evanno et al. (2005) method. All collection sites were included and are listed on the x-axis; HR=Horton Road, C=Canyon.

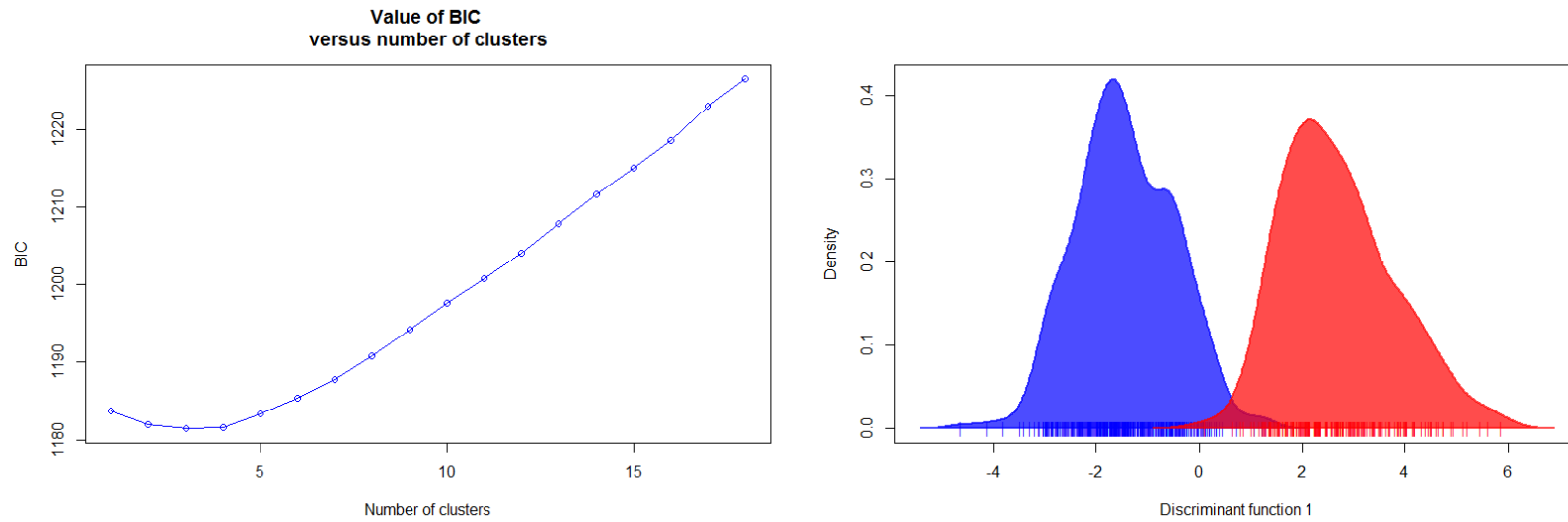


Figure C.11. San Clemente Island DAPC density plot for sequential k-means 2-cluster solution and associated BIC plot. The sequential k-means clustering algorithm indicates solutions based on 2-4 clusters are useful for describing the genetic structure of San Clemente Island (left). The DAPC density plot for the smallest value of K ($K=2$) is shown (right).

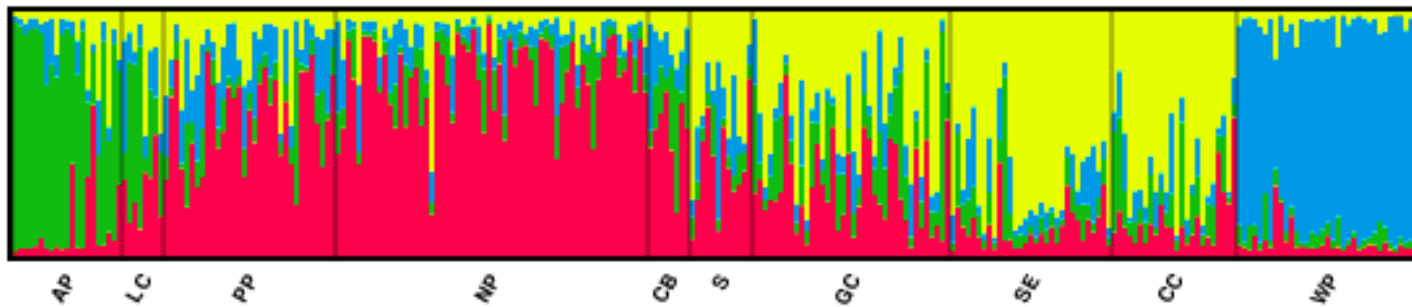


Figure C.12. Santa Barbara Island barplot for the Structure 4-cluster solution. Barplot showing individual coancestry proportions for the 2-cluster solution selected using the Evanno et al. (2005) method. All collection sites were included and are listed on the x-axis.

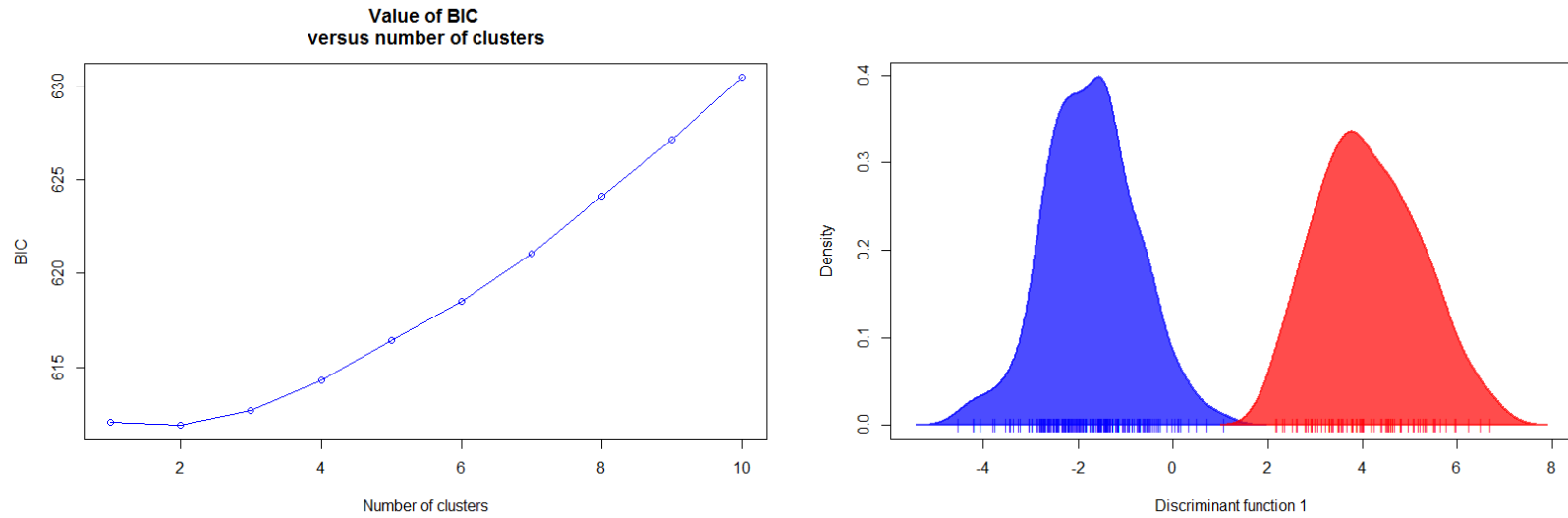


Figure C.13. Santa Barbara Island DAPC density plot for sequential k-means 2-cluster solution and associated BIC plot. The sequential k-means clustering algorithm indicates a 2-cluster solution is useful for describing the genetic structure of Santa Barbara Island (left). The DAPC density plot for K=2 is shown (right).

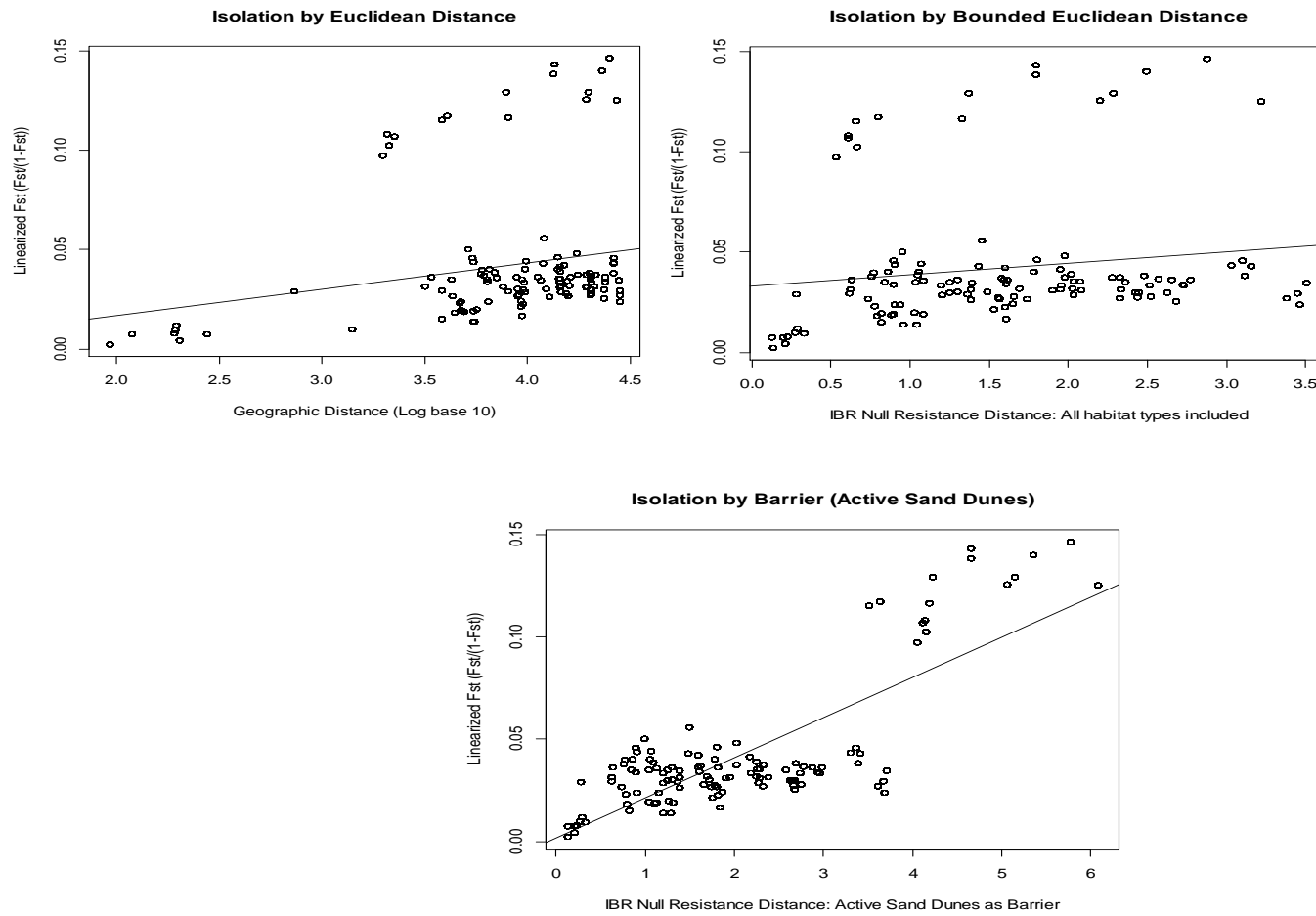


Figure C.14. San Clemente Island IBD, IBR, IBB null models. Figures plot linearized F_{st} values $\left(\frac{F_{st}}{1-F_{st}}\right)$ against log-transformed geographic distance in meters (top left), bounded Euclidean distance based on 100m cell sizes (IBR null model) (top right), and IBR null model with active sand dunes as an absolute barrier (bottom). See text for model selection procedures.

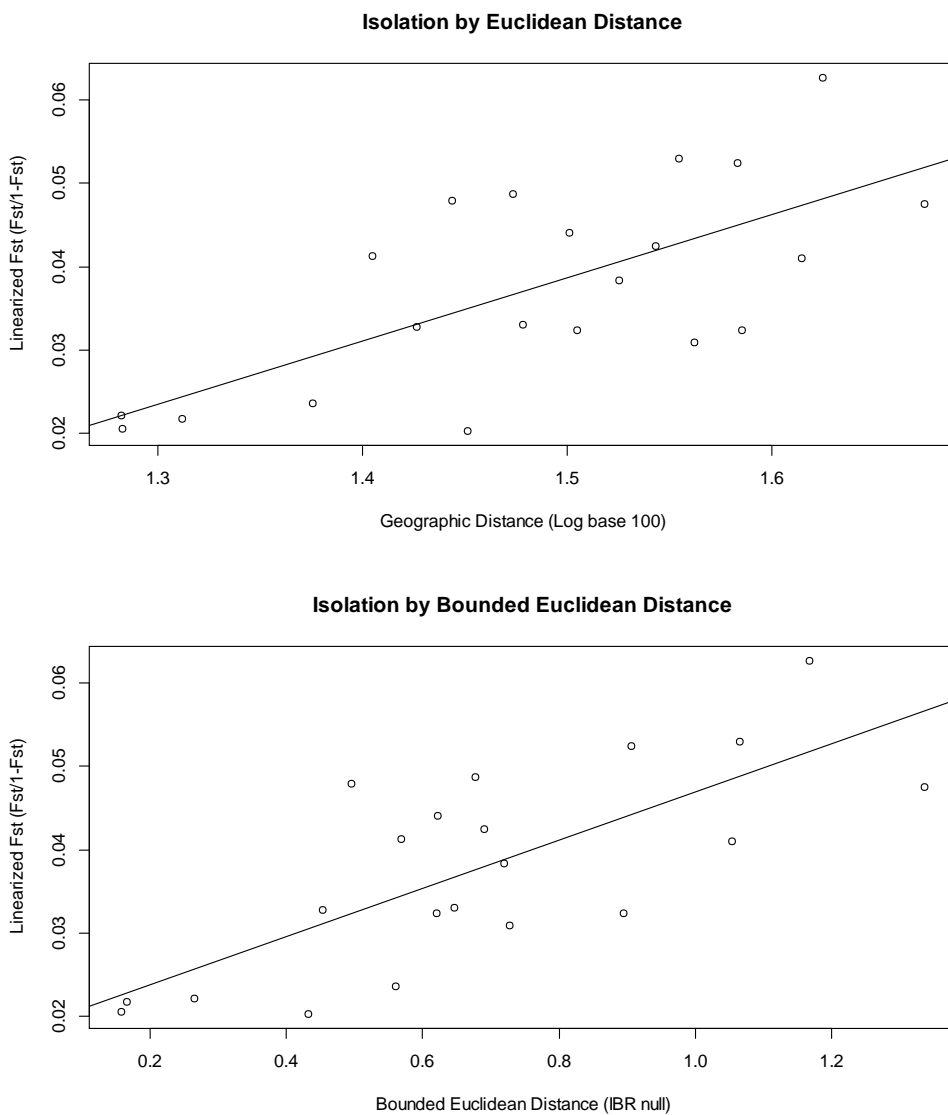


Figure C.15. Santa Barbara Island IBD and IBR null model plots. Figures plot linearized Fst values $\left(\frac{F_{St}}{1-F_{St}}\right)$ against log-transformed geographic distance in meters (top) and bounded Euclidean distance based on 5m cell sizes (IBR null)(bottom). See text for model selection procedures.

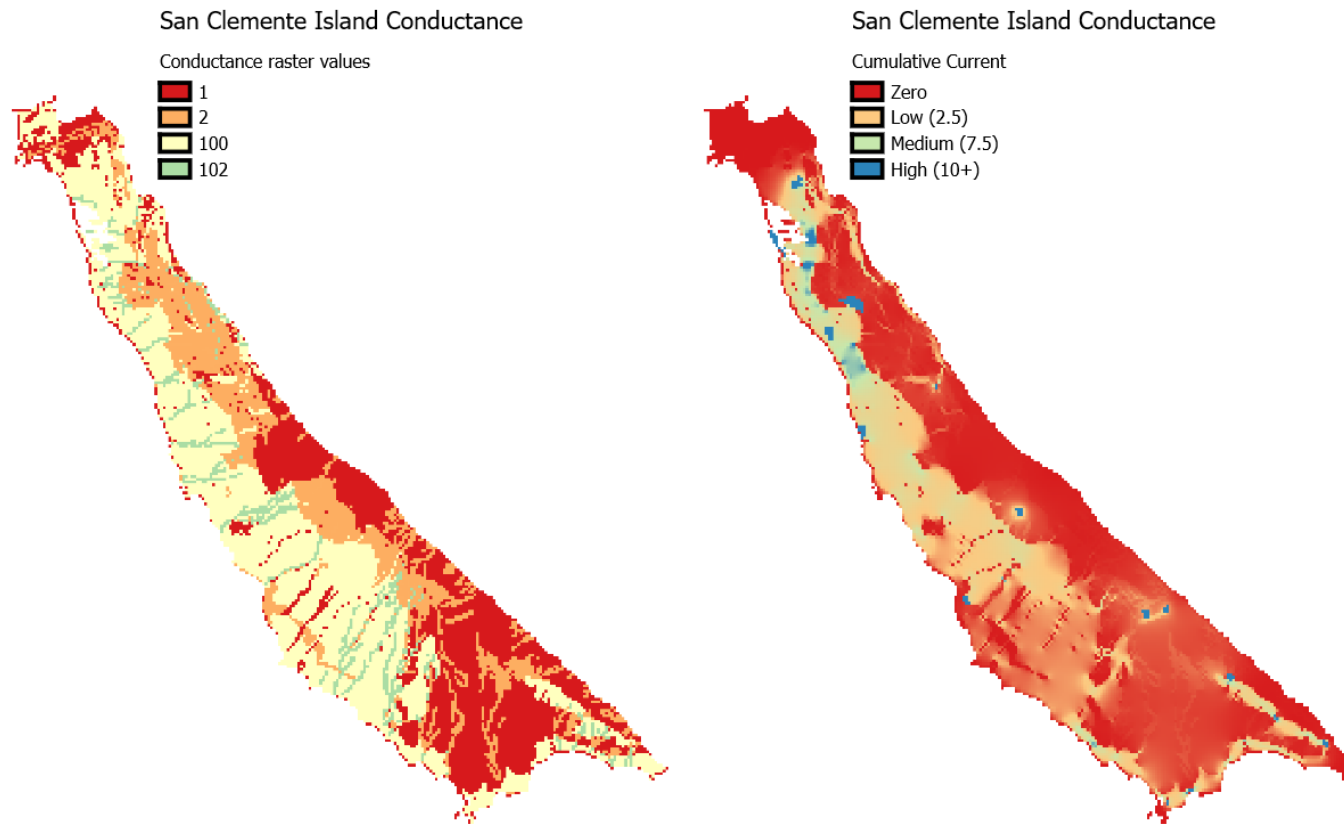


Figure C.16. San Clemente Island IBR conductance analysis. Left: Additive model of resistance with cell values. Model includes the null model (1), California boxthorn (100), Prickly pear cactus (100), grasslands (2), and canyons < 500 ft in length (2); values in the map represent base values and their additive components. Right: Resulting cumulative current map of conductance raster and focal regions formed by the collection site convex hulls for those sites included in Fst analyses. Current descriptions are qualitative with current values given in parentheses.

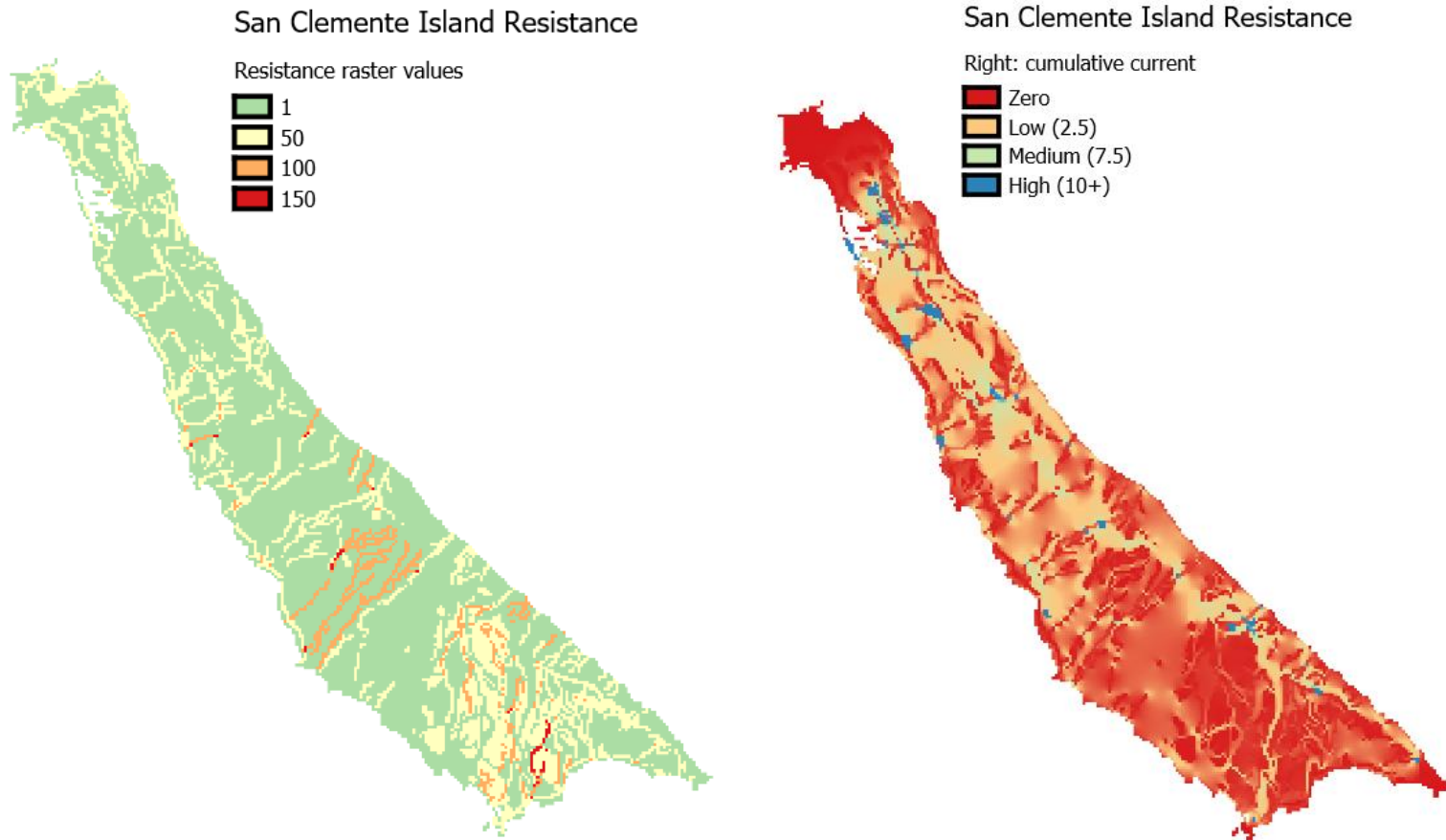


Figure C.17. San Clemente Island IBR resistance analysis. Left: Additive model of resistance with cell values. Model includes the null model (1), coastal cholla (50), canyons > 1000 ft long (100), canyons 500-1000 ft long (50), and secondary roads (50); values in the map represent base values and their additive components. Right: Resulting cumulative current map of resistance raster and focal regions formed by the collection site convex hulls for those sites included in Fst analyses. Current descriptions are qualitative with current values given in parentheses.

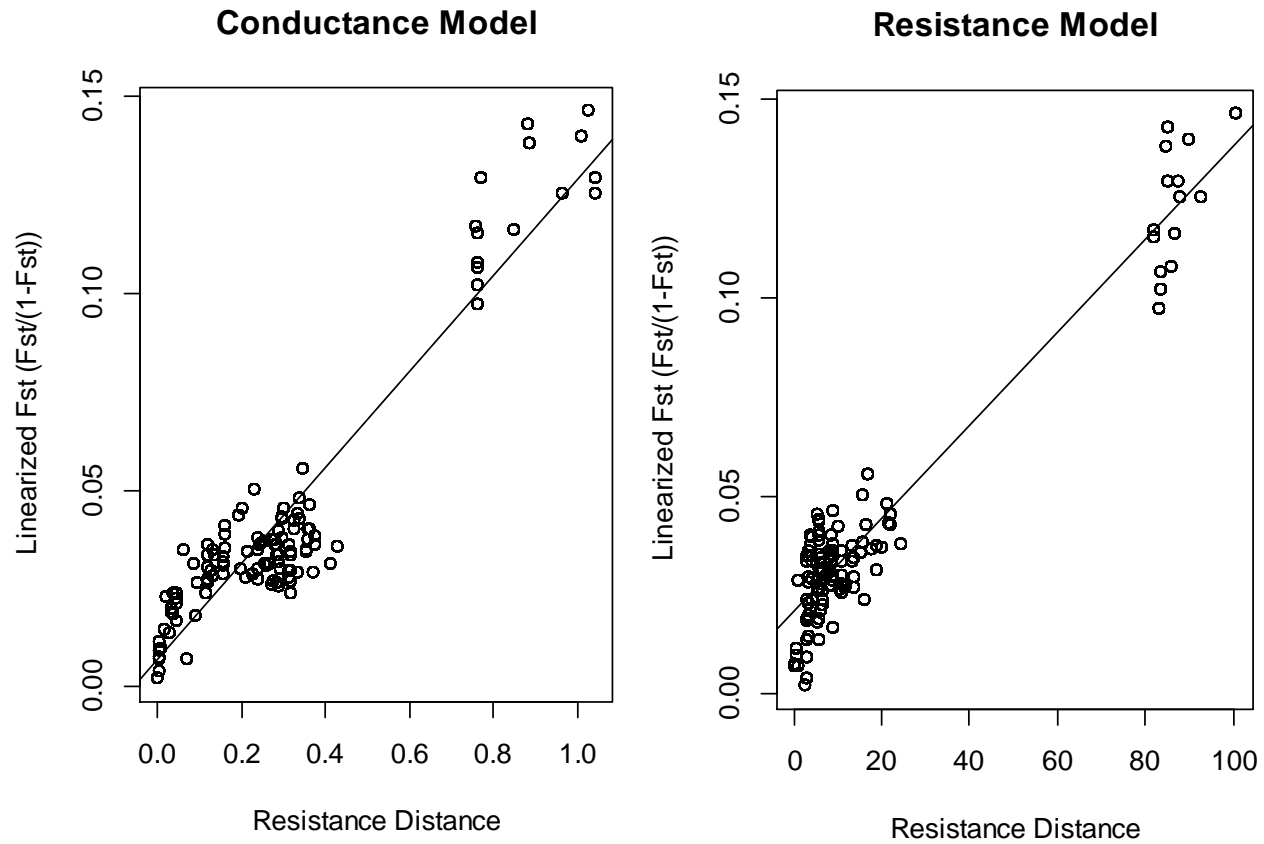


Figure C.18. San Clemente Island IBR plots. Left: Conductance model from Figure 7 with trend line of linearized Fst with resistance distance ($R^2=0.6461$). Right: Resistance model from Figure 8 with trend line of linearized Fst with resistance distance ($R^2=0.5125$).

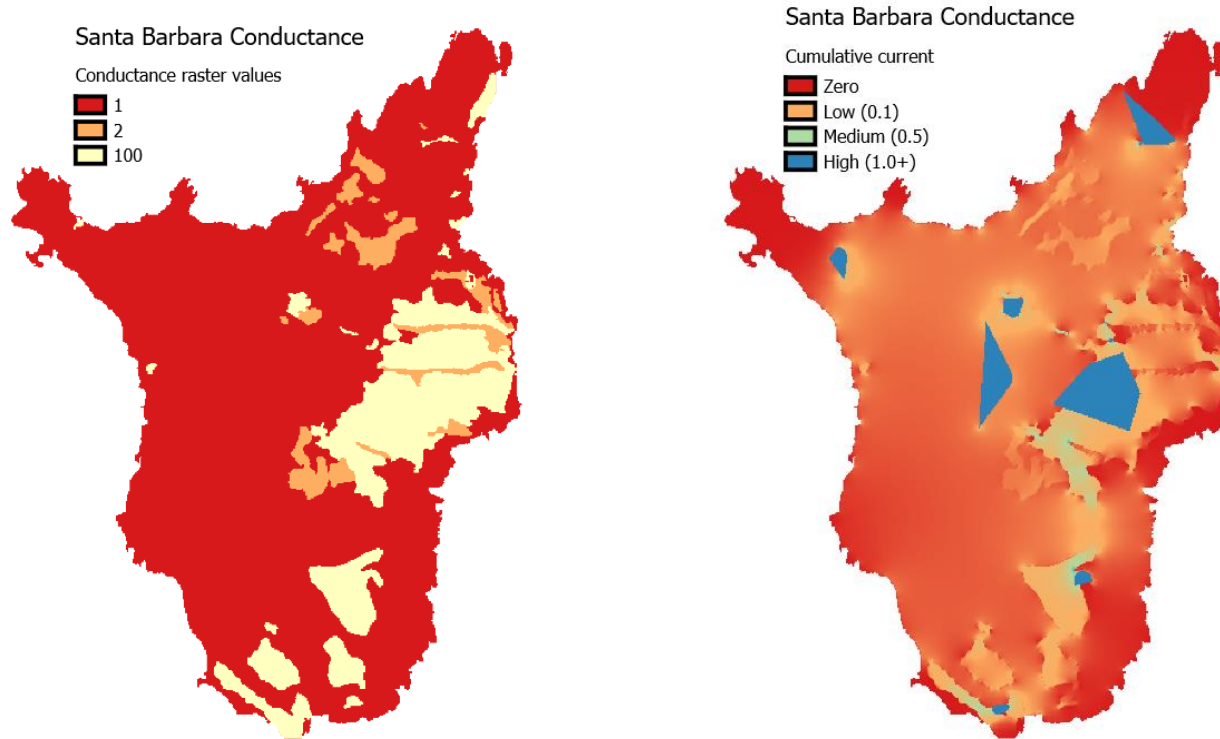


Figure C.19. Santa Barbara Island IBR conductance analysis. Left: Additive model of resistance with cell values. Model includes the null model (1), California boxthorn (100), Prickly pear cactus (100), and Giant Coreopsis (2); values in the map represent base values and their additive components. Right: Resulting cumulative current map of conductance raster and focal regions formed by the collection site convex hulls for those sites included in Fst analyses. Current descriptions are qualitative with current values given in parentheses.

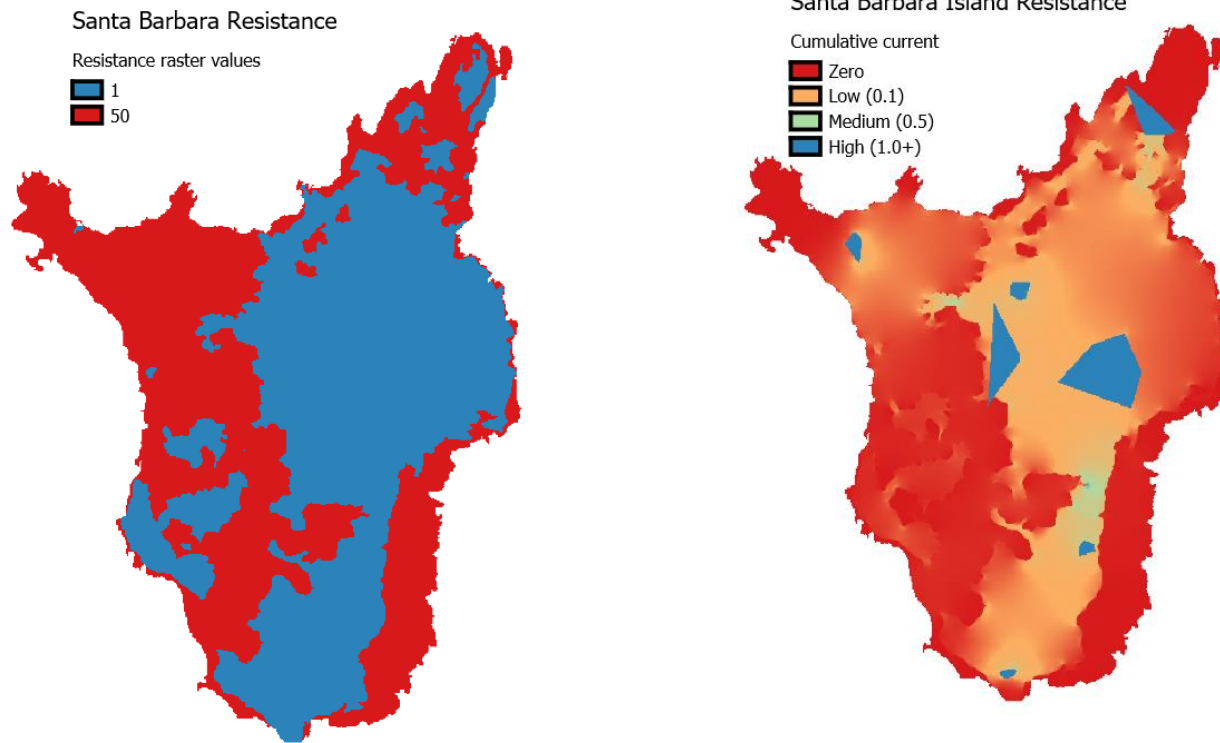


Figure C.20. Santa Barbara Island IBR resistance analysis. Left: Additive model of resistance with cell values. Model includes the null model (1), woolly seablite with crystalline iceplant (50) and common fiddleneck (50); values in the map represent base values and their additive components. Right: Resulting cumulative current map of resistance raster and focal regions formed by the collection site convex hulls for those sites included in Fst analyses. Current descriptions are qualitative with current values given in parentheses.

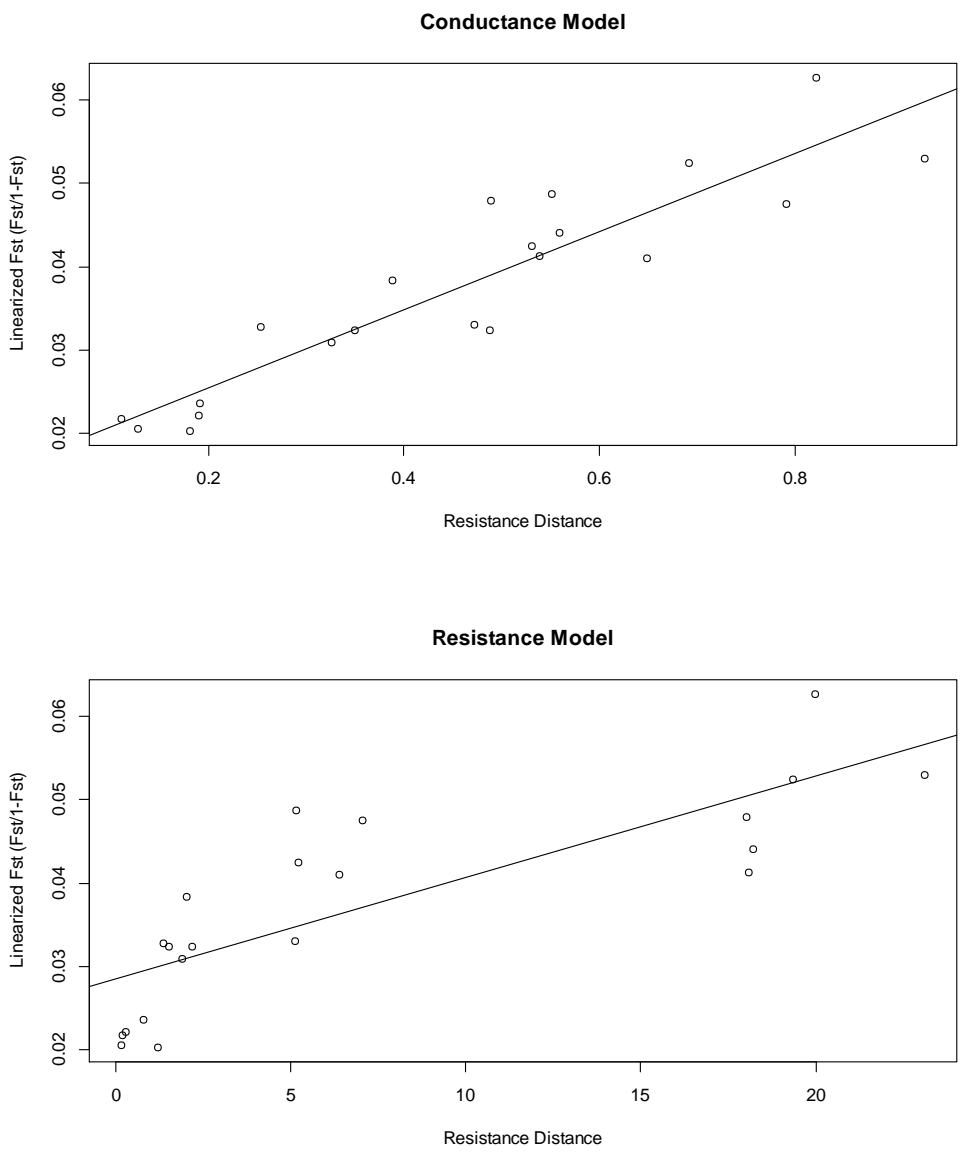


Figure C.21. Santa Barbara Island IBR plots. Top: Conductance model from Figure 10 with trend line of linearized Fst with resistance distance ($R^2=0.8877$). Bottom: Resistance model from Figure 11 with trend line of linearized Fst with resistance distance ($R^2=0.8582$).

Appendix D: Chapter 2 supplementary material

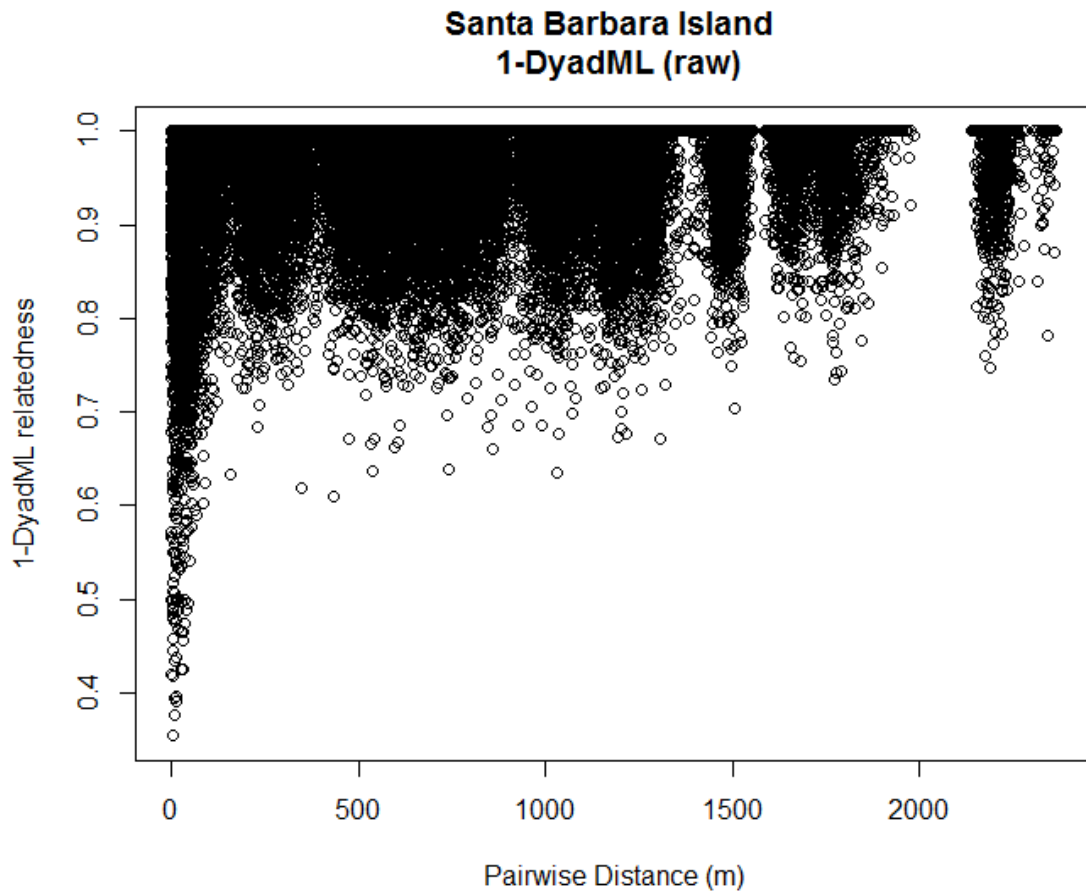


Figure D.1. Graph of raw data contributing to Santa Barbara Island DyadML analyses. X-axis represents pairwise distance between dyad members and Y is (un)relatedness as a distance measure suitable for variogram analyses.

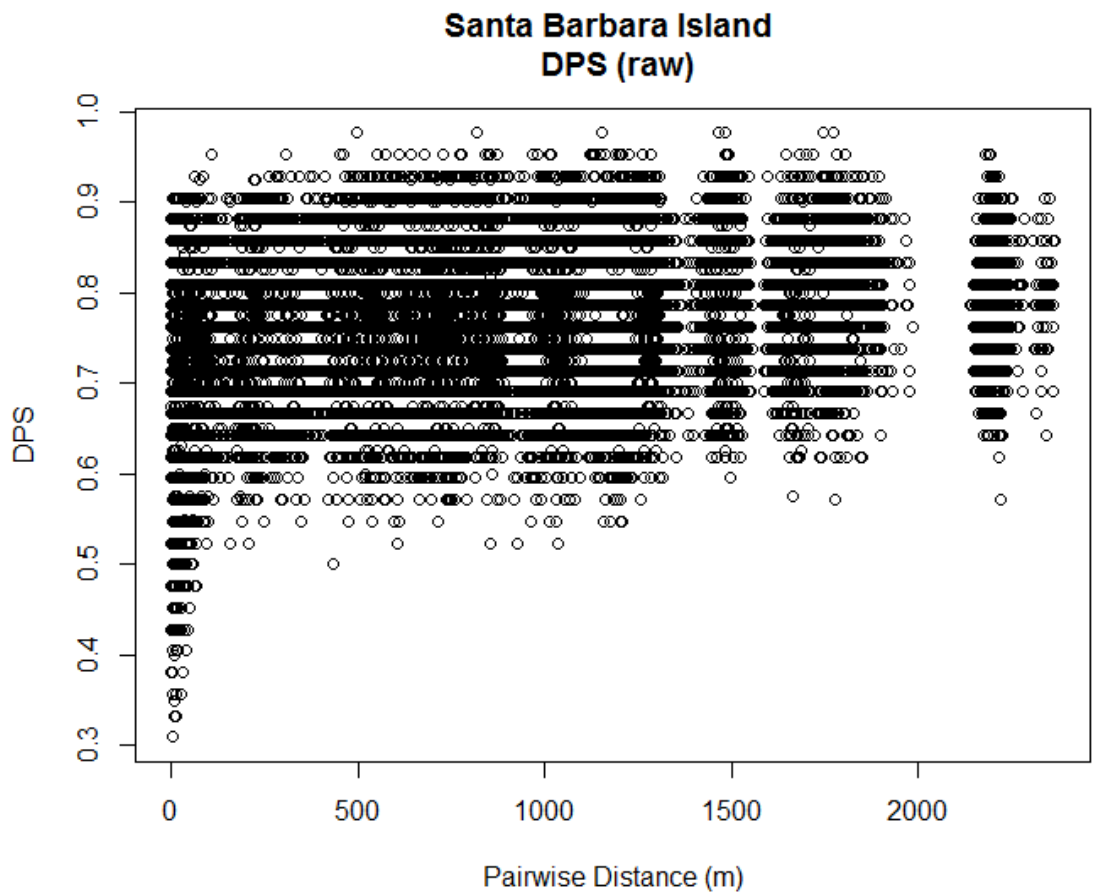


Figure D.2. Graph of raw data contributing to Santa Barbara Island DPS analyses. X-axis represents pairwise distance between dyad members and Y is the proportion of alleles no shared between dyad members.

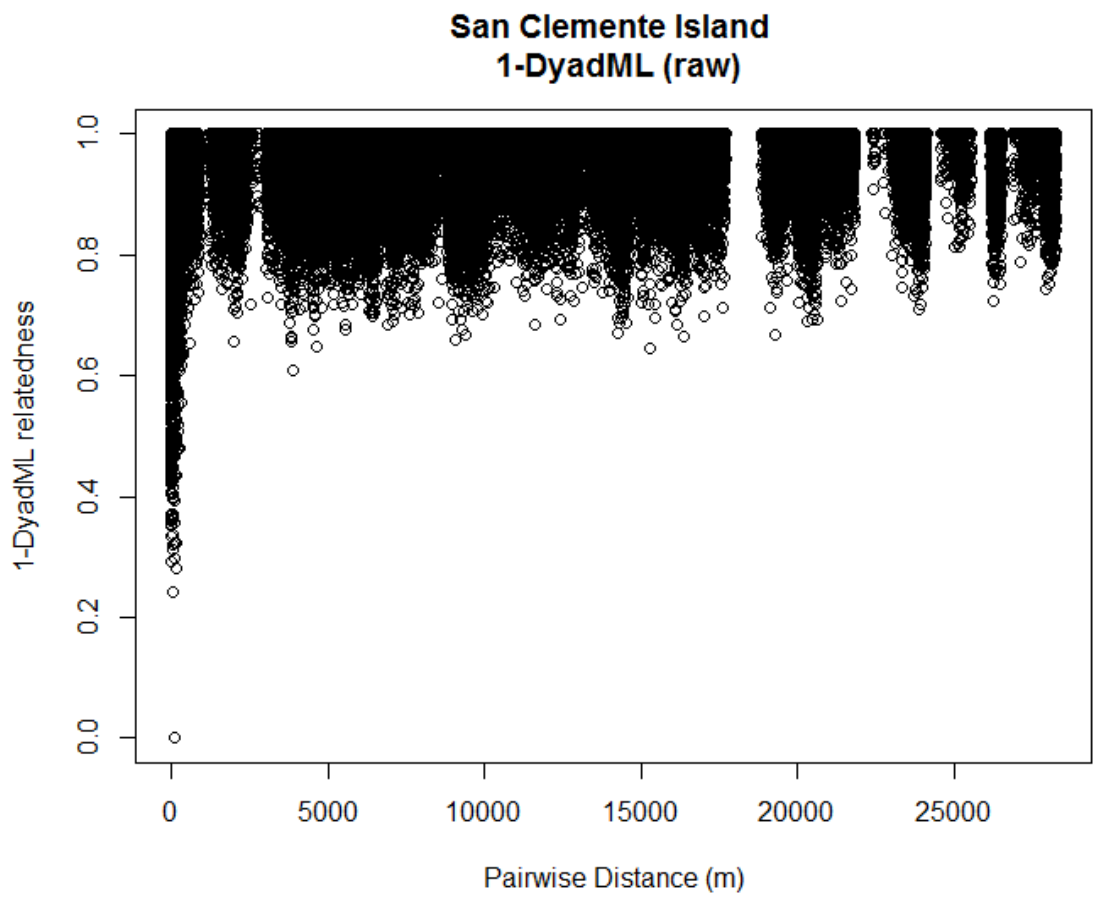


Figure D.3. Graph of raw data contributing to San Clemente Island DyadML analyses. X-axis represents pairwise distance between dyad members and Y is (un)relatedness as a distance measure suitable for variogram analyses.

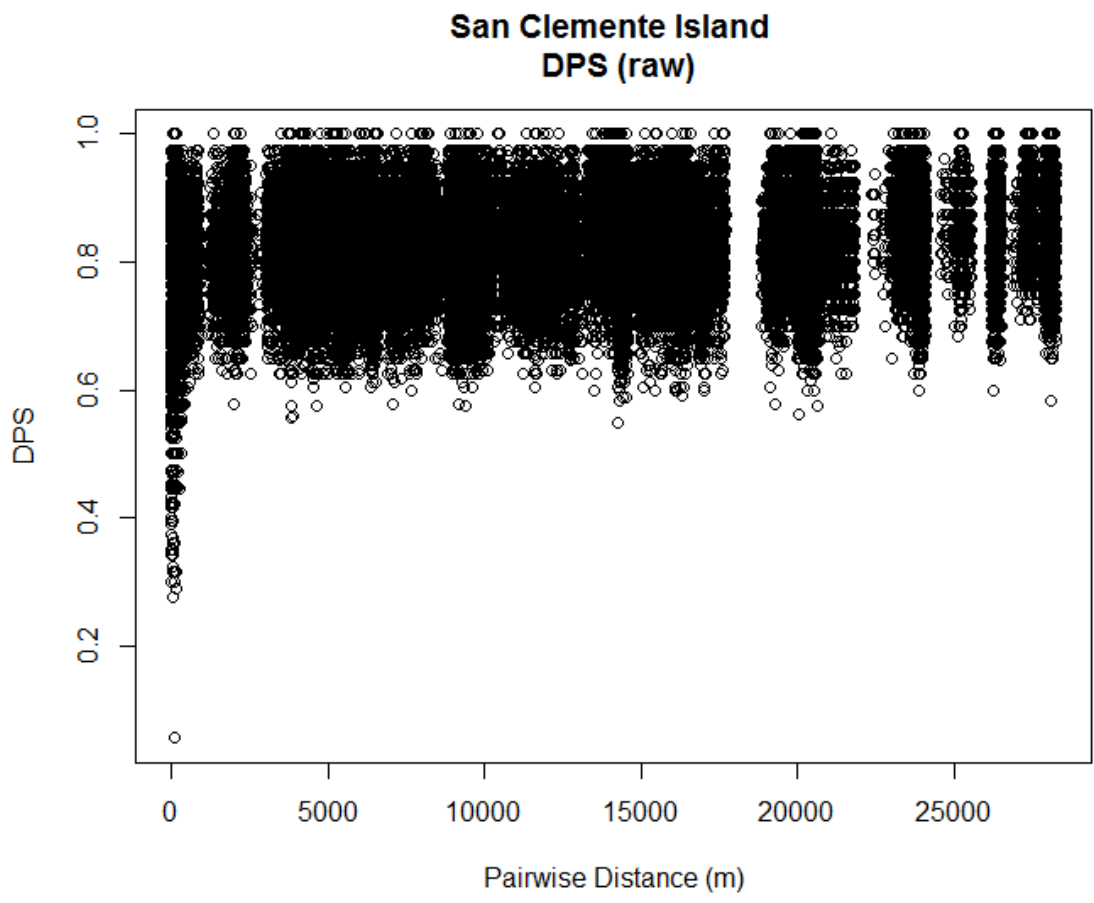


Figure D.4. Graph of raw data contributing to San Clemente Island DPS analyses. X-axis represents pairwise distance between dyad members and Y is the proportion of alleles no shared between dyad members.

Appendix E: Chapter 3 supplementary material

Table E.1. Life history parameters for *Xantusia riversiana* simulations. Demogenetic simulations incorporated the following life history parameters in a 4-stage model. Demographic stochasticity was implemented through the standard deviations given in parentheses for each variable. Males had a 50% probability of maturing when 2-3 years old and both sexes had 100% probability of maturing at 3+ years.

Age Class	Mortality (SD)	Male Maturity	Female Maturity	Fecundity (SD)
0	11.7 (13.45)	0	0	0
1	16.3 (16.05)	0	0	0
2	19.5 (21.15)	0.5	0	0
3	15.6 (18.63)	1.0	1.0	3.9 (1.15)

Figures: E.2.-E.14. Habitat suitability models and suitable patch distribution under all climate change scenarios. Models are identified by the year, climate model name, and RCP. Dark patches indicate suitable habitat based on the 0.1095 threshold value. Gray indicates unsuitable habitat below the threshold

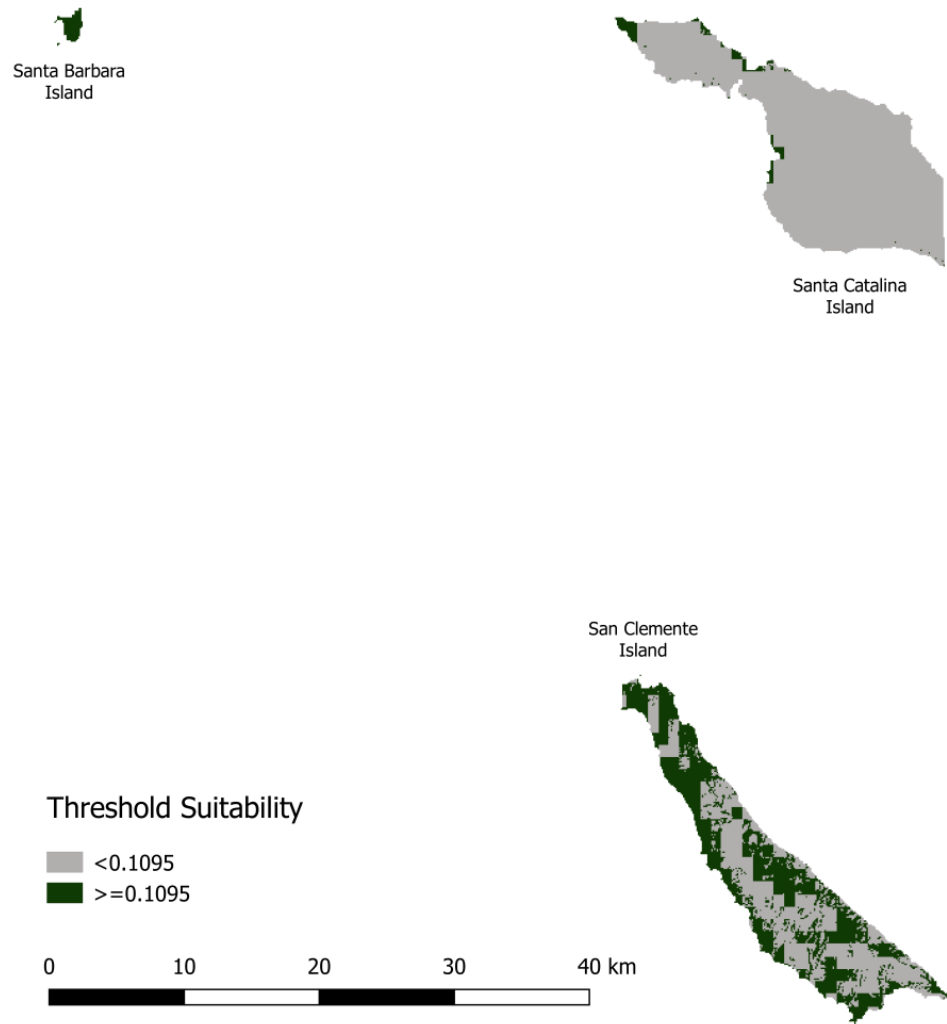


Figure E.2. Contemporary (2007) habitat suitability.

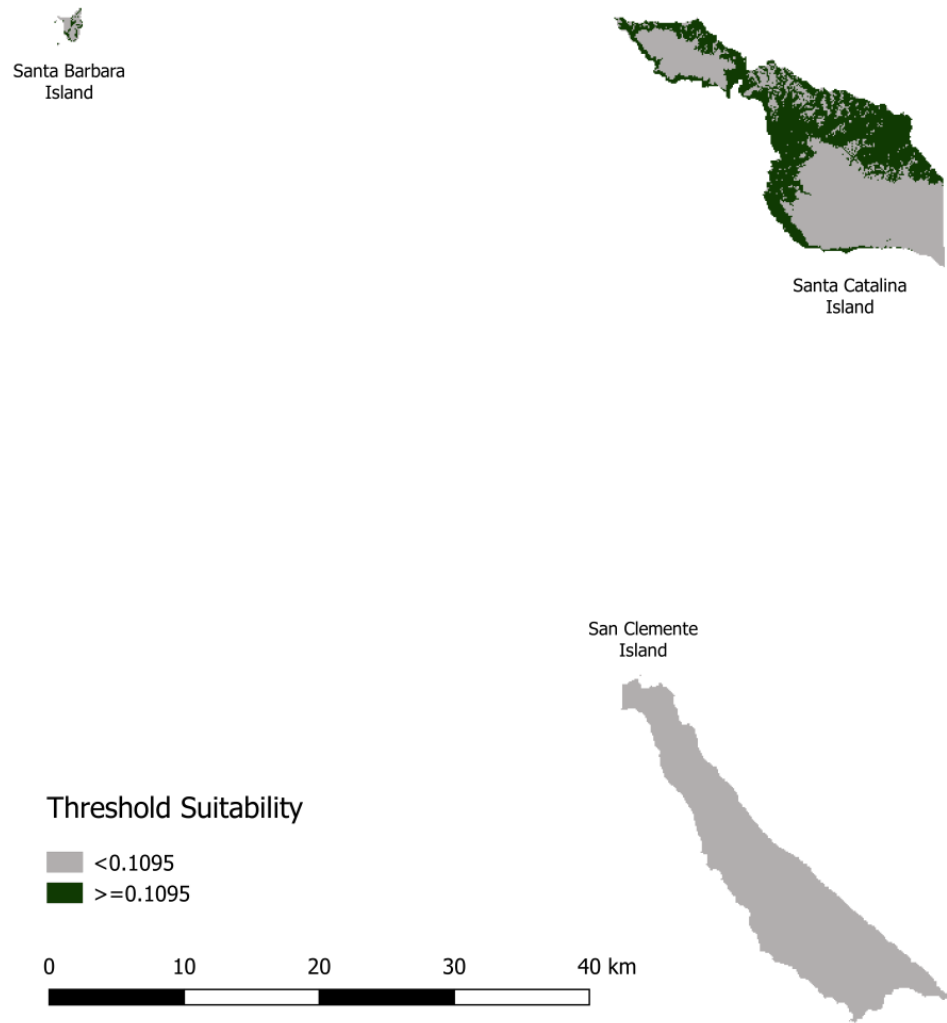


Figure E.3. 2038 CanESM 4.5 habitat suitability.

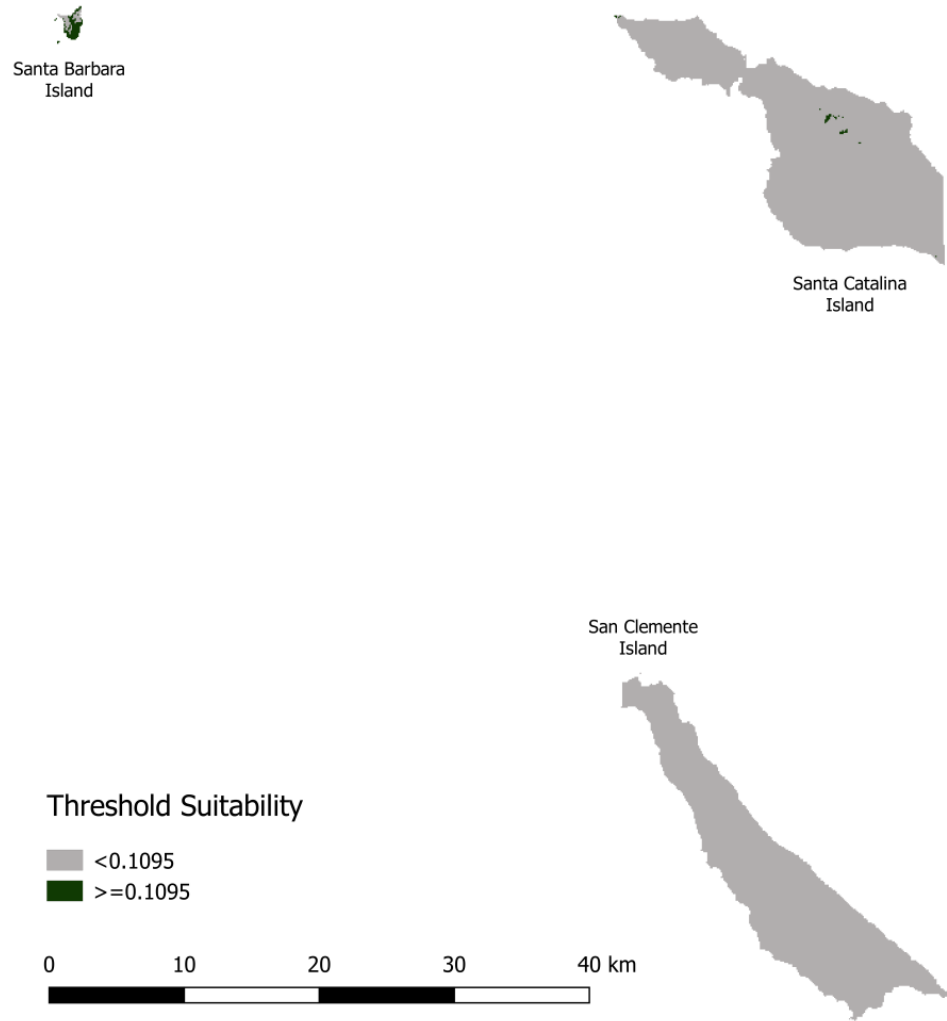


Figure E.4. 2038 CanESM 8.5 habitat suitability.

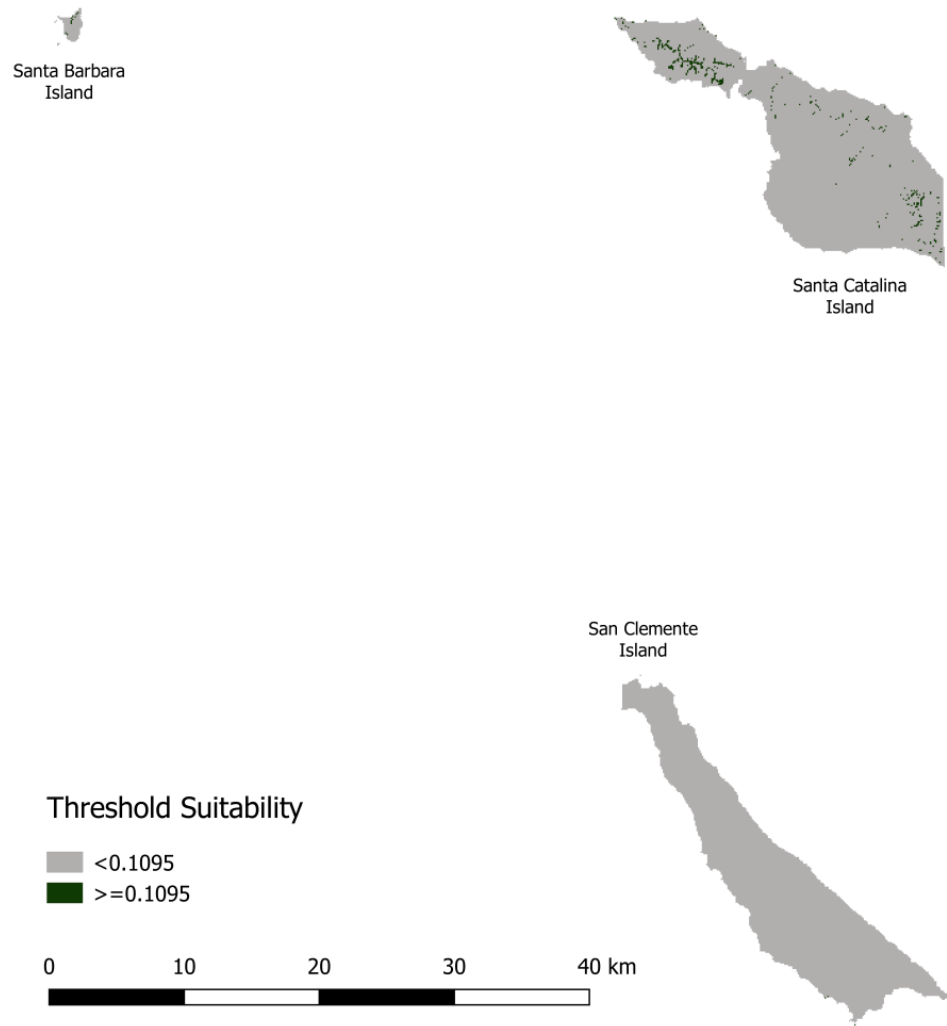


Figure E.5. 2038 Miroc 4.5 habitat suitability.

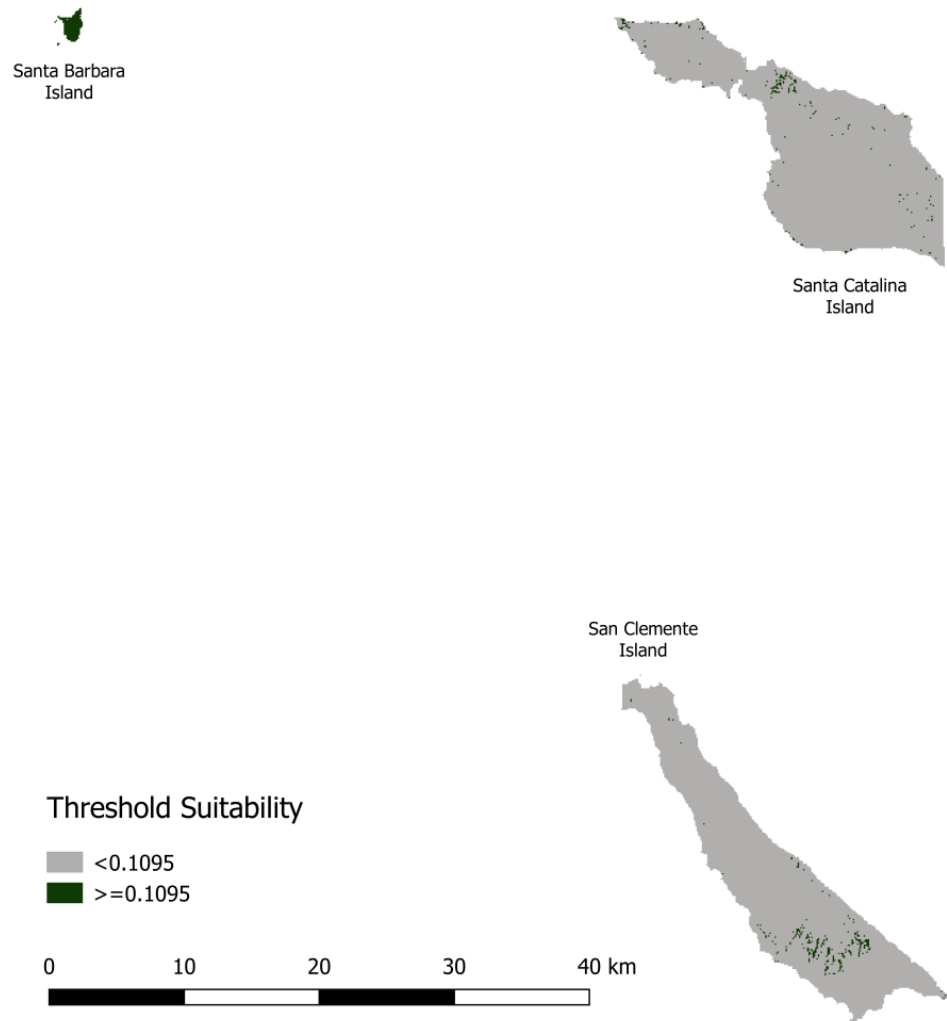


Figure E.6. 2038 Miroc 8.5 habitat suitability.

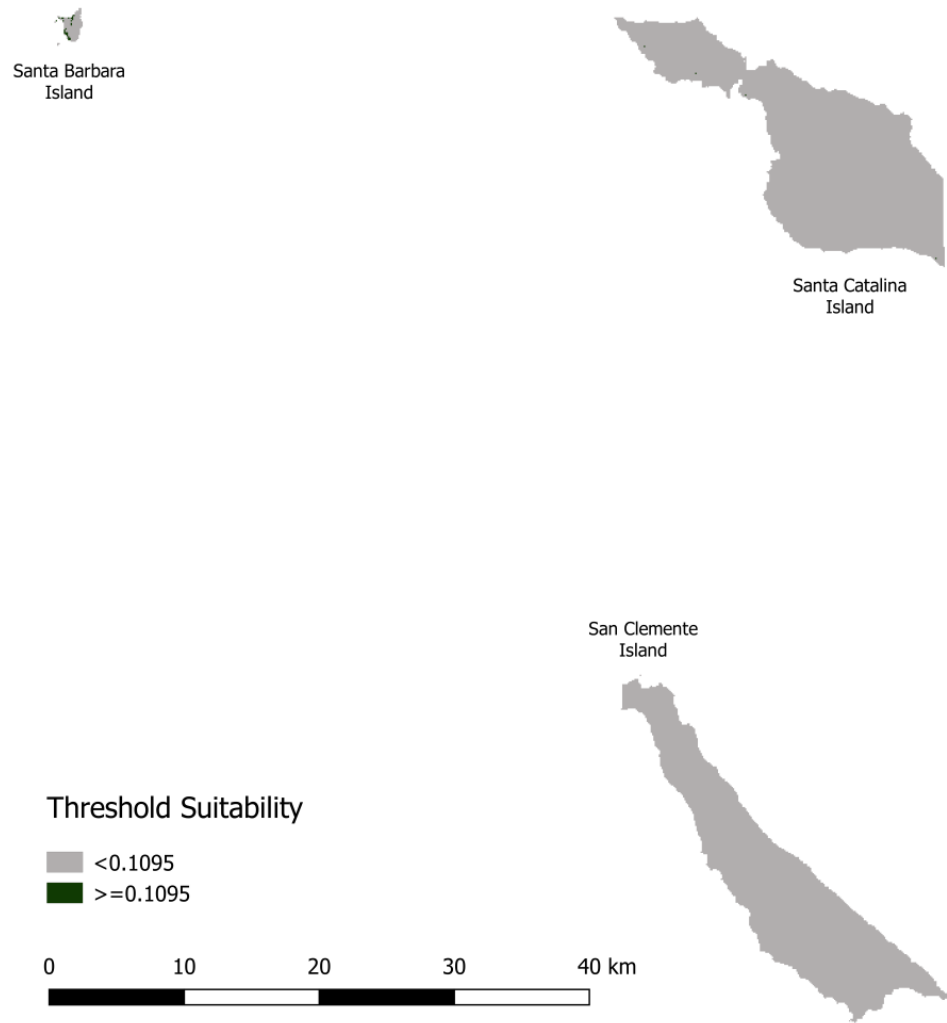


Figure E.7. 2069 CanESM 4.5 habitat suitability.

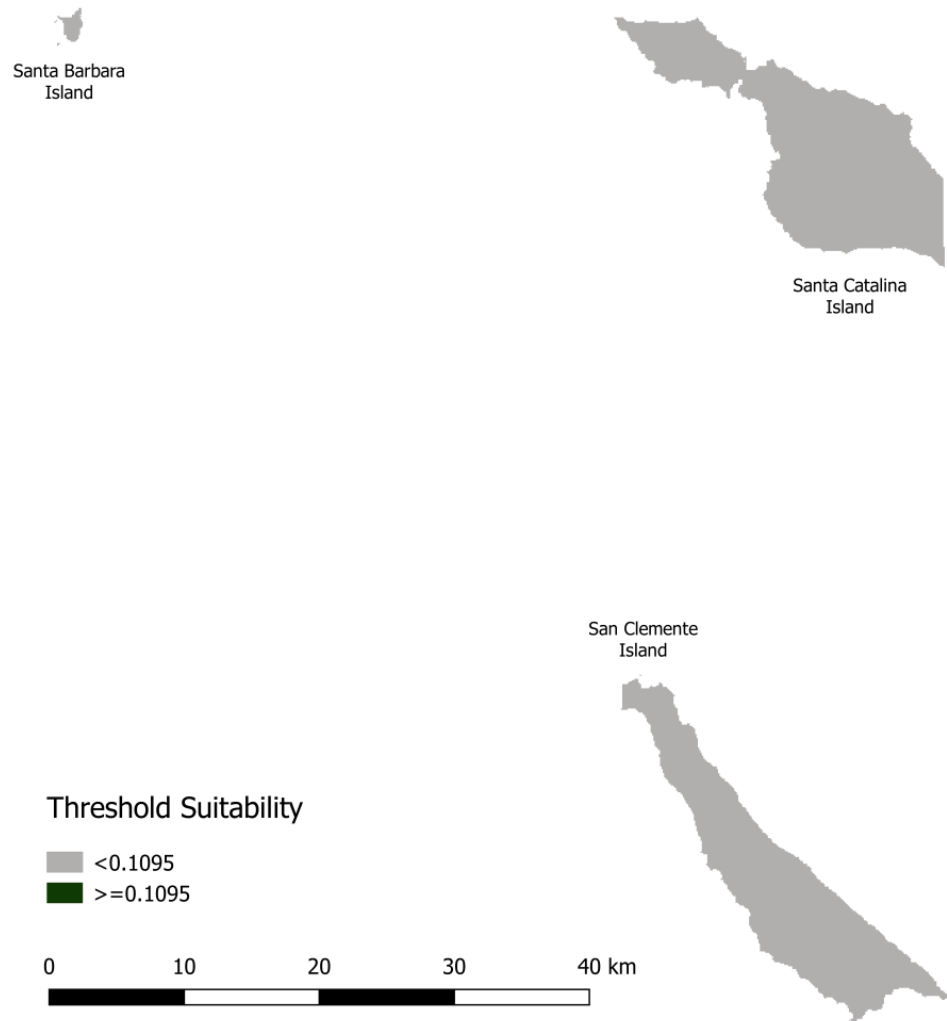


Figure E.8. 2069 CanESM 8.5 habitat suitability.

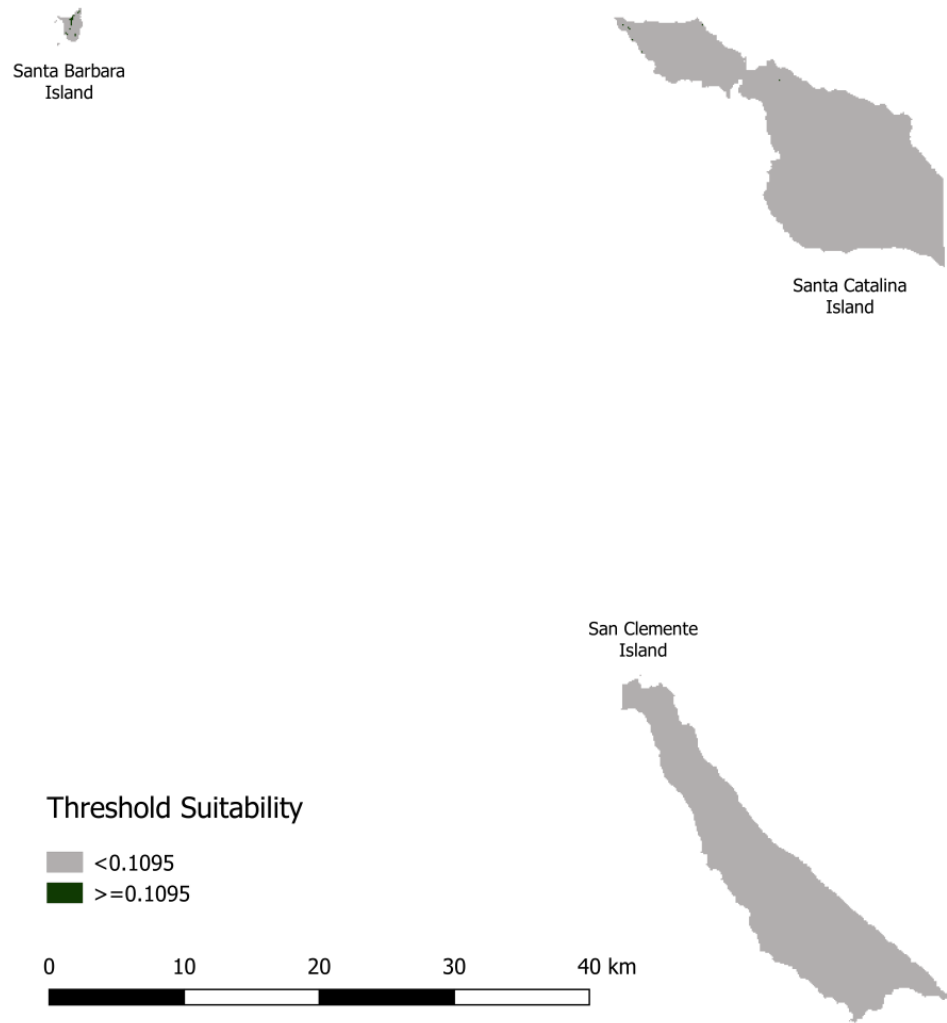


Figure E.9. 2069 Miroc 4.5 habitat suitability.

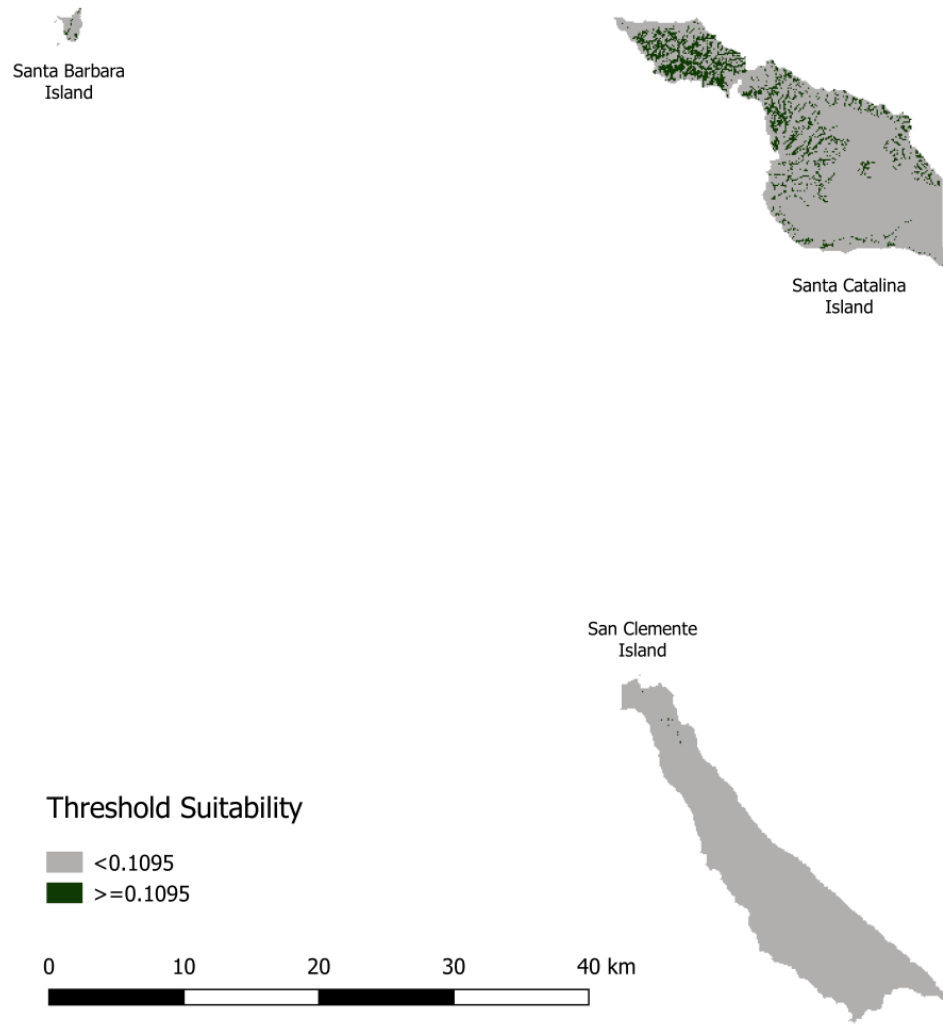


Figure E.10. 2069 Miroc 8.5 habitat suitability.

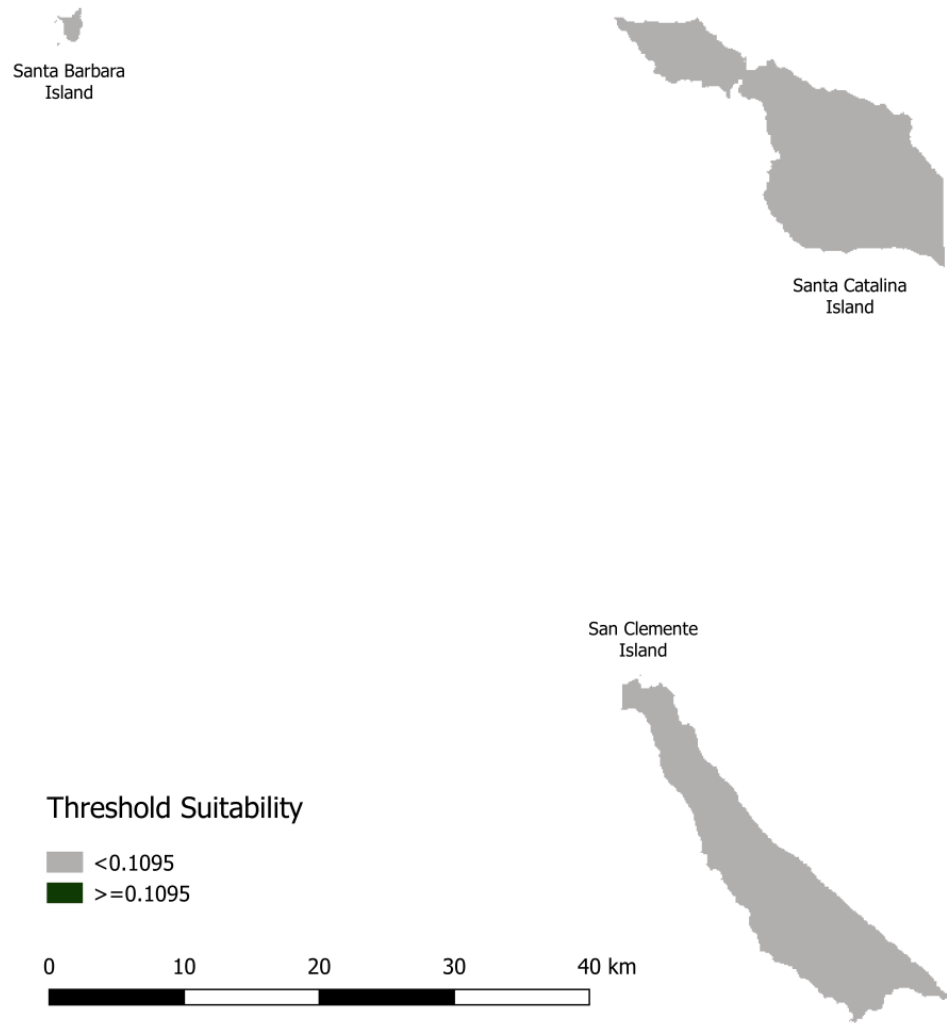


Figure E.11. 2100 CanESM 4.5 habitat suitability.

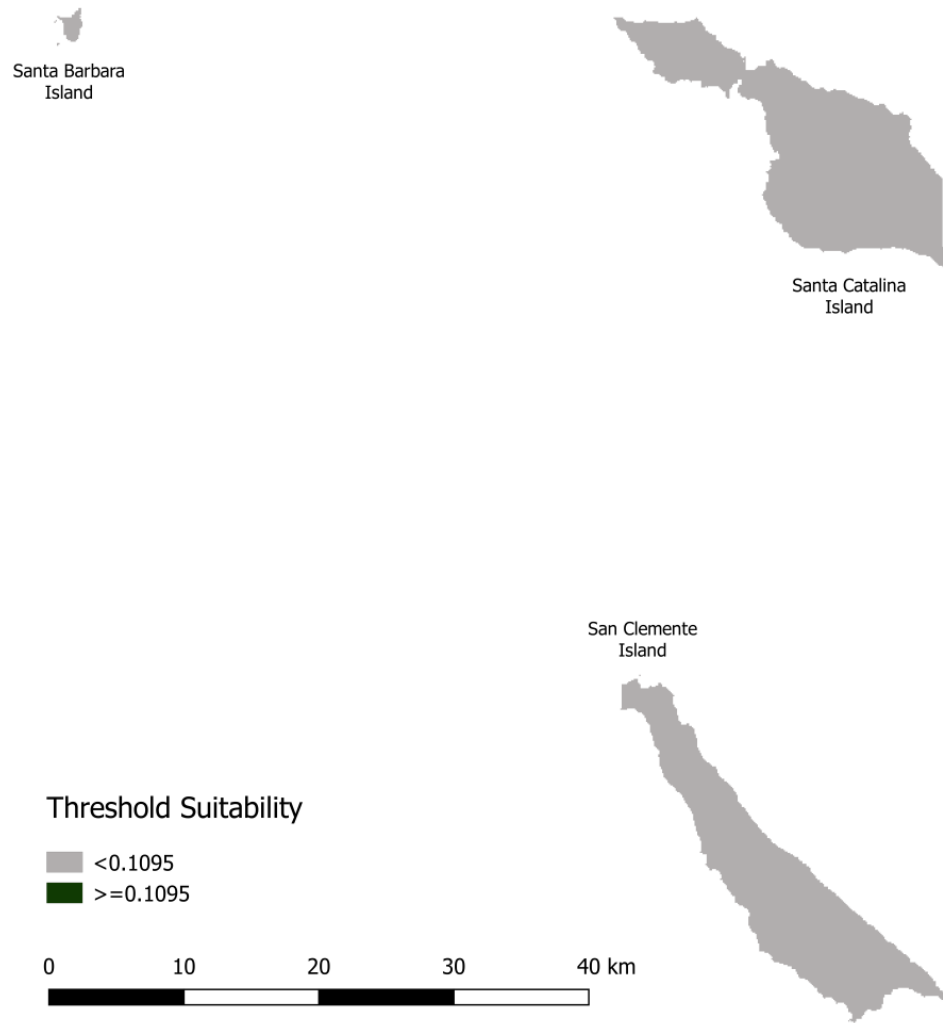


Figure E.12. 2100 CanESM 8.5 habitat suitability.

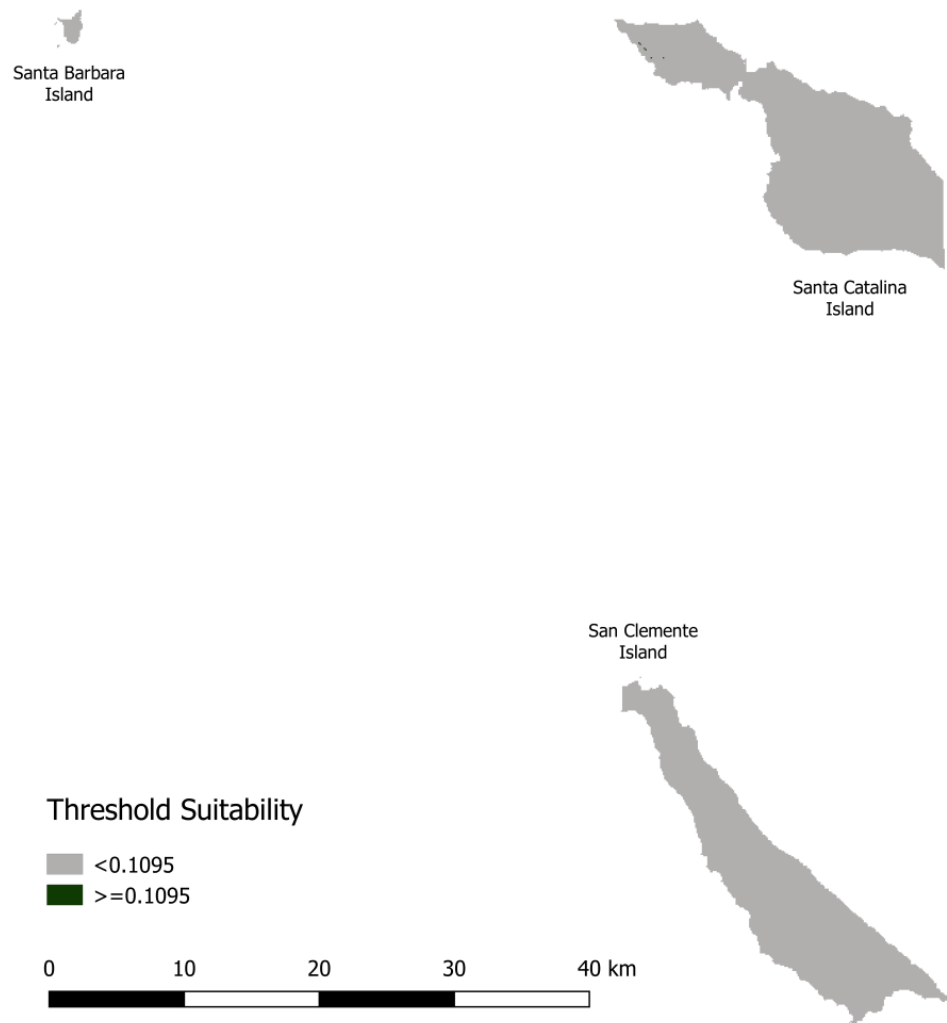


Figure E.13. 2100 Miroc 4.5 habitat suitability.

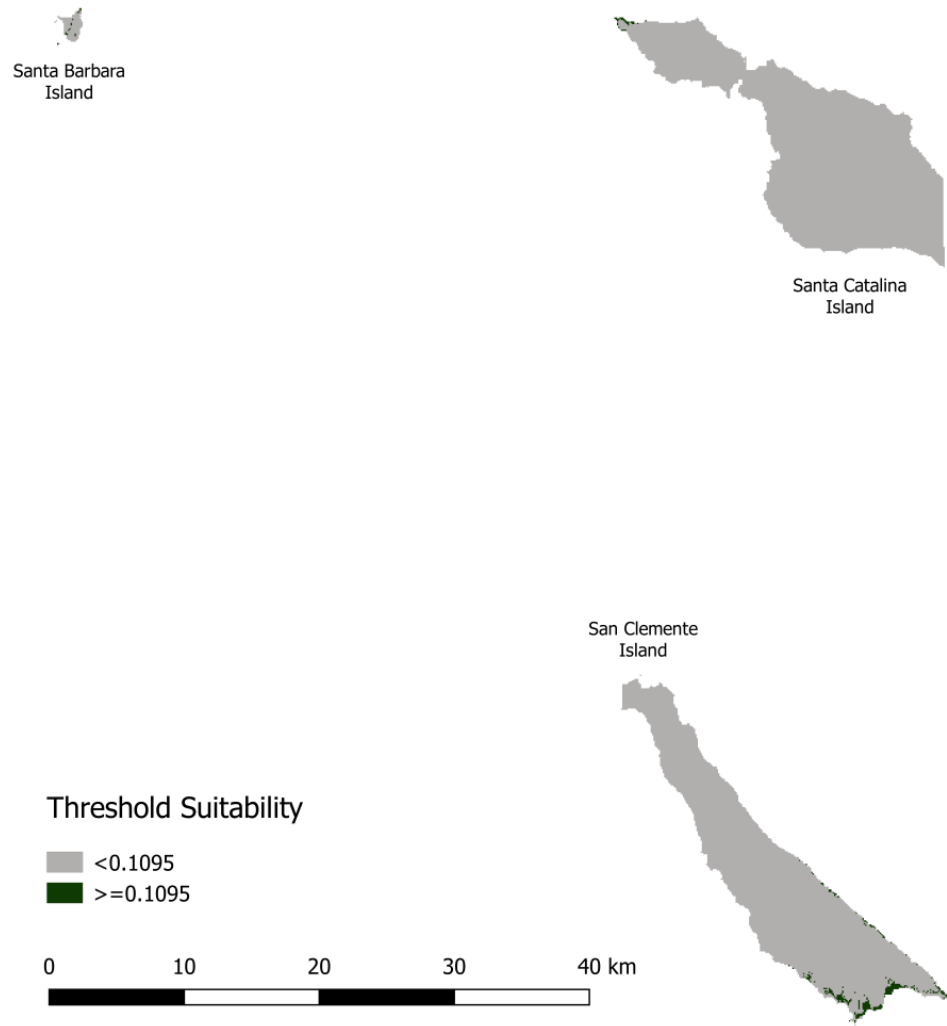


Figure E.14. 2100 Miroc 8.5 habitat suitability.